JPRS L/10417

26 March 1982

Translation

THEORETICAL AND EXPERIMENTAL INVESTIGATIONS OF SURFACE AND INTERNAL WAVES

Ed. by

B.A. Nelepo

FBIS FOREIGN BROADCAST INFORMATION SERVICE

NOTE

JPRS publications contain information primarily from foreign newspapers, periodicals and books, but also from news agency transmissions and broadcasts. Materials from foreign-language sources are translated; those from English-language sources are transcribed or reprinted, with the original phrasing and other characteristics retained.

Headlines, editorial reports, and material enclosed in brackets [] are supplied by JPRS. Processing indicators such as [Text] or [Excerpt] in the first line of each item, or following the last line of a brief, indicate how the original information was processed. Where no processing indicator is given, the information was summarized or extracted.

Unfamiliar names rendered phonetically or transliterated are enclosed in parentheses. Words or names preceded by a question mark and enclosed in parentheses were not clear in the original but have been supplied as appropriate in context. Other unattributed parenthetical notes within the body of an item originate with the source. Times within items are as given by source.

The contents of this publication in no way represent the policies, views or attitudes of the U.S. Government.

APPROVED FOR RELEASE: 2007/02/09: CIA-RDP82-00850R000500040063-3

JPRS L/10417

26 March 1982

THEORETICAL AND EXPERIMENTAL INVESTIGATIONS OF SURFACE AND INTERNAL WAVES

Sevastopol' TEORETICHESKIYE I EKSPERIMENTAL'NYYE ISSLEDOVANIYA POVERKHNOSTNYKH I VNUTRENNIKH VOLN in Russian 1980 pp 1-202

[Translation of "Theoretical and Experimental Investigations of Surface and Internal Waves", edited by B. A. Nelepo, academician Ukrainian Academy of Sciences, Morskoy gidrofizicheskiy institut AN USSR (MGI AN USSR), 300 copies, 202 pages]

[I - USSR - E FOUO]

FOR OFFICIAL USE ONLY

APPROVED FOR RELEASE: 2007/02/09: CIA-RDP82-00850R000500040063-3

[Text] Annotation. This collection of articles contains the results of theoretical and experimental investigations of surface, barotropic and internal waves arising in the ocean under the influence of periodic, moving and pulsed disturbances. These disturbances are wind, pressure formations, barotropic waves and submarine earthquakes. The articles discuss the dependence of the characteristics of wave processes on the parameters of the operative forces, sea medium and bottom relief.

The collection is intended for specialists in the field of marine physics and hydrodynamics.

Preface. The Second Seminar of Directors and Participants in the Interdepartmental Project "Volna" ["Wave"] was held in Sevastopol' during the period 26-30 November 1979 at the Marine Hydrophysical Institute of the Ukrainian Academy of Sciences. The theme of the seminar was: "Theoretical and Experimental Investigations of Surface and Internal Waves in the Ocean."

The organizers of this meeting of scientists were the Scientific Council of the USSR State Committee on Science and Technology on the Problem "Study of the Oceans and Seas and Use of Their Resources," the Commission on the Problem of the World Ocean of the USSR Academy of Sciences Presidium and the Marine Hydrophysical Institute of the Ukrainian Academy of Sciences as the coordinating organization of the "Volna" project.

The seminar was attended by specialists of the Marine Hydrophysical Institute of the Ukrainian Academy of Sciences, the Institute of Oceanology of the USSR Academy of Sciences, Acoustics Institute, Moscow State University, Hydromechanics Institute of the Ukrainian Academy of Sciences, Central Scientific Research Institute imeni A. N. Krylov, Soyuzmorniiproyekt, Institute of Applied Physics of the USSR Academy of Sciences, Northern Caucasus Scientific Center of Institutes of Higher Education, Siberian Department of the USSR Academy of Sciences, Far Eastern Scientific

Center of the USSR Academy of Sciences, State Committee on Hydrometeorology and Environmental Monitoring of the USSR Council of Ministers and a number of other organizations.

More than 70 scientific reports were presented and discussed. These dealt with the present-day status of theoretical and experimental investigations of wave processes in the ocean and timely directions in work in this field during 1981-1985. There was a scientific discussion of a broad range of questions relating to study of wind waves, mathematical modeling of the processes of generation and propagation of surface and internal waves in the open ocean and in the coastal zone, experimental investigation of internal waves under in situ and laboratory conditions.

The work of the seminar transpired in plenary and section meetings in two sections: surface and internal waves. The participants in the meeting expressed an interest in holding a scientific conference in 1980 and the publication of a specialized collection of articles.

The collection of articles contains presentations of studies presented at the seminar and devoted to theoretical and experimental investigations of surface and internal waves generated in the ocean by periodic, pulsed and moving disturbances.

The first section includes articles which examine surface and long waves arising in a barotropic ocean. The diffraction of waves by spatial inhomogeneities of bottom relief is studied; the influence of the velocity shear of sea currents on three-dimensional waves generated by a moving pressure region is investigated; computations of the distributions of orbital velocities of wind waves are given; the role of the ice cover in the process of propagation of flexural-gravitational waves is analyzed. In the case of long waves a study is made of the generation of seismic waves during the movement of tsunamis in a basin of variable depth, tsunami waves are analyzed on the basis of observational data in the neighborhood of Iturup Island, evolution of axisymmetric disturbances is studied, and the influence of viscosity and the β-effect on waves generated by periodic disturbances in a basin of variable depth is investigated.

The second section of this collection includes articles which examine internal waves. Long-period spatial internal waves arising from nonaxisymmetric initial disturbances in the absence of a flow are analyzed; nonstationary short-period plane internal waves in the presence of a flow with a sharp change in velocity are studied; the distorting influence of fine stratification on free and forced waves is investigated; an evaluation of the possible values of elements of internal waves in the zone of the southern polar front is given; the variability of the energy density of internal waves with depth is considered; the influence of viscosity on wave processes in the stratified ocean is analyzed.

SURFACE WAVES

SOME PROBLEMS IN WAVE DIFFRACTION AND SCATTERING BY SPATIAL INHOMOGENEITIES IN OCEAN AND ATMOSPHERE

Sevastopol' TEORETICHESKIYE I EKSPERIMENTAL'NYYE ISSLEDOVANIYA POVERKHNOSTNYKH I VNUTRENNIKH VOLN in Russian 1980 (manuscript received 7 Jun 80) pp 7-18

[Article by I. T. Selezov]

[Text]

Abstract: The problems of the theory of waves are considered when axisymmetric inhomogeneities are present. Some precise solutions are found and the methods of generalized power series and approximation of solutions by polynomials are set forth.

The diffraction of waves in the broad sense is the deviation of wave movements from the laws of geometrical optics. This phenomenon is generated when the medium contains some inhomogeneities localized or distributed in space.

As is well known, the application of rigorous methods of mathematical physics to solution of the problems of wave propagation, diffraction and scattering is limited and belongs to classical problems. Recently approximate analytical and numerical methods are being developed [1, 4, 6-9, 11-15].

1. Introduction. The classical problem of the theory of nonstationary diffraction is formulated in the following way [5]. Assume that some closed region R with the boundary ∂R is stipulated in the region Q, oriented in a rectangular Cartesian coordinate system x, y, z and a plane wave is propagated along the Ox-axis (Fig. 1). Then the diffraction problem is reduced to the Cauchy problem or the boundary-value problem for an equation in partial derivatives (or system of equations) in the Q region, whose coefficients experience discontinuities of the first kind on the ∂R surface. The ∂R surface is characterized by a curvilinear coordinate system.

We will assume that the field in the external region Q is described by the wave equation for the function $\varphi(x, y, z, t)$

$$\left(\nabla^2 - \frac{1}{c^2}\frac{\partial^2}{\partial t^2}\right)\varphi = 0. \qquad (1.1)$$

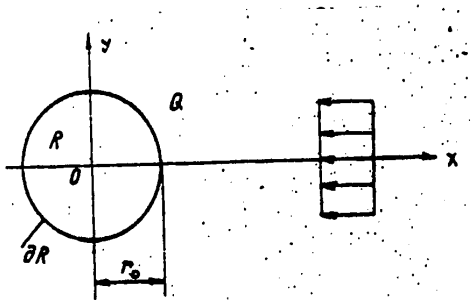

Fig. 1.

The φ function is represented in the form of the sum of the incident φ_i and the scattered φ_s fields $\varphi = \varphi_i + \varphi_s$, where $\varphi_i(x,0,0,t) = F(x + ct)$.

We will assume that at the time t = 0 the leading edge of the wave touches the ∂R surface. This is equivalent to the following: for the sought-for function φ and its derivative t the following initial conditions are stipulated

$$\varphi|_{t=0} = \frac{\partial \varphi}{\partial t}\Big|_{t=0} = 0, \qquad \varphi_i = H(r_0 - x)F(x+ct). \tag{1.2}$$

The boundary-value conditions in the simplest variant have the form of Dirichlet or Neumann conditions

$$\varphi|_{\partial R} = 0, \quad \frac{\partial \varphi}{\partial n}\Big|_{\partial R} = 0. \tag{1.3}$$

In addition, the solution must satisfy the attenuation condition at infinity.

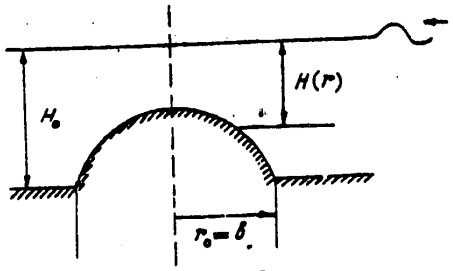

Fig. 2.

After the substitution of $\varphi = \varphi_i + \varphi_s$ into (1.1)-(1.3) we obtain a homogeneous equation relative to φ_s, since φ_i satisfies the wave equation, and inhomogeneous boundary-value conditions, since φ_i is a stipulated function.

Scattered and incident fields in diffraction problems are described in different coordinate systems. Accordingly, one of the fields must be restructured into another coordinate system, which is not a simple problem.

Depending on the properties of the R region, which in diffraction theory is called an inhomogeneity, obstacle, scatterer or diffracting body, it is possible to distinguish three cases: ideally reflecting or translucent body, the field does not enter into the R region; transparent object whose properties are different

from the surrounding medium, but are constant, that is, in the R region are not dependent on space coordinates; an arbitrary inhomogeneity whose properties in the R region are dependent on the space coordinates. In the two latter cases, in addition to the external problem, it is also necessary to solve the internal problem.

The first case includes: absolutely rigid body in an acoustic field, ideally conducting in an electromagnetic field and a vertical cylinder (junction) protruding above the free surface in the field of surface gravitational waves. As an example for the second and third cases we can use an underwater projection with a constant or variable depth (Fig. 2) in the field of surface gravitational waves.

If the function φ is represented in the form of a monochromatic travelling wave

$$\varphi_i = \varphi_0 e^{i(kx+\omega t)}, \quad k = \frac{\omega}{c}, \tag{1.4}$$

we obtain the stationary diffraction problem. It is assumed that $-\infty<t<\infty$. The sought-for function, in accordance with (1.4) can be cited in the form

$$\varphi(x, y, z, t) = \tilde{\varphi}(x, y, z)\, e^{i\omega t}. \tag{1.5}$$

The stationary diffraction problem is formulated on the basis of (1.1), (1.5) in the form of a boundary-value problem for the Helmholtz equation

$$(\nabla^2 + k^2)\,\tilde{\varphi} = 0. \tag{1.6}$$

As before the solution is represented by the sum $\tilde{\varphi} = \tilde{\varphi}_1 + \tilde{\varphi}_3$. The boundary-value conditions are similar for ∂R. In addition, in order to ensure uniqueness of the solution we introduce the radiation condition and the condition of limitation at infinity -- the Sommerfeld conditions. They have the form in three- and two-dimensional cases

$$\lim_{r\to\infty} r\left(\frac{\partial\tilde{\varphi}}{\partial r} - ik\tilde{\varphi}\right) = 0, \quad \lim_{r\to\infty}\sqrt{r}\left(\frac{\partial\tilde{\varphi}}{\partial r} - ik\tilde{\varphi}\right), \quad \lim_{r\to\infty}\tilde{\varphi} = 0. \tag{1.7}$$

2. Formulations of some problems. We will examine an axisymmetric inhomogeneity whose center is matched with the origin of cylindrical (r, θ, z) and spherical (r, θ, φ) coordinate systems: $f = f(r)$, $0 \leqslant r \leqslant r_0$. Outside the inhomogeneity $r > r_0$ the properties of the medium are constant.

A plane monochromatic wave travels from infinity; it partially bypasses the obstacle, is partially reflected and partially passes through the inhomogeneity, being refracted (Fig. 2).

Within the framework of a long-wave approximation, for a wave in water the problem is formulated relative to the velocity potential φ. In the region of variable depth $H = H(r)$ we obtain the differential equation [9]

$$\vec{\nabla}\left[\frac{H(\vec{x})}{H_0}\vec{\nabla}\varphi(\vec{x},t)\right]-\frac{1}{c_0^2}\frac{\partial^2\varphi(\vec{x},t)}{\partial t^2}=0,\quad 0<r\leqslant r_0, \tag{2.1}$$

in the region of constant depth

$$\nabla^2\varphi_2-\frac{1}{c_0^2}\frac{\partial^2\varphi_2}{\partial t^2}=0,\quad r>r_0,\quad c_0^2=gH_0. \tag{2.2}$$

In the case of an acoustic medium we obtain differential equations in the region of variable density $\rho_0 = \rho_0(r)$ [9]

$$\rho_0(\vec{x})\vec{\nabla}\cdot\left[\frac{1}{\rho_0(\vec{x})}\vec{\nabla}p(\vec{x},t)\right]-\frac{1}{c_0^2(\vec{x})}\frac{\partial^2 p(\vec{x},t)}{\partial t^2}=0,\ 0<r\leqslant r_0 \tag{2.3}$$

and in the region of constant density

$$\nabla^2\rho_2-\frac{1}{c_0^2}\frac{\partial^2\rho_2}{\partial t^2}=0,\quad r>r_0. \tag{2.4}$$

The propagation of electromagnetic waves in an inhomogeneous medium is described by the Maxwell equations [9]

$$\vec{\nabla}\times\vec{H}=\vec{j}+\frac{\partial\vec{D}}{\partial t},\quad \vec{\nabla}\cdot\vec{D}=\rho_e,\quad \vec{\nabla}\times\vec{E}=-\frac{\partial\vec{B}}{\partial t},\quad \vec{\nabla}\cdot\vec{B}=0. \tag{2.5}$$

In a general case of an anisotropic medium the vectors $\vec{H}$ and $\vec{B}$, $\vec{E}$ and $\vec{D}$ are non-collinear and are related by the material equations (summing for j)

$$D_i=\varepsilon_{ij}(\vec{x})E_j,\quad B_i=\mu_{ij}(\vec{x})H_j,\quad j_i=\sigma_{ij}(\vec{x})E_j.$$

In the case of plasma inhomogeneities in the atmosphere it is possible to consider an isotropic medium with the following properties: $\varepsilon = \varepsilon(\vec{x})$, μ= const, σ = const. The system of equations (2.5) can be reduced to two hyperbolic "decision" equations in the region of the inhomogeneous medium:

$$\nabla^2\vec{E}-\frac{1}{c^2(\vec{x})}\frac{\partial^2\vec{E}}{\partial t^2}-\vec{\nabla}(\vec{\nabla}\cdot\vec{E})-\mu\sigma\frac{\partial\vec{E}}{\partial t}=0, \tag{2.6}$$

where $c^2(\vec{x}) = 1/\mu\varepsilon(\vec{x})$. $\nabla^2\vec{H}-\frac{1}{c^2(\vec{x})}\frac{\partial^2\vec{H}}{\partial t^2}-\mu\sigma\frac{\partial\vec{H}}{\partial t}+\left[\vec{\nabla}c(\vec{x})\right]\times\frac{\partial\vec{E}}{\partial t}=0,$

In the case of a uniform medium from (2.6) we obtain wave equations relative to $\vec{E}$ and $\vec{H}$.

The formulation of the diffraction problem in each of the cited cases includes: stipulation of the incident field, which we use in the form of a plane, arriving from infinity, traveling wave which in an acoustic case has the form

$$p_i=p_0e^{i(k_2x+\omega t)}=p_0e^{i(k_2r\cos\theta+\omega t)}, \tag{2.7}$$

where $k_2 = \omega/c_0$, θ is the angle between the x-axis and the radius-vector of the moving coordinate; the conditions for the coupling of the sought-for functions and their derivatives at the discontinuity of the homogeneous and inhomogeneous media are stipulated. In the case of a spherical or cylindrical inhomogeneity they have the form

$$p|_{r=r_0} = p_2|_{r=r_0}, \quad \frac{1}{\rho_0(r)}\frac{\partial p}{\partial r}\Big|_{r=r_0} = \frac{\partial p_2}{\partial r}\Big|_{r=r_0}; \tag{2.8}$$

the Sommerfeld radiation conditions (1.7).

In an investigation of waves on water within the framework of a long-wave approximation the coupling conditions for φ are similar to (2.8). For electromagnetic waves at the discontinuity of media we obtain the conditions

$$(\vec{B}^1 - \vec{B}^2)\cdot\vec{n} = 0, \quad (\vec{D}^1 - \vec{D}^2)\cdot\vec{n} = 0,$$
$$(\vec{H}^1 - \vec{H}^2)\times\vec{n} = 0, \quad (\vec{E}^1 - \vec{E}^2)\times\vec{n} = 0. \tag{2.9}$$

3. Precise solutions. In all formulations the problems of diffraction of monochromatic waves are reduced to solution of the Helmholtz equation with variable coefficients. For inhomogeneities with cylindrical and spherical symmetry it is possible to use the method of separation of variables, which leads to an investigation of an ordinary differential equation with variable coefficients. In some special cases this equation allows the formulation of precise solutions.

For example, for the problem of diffraction of acoustic waves (1.7), (2.3), (2.4), (2.7), (2.8) we obtain solutions in the external region $r > r_0$

$$p_2 = p_i + p_s = \sum_{m=0}^{\infty}\left[\varepsilon_m i^m J_m(k_2 r) + a_m H_m^{(2)}(k_2 r)\right]\cos m\theta \tag{3.1}$$

and in the internal region

$$p = \sum_{m=0}^{\infty} b_m R_m(r)\cos m\theta, \tag{3.2}$$

where R_m is a solution of the equation in the region $r \leqslant r_0$;

$$\frac{d^2R_m}{dr^2} + \left[\frac{1}{r} - \frac{\rho_0'(r)}{\rho_0(r)}\right]\frac{dR_m}{dr} + \left[k_0^2(r) - \frac{m^2}{r^2}\right]R_m = 0. \tag{3.3}$$

Here $J_m(\zeta)$ and $H_m^{(2)}(\zeta)$ are cylindrical Bessel and Hankel functions; ε_m and B_m are unknown coefficients which are determined from the coupling conditions (2.8) after the substitution of (3.1) and (3.2) in them. Equation (3.3) allows two classes of precise solutions. With $\rho_0(r) = Ae^{-ar}$, $C_0^2(r) = C_0^2 = \text{const}$, A = const, a = const the solution is expressed in degenerate hypergeometric functions ${}_1F_1(\alpha', \beta, \gamma)$ with $a^2 \neq 4k_0^2$,

$$R_m = r^2\left(\sqrt{a^2 - 4k_0^2}\right)^{m+0,5} e^{-\left(a + \sqrt{a^2-4k_0^2}\right)r/2} \times {}_1F_1\left(m + \frac{1}{2} + \frac{a}{2\sqrt{a^2-4k_0^2}}, 2m+1, \sqrt{a^2-4k_0^2}\right).$$

In the case $a^2 = 4k_0^2$ the solution is written in Weber functions

$$R_m = e^{-ar}\varepsilon_{2m}\left(\sqrt{2ar}\right).$$

For inhomogeneities of the type

$$\rho_0(r) = Ar^{\alpha}, \quad c_0^2(r) = c_0^2 r^{-\alpha}$$

we obtain a solution in Bessel functions $J_\nu(z)$ with $\alpha \neq -2$

$$R_m = r^{\alpha/2} J_\nu\left(\frac{2k_0}{2+\alpha} r^{(2+\alpha)/2}\right), \quad \nu = \sqrt{\alpha^2+4m^2}/(2+\alpha);$$

with $\alpha = -2$

$$R_m = r^{(\mu-2)/2}, \quad \mu = 2\sqrt{1+m^2-k_0^2}.$$

Similar solutions were obtained for the problems of diffraction of surface gravitational waves (1.7), (2.1), (2.2), (2.7), (2.9) [9].

4. Approximate solutions. In the case of arbitrary axisymmetric inhomogeneities which are approximated by power-law polynomials or are stipulated at once in such a form the problems are reduced to solution of an equation in the form

$$x^2 y'' + \left(\sum_{n=0}^{\infty} a_n x^n\right) x y' + \left(\sum_{n=0}^{\infty} \beta_n x^n\right) y = 0. \tag{4.1}$$

We will assume that this equation satisfies the Fuchs theorem [10] ($y = y(x)$; a_n, b_n are known coefficients). According to the method of generalized power series (Frobenius method) the solution is represented in the form of a convergent generalized power series

$$y = x^\nu \sum_{n=0}^{\infty} \alpha_n x^n, \tag{4.2}$$

where the ν and α_n values are determined from the recurrent relationships, which follow from (4.1) after the substitution of (4.2). This method is conveniently used in complex problems, but it is characterized by slow convergence of series in the form (4.2).

The method of approximation of solutions by algebraic polynomials is more effective. These are selected from the condition of a best approximation for the norm in the space of piecewise-continuous functions C.

We will examine an equation with polynomial coefficients $a_0(x)$, $a_1(x)$, $a_2(x)$ [2,3]

$$a_0(x)\, y'' + a_1(x)\, y' + a_2(x) \cdot y = 0$$

and we will assume that the degree of each of the polynomials a_5 does not exceed the number $\ell + 1 - s$. We will demonstrate that it is equivalent to the Volterra equation of the second kind in the interval [a, b]

$$y(x) = \int_a^x \frac{P_\ell(x,\xi)}{a_0^{\ell+1}(x)}\, y(\xi)\, d\xi + \frac{f(x)}{a_0^{\ell+1}(x)}, \tag{4.3}$$

where $a_0^{\ell+1}$ is a polynomial of a degree not higher than $\ell + 1$; $P_\ell(x, \xi)$ is a polynomial in the variables x and ξ not exceeding the number ℓ:

$$P_\ell(x,\xi) = 2a_0'(\xi) - a_1(\xi) + (x-\xi)\left[a_0''(\xi) - a_1'(\xi) + a_2(\xi)\right] = \sum_{i+j\leq\ell} a_{ij} x^i \xi^j;$$

$$f(x) = a_0(a)\,\gamma + (x-a)\left\{ a_0(a)\,\delta + \left[a_1(a) - a_0'(a) \right]\gamma \right\} = f_1 + f_2 x .$$

For finding an approximate solution $y_n(x)$ of the integral equation (4.3) we substitute for it an operator equation in the form

$$a_0^{\ell+1}(x)\, y_n(x) = \int_a^x P_\ell(x,\xi)\, y_n(\xi)\, d\xi + f(x) - \varepsilon_n(x), \tag{4.4}$$

where

$$y_n(x) = \sum_{i=0}^{n} c_i x^i ; \quad a_0^{\ell+1}(x) = \sum_{i=0}^{\ell+1} a_i x^i ;$$

$$\varepsilon_n(x) = \sum_{i=1}^{\ell+1} \tau_{n+i}\, T_{n+i}\left(\frac{x-a}{\beta-a}\right); \quad T_{n+i}\left(\frac{x-a}{\beta-a}\right) = \sum_{j=0}^{n+i} \theta_j^{(n+i)} x^j .$$

Here $T_k(\zeta)$ are Chebyshev polynomials; τ_{n+i} are auxiliary parameters.

Equating the coefficients with identical powers of x, we obtain a system of $n + \ell + 2$ linear algebraic equations for determining the coefficients c_i and τ_{n+i}. For evaluating the deviation of the approximate solution $y_n(x)$ of the equation from the precise solution the following is correct:

$$\left| y(x) - y_n(x) \right| \leq \frac{1}{c_1}\left(\sum_{i=1}^{\ell+1} \left| \tau_{n+i} \right| \right) e^{\int_0^x \left| \frac{P_\ell(x,\xi)}{a_0(x)} \right| d\xi} ,$$

where

$$c_1 = \min_{x \in [a,\beta]} a_0(x) .$$

The indicated method was tested in test problems and was applied to solution of a number of wave diffraction problems [1, 13].

We will examine the problem of diffraction of surface gravitational waves on an axisymmetric obstacle of variable depth H(r), $0 \leqslant r \leqslant b$ (Fig. 2), which we will represent in the form of a polynomial of the degree N

$$H(r) = \sum_{n=0}^{N} h_n r^n .$$

Incident on the obstacle is a wave having the velocity potential

$$\varphi_i = A\, e^{i(k_2 r \cos\theta + \omega t)} .$$

The velocity potential φ in the region of variable depth $0 \leqslant r \leqslant b$ satisfies the equation (long-wave approximation)

$$\frac{\partial^2\varphi}{\partial r^2}+\left[\frac{1}{r}+\frac{H'(r)}{H(r)}\right]\frac{\partial\varphi}{\partial r}+\frac{1}{r^2}\frac{\partial^2\varphi}{\partial\theta^2}+\frac{k_2^2}{H(r)}\varphi=0. \tag{4.5}$$

In the outer region $r>b$, where the fluid depth is constant, we obtain

$$\frac{\partial^2\varphi_2}{\partial r^2}+\frac{1}{r}\frac{\partial\varphi_2}{\partial r}+\frac{1}{r^2}\frac{\partial\varphi_2}{\partial\theta^2}+k_2^2\varphi_2=0. \tag{4.6}$$

The solutions are joined together using the coupling conditions

$$\varphi\big|_{r=b}=\varphi_2\big|_{r=b},\quad \frac{\partial\varphi}{\partial r}\Big|_{r=b}=\frac{\partial\varphi_2}{\partial r}\Big|_{r=b}. \tag{4.7}$$

We will break down the region of variable depth into two regions. In the region $0\leqslant r<a$, where a is the minimum (in absolute value) root of the polynomial H(r), the velocity potential φ_1 satisfies the equation (4.5) and a solution can be obtained by the method of generalized power series or by some other method.

In the region $a\leqslant r\leqslant b$ the velocity potential also satisfies equation (4.5), but the polynomial H(r) has a complex root, in absolute value less than b. In the region $r>b$ the velocity potential φ_2 satisfies equation (4.6).

The solution of equation (4.5) in the region $0\leqslant r<a$ is written in the form of a series

$$\varphi_1=\sum_{m=0}^{\infty}\beta_m R_m^1(r)\cos m\theta,\quad R_m^1(r)=r^m\sum_{s=0}^{\infty}\alpha_s r^s. \tag{4.8}$$

The solution in the region $a\leqslant r\leqslant b$ is obtained by the method of approximation by polynomials. From (4.5), after separation of variables, we obtain an equation of the type

$$H(x)x^2y''+\left[H(x)x+x^2H'(x)\right]y'+\left[k_2^2x^2-m^2H(x)\right]y=0. \tag{4.9}$$

Since in equation (4.4) ℓ is such a minimum whole number that with all s = 0, 1, 2 the degree of each of the polynomials $a_s(x)$ does not exceed the number $\ell+1-3$, we find $\ell=N+1$. In this case

$$P_{N+1}(x,\xi)=q_1\xi+q_2\xi+q_3\xi^2+q_{21}\xi x+\ldots+q_{2N+1}\xi^{N+1}+q_{2N+2}\xi^N, \tag{4.10}$$

$$q_{2k-1}=\begin{cases}h_{k-1}\left[2(k+1)-m^2\right], & k=1,2,4,\ldots,N+1,\\ h_2\left(3-m^2+k_2^2\right), & k=3,\end{cases} \tag{4.11}$$

$$q_{2(k+1)}=\begin{cases}h_k\left(1+k-m^2\right), & k=0,1,3,4,\ldots,N,\\ -h_2\left(3+k_2^2-m^2\right), & k=2,\end{cases}$$

$$f(x)=f_1+f_2x,\quad f_1=2H(a)a^2\gamma-H(a)a^3\delta,$$

$$f_2=H(a)a^2\delta-H(a)a\gamma.$$

The integral equation corresponding to (4.9) and the parameters entering into it have the form (4.4) with the replacement $\ell = N + 1$ and

$$a_0^{N+2}(x) = \sum_{i=0}^{N} h_i x^{i+2}.$$

Taking into account (4.10), (4.11) and the expressions for $y_n(x)$, $a_0^{N+2}(x)$, $\varepsilon_n(x)$ from the above equation we obtain a system of $n + N + 3$ linear algebraic equations for determining the coefficients c_i and the auxiliary parameters τ_{n+1}

$$\sum_{i=0}^{N} c_i \sum_{j=0}^{N} q_{2j+k+1} \frac{a^{i+j+2-k}}{i+j+2-k} + \sum_{i=1}^{N+2} \tau_{n+i} \theta_k^{(n+i)} = f_{1+k}, \quad k=0,1; \tag{4.12}$$

$$\sum_{i=\max(0,k-n-2)}^{\min(k-2,N)} c_{k-2-i} \left[h_i - \frac{q_{2i+1}}{k} - \frac{q_{2i+2}}{k-1} \right] + \sum_{i=\max(1,k-n)}^{N+2} \tau_{n+1} \theta_k^{(n+i)} = 0,$$

$$k = 2, 3, \ldots, n+1.$$

The final solution in the region $a \leqslant r \leqslant b$ has the form

$$\varphi = \sum_{m=0}^{\infty} \left[\gamma_m \cdot y_{n1}(r) + \delta_m y_{n2}(r) \right] \cos m\theta. \tag{4.13}$$

In the region $r > b$ we obtain the solution

$$\varphi_2 = \sum_{m=0}^{\infty} a_m \cdot H_m^{(2)}(k_2 r) \cos m\theta. \tag{4.14}$$

After substitution of the solutions (4.8), (4.13) and (4.14) into coupling conditions of the type (4.7) at two discontinuities we obtain a system of linear algebraic equations relative to the unknown coefficients a_m, b_m, γ_m, δ_m.

On the basis of the derived precise and approximate solutions we analyzed the influence of the degree of the determined inhomogeneity on the directional diagram. and the scattering cross sections of acoustic, electromagnetic and surface gravitational waves [9]. Figure 3 shows an example of the total scattering cross section Q in dependence on wave number $k_2 = 2\pi/\ell$ for a cylindrical density inhomogeneity $\rho_0(r) = \rho_c + (1 - \rho_c)r^2$, $\rho_c = 3/2$ in an acoustic medium. At the boundary of the contact with the external medium $r = 1$ and $\rho_0 = 1$, at the center of the inhomogeneity $r = 0$ and $\rho_0 = \rho_c = 3/2$.

In Fig. 4 similar results are given for the scattering of electromagnetic waves by an inhomogeneity of the dielectric constant ε, also changing. The cited cross sections reveal extrema, which is of great interest for an analysis of the influence of inhomogeneities on wave propagation. From a comparison of solutions for the averaged constant inhomogeneity (ρ_0 or ε = const) and a real inhomogeneity

$\rho_0(r)$ or $\varepsilon(r)$ it can be seen that a real inhomogeneity is characterized by lesser total cross sections and can generate local resonances.

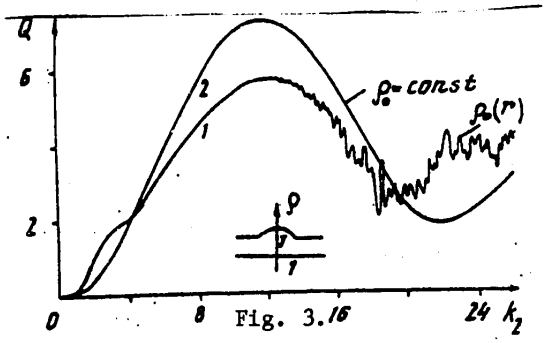

Fig. 3.

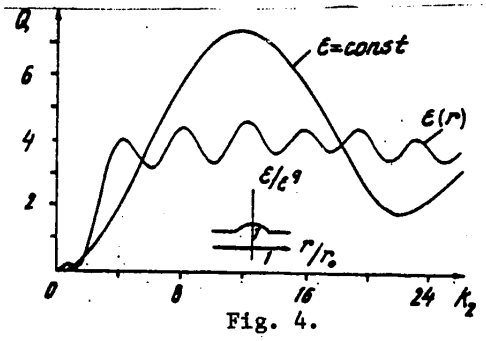

Fig. 4.

We note in conclusion that the characteristics of scattering of waves by inhomogeneities near a plane boundary (in a semibounded region) can be obtained by the images method in the form of the sum of multiply scattered fields [5,6]. We also note that for solution of problems of nonstationary wave defraction a method based on the analytical derivation of a precise solution in the space of Laplacian time images and with numerical transformation to the original is effective [7].

BIBLIOGRAPHY

1. Veselaya, O. G. and Yakovlev, V. V., "Approximation of Solution of Problems in the Diffraction of Surface Gravitational Waves on an Axisymmetric Obstacle by Polynomials," GIDROMEKHANIKA (Hydromechanics), 39, pp 51-57, 1979.

2. Dzyadyk, V. K., "Approximate Method for Approximating Solutions of Series of Linear Differential Equations by Algebraic Polynomials," IZV. AN SSSR: SER. MAT. (News of the USSR Academy of Sciences: Mathematical Series), 38, No 4, pp 937-967, 1974.

3. Dzyadyk, V. K., "Application of Linear Operators to an Approximate Solution of Ordinary Differential Equations," VOPROSY TEORII PRIBLIZHENIYA FUNKTSIY I IKH PRILOZHENIYE (Problems in the Theory of Approximation of Functions and Their Application), Kiev, pp 61-96, 1976.

4. Dotsenko, S. F. and Cherkesov, L. V., "Diffraction of a Surface Gravitational Wave on a Small Irregularity on the Bottom," PMM (Applied Mathematics and Mechanics), 43, No 4, pp 639-646, 1979.

5. Selezov, I. T., "Diffraction of Waves on Convex Bodies in Semibounded Regions," PRIKL. MEKHANIKA (Applied Mechanics), 6, No 3, pp 38-46, 1970.

6. Selezov, I. T. and Krivonos, Yu. G., "Scattering of Acoustic Waves on a Cylinder in a Semibounded Region," GIDROMEKHANIKA, No 15, pp 99-106, 1969.

7. Selezov, I. T. and Tkachenko, V. A., "Investigation of Unsteady Waves by the Method of Numerical Inversion of the Laplace Transform," TEORIYA DIFRAKTSII I RASPROSTRANENIYA VOLN. 7-y VSESOYUZNYY SIMPOZIUM PO DIFRAKTSII I RASPROSTRANENIYU VOLN (Theory of Wave Diffraction and Propagation. Seventh All-Union Symposium on Wave Diffraction and Propagation), Vol 3, Moscow, AN SSSR, pp 133-136, 1977.

8. Selezov, I. T. and Yakovlev, V. V., "Some Problems in the Diffraction of Plane Waves on a Cylinder With a Variable Density," AKUST. ZHUR. (Acoustics Journal), 23, No 6, pp 85-92, 1977.

9. Selezov, I. T. and Yakovlev, V. V., DIFRAKTSIYA VOLN NA SIMMETRICHNYKH NEODNORODNOSTYAKH (Wave Diffraction on Symmetric Inhomogeneities), Kiev, "Naukova Dumka," 1978, 146 pages.

10. Trikomi, F., DIFFERENTSIAL'NYYE URAVNENIYA (Differential Equations), Moscow, IL, 1962, 352 pages.

11. Cherkesov, L. V., POVERKHNOSTNYYE I VNUTRENNIYE VOLNY (Surface and Internal Waves), Kiev, "Naukova Dumka," 1973, 248 pages.

12. Cherkesov, L. V., GIDRODINAMIKA POVERKHNOSTNYKH I VNUTRENNIKH VOLN (Hydrodynamics of Surface and Internal Waves), Kiev, "Naukova Dumka," 1976, 364 pages.

13. Yakovlev, V. V., "Approximation of Solution of the Problem of Wave Diffraction on an Arbitrary Inhomogeneity by Polynomials," PRIKL. MEKHANIKA (Applied Mechanics), 13, No 2, pp 40-47, 1976.

14. Garrison, C. J. and Rao, V. S., "Interaction of Waves With Submerged Objects," J. WATERW. HARBORS AND COAST ENG. DIV. PROC. AMER. SOC. CIV. ENG., 97, No 2, pp 259-277, 1971.

15. Mei, Ch. C., "Numerical Methods in Water-Wave Diffraction and Radiation," ANNUAL REVIEW OF FLUID MECHANICS, Vol 10, pp 393-416, 1978.

NONSTATIONARY THREE-DIMENSIONAL WAVES IN A FLOW OF HOMOGENEOUS FLUID WITH VELOCITY SHEAR

Sevastopol' TEORETICHESKIYE I EKSPERIMENTAL'NYYE ISSLEDOVANIYA POVERKHNOSTNYKH I VNUTRENNIKH VOLN in Russian 1980 (manuscript received 28 Feb 80) pp 19-26

[Article by A. M. Suvorov, A. N. Tananayev and L. V. Cherkesov]

[Text]

Abstract: An analysis of the amplitude characteristics of a three-dimensional wave trace caused by a region of atmospheric pressure disturbances is given within the framework of linear theory. The current velocity gradient is assumed to be constant with depth and the fluid is assumed to be homogeneous.

In [1] the authors gave an asymptotic analysis of the pattern of development of three-dimensional surface waves and numerical methods were employed in studying the dependence of limiting angles of the wave trace, phase portraits and velocities of propagation of the leading edges of transverse and longitudinal waves on current velocity shear. Current velocity was assumed to be a linear function of depth ($U(z) = U_1 + a(z + H)$). The wave-forming effect of a ship was replaced by a region of normal stresses moving at a constant velocity. In this article we give an investigation of the amplitude characteristics of wave movement.

The expression for deviation of the free surface of the fluid from an undisturbed position in a coordinate system related to a moving region of normal stresses has the form [1]

$$\zeta = \frac{p_0}{4\pi^2\rho} \operatorname{Re} \int_0^{\infty} \int_{-\pi/2}^{3\pi/2} \frac{r^2 F(\beta, r) \operatorname{th} rH}{\delta \Delta} \left(1 - e^{-i\Delta t}\right) e^{irR\cos(\theta-\beta)} d\theta dr, \qquad (1)$$

where

$$\delta = \left(\delta_1^2 + gr \operatorname{th} rH\right)^{1/2}; \quad \delta_1 = 0{,}5\, a\cos\theta \operatorname{th} rH; \quad \Delta = rU_2\cos\theta - \delta_1 - \delta;$$

$$x = R\cos\gamma; \quad y = R\sin\gamma; \quad m = r\cos\theta; \quad n = r\sin\theta;$$

$$U_2 = U_1 + V + \Delta u; \quad \Delta u = aH;$$

$\overline{f}(\theta, r)$ is the Fourier transform of a function even relative to x and y, describing the form of the imparted disturbance; V is the velocity of movement of a spatially localized region of normal stresses. Due to the symmetry of z relative to y we will limit ourselves to an investigation of the wave trace in the half-plane $0<\gamma<\pi$.

The integrand in (1) has a pole with respect to θ at the points

$$\cos^2\theta = \frac{g\,\mathrm{th}\,rH}{U_2\left(rU_2 - a\,\mathrm{th}\,rH\right)}. \tag{2}$$

Analyzing then the internal integral with respect to θ by the methods of the theory of residues [1, 2], we obtain

$$\zeta = -\frac{\rho_0}{2\pi\rho} I_m \int_0^\infty \chi(r)\xi(r) e^{iRN(r,\gamma)} dr + O(R^{-1}), \quad 0<\gamma<\frac{\pi}{2}, \tag{3}$$

$$\xi(r) = \frac{r f(\theta_1, r)}{\sqrt{g}\sqrt{\frac{U_2\left(rU_2 - a\,\mathrm{th}\,rH\right)}{\mathrm{th}\,rH} - g}}; \quad N = r\cos(\theta_1 - \gamma);$$

θ_1 is a root of equation (2); $-\pi/2 < \theta_1 < 0$; $\chi(r) = 0$ for the r value, satisfying the inequalities

$$g\,\mathrm{th}\,rH > V_2\left(rU_2 - a\,\mathrm{th}\,rH\right) > 0, \quad v < v_1;$$

$\chi(r) = 1$ for the remaining r values from the integration interval;

$$v = tR^{-1}U_2; \quad v_1 = \frac{rU_2 - 0{,}5\,a\,\mathrm{th}\,rH}{rU_2 - a\,\mathrm{th}\,rH}(\cos\gamma - \mathrm{ctg}\,\theta_1 \sin\gamma).$$

For computing the integral (3) from the rapidly oscillating function we use the method described in [3]. Here the integral

$$J = \int_0^1 F(z) e^{iR\varphi(z)} dz,$$

where R is a large real parameter; F(z), $\varphi(z)$ are functions continuous together with their derivatives to the third degree, represented in the following way:

$$J = h\sum_{k=0}^{N-1} e^{iR\ell_k} \int_0^1 F(zh + kh)\, e^{iR(p_k z^2 + q_k z)} dz, \tag{4}$$

where N is the number of regions into which the integration segment is broken down [0,1]: $h = N^{-1}$; $\varphi(z) = p_k z^2 + q_k z + \ell_k$ for [kh, (k + 1)h]. The quadrature formula for the integral (4) has the form

$$\int_0^1 F_k e^{iR(p_k z^2 + q_k z)} dz \approx C_1(p_k, q_k) F_k(0) + C_2(p_k, q_k) F_k\left(\frac{1}{2}\right) + C_3(p_k, q_k) F_k(1) \tag{5}$$

where the coefficients $C_s(p_k, q_k)$ (s = 1, 2, 3) are found from the expressions cited in [3].

In computing the integral (3) the upper finite limit was replaced by a finite value which together with the h value was selected on the basis of adjustment computations. The integration segment [a, b] with $a \neq b$ was reduced to [0, 1] by the substitution $r = a + (b - a)z$.

All the computations of the form of the sea surface were made for a disturbance in the form

$$f(x, y) = \exp\left[-\left(\beta x^2 + cy^2\right)\right],$$

approximately modeling the wave-forming effect of moving surface ships. The parameters of the problem were selected as follows: H = 20 m, q = 9.81 $m \cdot sec^{-2}$, U_2 = 13.2 $m \cdot sec^{-1}$, ρ 1024 $kg \cdot m^{-3}$, B = 0.005 m^{-2}, c = 0.03 m^{-2}, $p_0 = 2 \cdot 10^4$ Pa. All the results of computations of wave profiles cited below can also be used for other p_0 values with the introduction of a constant conversion factor since p_0 is the amplitude factor in expression (3).

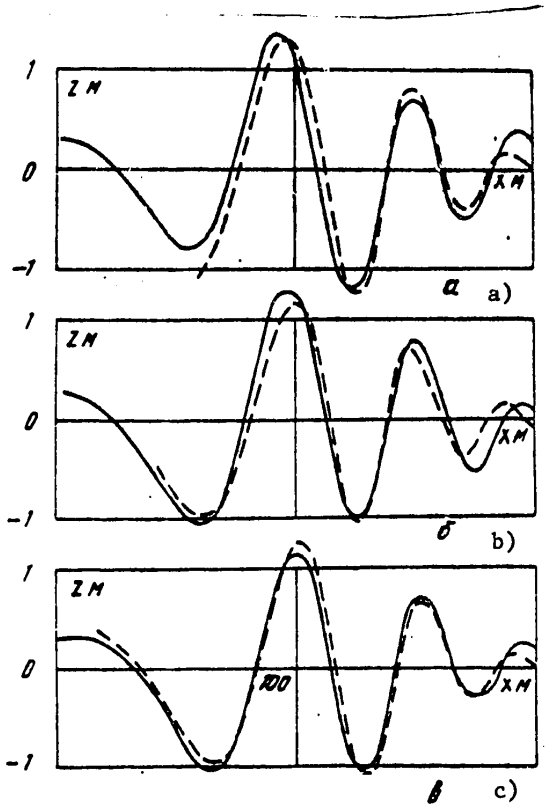

Fig. 1.

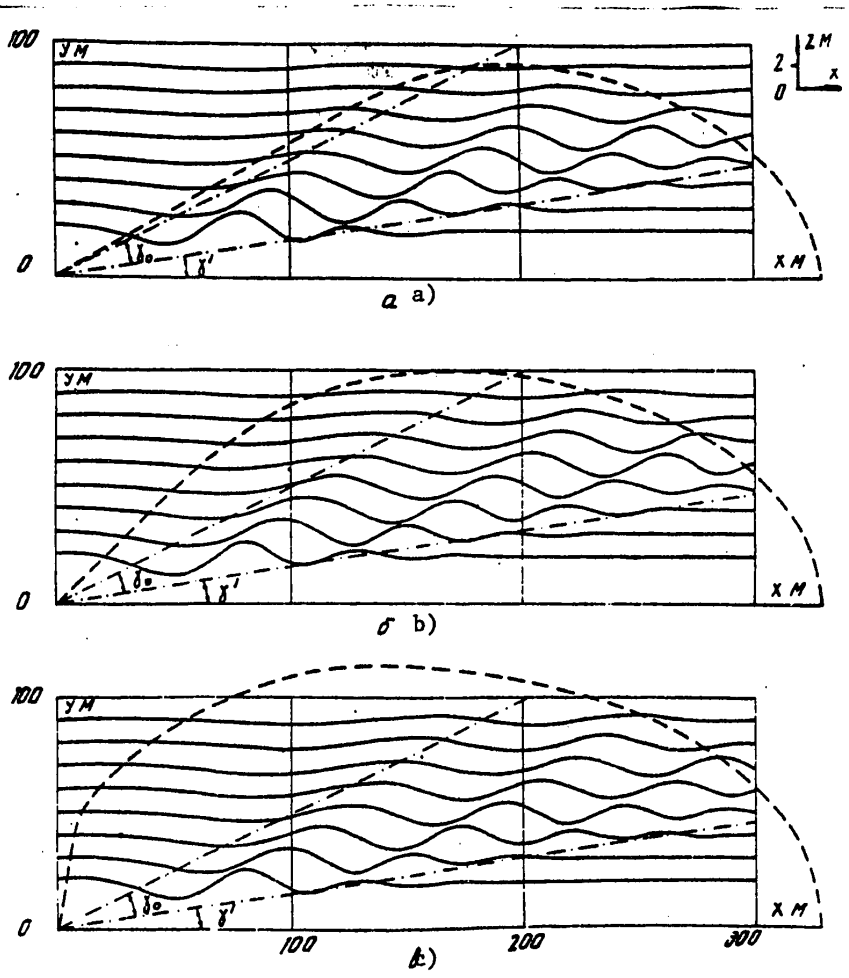

Fig. 2.

Figure 1 shows profiles of the wave-covered sea surface for y = 30 m, t = 25 sec and three values of the current velocity shear

$$a - \Delta u = 2\ \text{m}\cdot\text{sec}^{-1},$$
$$\delta - \Delta u = 0,\ B - \Delta u = -2\ \text{m}\cdot\text{sec}^{-1}.$$

The solid curves were constructed using formula (3); the dashed curves were constructed using the asymptotic expressions (2.3), (2.4) in [1], obtained from (3) by the stationary phase method. In the middle part of all three figures the sea surface profiles described by the integral and asymptotes are virtually the same. At the beginning and end of the profiles the differences in the form of the sea surface increase. This result is attributable to the fact that in these regions we find the boundaries of the limiting angles of the wave trace and the leading edges of the

developing ship waves (Fig. 2 [1]), in whose neighborhood asymptotic behavior of the type (2.3), (2.4) is not applicable.

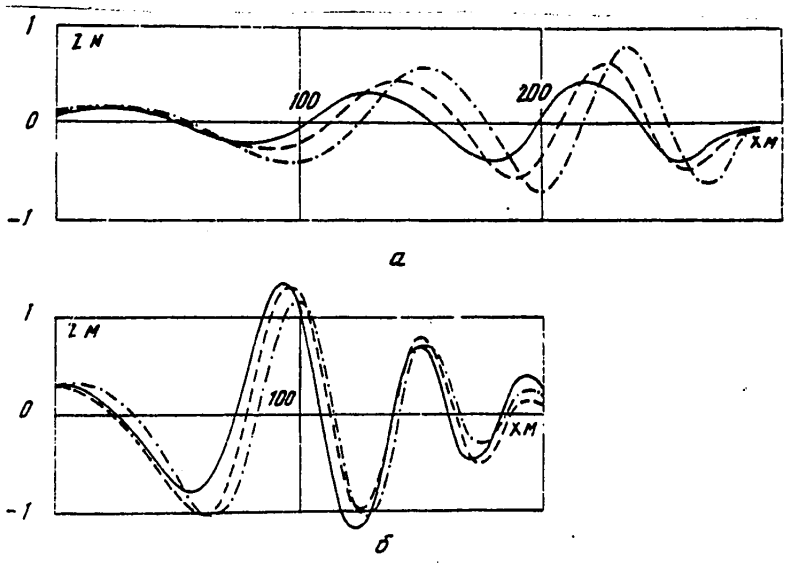

Fig. 3.

Figure 2,a,b,c gives some idea concerning the form of the sea surface for a section along $y = (20 + 10\ell)$ m, $\ell = 0, 1, \ldots, 7$, $t = 25$ sec and the same current velocity shears as in Fig. 1,a,b,c. The scale along the z-axis is localized in the upper part of the figure at the right; the computations for Figures 2, 3, 4 were made using expression (3). The dashed curves show the regions of localization of the wave trace constructed using the asymptotic expressions from [1]; the dot-dash curves represent visually discriminated sectors with an angle γ_0 in which the main wave disturbances are actually concentrated. The asymptotes give exaggerated values of the area of regions in which the main wave disturbances are situated (Fig. 2,b for $\Delta u = 0$ and 2,c for $\Delta u = -2$ m·sec^{-1}); the positioning of the sector with the angle γ_0 relative to the horizontal x-axis and the value of the γ_0 angle are virtually not dependent on the current velocity shear (in all three cases $\gamma_0 \approx 18$, $\gamma'_0 \approx 9°$).

Figure 3 illustrates profiles of the sea surface with $t = 25$ sec, $y = 80$ m (Fig. 3,a), $y = 30$ m (Fig. 3,b) and different values of the current velocity shear: $\Delta u = 2$ m·sec^{-1} -- solid curves, $\Delta u = 0$ -- dashed curves and $\Delta u = -2$ m·sec^{-1} -- dot-dash curves. It can be seen that an increase in the difference in current velocities $\Delta u = -2 - 2$ m·sec^{-1} leads to a displacement of the wave crests in the direction of lesser values of the horizontal coordinate x. The height of the two most positive crests for the profile for $y = 80$ m decreases by approximately a factor of 1.8-2; the height of the most positive crest for $y = 30$ m increases insignificantly.

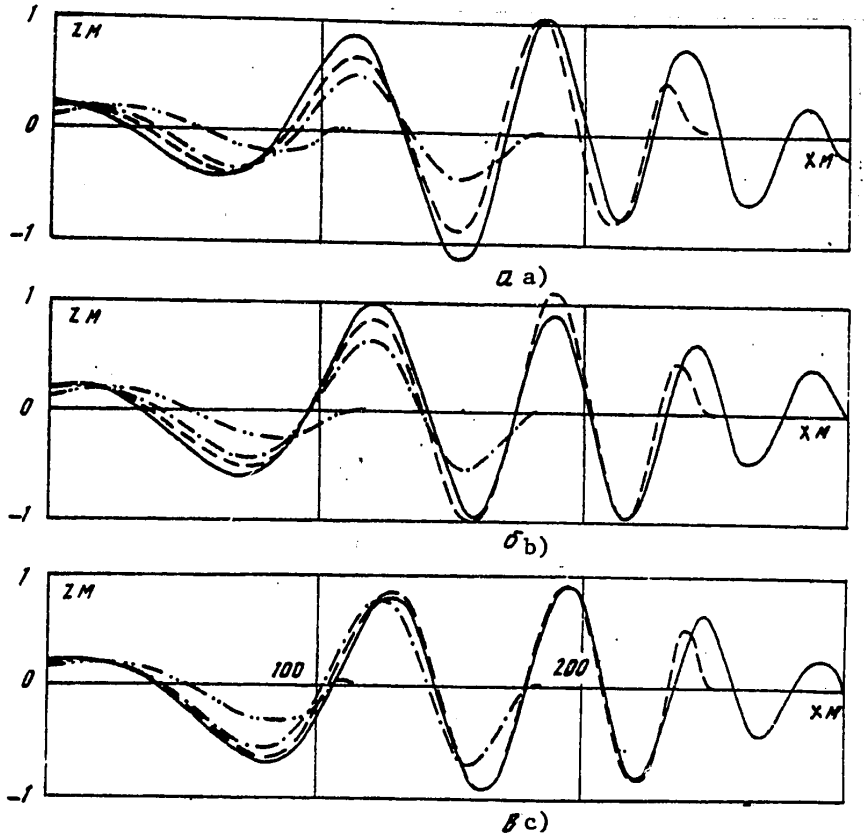

Fig. 4.

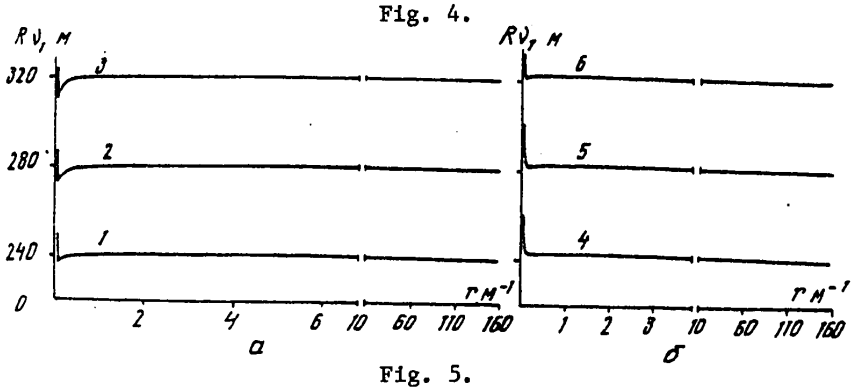

Fig. 5.

Figure 4,a,b,c shows profiles of the sea surface for y = 50 m, illustrating the process of development of the wave pattern for different moments in time after onset of operation of the source of disturbances: t = 10 sec -- dot-dash curves with two

points, t = 15 sec -- dot-dash curves with one point, t = 20 sec -- dashed curves and t = 50 sec -- solid curves. One of the interesting features of these results is a more rapid arrival of the wave disturbances in a stationary regime for $\Delta u = -2$ m·sec^{-1} in comparison with the cases $\Delta u = 0$ and 2 m·sec^{-1}. Thus, with a change in t from 10 to 20 sec the height of the positive crest falling in the region of values of the horizontal coordinate x somewhat exceeding 100 m really changes very little for $\Delta u = -2$ m·sec^{-1}; for $\Delta u = 0$ and 2 m·sec^{-1} it increases by a factor of approximately 1.6-1.7. This fact is also illustrated by the table, in which for y = 50 m and three current velocity shear values Δu we have given the values of sea surface deviation from a horizontal level.

Table 1

Δu = 2 м·с$^{-1}$				Δu = 0				Δu = -2 м·с$^{-1}$ м·sec^{-1}			
t, с / x, м	25	50	100	t, с / x, м	25	50	100	t, с / x, м	25	50	100
112	0,73	0,83	0,87	122	0,90	0,97	0,99	128	0,84	0,80	0,80
153	-1,05	-1,16	-1,19	160	-1,03	-0,91	-0,88	164	-0,88	-0,94	-0,94
186	1,15	1,07	1,03	191	0,94	0,88	0,89	195	0,93	0,92	0,92
215	-1,01	-0,77	-0,75	219	-0,78	-0,95	-0,99	222	-0,85	-0,81	-0,81

It was noted in [1], with transformation from a double integral (1.8) for θ and r to a single integral (1.9) for r with integration limits from r_1 to $+\infty$, that (1.9) is correct in the region of ν_1 values in which the inverse function $r(\nu_1)$ is unambiguous. Here r_1 is a root of the equation $\nu = \nu_1$. We will examine this in greater detail.

A numerical analysis of the $\nu_1(r)$ function in the range of parameters of the problem for which computations were carried out in [1] indicated that for $\Delta u = 0$ and 2 m·sec^{-1} it decreases monotonically, with $\lim_{r\to\infty} R\,\nu_1(r) = x$. Accordingly, the inverse function will be monotonic and unambiguous. Curves of the $R\,\nu_1(r)$ function in the region of its determination for $\Delta u = -2$ m·sec^{-1} and two y values are represented in Fig. 5,a (y = 4 m) and Fig. 5,b (y = 12 m). Here $R = \sqrt{x^2 + y^2}$ is not dependent on r. Curves 1-3, 5 and 6 have a local minimum for small r values and a less conspicuous local maximum in the case of greater r values. The value of the function at the point of the local maximum r^* satisfied the condition $R\,\nu_1(r^*) > x$, $\lim_{r\to\infty} R\,\nu_1(r) = x$. Curve 4 is a monotonic function of r.

The values of the variable r which is used in integration in the single integral must satisfy the condition $\nu > \nu_1$. Then in the case of a monotonic function $R\,\nu_1(r)$ the integration interval assumes the form $[\tau_1, +\infty]$. For the function $R\,\nu_1(r)$ with a local maximum there can be a variant in which the integration interval is broken down into two parts $[r_1, r_2] \cup [r_3 + \infty]$, where r_2, r_3 are roots of the equation $\nu = \nu_1$. This fact must be taken into account in a numerical analysis of the single integral and in its computation by the stationary phase method since it is not excluded that the stationary points can fall in the interval $[r_2, r_3]$.

Summary

a) It has been established that for all the current velocity shear values used in the computations the sea surface profiles constructed on the basis of asymptotic formulas and using a more precise integral expression for all practical purposes differ little from one another within the region delimited by the horizontal x-axis, the leading edges of the developing waves and the boundaries of the limiting angles. In the neighborhood of the region boundaries there are significant differences in the form of the profiles.
b) The main wave disturbances are concentrated in the sector between the rays drawn at the angles ~ 9 and $\sim 27^\circ$ to the x-axis.
c) The arrival of the wave disturbances in a stationary regime occurs more rapidly for negative values of the current velocity shear.

BIBLIOGRAPHY

1. Suvorov, A. M., Tananayev, A. N. and Cherkesov, L. V., "Nonstationary Three-Dimensional Waves in a Flow of a Homogeneous Fluid With a Velocity Shear," POVERKHNOSTNYYE I VNUTRENNIYE VOLNY (Surface and Internal Waves), Sevastopol', Izd. MGI AN Ukrainskoy SSR, pp 14-21, 1979.

2. Cherkesov, L. V., NEUSTANOVIVSHIYESYA VOLNY (Unsteady Waves), Kiev, "Nauka Dumka," 1970, 198 pages.

3. Zhileykin, Ya. M. and Kukarkin, A. B., "Computation of Integrals of Rapidly Oscillating Functions," VYCHISLITEL'NYYE METODY I PROGRAMMIROVANIYE (Computation Methods and Programming), Moscow, MGU, 1977.

EFFECT OF CURRENT VELOCITY SHEAR ON AMPLITUDES OF WAVES GENERATED IN HOMOGENEOUS FLUID BY MOVING PRESSURE REGION

Sevastopol' TEORETICHESKIYE I EKSPERIMENTAL'NYYE ISSLEDOVANIYA POVERKHNOSTNYKH I VNUTRENNIKH VOLN in Russian (manuscript received 19 Jun 80) pp 27-35

[Article by V. F. Sannikov and L. V. Cherkesov]

[Text]

Abstract: A study was made of the influence of current velocity shear on the amplitudes of waves generated by surface pressure disturbances moving uniformly and linearly. It is demonstrated that the shear of the transverse velocity component exerts a considerable influence on the phase configuration of the wave trace and increases the maximum surface rises of the fluid. The influence of current velocity shear is most conspicuous with small velocities of movement of the disturbance.

The waves forming during the movement of pressures along the surface of a homogeneous fluid have been studied quite completely. The author of [6] for the first time proposed a theory which describes the types of crests in a system of waves forming on the surface of deep water during movement of a point pressure disturbance with a constant velocity. Then this theory was developed for a fluid of finite depth [6]. In [1] a study was made of the development of waves arising during movement of a region of surface pressures from a state of rest in a deep fluid of finite depth.

The study of spatial waves generated by surface pressures in flows with a current velocity variable in depth began relatively recently. Steady waves in a fluid with a current velocity profile which is linear and constant in direction were examined in [7], and unsteady waves were examined in [2]. The influence of a change in current velocity and its direction with depth on the structure and geometry of the wave trace was investigated in [3]. It was found that allowance for the vertical inhomogeneity of a current leads to some qualitatively new effects in the system of waves arising beyond the region of pressures. In the case of great current velocity drops with depth even in a plane flow the structure of the wave trace differs substantially from the well-known ship waves and as a result of change in the

direction of current velocity with depth at the surface of the fluid the wave trace is deformed in a definite way and becomes asymmetric. This article represents a continuation of the investigations begun earlier in [3]. A study is made of the influence of current velocity shear on the amplitudes of waves generated by atmospheric pressures moving linearly and uniformly relative to the surface of a fluid. It is postulated that the current velocity components change linearly with depth.

1. Assume that $\vec{v}_0 = (u_0, v_0, 0)$ is the velocity of the undisturbed flow of a fluid of the depth H; u_0 and v_0 are linear functions of the vertical coordinate z. As a convenience we will assume that $\vec{v}_0(z)$ is the sum of current velocity and the velocity of pressure movement. The coordinate system was selected in such a way that its origin was situated on the undisturbed free surface, the z-axis is directed vertically upward and the direction of the $\vec{v}_0(0)$ vector coincides with the positive direction of the Ox-axis. A pressure in the form

$$p = -p_0 f(x, y). \tag{1}$$

is imparted to the free surface.

In [3] a solution was obtained for ζ -- rises of the free surface in the form of double, single integrals and asymptotic formulas not containing integrals. In the investigation of the dependence of wave amplitudes on the current parameters the computations were made using formulas containing single integrals. The computation of double integrals requires great expenditures of computer time and the asymptotic formulas not containing integrals are not uniformly suitable. In addition, it was assumed that the time elapsing from the onset of pressures (1) is quite great and movement can be considered steady. Computations of the rise of the free surface were made using the formula

$$\zeta = \frac{p_0}{\rho H c^2 \varkappa} \sum_{m=1}^{2} \int_{r_0}^{\infty} r \bar{f}\left(\frac{r\cos\theta_m}{H}, \frac{r\sin\theta_m}{H}\right) \frac{\sin\left[r(x_1\cos\theta_m + y_1\sin\theta_m)\right]}{\sqrt{\beta^2 - 1 - a + \varkappa^{-1} r \operatorname{cth} r}} \chi_m \, dr + O(R^{-1}) \tag{2}$$

where ρ is fluid density

$$c = u_0(0); \quad \varkappa = gHc^{-2}; \quad a = (c\varkappa)^{-1}\frac{d}{dz}u_0; \qquad \beta = (2c\varkappa)^{-1}\frac{d}{dz}v_0;$$

g is the acceleration of gravity; $x_1 = x/H$; $y_1 = y/H$; $R = \sqrt{x_1^2 + y_1^2}$; $\bar{f}$ is a Fourier transform of the function f(x,y);

$$\theta_m = \operatorname{arctg}\left[-\beta + (-1)^m \sqrt{\beta^2 - 1 - a + \varkappa^{-1} r \operatorname{cth} r}\right];$$

r_0 is the minimum of all $r \geqslant 0$ for which the integrand in (2) is nonnegative; $\chi_m = 1$, if $(-1)^m(\sin\theta_m x_1 - \cos\theta_m y_1) > 0$ and $\chi_m = 0$ in the opposite case. The computations were made for the function

$$f(x, y) = \frac{1}{2\pi a_1 \beta_1} \exp\left[-\frac{x^2}{2a_1^2} - \frac{y^2}{2\beta_1^2}\right], \quad \bar{f}(\mu, \nu) = \frac{1}{2\pi} \exp\left[-\frac{1}{2}(a_1\mu)^2 - \frac{1}{2}(\beta_1\nu)^2\right]. \tag{3}$$

The integrals (2) have the following characteristics which must be taken into account in the computations: infinite upper limit, the integrand can be unlimited with $r = r_0$ and rapidly oscillate with large x_1 and y_1 values. We will first evaluate the residual term of the integral, rejectable with replacement of the infinite

upper limit by a finite interval

$$\left|\int_{r_2}^{\infty} rf\,\frac{\cos[r(x_1\cos\theta_m + y_1\sin\theta_m)]}{\sqrt{\beta^2 - 1 - a + \varkappa^{-1} r\,\mathrm{cth}\,r}}\,\chi_m\,dr\right| \leqslant \frac{1}{\sqrt{\beta^2 - 1 - a + \varkappa^{-1} r_2\,\mathrm{cth}\,r_2}}\int_{r_2}^{\infty} rf\,dr \leqslant \tag{4}$$

$$\leqslant \frac{1}{2\pi\sqrt{\beta^2 - 1 - a + \varkappa^{-1} r_2\,\mathrm{cth}\,r_2}}\cdot\frac{e^{-0{,}5\,a_2^2 r_2^2}}{a_2^2},$$

where $a_2 = \max(a_1, b_1)/H$. Selecting the upper limit r_2 adequately large, it is possible to make expression (4) as small as desired. The singularity of the integrand at the point $r = r_0$ is eliminated by the substitution $r = r_0 + u^2$. The computation of the integrals (2) in the case of high x_1 and y_1 values requires the use of quadrature formulas of the Philon type [4] or a great number of nodes in the Gauss or Simpson formulas. With the use of the last integrals (2) it is possible for different x_1 and y_1 to compute the quadrature formulas without scaling of the weights. In this article we have used the Gauss formulas with the number of nodes being n = 40 [4]. With a parallel organization of the calculations the computation of the rise of the free surface at 3,600 points required only 5 minutes on an M-220 electronic computer. The computations were made for the following values of the parameters of the problem:

$$x_1 \leqslant 5{,}5,\ |y_1| \leqslant 3,\ a_1/H = b_1/H = 0{,}1,$$
$$a \in [-0{,}2;\ 0{,}2],\ \beta \in [0;\ 0{,}5],\ \varkappa \in [0{,}25;\ 4{,}75]. \tag{5}$$

In this case there did not have to be a further breakdown of the integration interval for achieving a relative accuracy of 10^{-2}–10^{-3}.

2. Figure 1 gives a general idea concerning the influence of the shear of the transverse component of current velocity on the wave trace behind the moving pressure region. The values of the lines of equal deviation ζ from the undisturbed level, shown in the figure, were normalized to the maximum ζ value in the region $0 \leqslant x_1 \leqslant 5.5$; $-2 \leqslant y_1 \leqslant 2$. The current velocity vector turns to the left with depth, in the direction of a negative direction of the y-axis. The extents of the conspicuous parts of the corresponding crests and troughs (level lines ±0.25) in the right and left parts of the figure differ by a factor of approximately 2.5. As follows from the results of the preceding study [3], with an increase in the β parameter the wave crests and troughs in the right part of the wave trace are displaced toward the Ox-axis, but never pass beyond it. The computations indicated that the maximum values of the ζ deviations from the undisturbed level are approximately equal to the left and right of the Ox-axis for all values of the parameters (5). Thus, the transverse current velocity shear can lead to substantial changes in the phase configuration of the trace.

Figure 2 makes possible a more detailed tracing of changes in the wave trace occurring with a change in the parameter b of shear of the transverse component of current velocity. As the scale unit along the z-axis we took the maximum value $\zeta(x_1, y_1)$ in the region $2 \leqslant x_1 \leqslant 5$, $|y_1| \leqslant 1.5$; when there is no current velocity shear (a = b = 0), $\mathcal{H} = 2$. With an increase in the b parameter there is also an increase in wave amplitude. In the cross section (Fig. 2,a) the z extrema with an increase in b are displaced in the direction of the current velocity shear; in this case the distances between adjacent extrema decrease in the region $y > 0$ and increase in the region $y < 0$. In the longitudinal sections (Fig. 2,b) the ζ extrema with an increase in b are displaced to the right (in the direction of greater x

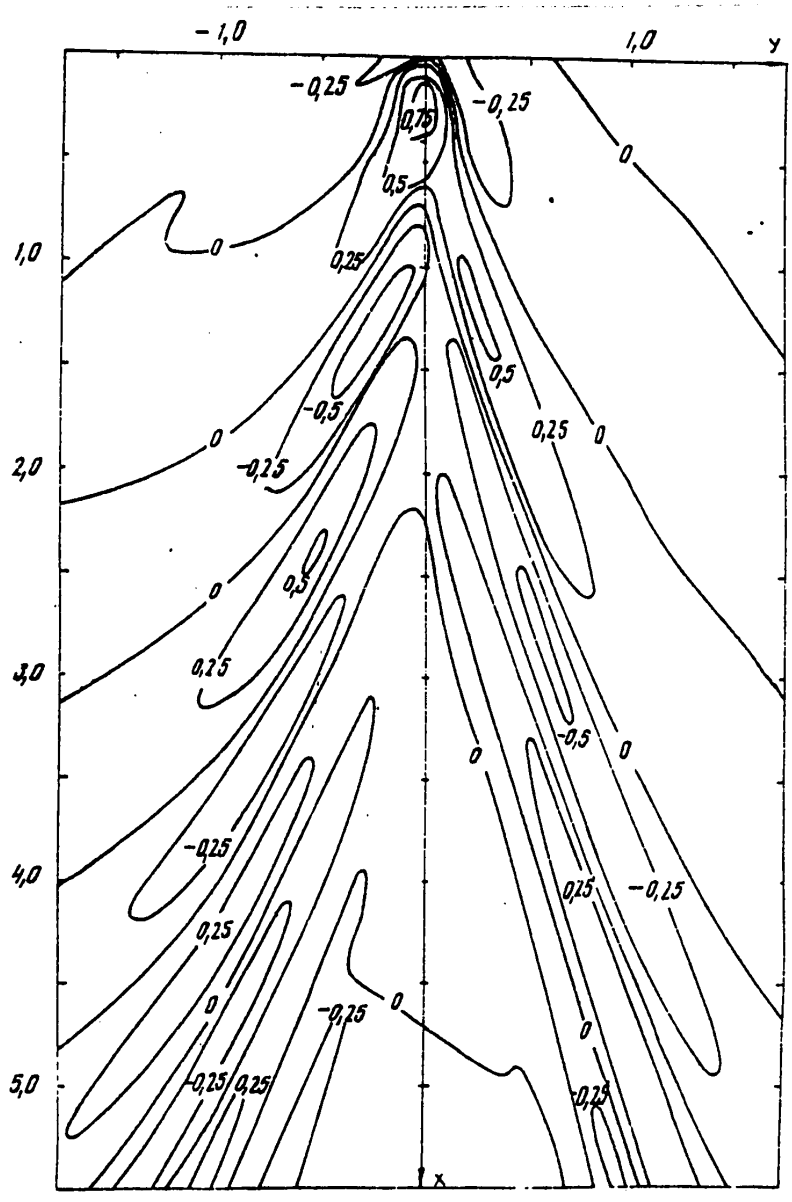

Fig. 1. Relief of free surface behind moving region of pressures with shear of the transverse component of current velocity for a = 0, b = 0.5, $\mathcal{K}$ = 2.

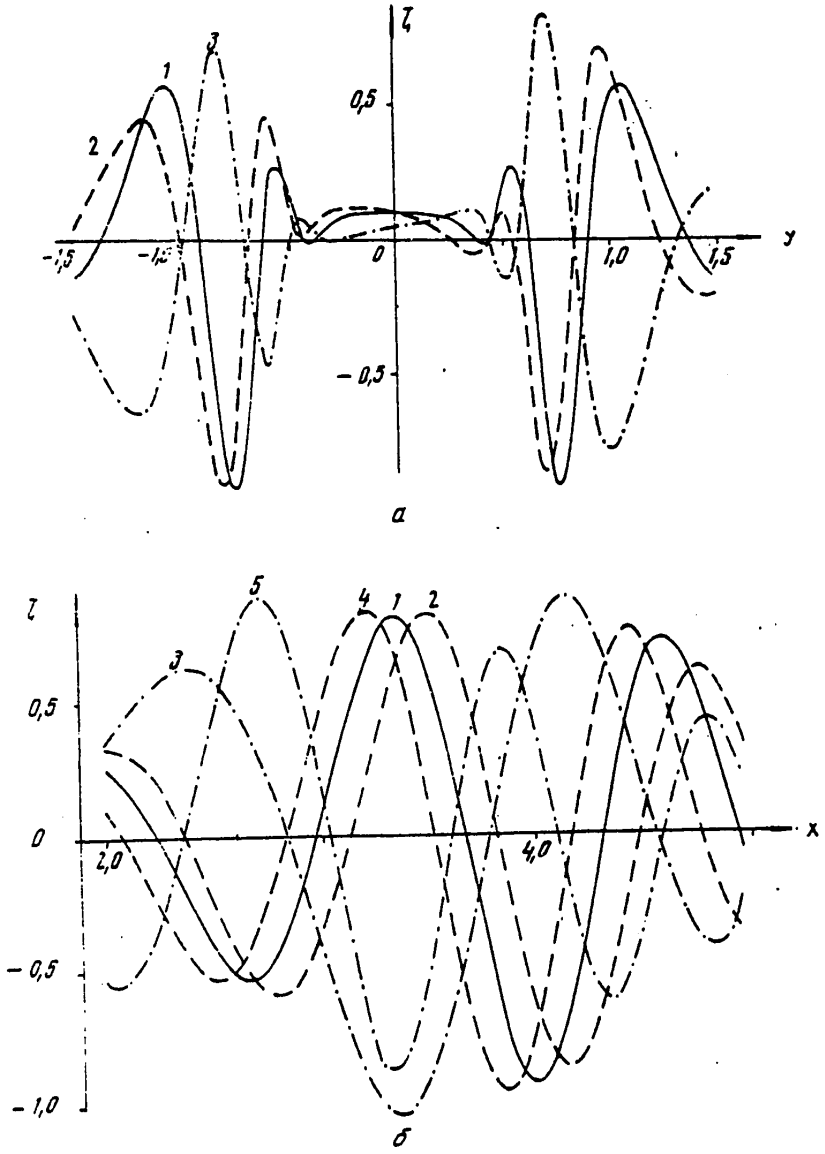

Fig. 2. Profile of fluid surface in transverse and longitudinal sections for a = 0, $\mathcal{H}$ = 2 for different b values: a) curves 1, 2, 3 correspond to the values b = 0, 0.1, 0.5 with x_1 = 4; b) curves 1, 2, 3 correspond to the values b = 0, 0.1, 0.5 with y_1 = 0.75, and curves 4, 5 correspond to values b = 0.1, 0.5 with y_1 = -0.75.

values) in the region y > 0, the distances between adjacent extrema increase. In the region y > 0 the ζ extrema are displaced to the left with an increase in b and the distances between adjacent extrema decrease.

Table 1

Maximum Deviations of Fluid Surface From Undisturbed Level

$\varkappa$ \ θ	0	0,1	0,2	0,3	0,4
0,25	15,18	15,18	15,20	15,20	15,20
0,50	21,42	21,80	21,94	21,97	21,98
1,00	28,06	28,30	28,62	28,99	29,35
1,50	35,94	37,19	38,31	39,35	38,46
1,75	36,22	37,45	38,92	39,64	39,34
2,00	38,38	39,61	40,85	41,96	42,49
2,25	37,37	37,65	36,75	41,27	43,43
2,50	34,63	35,17	36,03	37,43	39,84
3,00	25,30	25,96	28,25	32,23	35,62
4,00	7,26	7,88	9,86	13,74	20,14
4,75	1,39	1,55	2,26	4,10	6,02

Table 2

Joint Effect of Influence of Shears of Longitudinal and Transverse Components of Current Velocity on Maximum $|Z|$ Values

$\varkappa$ \ a \ δ	0,1				0,2			
	-0,2	-0,1	0,1	0,2	-0,2	-0,1	0,1	0,2
0,25	15,13	15,16	15,21	15,24	15,14	15,17	15,22	15,25
0,50	21,77	21,73	21,86	21,92	21,77	21,85	22,03	22,16
1,00	28,12	28,31	30,64	32,41	28,35	28,61	29,85	32,47
1,25	33,74	33,94	35,61	34,36	31,29	32,88	36,82	36,08
1,50	33,16	39,04	34,75	35,01	37,15	39,63	35,92	36,43
1,75	41,21	37,02	37,47	36,39	41,28	37,93	38,76	37,65
2,00	39,58	39,88	36,24	33,53	40,25	41,42	37,83	33,45
2,25	42,14	41,47	34,11	30,27	43,58	42,82	34,44	31,11
2,50	42,58	39,27	30,61	23,39	45,57	38,24	32,18	25,93
3,00	40,67	31,92	19,89	13,38	40,69	34,76	21,76	14,53
4,00	24,44	15,42	3,62	1,22	28,60	17,77	4,67	1,75
4,75	12,18	5,02	0,32	-	15,24	6,85	0,55	0,09

An analysis of the results of computations shows that the transverse velocity shear, directed in the negative direction of the y-axis, elongates the wave crests in the region $y>0$ and turns them toward the Ox-axis (the angle between the crest and the Ox-axis becomes less). In the region $y = 0$ the transverse velocity shear shortens the wave crests and increases the angles between the crests and the Ox-axis. The lengths of the waves increase in the region $y>0$ and decrease in the region $y<0$. With an increase in the b parameter the amplitudes of the waves increase.

3. We will make an analysis of the dependence of the maximum deviations of the free surface on the values of the parameters a, b, $\mathcal{H}$. The maximum $|\zeta|$ values were determined for the region $2 \leqslant x_1 \leqslant 5$, $-1.5 \leqslant y_1 \leqslant 1.5$. The max $|\zeta|$ values are given in the tables with an accuracy to the factor $p_0/(2\pi\rho Hc^2\mathcal{H})$.

Table 1 gives the results of max $|\zeta|$ computations for a = 0 and a series of $\mathcal{H}$ and b values. The author of [3] gave the critical value of the parameter $\mathcal{H} = (1 + a - b^2)^{-1}$, with transition through which there is a change in the composition of the wave trace. For a = 0 and $0 \leqslant b \leqslant 0.4$ the critical $\mathcal{H}$ value falls in the interval $1 \leqslant \mathcal{H} \leqslant 1.2$. It is interesting that with a fixed value of the b parameter the maximum $|\zeta|$ deviations are attained with $\mathcal{H} = \mathcal{H}_2 \approx 2$, that is, greater than the critical value. An analysis of the results of computations cited in Table 1 indicates that for $b \leqslant 0.4$ and $\mathcal{H} \leqslant \mathcal{H}_2$ the changes in the maximum deviations of the free surface do not exceed 10-12%. The influence of the transverse shear of current velocity is greater with large $\mathcal{H}$ values (or small velocities of movement of the region of pressures relative to the free surface). For example, with $\mathcal{H} = 2$ the change in the max $|\zeta|$ value is 10.7% with a change in b 0-0.4 and for $\mathcal{H} = 4.75$ the max $|\zeta|$ value with b = 0.4 is almost six times greater than the corresponding value with b = 0. In addition, with a decrease in $\mathcal{H}$ the changes in the max $|\zeta|$ values decrease with a change in the b parameter. With an increase in the b parameter for all $\mathcal{H}$ there is also an increase in the maximum deviations of the free surface from the undisturbed level.

We will examine the joint effect of the influence of shears of the longitudinal and transverse current velocity components on wave amplitudes. The results of computations for b = 0.1, 0.2 and a number of values of the a and $\mathcal{H}$ parameters are given in Table 2. The critical values of the $\mathcal{H}$ parameter here fall in the interval $0.84 < \mathcal{H} < 1.32$. An analysis of the results of computations shows that with allowance for the shear of the longitudinal component of current velocity the principal effect of presence of a shear of the transverse component is reflected in an increase in the amplitude of waves. The influence of longitudinal shear is more varied. With small $\mathcal{H}$ values with an increase in the a parameter there is an increase in the max $|\zeta|$ values; with large $\mathcal{H}$ values the picture is the reverse. A change in a is reflected to a greater degree in the case of great $\mathcal{H}$. The position of the maximum max $|\zeta|$ values (with respect to $\mathcal{H}$) is dependent on the a value to a greater degree than on b. With a decrease in a there is an increase in $\mathcal{H}$ at which max $|\zeta|$ attains its greatest value. For example, with b = 0.1 and a = -0.2 the greatest max $|\zeta|$ value is attained with $\mathcal{H} = 2.5$ and with this same b value and a = 0.1 with $\mathcal{H} = 1.75$. We also note that these $\mathcal{H}$ values are greater than the corresponding $\mathcal{H}$ values.

Summary

The intensity of shear of the transverse component of current velocity v_{0z} exerts a substantial influence on the phase configuration of the wave trace. With an increase in $|v_{0z}|$ the wave crests from one side of the wave trace (symmetrical with $v_{0z} = 0$) become longer, and on the other side -- shorter. In this case the wave crests are turned relative to the pressure epicenter in the direction of rotation of the current velocity vector with depth (Fig. 1).

The maximum displacement of the free surface is an increasing function of the shear modulus of the transverse component of current velocity $|v_{0}{}^{z}|$.

The greatest displacements of the free surface are attained with velocities C of movement of disturbances less than the velocities of propagation of long waves (critical).

In the case of small (in comparison with the critical values) velocities of movement of disturbances the maximum displacements of the free surface increase with an increase in u_{0z}, the shear of the longitudinal component of current velocity, and decrease with large C values.

The influence of shear of current velocity on the amplitudes of waves is most conspicuous in the case of small velocities of movement of disturbances. For example, for a C velocity half as great as the critical value the wave amplitudes can change by a factor of 20 or more with a change in the shear parameters in the intervals indicated in (5). In addition, the changes in maximum amplitudes of waves do not exceed 15% for velocities of movement of disturbances greater than the critical values.

BIBLIOGRAPHY

1. Cherkesov, L. V., NEUSTANOVIVSHIYESYA VOLNY (Unsteady Waves), Kiev, "Naukova Dumka," 1970, 196 pages.

2. Suvorov, A. M., Tananayev, A. N. and Cherkesov, L. V., "Nonstationary Spatial Waves in a Flow of a Homogeneous Fluid With Velocity Shear," POVERKHNOSTNYYE I VNUTRENNIYE VOLNY (Surface and Internal Waves), Sevastopol', Izd. MGI AN Ukrainskoy SSR, pp 14-21, 1979.

3. Sannikov, V. F., "Ship Waves in a Homogeneous Sea With a Linear Current Velocity Profile With Depth," POVERKHNOSTNYYE I VNUTRENNIYE VOLNY, Sevastopol', Izd. MGI AN Ukrainskoy SSR, pp 22-31.

4. Abramovits, M. and Stigan, I., SPRAVOCHNIK PO SPETSIAL'NYM FUNKTSIYAM S FORMULAMI, GRAFIKAMI I TABLITSAMI (Handbook on Special Functions With Formulas, Graphs and Tables), Moscow, "Nauka," pp 673-720, 1979.

5. Kelvin (W. Thomson), "On the Waves Produced by a Single Impulse in Water of Any Depth or in Dispersive Medium," PROC. ROY. SOC. LONDON, Ser. A, Vol 42, pp 80-85, 1887.

6. Havelock, T., "The Propagation of Groups of Waves in Dispersive Medium With Application to Waves on Water Produced by a Travelling Disturbance," PROC. ROY. SOC., LONDON, Ser. A, Vol 81, No 549, pp 398-430, 1908.

7. Kolberg, F., "Untersuchung des Wellenwiderstandes von Schiffen auf flachen Wasser gleichformig scherender Grundstromung," ZEITSCHRIFT ANGEW. MATH., B 39, H 7/8, 253-279, 1959.

UNSTEADY THREE-DIMENSIONAL WAVES IN A FLOW OF HOMOGENEOUS FLUID WITH VELOCITY SHEAR

Sevastopol' TEORETICHESKIYE I EKSPERIMENTAL'NYYE ISSLEDOVANIYA POVERKHNOSTNYKH I VNUTRENNIKH VOLN in Russian 1980 (manuscript received 28 Feb 80) pp 36-44

[Article by A. M. Suvorov and A. N. Tananayev]

[Text]

Abstract: A study was made of the process of development of three-dimensional surface waves generated by moving atmospheric pressure disturbances. Flow velocity is a piecewise-linear function of the vertical coordinate, which makes it possible, with a sufficient degree of accuracy, to approximate both the direction and velocity modulus of real currents in the ocean. The article gives a method for the analysis of three-dimensional waves in an N-layer (with respect to current velocity) sea. The special case with N = 1 is examined.

The theory of ship waves is one of the complex branches of modern hydrodynamics of the sea [1-4], and at the same time is quite important for practical applications. Emphasis has been on study of wave movement in a medium at rest in an undisturbed state or in a fluid flow having a velocity constant in depth. Recently interest has been shown in investigation of the influence of the vertical structure of currents on the parameters of three-dimensional waves [5, 6, 13]. In these studies current velocity was assumed to be a linear function of depth. However, observations show [7, 9] that one of the characteristic features of horizontal currents in the ocean is a quite complex dependence of their velocity and direction on depth. In this article we investigate unsteady three-dimensional surface waves for a piecewise-linear vertical profile of flow velocity making it possible with an adequate degree of accuracy to approximate real currents in the ocean.

1. We will examine the flow of an ideal incompressible homogeneous fluid of constant depth unbounded in horizontal directions (see Fig. 1). Here $z = -h_j (j = 0.1, \ldots; h_0 = 0)$ -- the vertical coordinates of the points at which the modulus and direction of the velocity vector of the horizontal current are stipulated (for example, on the basis of oceanic measurement data). In the intervals between these points the components of the current velocity vector along the x_1 and y_1 axes were approximated by linear functions of depth

$$U_j = b_j z + c_j , \quad V_j = d_j z + e_j . \tag{1.1}$$

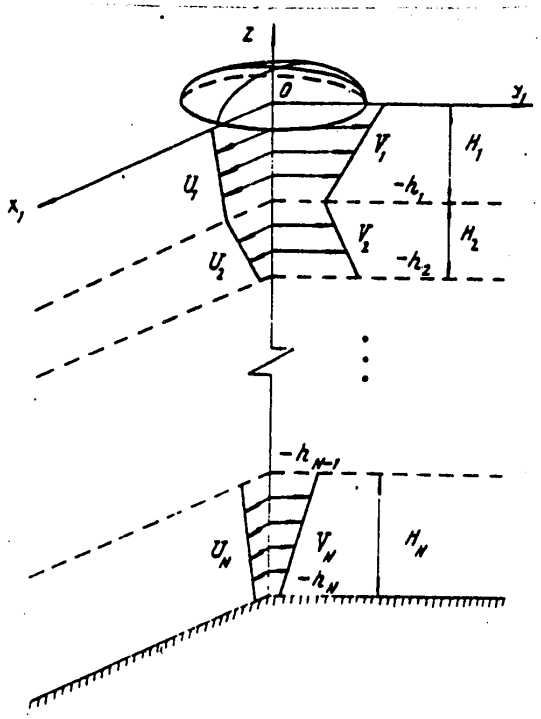

Fig. 1.

It is also assumed that

$$U_j = U_{j+1} = U_j' , \quad V_j = V_{j+1} = V_j' \quad \text{with} \quad z = -h_j \quad (j = 1, \ldots, N-1) ,$$

the derivatives of current velocity at these points can have discontinuities of the first kind.

Assume that a region of atmospheric pressure disturbances in the form

$$p_a = p_0 f(x_1 + U_0 t , y_1 + V_0 t) . \tag{1.2}$$

moving at a constant velocity is imparted to the surface of a fluid flow at the time t = 0.

Within the framework of linear theory we will investigate the process of development of three-dimensional waves generated by disturbances (1.2) and described by the following system of equations, boundary and initial conditions, written with (1.1) taken into account,

$$\rho\left(L_j u_j + \theta_j w_j\right) = -p_{jx_1}, \quad \rho\left(L_j v_j + \alpha_j w_j\right) = -p_{jy_1}, \quad \rho L_j w_j = -p_{jz}, \tag{1.3}$$

$$u_{jx_1} + v_{jy_1} + w_{jz} = 0 \quad \left(-\infty < x_1,\ y_1 < +\infty,\ -h_j < z < -h_{j-1},\ j = 1, \ldots, N\right);$$

$$w_N = 0 \qquad \left(z = -h_N\right),$$

$$w_j = w_{j+1} = L_{j+1}\zeta_{j+1}, \quad p_j = p_{j+1} \qquad \left(z = -h_j,\ j = 1, \ldots, N-1\right), \tag{1.4}$$

$$p_1 - \rho g \zeta_1 = p_a, \quad L_1 \zeta_1 = w_1 \qquad \left(z = 0\right);$$

$$u_j = v_j = w_j = \zeta_j = 0 \qquad \left(t = 0\right). \tag{1.5}$$

Here

$$L_j \equiv \frac{\partial}{\partial t} + U_j \frac{\partial}{\partial x_1} + V_j \frac{\partial}{\partial y_1};$$

are wave disturbances of velocity and pressure; ρ is fluid density; g is the acceleration of gravity; ζ_1 is the rise of the free surface; ζ_j (j = 2,...,N) is the displacement of the interface of the layers from an undisturbed position.

Then transforming to a coordinate system related to the moving region of atmospheric pressure disturbances

$$\left(x = x_1 + U_0 t, \quad y = y_1 + V_0 t\right),$$

using integral Fourier transforms for x, y and the Laplacian for t, we reduce (1.1) -(1.5) to such a boundary-value problem for the Fourier-Laplace transforms W_j of vertical velocity

$$W_{jzz} - r^2 W_j = 0 \quad \left(-h_j < z < -h_{j-1}\right); \tag{1.6}$$

$$W_N = 0 \qquad \left(z = -h_N\right),$$

$$W_j = W_{j+1}, \quad \mu_{j+1} W_{j+1} = \beta_{j+1}^2 \left[W_{jz} - W_{(j+1)z}\right] \quad \left(z = -h_j,\ j = 1, \ldots, N-1\right), \tag{1.7}$$

$$\mu_1 W_1 + \beta_1^2 W_{1z} = A \qquad \left(z = 0\right),$$

where

$$\mu_j = g c_j r^2 - a_j \beta_j, \quad \beta_j = \alpha + im U_j^0 + in V_j^0, \quad U_j^0 = U_0 + U_j', \quad V_j^0 = V_0 + V_j',$$

$$a_j = \beta_{jz} + \gamma_j \beta_{(j-1)z}, \quad \beta_{0z} = 0, \quad \beta_{jz} = im\delta_j + in\alpha_j,$$

$$c_j = 1 - \gamma_j, \quad \gamma_1 = 0, \quad \gamma_j = 1, \quad r^2 = m^2 + n^2,$$

$$A = -\frac{\rho_0 \beta_1 r^2 \bar{F}(m,n)}{\alpha \rho};$$

m, n, α are the parameters of the Fourier and Laplace transform.

The solution of equations (1.6) has the form

$$W_j = C_j \operatorname{sh} r(z+h_j) + C_j' \operatorname{ch} r(z+h_j)$$

and after substitution into the boundary conditions (1.7) gives the following system of algebraic equations for determining the unknown coefficients C_j and C_j':

$$\begin{gathered} C_N' = 0, \\ r\beta_{j+1}^2 C_j = C_{j+1}\rho_{j+1} + C_{j+1}' q_{j+1}, \\ r\beta_{j+1}^2 C_j' = C_{j+1}\rho_{j+1}' + C_{j+1}' q_{j+1}' \quad (j=1,\ldots,N-1), \\ C_1\rho_1 + C_1' q_1 = A. \end{gathered} \tag{1.8}$$

Here

$$\rho_j = \mu_j \operatorname{sh} rH_j + r\beta_j^2 \operatorname{ch} rH_j, \quad q_j = \mu_j \operatorname{ch} rH_j + r\beta_j^2 \operatorname{sh} rH_j,$$

$$\rho_j' = r\beta_j^2 \operatorname{sh} rH_j, \quad q_j' = r\beta_j^2 \operatorname{ch} rH_j.$$

After a number of transformations from (1.8) we obtain

$$C_j = \frac{AB_j}{d_N} s_j, \quad C_j' = \frac{AB_j}{d_N} s_j', \quad B_j = r^{j-1} \prod_{\ell=2}^{j} \beta_\ell^2,$$

$$s_N = 1, \quad s_N' = 0, \quad s_j = s_{j+1}\rho_{j+1} + s_{j+1}' q_{j+1},$$

$$s_j' = s_{j+1}\rho_{j+1}' + s_{j+1}' q_{j+1}', \quad d_0 = 1, \quad d_0' = 0,$$

$$d_j = \rho_j d_{j-1} + \rho_j' d_{j-1}', \quad d_j' = q_j d_{j-1} + q_j' d_{j-1}'.$$

We note that with j = 1 Bj = 1.

Taking these results into account and applying the inversion formulas, we derive an integral representation for z_j (j = 1,...,N)

$$z_j = \frac{-\rho_0}{4\pi^2\rho} \int_{-\infty}^{\infty}\int J_j e^{imx+inv}\, dm\, dn, \tag{1.9}$$

$$J_j = \frac{Fr^2}{2\pi i} \int_{s-i\infty}^{s+i\infty} \frac{F_j(\alpha, m, n)}{\alpha d_N} e^{\alpha t}\, d\alpha, \tag{1.10}$$

where

$$F_j(\alpha, m, n) = \beta_1 \beta_j^{-1} (s_j \operatorname{sh} rH_j + s_j' \operatorname{ch} rH_j) B_j .$$

For other hydrodynamic parameters, instead of the indicated F_j in (1.10) we will have the following expressions:

$$F_j = \beta_1 [s_j \operatorname{sh} r(z+h_j) + s_j' \operatorname{ch} r(z+h_j)] B_j \qquad \text{for } w_j,$$

$$F_j = \beta_1 \left\{ \operatorname{sh} r(z+h_j) \left[-s_j \left(\frac{im\beta_{jz}}{\beta_j r^2} + \frac{\beta_j}{\beta_j} \right) + s_j' \frac{im}{r} \right] + \right. \qquad \text{for } u_j,$$
$$\left. + \operatorname{ch} r(z+h_j) \left[-s_j' \left(\frac{im\beta_{jz}}{\beta_j r^2} + \frac{\beta_j}{\beta_j} \right) + s_j \frac{im}{r} \right] \right\} B_j$$

$$F_j = \beta_1 \left\{ \operatorname{sh} r(z+h_j) \left[-s_j \left(\frac{in\beta_{jz}}{\beta_j r^2} + \frac{d_j}{\beta_j} \right) + s_j' \frac{in}{r} \right] + \right. \qquad \text{for } v_j,$$
$$\left. + \operatorname{ch} r(z+h_j) \left[-s_j \left(\frac{in\beta_{jz}}{\beta_j r^2} + \frac{d_j}{\beta_j} \right) + s_j \frac{in}{r} \right] \right\} B_j$$

$$F_j = \beta_1 \rho r^{-2} [\operatorname{sh} r(z+h_j) (\beta_{jz} - r\beta_j s_j') +$$
$$+ \operatorname{ch} r(z+h_j) (\beta_{jz} s_j' - r\beta_j s_j)] B_j \qquad \text{for } p_j.$$

2. We will make an analysis of the integral (1.10). The poles of the integrand are the point $\alpha = 0$ and the roots of the equation

$$d_N(\alpha) = 0, \tag{2.1}$$

which with $\alpha = i\sigma$ undergoes transition into a dispersion relationship for periodic waves in a flow of a homogeneous fluid with a velocity shear. The left-hand side of equation (2.1) is a polynomial of the 2N-th degree relative to α and according to a corollary from the fundamental theorem of algebra [10] it has a unique expansion in the form

$$d_N(\alpha) = F'(m, n) \prod_{\ell=1}^{2N} (\alpha - \alpha_\ell) = i^{2N} F'(m, n) \prod_{\ell=1}^{2N} (\sigma - \sigma_\ell) = 0, \tag{2.2}$$

where F'(m,n) is a known higher coefficient, the expression for which, since it is unwieldy, is not given here. Applying the Cauchy residues theorem, from (1.10) we obtain

$$J_j = \frac{r^2 \bar{f}}{F'} \left[\frac{F_j(0, m, n)}{\prod_{\ell=1}^{2N} \alpha_\ell} + \sum_{k=1}^{2N} \frac{F_j(\alpha_k, m, n) e^{\alpha_k t}}{\alpha_k \prod_{\substack{\ell=1 \\ \ell \neq k}}^{2N} (\alpha_k - \alpha_\ell)} \right]. \tag{2.3}$$

The first expression in the brackets, not dependent on time, corresponds to stationary waves, whereas the second, consisting of the sum of 2N terms, describes the transient process.

For real m and n values equation (2.2) has real coefficients relative to σ. Accordingly, among the roots δ_ℓ of the equation there can be both real and paired-conjugate complex roots. The corresponding α_ℓ values will be either purely imaginary or complex. The real parts of each pair of complex roots α_ℓ have opposite signs. For complex roots with a positive real part the J_j value (2.3) increase exponentially with time. In this case with $t \to \infty$ limitation of the integral (1.9) can occur only due to interference of waves for different m and n.

An investigation of the parameters of a fluid flow for which among the roots δ_ℓ of the dispersion relationship there are conjugate-complex roots, is an important independent problem in the theory of hydrodynamic stability [11, 14].

We will assume that all the roots δ_ℓ are real expressions. However, in each specific case this fact must be checked.

Since $z_j \mid_{t=0} = 0$, due to the uniqueness of the Fourier transform, from (2.3) we obtain

$$\frac{F_j(0, m, n)}{\prod_{\ell=1}^{2N} \alpha_\ell} + \sum_{k=1}^{2N} \frac{F_j(\alpha_k, m, n)}{\alpha_k \prod_{\substack{\ell=1 \\ \ell \neq k}}^{2N} (\alpha_k - \alpha_\ell)} = 0.$$

With this result taken into account (2.3) assumes the form

$$J_j = \frac{-r^2 \bar{f}}{F'} \sum_{k=1}^{2N} \frac{F_j(\alpha_k, m, n)}{\alpha_k \prod_{\substack{\ell=1 \\ \ell \neq k}}^{2N} (\alpha_k - \alpha_\ell)} \left(1 - e^{\alpha_k t}\right). \tag{2.4}$$

Introducing integration for t, from (1.9), (2.4)

$$\zeta_j = -\frac{\rho_0}{4\pi^2 \rho} \sum_{k=1}^{2N} \zeta_{jk}, \tag{2.5}$$

where

$$\zeta_{jk} = \int_0^\infty \int_{-\pi/2}^{3\pi/2} \int_0^\nu \Phi_{jk} e^{iRN_k} \, d\xi \, d\theta \, dr,$$

$$\Phi_{jk} = \frac{r^2 \bar{f}(r, \theta) F_j(\alpha_k, r, \theta)}{F'(r, \theta) \prod_{\substack{\ell=1 \\ \ell \neq k}}^{2N} (\alpha_k - \alpha_\ell)}, \quad N_k = \sigma_k \xi R^{-1} + r \cos(\theta - \gamma), \tag{2.6}$$

$$x = R \cdot \cos\gamma, \quad y = R \sin\gamma, \quad m = R \cos\theta, \quad n = r \sin\theta.$$

3. We will investigate the asymptotic behavior of the integral (2.6) for large R and t values. We will use the stationary phase method for multidimensional integrals [12]. The stationary points are found using the following system of equations:

$$\begin{cases} \sigma_k = 0 & (3.1) \\ \frac{\partial \sigma_k}{\partial \theta} \xi R^{-1} - r \sin(\theta - \gamma) = 0 & (3.2) \\ \frac{\partial \sigma_k}{\partial r} \xi R^{-1} + \cos(\theta - \gamma) = 0 & (3.3) \end{cases}$$

taking into account the inequality

$$0 < \xi < t \ , \tag{3.4}$$

ensuring that the stationary points belong to the integration region. We will examine cases when the system (3.1)-(3.3) has only real roots. We will assume that equation (3.1) has at least one real root $\theta = \theta_\lambda(r)$, dependent on r. Then substituting $\theta = \theta_\lambda(r)$ into (3.2), (3.3), excluding ξ and taking into account that

$$\frac{\partial \theta_\lambda}{\partial r} = -\frac{\partial \sigma_k}{\partial r}\left(\frac{\partial \sigma_k}{\partial \theta_\lambda}\right)^{-1},$$

we find two equations for determining r_λ and ξ_λ

$$tg\,\gamma = \psi(r_\lambda) \ , \tag{3.5}$$

$$\xi_\lambda = \left(\frac{\partial \sigma_k}{\partial r}\right)^{-1} R \cos(\theta_\lambda - \gamma) \ , \tag{3.6}$$

where

$$\psi(r_\lambda) = \left.\frac{r\frac{\partial \theta_\lambda}{\partial r} tg\,\theta_\lambda - 1}{r\frac{\partial \theta_\lambda}{\partial r} + tg\,\theta_\lambda}\right|_{r=r_\lambda} . \tag{3.7}$$

The main term of the asymptotic representation for (2.6) in the case of one simple stationary point $B = (\theta_\lambda, r_\lambda, \xi_\lambda)$ assumes the form

$$I_{jk} = \sqrt{\frac{8\pi^3}{R|\det D_k|}}\, \Phi_{jk}(\beta) \exp\left[iN_{1k}(\beta) + i\frac{\pi}{4} \operatorname{sign} D_k \right], \tag{3.8}$$

where

$$N_{1k}(\beta) = \left[\sigma_k \xi + r R \cos(\theta - \gamma)\right]_\beta ; \quad D_k = \left\| \frac{\partial^2 N_{1k}(\beta)}{\partial z_r \partial z_s} \right\| -$$

is a matrix consisting of the second derivatives of N_{1k} for θ, r, ξ at the point B; $\overline{r}$, $\overline{s}$ = 1, 2, 3; sign D_k is a signature of a quadratic form with the matrix D_k. From (3.4), (3.6) we find that the wave corresponding to the stationary point B is localized in the region

$$0 < R < c_{k\lambda} t \ , \quad \text{where} \quad c_{k\lambda} = \frac{\partial \sigma_k}{\partial r} \cos^{-1}(\theta_\lambda - \gamma) \ -$$

is the velocity of motion of the leading edge of the disturbance. When there are several stationary points in (3.8) it is necessary to take the sum of the corresponding asymptotes.

4. We will examine special cases.

a) N = 1, $B_1 = V_1 = U_1 = V_0 = 0$ (a layer at rest in an undisturbed state of a fluid of finite depth). Then we have [4]

$$d_1 = gr^2 \operatorname{sh} rH_1 + r(\alpha + im U_0)^2 \operatorname{ch} rH_1 = r \operatorname{ch} rH_1 (\alpha - \alpha_1)(\alpha - \alpha_2),$$

$$\alpha_{1,2} = i\left(-mU_0 \pm \sqrt{gr \operatorname{th} rH_1}\right),$$

$$\psi(r) = g\frac{\operatorname{th} rH_1 + rH_1 \operatorname{sech}^2 rH_1}{2rU_0 - g \operatorname{th} rH_1 - rgH_1 \operatorname{sech}^2 rH_1}\sqrt{\frac{rU_0^2}{g \operatorname{th} rH_1} - 1}.$$

The function $\psi(r)$ for $U_0 c^{-1} \geqslant 1$ ($c = \sqrt{gH_1}$) decreases monotonically with an increase in $r \geqslant 0$, tending to zero when $r \to 0$ and assuming a maximum value $(U_0^{2s-2} - 1)^{-1/2}$ with $r = 0$. For $U_0^{c-1} < 1$ the $\psi(r)$ function becomes equal to zero with $r = r_0$, $r = \infty$ and and contains a single maximum with $r = r_3$ ($r_0 < r_5 < \infty$). In the region $r_0 \leqslant r \leqslant r_5$ $\psi(r)$ increases monotonically; with $r > r_5$ it decreases monotonically with an increase in r. It therefore follows that equation (3.5) with $U_0 c^{-1} \geqslant 1$ has one positive root r_2 for $0 < \gamma < \gamma_1$, where γ_1 = arc tg $(U_0^2 c^{-2} - 1)^{-1/2}$. With $U_0 c^{-1} < 1$ and $\gamma < \gamma_2$ (γ_2 = arc tg $\psi(r_5)$ equation (3.5) has two different positive roots $r = r_3$ and $r = r_4$ ($r_4 > r_3$), with $\gamma = \gamma_2$ -- one multiple root $r = r_5$. Accordingly, the wave movement will consist either of one longitudinal wave with $U_0 c^{-1} > 1$, $0 < \gamma < \gamma_1$, or of transverse and longitudinal waves with $U_0 c^{-1} < 1$, $0 < \gamma < \gamma_2$.

b) N = 1 (flow of a homogeneous fluid with a linear profile of current velocity in depth). We obtain

$$d_1 = \left(gr^2 - \alpha_1\beta_1\right) \operatorname{sh} rH_1 + r\beta_1^2 \operatorname{ch} rH_1 = r \operatorname{ch} rH_1 (\alpha - \alpha_1)(\alpha - \alpha_2),$$

$$\alpha_{1,2} = i\left[r \cos\theta U_1^\circ + r \sin\theta V_1^\circ - \frac{\operatorname{th} rH_1 (\beta_1 \cos\theta + \alpha_1 \sin\theta)}{2} \pm \right.$$

$$\left. \pm \sqrt{\frac{\operatorname{th}^2 rH_1 (\beta_1 \cos\theta + \alpha_1 \sin\theta)^2}{4} + gr \operatorname{th} rH_1}\right],$$

$$\operatorname{tg}\theta_{1,2} = \frac{-\delta_2 \pm \sqrt{\delta_2^2 - 4\delta_1\delta_3}}{2\delta_1}, \quad \delta_2 = \frac{2U_1^\circ V_1^\circ}{c^2} - \frac{\bar{r}}{g}(\beta_1 V_1^\circ + \alpha_1 U_1^\circ), \quad \bar{r} = \frac{\operatorname{th} rH_1}{rH_1},$$

$$\delta_1 = \frac{V_1^{\circ 2}}{c^2} - \bar{r}\left(1 - \frac{\alpha_1 V_1^\circ}{g}\right), \quad \delta_3 = \frac{U_1^{\circ 2}}{c^2} - \bar{r}\left(1 - \frac{\beta_1 U_1^\circ}{g}\right).$$

the $\psi(r)$ function after the substitution of $\mathrm{tg}\,\theta_{1,2}$ and $d\theta_{1,2}/dr$ into (3.7) proves to be quite complex for an analytical representation. A numerical analysis of the parameters of wave motion in the case of a current velocity direction constant in depth was carried out in [5] and with allowance for change in direction -- in [6].

BIBLIOGRAPHY

1. Stoker, D., VOLNY NA VODE (Waves on Water), Moscow, IL, 1959, 620 pages.

2. Sretenskiy, L. N., TEORIYA VOLNOVYKH DVIZHENIY ZHIDKOSTI (Theory of Wave Movements of a Fluid), Moscow, "Nauka," 1977, 816 pages.

3. Khaskind, M. D., GIDRODINAMICHESKAYA TEORIYA KACHKI KORABLYA (Hydrodynamic Theory of Ship Rolling), Moscow, "Nauka," 1973, 328 pages.

4. Cherkesov, L. V., NEUSTANOVIVSHIYESYA VOLNY (Unsteady Waves), Kiev, "Naukova Dumka," 1970, 196 pages.

5. Suvorov, A. M., Tananayev, A. N. and Cherkesov, L. V., "Nonstationary Three-Dimensional Waves in a Flow of Homogeneous Fluid With a Velocity Shear," POVERKHNOSTNYYE I VNUTRENNIYE VOLNY (Surface and Internal Waves), Sevastopol', Izd. MGI AN Ukrainskoy SSR, pp 14-21, 1979.

6. Sannikov, V. F., "Ship Waves in a Homogeneous Sea With a Linear Profile of Current Velocity in Depth," POVERKHNOSTNYYE I VNUTRENNIYE VOLNY, Sevastopol', Izd. MGI AN Ukrainskoy SSR, pp 22-31, 1979.

7. Monin, A. S., Kamenkovich, V. M. and Kort, V. G., IZMENCHIVOST' MIROVOGO OKEANA (Variability of the World Ocean), Leningrad, Gidrometeoizdat, 1974, 264 pages.

8. Titov, V. V. and Fomin, L. M., "Vertical Structure of Currents According to Measurement Data for the Indian Ocean," OKEANOLOGIYA (Oceanology), 9, No 4, pp 578-587, 1971.

9. Fomin, L. M., "Expeditionary Investigations of Structure of Ocean Currents," OKEANOLOGIYA, 3, pp 6-34, 1975.

10. Kurosh, A. G., KURS VYSSHEY ALGEBRY (Course in Higher Algebra), Moscow, "Nauka," 1971, 432 pages.

11. Lin'-Tszya-tszyao, TEORIYA GIDRODINAMICHESKOY USTOYCHIVOSTI (Theory of Hydrodynamic Stability), Moscow, IL, 1958, 194 pages.

12. Fedoryuk, M. V., "Stationary Phase Method for Multidimensional Integrals," ZHURN. VYCHISLIT. MAT. I MAT. FIZ. (Journal of Computation Mathematics and Mathematical Physics), 2, No 1, pp 145-150, 1962.

13. Kolberg, E., "Untersuchung des Wellenwiderstandes von Schiffen und flachen Wasser bei glichformig scheirender Grundstorung," ZEITSCHRIFT ANGEW. MATH., B 39, H 7/8, S 253-279, 1959.

14. Drazin, P. G. and Howard, L. N., "Hydrodynamic Stability of Parallel Flow of Inviscid," ADV. APPL. MATH., 9, No 1, pp 1-89, 1966.

COMPUTATIONS OF DISTRIBUTIONS OF ORBITAL VELOCITIES OF WIND WAVES

Sevastopol' TEORETICHESKIYE I EKSPERIMENTAL'NYYE ISSLEDOVANIYA POVERKHNOSTNYKH I VNUTRENNIKH VOLN in Russian 1980 (manuscript received 20 Sep 79) pp 45-54

[Article by L. A. Korneva and V. P. Liverdi]

[Text]

Abstract: Experimental data on interrelated two-dimensional, conditional and marginal distributions of orbital velocities and wave periods in the Black Sea and ocean are examined. There was found to be a change in the characteristics of the conditional distributions of orbital velocities in dependence on the ratio of the specific value of the period to its mean value according to the wave record. In computations of the mean orbital velocity it is recommended that the experimental curves of the distribution of orbital velocities be used. In order to accelerate computations data are given on the change in a single parameter of this distribution as a function of the stage in wave development.

The orbital velocity of wind waves can be determined for each wave by computations if at the same time the height and the period of the wave $v_i = \pi h_i/T_i$ are computed. Individual v_i values are random values. The description of their statistical behavior requires a study of the experimental orbital velocity distribution functions $\varphi(v)$. Still more precise information is given by a study of the two-dimensional distributions $\varphi(v,T)$. At the same time the initial experimental material obtained from the wave records are the heights h_i and periods T_i of the waves, constituting a system of two random values. This system can be described by a two-dimensional experimental statistical table of the values $n_{ij}(h_0, T_0)$, that is, by the number of cases stipulated at equal intervals Δh_0 and ΔT_0 of the relative values $h_0 = h/\bar{h}$ and $T_0 = T/\bar{T}$. Using such a table it is possible to compute the experimental values of the probability density of a two-dimensional distribution $\varphi(h_0, T_0)$, conditional distributions $\varphi(h_0 \mid T_0)$ and $\varphi(T_0 \mid h_0)$ and the marginal distributions $\varphi(h_0)$ and $\varphi(T_0)$. These three types of distributions are related to one

another by the theorem of multiplication of laws [1]

$$\varphi(h_0, T_0) = \varphi(T_0)\ \varphi(h_0 | T_0). \tag{1}$$

Historically it has so happened that the distributions $\varphi(T_0)$ and $\varphi(h_0)$ for wind waves were first studied using one-dimensional series h_0 and T_0, whereas the two-dimensional distribution was found using the multiplication theorem. For theoretical computations of $\varphi(h_0, T_0)$ it is convenient to consider h_0 and T_0 to be independent, that is, assume that $\varphi(h_0|T_0) = \varphi(h_0)$; then the theorem of multiplication of laws is simplified

$$\varphi(h_0, T_0) = \varphi(h_0)\ \varphi(T_0). \tag{2}$$

Later it was found that the experimental data on $\varphi(h_0|T_0)$ do not correspond to the assumption of a nondependence of this conditional distribution on T_0 [2]. This is the reason for the discrepancy between the experimental distributions and the theoretical distributions, obtained with use of the theorem of multiplication of laws for independent values. In our recent investigations in the Black Sea the basis for obtaining different distributions is the initial two-dimensional n_{ij} table having i rows for the h_0 values and j columns for the T_0 values. If it is taken into account that

$$\varphi(h_0 | T_0) = \frac{n_{ij}}{\sum_i n_{ij} \Delta h_0}, \qquad \varphi(T_0) = \frac{\sum_i n_{ij}}{\sum_{i,j} n_{ij} \Delta T_0},$$

it can then be shown that the theorem of multiplication of laws on the basis of the data in such a table is satisfied in general form (1), since

$$\varphi(h_0, T_0) = \frac{n_{ij}}{\sum_{i,j} n_{ij} \Delta h_0 \Delta T_0}.$$

It is possible to proceed from the main system (h_0, T_0) and the two-dimensional distribution $\varphi(h_0, T_0)$ corresponding to it to systems of values related to h_0, T_0.

In this study we will attempt to find $n_{ij}(h_0/T_0, T_0)$, $\varphi(h_0/T_0, T_0)$, and from them $\varphi(v_0)$ and $\varphi(v)$, where $v = \pi h/T$, and $v_0 = h_0/T_0 = v/v_*$; $v_* = \pi h/T$.

In order to obtain an $n_{ij}(h_0, T_0)$ table we used two two-dimensional tables (one of them included 4079 pairs of h_0, T_0 values, taken from wave records of the Black Sea, whereas the other included 8116 pairs of h_0, T_0 values obtained on voyages in the Atlantic Ocean [3]). The h_0 and T_0 values were used in computing $v_0 = h_0/T_0$ and the obtained orbital velocity value V_0 is assigned the number of cases of $n_{ij}(h_0, T_0)$ found in this same box in the table. Then a statistical table $n_{ij}(v_0, T_0)$ is obtained for equal intervals Δv_0 and ΔT_0. In our computations we stipulated $\Delta v_0 = 0.4$ and $\Delta T_0 = 0.2$. From the $n_{ij}(v_0, T_0)$ values we find all the other types

Table 1

Densities of Two-Dimensional Distribution $\varphi(v_0, T_0)\cdot 10^2$, Conditional Distribution $\varphi(v_0 \mid T_0)$ and Experimental Marginal Distributions $\varphi_{ex}(v_0)$, $\varphi_{ex}(T_0)$ for Black Sea

v_0 \ T_0	0,3	0,5	0,7	0,9	1,1	1,3	1,5	1,7	1,9	2,1	$\varphi_э(v_0)$
0,2	10,7	7,3 (0,20)	7,7 (0,08)	20,8 (0,17)	10,7 (0,09)	15,3	7,7	1,2	2,7	–	0,17
0,6	–	32,1 (0,90)	79,0 (0,84)	77,5 (0,62)	55,1 (0,48)	57,9	39,8	15,6	8,6	1,8	0,74
1,0	11,9	25,4 (0,71)	55,1 (0,59)	61,6 (0,49)	140,9 (1,30)	81,5	29,8	6,1	2,4	–	0,83
1,4	–	10,1 (0,28)	61,5 (0,65)	88,5 (0,71)	46,8 (0,41)	19,2	4,3	1,2			0,46
1,8	3,4	9,2 (0,26)	16,8 (0,18)	42,2 (0,34)	22,3 (0,20)	3,4	0,3				0,19
2,2	0,8	3,1 (0,08)	8,3 (0,09)	16,8 (0,13)	7,9 (0,07)	0,3					0,07
2,6		0,9 (0,03)	7,0 (0,07)	3,7 (0,03)	0,9 (0,008)						0,03
3,0		0,9 (0,03)	0,6 (0,006)	0,3 (0,002)	0,3 (0,003)						0,004
3,4		0,3 (0,01)	0,6 (0,006)	0,3 (0,002)							0,003
3,8		1,2 (0,03)	0,3 (0,008)								0,003
4,2		0,3 (0,01)									0,001
$\varphi_э(T_0)$	0,1	0,36	0,94	1,25	1,14	0,71	0,32	0,09	0,06	0,01	

$[\varphi_э = \varphi_{ex}]$

of distributions. Table 1 gives the probability of the two-dimensional distribution computed using the formula

$$\varphi(v_0, T_0) = \frac{n_{ij}}{\sum_{ij} \Delta v_0 \Delta T_0}. \quad (3)$$

The density of the conditional distribution of orbital velocity for a fixed period T_0 is computed for each column of the two-dimensional table

$$\varphi(v_0 | T_0) = \frac{n_{ij}(v_0, T_0)}{\sum_i n_{ij} \Delta v_0}. \quad (4)$$

The conditional distribution of the period for a fixed value can be computed for each line of the two-dimensional table

$$\varphi(T_0 | v_0) = \frac{n_{ij}}{\sum_j n_{ij} \Delta T_0}.$$

The total values in the table columns and rows are used in computing the marginal distributions of orbital velocity $\varphi(v_0)$ and period $\varphi(T_0)$ respectively

$$\varphi(T_0) = \frac{\sum_i n_{ij}}{\sum_{ij} n_{ij} \Delta T_0}, \qquad \varphi(v_0) = \frac{\sum_j n_{ij}}{\sum_{ij} n_{ij} \Delta v_0}. \quad (5)$$

The $\varphi_{ex}(T_0)$ values are given in Table 1 in the last additional row; the $\varphi_{ex}(v_0)$ values are given in the last column.

The $\varphi(v_0 | T_0)$ values can also be found using the theorem of multiplication of laws since they are equal to

$$\varphi(v_0 | T_0) = \frac{\varphi(v_0, T_0)}{\varphi(T_0)}.$$

These values are given in Table 1 in parentheses for some T_0 values. It can be seen that $\varphi(v_0 | T_0)$ differs from $\varphi(V_0)$. Naturally, the statistical characteristics of the conditional distributions will also differ from the characteristics of the marginal distributions, that is, will not be constant, but will change in dependence on the fixed T_0 value. An analysis of $\varphi(v_0 | T_0)$ and the statistical characteristics of this distribution (such as mean v_0, the dispersion σ_{v0}^2, the variation coefficient C_{vv0}) was made for the Black Sea and the Atlantic Ocean (Table 2). The changes in these characteristics are shown in Fig. 1. It can be seen that the considered statistics (statistical characteristics) are not constant but are dependent on T_0. With $T_0 = 0.85$ for the Black Sea and with $T_0 = 0.7$ for the ocean there is a maximum on the $v_0(T_0)$ curve. For σ_{v0}^2 there is a maximum with a value $T_0 = 0.6$ for the two considered regions. The variation coefficient Cv_{v0} changes smoothly from large values in the case of small T_0, attains values 0.52 with $T_0 = 0.8$ and then decreases to 0.35 with $T_0 = 2$. We investigated the experimental marginal distribution $\varphi(v_0) = \varphi(v)v_*$ for the Black Sea and $\varphi(v_0)$ for the

ocean. These distributions are characterized by the following statistics: $\bar{v}_0 = 1.03$, $\sigma_{v_0}^2 = 0.27$ for the Black Sea; $\bar{v}_0 = 1.04$, $\sigma_{v_0}^2 = 0.26$ for the ocean. It can be seen that the marginal distributions $\varphi(v_0)$ for both water regions are characterized by one and the same variation coefficient $Cv_{v_0} = 0.52$ and the value $v_0 = 1.03$-1.04. The greatest difference $\varphi(v_0 \mid T_0)$ from $\varphi(v_0)$ is observed for waves of short and long periods and the difference is less clearly expressed for periods close to the average.

Table 2

Statistical Characteristics of Conditional Distribution $\varphi(v_0 \mid T_0)$ as a Function of Different T_0

T_0	Black Sea			Ocean		
	$\bar{v}_0$	$C_{v v_0}$	$\sigma_{v_0}^2$	$\bar{v}_0$	$C_{v v_0}$	$\sigma_{v_0}^2$
0,2	0,78	0,75	0,26	0,84	0,78	0,30
0,4	0,85	0,65	0,34	1,10	0,68	0,36
0,6	1,10	0,56	0,36	1,15	0,54	0,36
0,8	1,18	0,49	0,32	1,14	0,48	0,31
1,0	1,14	0,44	0,25	1,08	0,44	0,21
1,2	1,02	0,40	0,17	0,95	0,42	0,14
1,4	0,89	0,38	0,11	0,82	0,39	0,10
1,6	0,76	0,38	0,07	0,71	0,37	0,07
1,8	0,67	0,35	0,05	0,64	0,36	0,06
2,0	0,63	0,34	0,04	0,62	0,34	0,05
2,2	0,60	0,34	0,03	0,60	0,38	0,05

Now we will examine in greater detail the marginal distribution $\varphi(h_0/T_0) = \varphi(v_0)$ because we must obtain from it the distribution $\varphi(v)\bar{v}$, where $v = \pi h/T$ is the true orbital velocity. For this we use the notation $\pi h/\bar{T} = v_*$, $\pi h/T = v$. Then $h_0/T_0 = v/v_* = v_0$. Thus, the distribution $\varphi(v_0)$ is the distribution $\varphi(v/v_*)$. For the linearly related arguments v and v/v_* there will be a correlation of the distributions themselves [1] in the form

$$\varphi(v/v_*) = \varphi(v)\, v_* .$$

With transformation from the v/v_* values to $v/\bar{v}$ we will assume that $v_* = \beta \bar{v}$. The β value is found from the experimental distribution $\varphi(v_0) = \varphi(v/v_*)$, computing the first moment of the distribution. It is equal to

$$(\overline{v/v_*}) = \int_0^\infty (v/v_*)\,\varphi\,(v/v_*)\,d(v/v_*). \qquad (6)$$

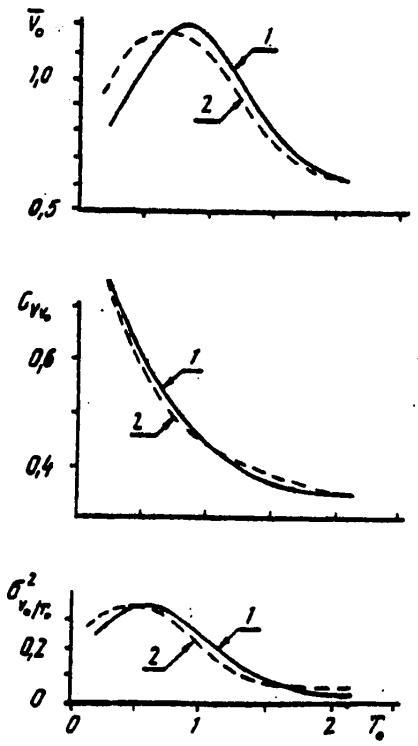

Fig. 1. Statistical characteristics $\bar{v}_0|T_0$, $C_{Vv0}|T_0$, $\sigma^2_{v_0}|T_0$ of the conditional distribution $\varphi(v_0|T_0)$: 1) Black Sea; 2) ocean.

Since the $\varphi(v_0)$ values are expressed in the numerical data (Table 1), computations of the first moment were made by the numerical integration method, where use was made of the method for computing the statistical characteristics by the approach of grouping of values by classes [4].

It was therefore found that for the distribution $\varphi(v_0)$ $\overline{(v/v_*)}$ = 1.03-1.04 for the Black Sea and the ocean respectively. It can be assumed that β = 1.04. The scaling of $\varphi(v_0)$ into $\varphi(v)\bar{v}$ was carried out on the assumption that $\varphi(v)\bar{v} = \varphi(v_0)\beta$ with the argument $v/\bar{v} = v/\beta\, v_*$.

Table 3 (columns 2,3) gave experimental data for the Black Sea and ocean and in Fig. 2 it can be seen that the experimental distributions of the orbital velocities of the two water regions coincide quite well.

Figure 3 shows the integral curves

$$F(v/\bar{v}) = \int_{0}^{v/\bar{v}} \varphi(v/\bar{v})\, d(v/\bar{v}),$$

whose values are expressed in percent (so-called guaranteed probability); using these curves it is possible to determine the ratio of wave velocity to mean orbital velocity for waves of stipulated guaranteed probability.

Table 3

Experimental Generalized Distribution $\varphi(v)\bar{v}$ for Black Sea and Ocean and Its Computation From $\varphi(h_0, n_h)$ and $\varphi(T_0, n_T)$

$v/\bar{v}$	Black Sea	Ocean	Computed $\varphi(v)\bar{v}$	
			$n_T=3$, $n_h=2$	$n_T=4$, $n_h=2$
0,2	0,20	0,16	0,39	0,42
0,4	0,44	0,43	0,66	0,65
0,6	0,73	0,71	0,80	0,76
0,8	0,85	0,90	0,80	0,76
1,0	0,90	0,89	0,67	0,66
1,2	0,86	0,73	0,50	0,53
1,4	0,42	0,48	0,36	0,38
1,6	0,29	0,32	0,26	0,26
1,8	0,20	0,21	0,18	0,20
2,0	0,13	0,14	0,13	0,14
2,2	0,07	0,07	0,09	0,10
2,4	0,04	0,04	0,07	0,07
2,6	0,02	0,02	0,05	0,05
2,8	0,01	0,01	0,04	0,04
3,0	0,01	0,01	0,03	0,03

For a comparison of the experimental material with the theoretical scheme we made computations of the theoretical value $\varphi(v_0)$ from $\varphi(h_0, T_0)$ in two variants:

$$\varphi_1(h_0, T_0) = 8\Gamma^2\left(\frac{3}{2}\right)\Gamma^3\left(\frac{4}{3}\right) h_0 T_0^2 \exp\left[-\Gamma^2\left(\frac{3}{2}\right)h_0^2 - \Gamma^3\left(\frac{4}{3}\right)T_0^3\right], \quad (7)$$

$$\varphi_2(h_0, T_0) = 8\Gamma^2\left(\frac{3}{2}\right)\Gamma^4\left(\frac{5}{4}\right) h_0 T_0^3 \exp\left[-\Gamma^2\left(\frac{3}{2}\right)h_0^2 - \Gamma^4\left(\frac{5}{4}\right)T_0^4\right]. \quad (8)$$

In both cases we will assume that $\varphi(h_0, T_0) = \varphi(h_0)\varphi(T_0)$, that is, that $\varphi(h_0)$ and $\varphi(T_0)$ are independent and their approximation was taken in the form of a Weibull distribution $\varphi(x) = nAx_0^{n-1} \exp[-Ax_0^n]$, where $A = \Gamma^n(n + 1/n)$. In the first variant $n_h = 2$, $n_T = 3$, in the second $n_h = 2$, $n_T = 4$. These n_h and n_T values were selected on the basis of the experimental values of the variation coefficients which we obtained $C_{VT_0} = 0.31$ and $C_{Vh_0} = 0.52$ for the Black Sea and $C_{VT_0} = 0.34$, $C_{Vh_0} = 0.52$ for the ocean [3, 5]. The determined $\varphi_1(h_0, T_0)$ and $\varphi_2(h_0, T_0)$ values were used in forming two variants of two-dimensional $\varphi(h_0, T_0)$ tables.

Computations were made for all the theoretical distributions.

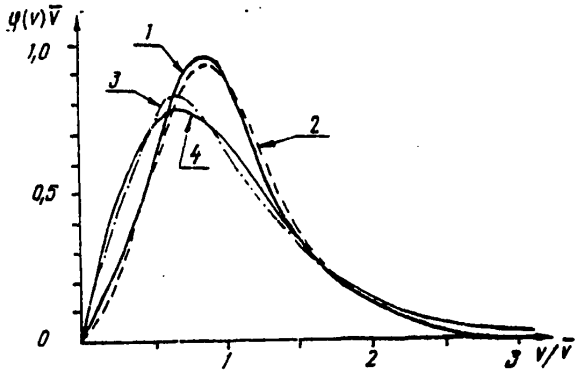

Fig. 2. Distributions $\varphi(v)\bar{v}$: 1) based on experimental data for the Black Sea; 2) on the basis of oceanic data; 3) computations of $\varphi(v)\bar{v}$ from $\varphi(h_0, n_h)$ $\varphi(T_0, n_T)$ with $n_h = 2$, $n_T = 3$ and 4) with $n_h = 2$, $n_T = 4$.

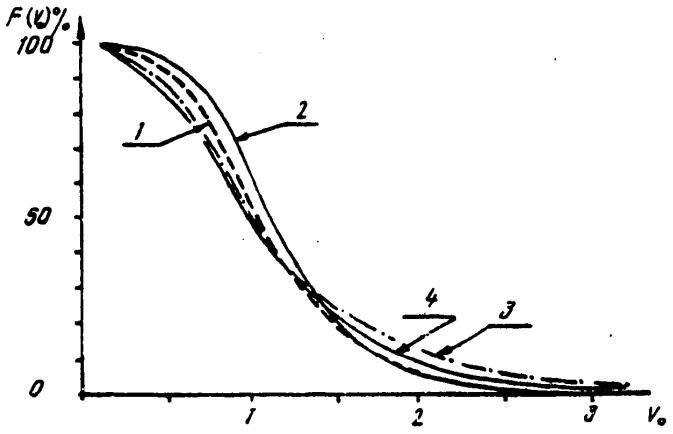

Fig. 3. Integral distribution -- guaranteed probability obtained from the corresponding curves in Fig. 2.

The computed distributions $\varphi(v_0)$ are given in Table 3 (columns 4, 5 and in Fig. 2). In comparing the different curves in Figures 2 and 3 we note that the two different variants with respect to n_T do not give a substantial difference in the values of the approximating computation curves $\varphi(v_0)$. A somewhat greater discrepancy is observed when they are compared with experimental data: the most probable $\hat{\varphi}(v)\bar{v}$ values (Fig. 2) do not coincide; for $v_0 < 1$ the theoretical guaranteed

probability curves are less than the experimental values (Fig. 3). Such a difference between the experimental and computed distributions should be expected since the fundamental assumption of theoretical computations on the equality $\varphi(v_0 \mid T_0) = \varphi(v_0)$ does not correspond to the dependence which we obtained between the conditional distributions and their statistical parameters on T_0, as was mentioned in the first part of the study.

It was demonstrated earlier in [3] on the basis of an analysis of $\varphi(\delta)$, and now in this article in the example of $\varphi(v)$, that the simplified theorem of multiplication of laws (2) is not applicable to computations of the original distribution of waves; it can be considered when $\varphi(h_0 \mid T_0)$ is unknown. In order to refine such computations it is necessary to apply the theorem of multiplication of laws in its general form (1), which agrees with the method which we used in computing different types of distribution on the basis of experimental two-dimensional tables. Accordingly, experimental curves and tables characterizing different distributions of orbital velocities are recommended.

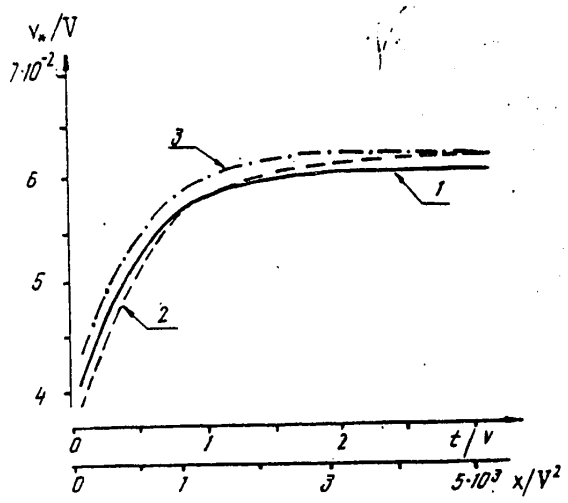

Fig. 4. Changes in V_*/V values at different stages in wave development (t/V): 1) on the basis of experimental data for the Black Sea; 2) for ocean; 3) our computations using the V. V. Shuleykin diagrams method [6].

As the distribution parameter $\varphi(v)$, changing in dependence on the stage of wave development, it is possible to use v_*/V. Its numerical value can be precomputed since it is related to $\bar{h}$ and $\bar{T}$, whose values are determined on the basis of the experimental data in [5]. Figure 4 shows the dependence of v_*/V on t/V, obtained from the dependence of $\bar{h}/V^2$ and $\bar{T}/V$ on t/V. As the latter we took the experimental dependences [3] for the Black Sea and ocean and the prognostic expressions in the V. V. Shuleykin method [6]. It can be seen that there is a specific difference in the course of development of waves in the Black Sea and ocean.

In conclusion we will generalize the scheme for computing orbital velocities. On the basis of the wave-forming factors V, t and x we determine t/V and x/V^2. If on the x-scale (Fig. 4) $x/V^2 < t/V$, the waves must be considered as not developed,

but rather developing [7] and the V_*/V values are determined in this case on the basis of t/V. Computations of well-developed waves are made from the dependence of v_*/V on x/V^2. Since the wind is stipulated, the numerical value of v_*/V and V makes it possible to determine the numerical value $v_* = Vv_*/V$. Then we determine $\bar{v} = \beta v_*$. On the basis of known $\bar{v}$ and the $\varphi(v)\underline{v}$ values we determine $\varphi(v)$, giving the probability of all values of specific $\bar{v} = Vv/V$ different from v. Using Fig. 3 we also determine the guaranteed probability of specific values of orbital velocities. Such a prediction thus gives not only the mean orbital velocity, but all its other values in this stage of wave development with an indication of their probability.

BIBLIOGRAPHY

1. Venttsel', Ye. S., TEORIYA VEROYATNOSTEY (Theory of Probabilities), Moscow, Fizmatgiz, 1962, 561 pages.

2. Davidan, I. N., Lopatukhin, L. I. and Rozhkov, V. A., VETROVOYE VOLNENIYE KAK VEROYATNOSTNYY GIDRODINAMICHESKIY PROTSESS (Wind Waves as a Stochastic Hydrodynamic Process), Leningrad, Gidrometeoizdat, 1978, 285 pages.

3. Korneva, L. A. and Liverdi, V. P., "Distribution of Wave Elements and Wave Steepness in Black Sea," KOMPLEKSNYYE ISSLEDOVANIYA CHERNOGO MORYA (MEZHDUVEDOMSTVENNAYA PROGRAMMA SKOICh) (Multisided Investigations of the Black Sea (Interdepartmental SKOICh Program)), Sevastopol', Izd. MGI AN Ukrainskoy SSR, pp 59-70, 1979.

4. Korneva, L. A., "Statistical Characteristics of Variability of Wave Elements in the Coastal Zone of a Deep Sea (Results of Registry of Waves by the A. A. Ivanov Wave Recorder)," TRUDY MGI (Transactions of the Marine Hydrophysical Institute), Vol 23, Moscow, pp 44-65, 1961.

5. Korneva, L. A. and Liverdi, V. P., "Statistics of Distributions and Spectra of Internal Waves," Sevastopol', Izd. MGI AN Ukrainskoy SSR, pp 109-118.

6. Shuleykin, V. V. and Korneva, L. A., "Development of a Method for Precomputing Waves of a Fixed Guaranteed Probability Using the Results of an Investigation of Waves in a Storm Basin in the Ocean," ISSLEDOVANIYA V OBLASTI FIZIKI OKEANA (Investigations of Oceanic Physics), Sevastopol', Izd. MGI AN Ukrainskoy SSR, pp 39-48, 1969.

7. Korneva, L. A., "Maximum and Energy Width of Wind Wave Spectrum," IZV. AN SSSR: FAO (News of the USSR Academy of Sciences: Physics of the Atmosphere and Ocean), Vol 13, No 7, pp 759-765, 1977.

EFFECT OF GEOMETRY OF PRESSURE DISTURBANCES ON CHARACTERISTICS OF CAPILLARY-GRAVITATIONAL WAVES

Sevastopol' TEORETICHESKIYE I EKSPERIMENTAL'NYYE ISSLEDOVANIYA POVERKHNOSTNYKH I VNUTRENNIKH VOLN in Russian 1980 (manuscript received 19 Jun 80) pp 55-64

[Article by V. V. Trepachev]

[Text]

Abstract: The effect of the geometry of pressure disturbances on the amplitude of generated capillary-gravitational waves at the surface of a homogeneous ideal incompressible fluid of infinite depth is investigated. The pressure disturbance is modeled by a normal stress changing harmonically with time. The article examines the case of generation of surface waves by a platform of ice of finite width oscillating under the influence of a pressure disturbance at its surface. In this problem the pressure of the platform on the fluid is an unknown function and is determined by solution of a mixed problem.

Capillary-gravitational waves caused by surface normal pressures have been studied by the authors of [1, 3, 15]. Problems relating to forced oscillations and diffraction in the presence of a plate of finite width without allowance for surface tension were investigated in [1, 2, 14]. The influence of surface tension and the finiteness of depth was examined in [9].

1. We will examine the problem of forced harmonic oscillations of an ideal incompressible fluid of infinite depth

$$\frac{\partial u}{\partial t} = -\frac{1}{\rho}\frac{\partial p}{\partial x} - \mu u, \quad \frac{\partial v}{\partial t} = -\frac{1}{\rho}\frac{\partial p}{\partial y} - \mu v,$$
$$\frac{\partial u}{\partial x} + \frac{\partial v}{\partial y} = 0, \quad p = p_2 + \rho g y, \tag{1.1}$$
$$-p + \rho g \zeta - \alpha \frac{\partial^2 \zeta}{\partial x^2} = -p^*, \quad \frac{\partial \zeta}{\partial t} = v, \quad y = 0,$$

$$p^* = p^*(x)\, e^{i\omega t}, \qquad u = v = \rho = 0, \quad t < 0,$$

$$(\zeta, u, v, p) \to 0, \qquad (x^2 + z^2)^{1/2} \to \infty.$$

Here u, v are the components of horizontal and vertical velocity; ζ (x,t) is the form of the fluid surface; α is the surface tension coefficient; g is the acceleration of free falling; $\mu > 0$ is the Rayleigh dissipation coefficient [1].

The origin of the Cartesian coordinate system was selected at the undisturbed fluid surface; the y-axis was directed vertically upward. The movement of the fluid was caused by harmonic oscillations of normal pressure P^* with the frequency ω. The motion of the fluid at the initial moment in time is eddy-free and therefore even in the presence of Rayleigh forces the Lagrangian theorem of conservation of potential motion remains correct [1]. Introducing potential using the formulas

$$u = \frac{\partial \varphi}{\partial x} e^{i\omega t}, \quad v = \frac{\partial \varphi}{\partial y} e^{i\omega t}, \quad \zeta = \eta(x) e^{i\omega t}, \tag{1.2}$$

from (1.1) we have a formulation of the problem for potential

$$\frac{\partial^2 \varphi}{\partial x^2} + \frac{\partial^2 \varphi}{\partial y^2} = 0, \quad \frac{p^*(x)}{\rho} = \frac{gi}{\omega}\left(\frac{\partial \varphi}{\partial y} - \nu\varphi - \frac{\alpha}{\rho g}\frac{\partial^3 \varphi}{\partial x^2 \partial y}\right), \quad y = 0, \tag{1.3}$$

$$\omega\eta(x) = -i\frac{\partial \varphi}{\partial y}, \quad y = 0, \quad \nu = \left(\omega^2 - \mu i\omega\right)/g, \tag{1.4}$$

$$\left(\frac{\partial \varphi}{\partial x}, \frac{\partial \varphi}{\partial y}, \frac{\partial^2 \varphi}{\partial x \partial y}, \eta\right) \to 0, \quad (x^2 + y^2)^{1/2} \to \infty.$$

Applying to (1.3) the Fourier transform for the x-coordinate, using the contraction theorem, we obtain integral representations for potential φ and rise of the fluid surface η

$$\varphi(x,y) = -\frac{i\omega}{2\pi\rho g}\int_{-\infty}^{\infty} p^*(\alpha)\,d\alpha \int_0^{\infty} \frac{e^{ky}}{\Delta}\left[e^{-ik(x-\alpha)} + e^{ik(x-\alpha)}\right]dk, \tag{1.5}$$

$$\eta(x) = -\frac{1}{2\pi\rho g}\int_{-\infty}^{\infty} p^*(\alpha)\,d\alpha \int_0^{\infty} \frac{k}{\Delta}\left[e^{-ik(x-\alpha)} + e^{ik(x-\alpha)}\right]dk, \tag{1.6}$$

$$\Delta = k\left(1 + \frac{\alpha}{\rho g}k^2\right) - \nu. \tag{1.7}$$

Here ν was determined by formula (1.4); k is the wave number.

The Δ value on the real k-axis with $\mu \neq 0$ does not become equal to zero; there are no free waves in the solution. The use of the complex frequency method $\omega = \omega_1 - i\omega_2$, $\omega_2 > 0$ [6] in this problem gives a result equivalent to the Rayleigh method. These two methods and others, as well as their correspondence to radiation

principles, were investigated in [1, 5-8].

2. It has been demonstrated that the dispersion relationship (1.7)

$$k\left(1+\frac{\alpha}{\rho g}k^2\right)-\nu=0 \tag{2.1}$$

has three complex roots with $\mu \neq 0$:

$$k_0,\quad Re(k_0)>0,\quad Im(k_0)<0\ ; \tag{2.2}$$

$$m_1=-\frac{k_0}{2}+i\sqrt{\frac{g\rho}{\alpha}+\frac{3}{4}k_0^2},\quad m^2=\frac{g\rho}{\alpha}+\frac{3}{4}k_0^2\ ; \tag{2.3}$$

$$m_2=-\frac{k_0}{2}-i\sqrt{\frac{g\rho}{\alpha}+\frac{3}{4}k_0^2},\qquad Re\sqrt{m^2}>0. \tag{2.4}$$

With $\alpha=\mu=0$ the root $k_0=\omega^2/g$ [1]; computation of the complex root k_0 (situated in the fourth quadrant of the complex wave number k) is convenient by the successive approximations method [13]

$$k_{n-1}\frac{g}{\omega^2}=\frac{1-\mu i/\omega}{1+\alpha k_n^2/\rho g},\quad k_{n+1}\frac{g}{\omega^2}=A(k_n),\quad n=1,2,3\ldots,$$
$$\lim_{n\to\infty}k_n=k_0,\quad k_0\approx k_2=\nu/\left(1+\alpha\nu^2/\rho g\right),\quad \nu\to 0. \tag{2.5}$$

For the contraction operator A(k) we obtain the evaluation

$$\left|A(k_{n+1})-A(k_n)\right|<\left|k_{n+1}-k_n\right|\varepsilon, \tag{2.6}$$

$$k_n,\ k_{n+1}\in\left\{|k|<\frac{\varepsilon\rho g}{2\alpha\left(1+\mu^2/\omega^2\right)},\quad Re\,k\geq|Im\,k|>0\right\}. \tag{2.7}$$

Here ε is equal to a unit length in the selected system of units. With $\mu=0$ in a volume of fluid under the free surface an arbitrariness in finding of the solutions appears which is determined by functions of the type

$$\varphi=Ce^{-im_1z},\quad \bar{C}e^{im_2\bar{z}}\ ; \tag{2.8}$$

$$\varphi=De^{-im_2z},\quad \bar{D}e^{im_1\bar{z}}\ ; \tag{2.9}$$

$$z=x+iy,\quad x>0,\quad y\leq 0. \tag{2.10}$$

Here

$$m_1=-k_0/2+im,\quad m_2=\bar{m}_1,\quad k_0,\quad m>0,$$
$$\bar{z}=x-iy,\quad \mu=0,\quad \rho^*(x)=0,\quad x>0. \tag{2.11}$$

The solutions (2.8), (2.9) satisfy the Laplace equation and the free-surface condition (1.3), (2.11). The solutions (2.8) are exponentially increasing in the fluid volume under the free surface (2.10). The first solution (2.9) corresponds to the wave process propagating from the depth of the fluid; the second solution (2.9) determines the wave process propagating into the depth of the fluid. For the

solution of (2.9) in the volume of fluid beneath the free surface (2.10) there are two qualitatively different zones

$$y < -2m\,x / k_0 , \tag{2.12}$$

$$y \geq -2m\,x / k_0 . \tag{2.13}$$

In (2.12) the solutions of (2.9) increase exponentially; in (2.13) they decrease exponentially. In order to satisfy the condition of decrease of the solution in the entire region under the free surface of the fluid (2.10) it must be assumed that C = D = 0. The arbitrariness in solution of the problem, supplied with the root of the dispersion relationship k_0, with $\mu = 0$, was studied in [1, 2]. With $\mu \neq 0$ the solution, determined by the root k_0, represents a wave penetrating into the depth of the fluid only in the region $x > 0$, $y < 0$, $y/x > \mathrm{Re}(k_0)/\mathrm{Jm}(k_0)$. The non-dependence of the Rayleigh dissipation coefficient μ on wave scale makes difficult the applicability of the model in [6]. We will examine the dispersion relationship for a viscous incompressible fluid [15] (with a Laplace transform parameter $s = i\omega$)

$$gk - 4k^3\varepsilon^2 p + (i\omega + 2\varepsilon k^2)^2 = gk - \omega^2 + 4k^2 i\omega\varepsilon \frac{p}{p+k} = 0, \tag{2.14}$$

where

$$p = \sqrt{k^2 + i\omega/\varepsilon}\ , \quad \mathrm{Re}\, p > 0.$$

The influence of viscosity is determined by the value of the last term in equation (2.14), the factor $p/(p + k) \sim 1$, $k \to 0$; $p/(p + k) \sim 1/2$, $k \to \infty$; the mean is $p/(p + k) \sim 3/4$, $k \in (k \to 0,\ k \to \infty)$.

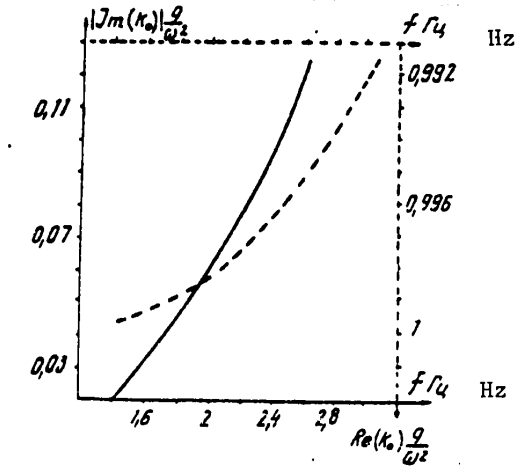

Fig. 1.

Using the mean value of the factor $p/(p + k)$ for the wave number and making one iteration in (2.14) (with an initial value $k = \omega^2/g$), we have an evaluation of the order of magnitude of

$$\mu(\omega, \varepsilon) \approx \frac{\vartheta \omega^4 \varepsilon}{g^2}. \tag{2.15}$$

Here ε is the kinematic viscosity coefficient. The results of computations of the k_0 of the dispersion relationship (2.1) are reflected in Fig. 1.

3. We will study the form of the fluid surface $\eta(x)$ for pressure disturbances $p^*(x)$ exerting a direct effect on the fluid surface. We will examine pressure in the form

$$p_1^*(x) = Q\delta(x), \quad \tilde{p}_1^* = Q, \tag{3.1}$$

$$p_2^*(x) = \begin{cases} Q/2a, & |x| < a, \\ 0, & |x| > a, \end{cases} \quad \tilde{p}_2^* = Q\frac{\sin ka}{ka}, \tag{3.2}$$

$$p_3^*(x) = \begin{cases} \frac{Q}{\pi a^2}\sqrt{a^2 - x^2}, & |x| < a, \\ 0, & |x| > a, \end{cases} \quad \tilde{p}_3^* = Q\frac{J_1(ka)}{ka}, \tag{3.3}$$

$$p_4^*(x) = \frac{Qa}{\pi(a^2 + x^2)}, \quad \tilde{p}_4^* = Qe^{-|k|a}. \tag{3.4}$$

Here

$$\tilde{p}_n^* = \int_{-\infty}^{\infty} p_n^*(x) e^{ikx} dk, \quad n = 1 \div 4;$$

δ is the Dirac delta function; J_1 is a Bessel function of the first kind; Q is the magnitude of the total force acting on the loaded water surface, related to a unit width. Using contour integration [10] from (1.6), (3.1)-(3.4) we determine

$$\eta(x) = \frac{\tilde{p}_n^*(k_0)}{\rho g}\frac{ik_0 e^{-ik_0|x|}}{1 + \vartheta\alpha k_0^2/\rho g} - \frac{\nu}{\pi\rho g}\int_0^{\infty} \frac{\nu \tilde{p}_n^*(i\nu)e^{-\nu|x|}}{\nu^2 + \nu^2(1 - \alpha\nu^2/\rho g)^2} d\nu, \tag{3.5}$$

$$|x| \geq 0, \ n = 1; \quad |x| > a, \ n = 2, 3;$$

$$\eta(x) = \frac{Qe^{-k_0 a}}{\rho g}\frac{ik_0 e^{-ik_0|x|}}{1 + \vartheta\alpha k_0^2/\rho g} - \frac{Q}{\pi\rho g}\int_0^{\infty} \nu e^{-\nu|x|} \times$$

$$\times \frac{[\nu\cos\nu a + \nu\sin\nu a\left(1 - \frac{\alpha}{\rho g}\nu^2\right)]}{\nu^2 + \nu^2(1 - \alpha\nu^2/\rho g)^2} d\nu, \quad |x| \geq 0. \tag{3.6}$$

Applying the method of integration by parts to (3.5) and (3.6) we obtain asymptotic formulas of the fluid surface type

$$\eta_1(x) \sim \frac{Q}{a\rho g}\left\{\frac{ik_0 e^{-ik_0|x|}}{1 + \vartheta\alpha k_0^2/\rho g} - \frac{\nu a}{\pi}\frac{1}{x^2\nu^2}\left[1 - \frac{6}{x^2\nu^2}\right]\right\}, \tag{3.7}$$

$$\eta_2(x) \sim \frac{Q}{a\rho g}\left\{\frac{i\sin(k_0 a)e^{-ik_0|x|}}{1+\beta\alpha k_0^2/\rho g} - \frac{\nu a}{\pi}\frac{1}{x^2\nu^2}\left[1-\frac{a^2\nu^2-6}{x^2\nu^2}\right]\right\},$$

$$\eta_3(x) \sim \frac{Q}{a\rho g}\left\{\frac{iJ_1(k_0 a)e^{-ik_0|x|}}{1+\beta\alpha k_0^2/\rho g} - \frac{\nu a}{\pi}\frac{1}{x^2\nu^2}\left[1+\frac{\beta}{4}\frac{a^2\nu^2-16}{x^2\nu^2}\right]\right\}, \qquad (3.7)$$

$$\eta_4(x) \sim \frac{Q}{a\rho g}\left\{\frac{ik_0 a e^{-k_0 a}e^{-ik_0|x|}}{1+\beta\alpha k_0^2/\rho g} - \frac{\nu a}{\pi}\frac{1}{x^2\nu^2}\left[1+\frac{\beta(2\nu a-\nu^2a^2-2)}{x^2\nu^2}\right]\right\};$$

$$|x|\nu \to \infty, \quad |x|/a \to \infty. \qquad (3.8)$$

Here $\eta_n(x)$ (n = 1-4) correspond in number to the stresses (3.1)-(3.4); k_0 is the root of the dispersion relationship (2.2). Multiplying (3.7) by $e^{i\omega t}$, we draw the conclusion that the solution consists of a travelling wave and level fluctuations. The level fluctuations decrease exponentially with distance. The level fluctuations for the pressure $p_3^*(x)$ in the region of parameters (3.8) are half as great as for the pressures $p_1^*(x)$, p_2^*, p_4^*.

The principal terms of the asymptotic forms of level fluctuations for the pressures p_1^*, p_2^*, p_4^* coincided and for the pressures p_2^*, p_3^*, p_4^* have a single type -- the type of the main term of the asymptotic form of level fluctuation caused by a deltalike pressure $p_1^*(x) = Q\,\delta(x)$.

In the considered examples the influence of the geometry of the pressure disturbance on fluctuations of fluid level is manifested in the higher terms of the approximation of asymptotic forms over great distances (3.7), (3.8).

According to (3.7), (2.2), the wave terms decrease with distance exponentially, whereas fluctuations of fluid level decrease in conformity to a power law, and at quite great distances from the pressure epicenter only fluctuations of the fluid level are observed.

The general form of the wave term is represented by the term outside the integral in formula (3.5). Computations show that an increase in the frequency of the forced oscillations ω (g, α are fixed, $\mu = 3\omega^4\varepsilon/g^2$ (2.5)) decreases the wavelength $\lambda = 2\pi/\mathrm{Re}(k_0)$ and the value of the amplitude factor $\exp(\mathrm{Jm}(k_0)\,|\,x\,|\,)$, $\mathrm{Jm}\,k_0 < 0$, $|\,x\,| = \mathrm{const}$. We will study the behavior of wave amplitude without taking into account the spatial variability factor $\exp(-i\,k_0\,|\,x\,|\,)$. For pressures (3.1)-(3.4) it has the form

$$A_1 = \frac{k_0}{1+3\alpha k_0^2/\rho g}, \quad A_2 = \frac{\sin k_0 a}{1+3\alpha k_0^2/\rho g},$$
$$A_3 = \frac{J_1(k_0 a)}{1+3\alpha k_0^2/\rho g}, \quad A_4 = \frac{k_0 e^{-k_0 a}}{1+3\alpha k_0^2/\rho g}. \tag{3.9}$$

The values of the amplitudes A_n (n = 1-4) with each fixed surface tension value α, according to the "compressed images" principle (2.6), in the region of the complex wave number (2.7), can be investigated as a function of one complex variable k_0. The poles of the amplitudes A_n (n = 1-4) are purely imaginary $k_0 = \pm\sqrt{\rho g/3\alpha}$ and do not belong to the region of determination (2.7). In accordance with the properties of the harmonic functions [10] the Re A_n, Jm A_n values cannot attain their extremal values at the internal points of the determination region and in the neighborhood of the zeroes of their first derivatives have a saddlelike form. A special case of internal points in the region (2.7) is real k_0 values ($\mu = 0$, ideal fluid without dissipation). Hence we draw the conclusion that

$$|A_n(k_0)| > |A_n(\mathrm{Re}\, k_0)| : \frac{\partial A_n}{\partial k} = 0, \quad k = \mathrm{Re}\, k_0 > 0, \quad n = 1 \div 4. \tag{3.10}$$

According to (3.10), the moduli of the amplitudes A_n, with allowance for dissipation, are greater than the moduli of the extremal values A_n for a fluid without allowance for dissipation with equal wave lengths. Without allowance for dissipation we derived the formulas

$$\left|\frac{A_2}{A_1}\right| < 1, \quad \left|\frac{A_3}{A_1}\right| < 1, \quad \left|\frac{A_4}{A_1}\right| < 1, \quad \mu = 0, \quad 0 < \omega < \infty;$$
$$A_1 < \frac{1}{2}\sqrt{\frac{g\rho}{3\alpha}}, \quad 0 < \omega < \infty, \quad \omega \neq \omega^*, \quad \mu = 0, \tag{3.11}$$
$$\omega^* = \sqrt{\frac{4}{3} g \sqrt{\frac{g\rho}{3\alpha}}}, \quad \lambda^* = 2\pi\sqrt{\frac{3\alpha\rho}{g}}.$$

According to (3.11), the amplitude A_1 ($\mu = 0$) has one maximum at the frequency ω^* (α = 70 dynes/cm, λ^* = 2.9 cm, $f^* = 2\pi/\omega^*$ = 8.46 Hz). With large $k_0 a$ values the amplitude A_4 is an exponentially decreasing function, and the amplitude A_3 has an asymptote [11] in the form

$$A_3 \sim \sqrt{\frac{2}{\pi k_0 a}} \frac{\cos(k_0 a - 3\pi/4)}{1+3\alpha k_0^2/\rho g}. \tag{3.12}$$

With small values $k_0 a$ the amplitudes A_2, A_3, A_4 have an order of change equivalent to A_1.

4. The force effect of a rigid freely floating ice platform of finite width at the surface of a fluid with harmonic oscillations of pressure at the surface of the platform is determined from solution of the problem

$$\Delta\varphi = 0, \quad \frac{\partial\varphi}{\partial y} = v(x), \quad |x| < a, \quad y = 0; \tag{4.1}$$

$$p^*(x) = \frac{\rho i}{\omega} f(x), \quad p^*(x) = 0, \quad |x| > a; \tag{4.2}$$

$$f(x) = \frac{\partial\varphi}{\partial y} - \nu\varphi - \beta\frac{\partial^3\varphi}{\partial x^2\partial y}, \quad y = 0, \quad \nu = \frac{\omega^2}{g}, \quad \beta = \frac{\alpha}{\rho g}. \tag{4.3}$$

Here $p^*(x)$ is the pressure of the ice platform on the water; v(x) is the velocity of points on the ice platform in a vertical direction (known value). By the method developed in [1] the solution (4.1)-(4.3) is reduced to solution of an integro-differential equation relative to the f(x) function (4.3)

$$f(x) - \beta\frac{\partial^2 f}{\partial x^2} = f(0) - \beta f''(0) + \int_0^x W(\alpha)\,d\alpha + \frac{\nu}{\pi}\int_{-a}^{a} f(\alpha)\ln\left|\frac{\alpha - x}{x}\right| d\alpha, \tag{4.4}$$

$$W(x) = f'(0) + i\nu f(0) - \beta f'''(0) + \frac{\nu}{\pi}\int_c \frac{f(\alpha)\,d\alpha}{\alpha} + \int_0^x \left(\frac{\partial^2 v}{\partial x^2} + \nu v + \beta^2\frac{\partial^6 v}{\partial x^6}\right) \tag{4.5}$$

The problem (4.3) is soluble in a class of harmonic functions with satisfaction of the conditions

$$\begin{aligned}
&-v(0) + f(0) + \frac{\nu}{2}\varphi(0) + \beta v_{xx}''(0) = 0,\\
&-v'(0) + f'(0) + \nu u(0) + \beta v_{xxx}'''(0) = 0,\\
&-v''(0) + f''(0) + \nu u'(0) + \beta v_{xxxx}^{IV}(0) = 0,\\
&-v'''(0) + f'''(0) + \nu u'(0) + \beta v_{xxxxx}^{V}(0) = 0,\\
&-v(r) + f(r) + \frac{\nu}{2}\varphi(r) + \beta v_{xx}''(r) = 0.
\end{aligned} \tag{4.6}$$

with

$$m_0 r \neq n\pi, \quad 0 < r < a, \quad n = 0, 1, 2 \ldots . \tag{4.7}$$

Here φ is the potential determined from (1.5) by a limiting Rayleigh transition [1], $u = \partial\varphi/\partial x$ is horizontal velocity; m_0 is a real positive root of the equation $\nu^2 - m^2(1 + B^2m^4)$. In the derivation of (4.5)-(4.7) we used the conditions of absence of arbitrariness (2.8), (2.9). The nonsatisfaction of the conditions (4.7) in limiting cases a = 0, $\nu = 0$ ($\nu = 0 \sim m_0 = k_0 = 0$) gives a solution in the class of generalized functions. With a = 0 the solution has the form (3.1). With $\nu = 0$, $v/\omega = h = \text{const}$ (4.1) the pressure consists of hydrostatic and capillary

(two delta functions along the edges $x = \pm a$; a solution was obtained by the method in [12]). The total force acting on the platform in a unit width ℓ, with $\nu = 0$, is equal to

$$Q = \int_{-a}^{a} p^*(x)\,dx = 2\rho g h a \ell \left[1 + \sqrt{\frac{\alpha}{\rho g a^2}}\right]. \qquad (4.8)$$

Here h is the depth of platform submergence. The contribution of capillary pressure to the total force Q with large a is really small. A numerical analysis of the problem (4.1)-(4.3) was made by the trapezia method [4]. The results of computations of pressure and the modulus of wave amplitude are given in Figures 2 and 3.

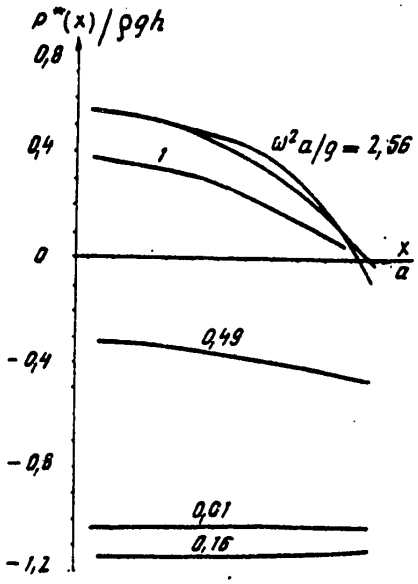

Fig. 2.

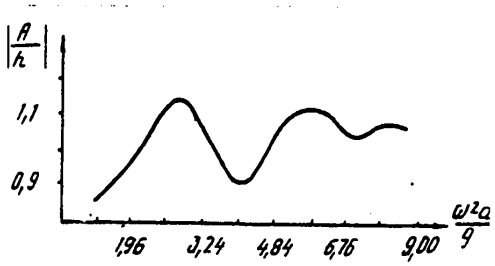

Fig. 3.

With small values of the parameters $\omega^2 a/g$, $\alpha/\rho g a^2$ the pressure developed at the fluid surface by the ice platform is close to hydrostatic (Fig. 2). The high-frequency asymptote of the dynamic part of the pressure is analyzed using the formulas (3.3), (3.9), (3.12). The results of the work are in qualitative agreement with [1, 2]. The main conclusion is that pressure distributed over the entire area of the fluid (3.4) causes traveling waves of lesser amplitude than concentrated pressures when there is an identical total force.

BIBLIOGRAPHY

1. Sretenskiy, L. N., TEORIYA VOLNOVYKH DVIZHENIY ZHIDKOSTI (Theory of Wave Movements of a Fluid), Moscow, "Nauka," 1977, 815 pages.

2. Khaskind, M. D., GIDRODINAMICHESKAYA TEORIYA KACHKI KORABLYA (Hydrodynamic Theory of Ship Rolling), Moscow, "Nauka," 1973, 327 pages.

3. Cherkesov, L. V., POVERKHNOSTNYYE I VNUTRENNIYE VOLNY (Surface and Internal Waves), Kiev, "Naukova Dumka," 1973, 247 pages.

4. Pavlenko, P. Ye., IZBRANNYYE TRUDY (Selected Works), Kiev, "Naukova Dumka," 1978, 222 pages.

5. Gossard, E. E. and Khuk, U. Kh., VOLNY V ATMOSFERE (Atmospheric Waves), Moscow, "Mir," 1978, 277 pages.

6. Andronov, A. A. and Fabrikant, A. L., "Landau Attenuation, Wind Waves and Whistles," NELINEYNYYE VOLNY (MATERIALY 4-ya VSESOYUZNOY SHKOLY PO NELINEYNYM VOLNAM) (Nonlinear Waves (Materials of the Fourth All-Union School on Nonlinear Waves)), Moscow, "Nauka," 1979, 78 pages.

7. Vorovich, I. I. and Babeshko, V. A., DINAMICHESKIYE SMESHANNYYE ZADACHI TEORII UPRUGOSTI DLYA NEKLASSICHESKIKH OBLASTEY (Dynamic Mixed Problems in Elasticity Theory for Nonclassical Regions), Moscow, "Nauka," 1979, 319 pages.

8. Abramyan, B. A., et al., RAZVITIYE TEORII KONTAKTNYKH ZADACH V SSSR (Development of the Theory of Contact Problems in the USSR), Moscow, "Nauka," 1976, 492 pages.

9. Andreyeva, T. I., Potetyunko, E. N. and Trepachev, V. V., "Waves Caused by a Vibrator," TEZISY DOKL. VSESOYUZN. NAUCHN. KONF. PO SMESHANNYM ZADACHAM MEKHANIKI DEF. TELA (Summaries of Reports at the All-Union Scientific Conference on Mixed Problems in the Mechanics of Deformable Bodies), Part 1, Rostov-na-Donu, 1977, 158 pages.

10. Lavrent'yev, M. A. and Shabat, M. B., METODY TEORII FUNKTSIY KOMPLEKSNOGO PEREMENNOGO (Methods in the Theory of Functions of a Complex Variable), Moscow, "Nauka," 1973, 736 pages.

11. Gradshteyn, I. S. and Ryzhik, I. M., TABLITSY INTEGRALOV, SUMM, RYADOV I PROIZVEDENIY (Tables of Integrals, Summs, Series and Products), Fifth Edition, Moscow, "Nauka," 1971, 1108 pages.

12. Zabreyko, P. P., et al., INTEGRAL'NYYE URAVNENIYA (Integral Equations), SMB, Moscow, "Nauka," 1968, 448 pages.

13. Kolmogorov, A. N. and Fomin, S. V., ELEMENTY TEORII FUNKTSIY I FUNKTSIONAL'NOGO ANALIZA (Elements of the Theory of Functions and Functional Analysis), Third Edition, Moscow, "Nauka," 1972, 496 pages.

14. Vityuk, V. F., "Diffraction of Surface Waves on Docks of Finite Width," PMM (Applied Mathematics and Mechanics), Vol 34, No 1, pp 32-40, 1970.

15. Potetyunko, E. N., ASIMPTOTICHESKIY ANALIZ POVERKHNOSTNYKH VOLN (Asymptotic Analysis of Surface Waves), ISKNTsVSh, No 4, pp 71-74, 1973.

UNSTEADY FLEXURAL-GRAVITATIONAL WAVES FROM IMPULSE DISTURBANCES UNDER ICE COMPRESSION CONDITIONS

Sevastopol' TEORETICHESKIYE I EKSPERIMENTAL'NYYE ISSLEDOVANIYA POVERKHNOSTNYKH I VNUTRENNIKH VOLN in Russian 1980 (manuscript received 8 Apr 80) pp 65-73

[Article by A. Ye. Bukatov and A. A. Yaroshenko]

[Text]

Abstract: A study was made of the process of development of waves from impulse disturbances in a sea covered with ice. Ice compression and dilatation are taken into account. It is demonstrated that ice compression increases and dilatation decreases the time required for waves to pass through a stipulated point. In addition, ice compression can lead to the formation of compression waves not arising in the absence of compressive forces. The conditions for generation of these waves were determined and the dependence of their elements on the magnitude of the compressive force were determined.

Unsteady oscillations of the ice cover in the absence of dilatational and compressive forces were investigated in [1-3]. The development of flexural-gravitational waves, caused by periodic disturbances under conditions of longitudinal dilatation, was studied in [4], and in the case of longitudinal compression in [5].

In this article we give an analysis of the influence of longitudinal compression and dilatation on waves from impulse disturbances. As the wave generator we will examine a small displacement of a sector of the bottom of the basin occurring with the vertical velocity

$$w = af(x)\varphi(t), \quad \varphi(0) = 0, \tag{1.1}$$

beginning from the moment in time t = 0. The investigation was carried out on the assumption that prior to the onset of exposure to disturbance the fluid is at rest and the ice-water surface is horizontal. The velocity potential φ of wave movement of the fluid under conditions of longitudinal dilatation [2,6] is determined from the equation

$$\varphi_{xx} + \varphi_{zz} = 0, \quad -H < z < 0, \quad |x| < \infty \tag{1.2}$$

the boundary and initial conditions

$$D_1 \zeta_{xxxx} - Q_1 \zeta_{xx} + \varkappa \zeta_{tt} + \zeta + \frac{1}{g}\varphi_t = 0 \qquad \text{with } z = 0,$$

$$\varphi_z = w \text{ with } z = -H, \quad \varphi_2 = \zeta_t \text{ with } z = 0, \quad \varphi = \zeta = 0 \text{ with } t = 0. \tag{1.3}$$

Here

$$D_1 = \frac{D}{\rho_1 g}; \quad Q_1 = \frac{Q}{\rho_1 g}; \quad \varkappa_1 = \frac{\rho_1 h}{\rho g}; \quad D = \frac{Eh^3}{12(1-\mu^2)};$$

E, h, ρ_1, μ are the modulus of normal elasticity, thickness, density and Poisson coefficient of ice; ρ is fluid density; Q is the longitudinal dilatational force imparted to a unit width of the ice plate; ζ is flexure of the ice or the rise of the ice-water surface.

Applying the Fourier transform for x and the Laplace transform for t for solution of the problem, we find

$$\zeta = \frac{a}{\sqrt{2\pi}} \int_{-\infty}^{\infty} \frac{\bar{f}(r)}{\operatorname{ch} rH} K(r,t) e^{irx}\, dr, \quad K = \frac{1}{2\pi i} \int_{\omega-i\infty}^{\omega+i\infty} \frac{\alpha \psi(\alpha)}{\alpha^2 B_1 + B_2} e^{\alpha t}\, d\alpha, \tag{1.4}$$

$$B_1 = 1 + \varkappa_1 \cdot rg \operatorname{th} rH, \quad B_2 = rg\, B_1(r) \operatorname{th} rH, \quad \theta_1 = 1 + Q_1 r^2 + D_1 r^4,$$

where $\bar{f}(r)$ is the Fourier transform of the function f(x); $\bar{\psi}(\alpha)$ is the Laplace transform of the $\psi(t)$ function. Hence for $\psi(\alpha) = \delta(t - t_0)$, $t_0 > 0$, where $\delta(t)$ is the Dirac delta function, we obtain

$$\zeta = \frac{1}{2\sqrt{2\pi}} \int_{-\infty}^{\infty} \frac{\bar{f}(r)}{B_1 \operatorname{ch} rH} \left[e^{i|x| M_1(r)} + e^{i|x| M_2(r)} \right] dr, \tag{1.5}$$

$$M_{1,2} = r \operatorname{sign} x \pm \nu \tau(r), \quad \nu = \frac{t}{|x|}, \quad \tau(r) = \left(B_2 / B_1\right)^{1/2}.$$

Here the subscript 1 on $t_1 = t - t_0$ has been omitted. From (1.5), using the stationary phases method, we find an asymptotic expression for ζ. The presence of stationary points for the phase functions $M_{1,2}(r)$ with fixed ν is determined by the behavior of the function $\tau'(r)$. Its dependence on the magnitude of the dilatational force is similar to the dependence of the frontal velocity of nonattenuating waves generated by disturbances which are periodic in time. It was studied in [4] and is illustrated there in Fig. 2. It follows from the data in the figure that M_2 with $\nu^{-1} < u_2$ does not have stationary points (true roots of the equation $M_2'(r) = 0$). For $\nu^{-1} > u_1$ and $u_2 < \nu^{-1} < u_1$ the stationary points will be $r = r_2$ and $r = r_1$, $r = r_2$ if $x > 0$ or $r = -r_2$ and $r = -r_1$, $r = -r_2$, if $x < 0$. The conditions for existence of the stationary points for $M_1(r)$ are the same as for $M_2(r)$ and the stationary points for M_2 differ from the points for M_1 only in sign.

Here $u_1 = \lim_{r \to 0} \tau'(r) = \sqrt{gH}$; $u_2 = \tau'(r_0)$; r_0 is a positive root of the equation $\tau''(r) = 0$, the stationary points $r = \pm r_2$ are governed by the elastic forces of the ice cover.

Thus, after use of the stationary phases method we find

$$\zeta = \begin{cases} \zeta_2 + O\left(\frac{1}{|x|}\right), & |x| > u_1 t, \\ \zeta_1 + \zeta_2 + O\left(\frac{1}{|x|}\right), & u_2 t < |x| < u_1 t, \\ O\left(\frac{1}{|x|}\right), & |x| < u_2 t, \end{cases} \tag{1.6}$$

$$\zeta_k = \frac{1}{|x|} A(r_k) \cos\left[r_k |x| - t\tau(r_k) - (-1)^k \frac{\pi}{4}\right], \quad k = 1, 2,$$

$$A = \frac{\bar{f}(r)}{B_1(r) \operatorname{ch} rH \sqrt{j \tau''(r)}}, \quad j = \begin{cases} -1, & k = 1, \\ 1, & k = 2. \end{cases}$$

Accordingly, the wave ζ_2, caused by elastic forces, arrives at a fixed point earlier than the gravitational wave ζ_1, in this case not having a clearly expressed leading edge. The leading edge of the gravitational waves moves from the epicenter of the disturbances with the velocity u_1. The trailing edges of the elastic and gravitational waves coincide with one another and move with the identical velocity u_2, dependent on the ice thickness, the modulus of normal elasticity of the ice and the magnitude of the dilatational force. A large dilatational force also corresponds to a high velocity of the trailing edge. Qualitatively there is the same character of the dependence of u_2 on ice thickness.

In a general case it is impossible to find an analytical expression for the stationary points (roots of the equations $M'_{1,2}(r) = 0$) as functions of x and t, but numerically they can be found with the required degree of accuracy with stipulated x and t and thus it is possible to form a quantitative picture of the change in ζ with the course of time at an arbitrary fixed point and the pattern of waves at a fixed moment in time.

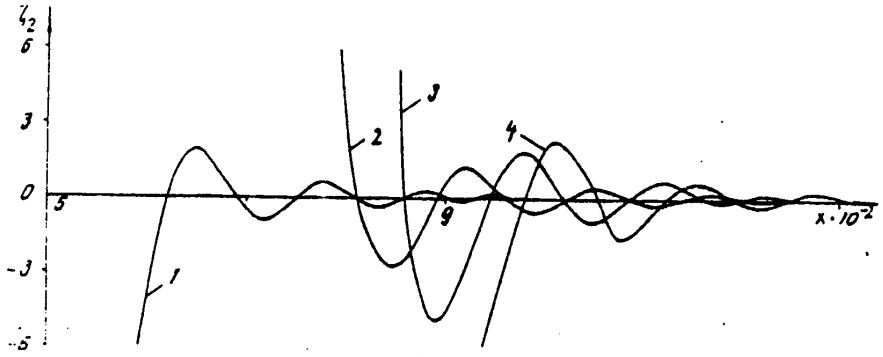

Fig. 1.

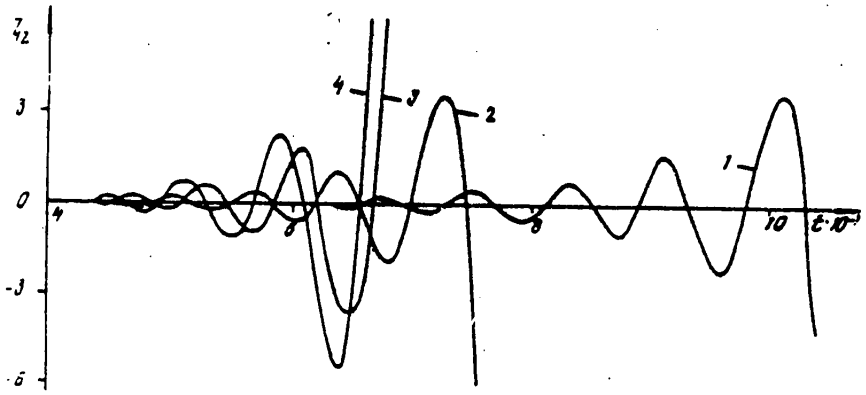

Fig. 2.

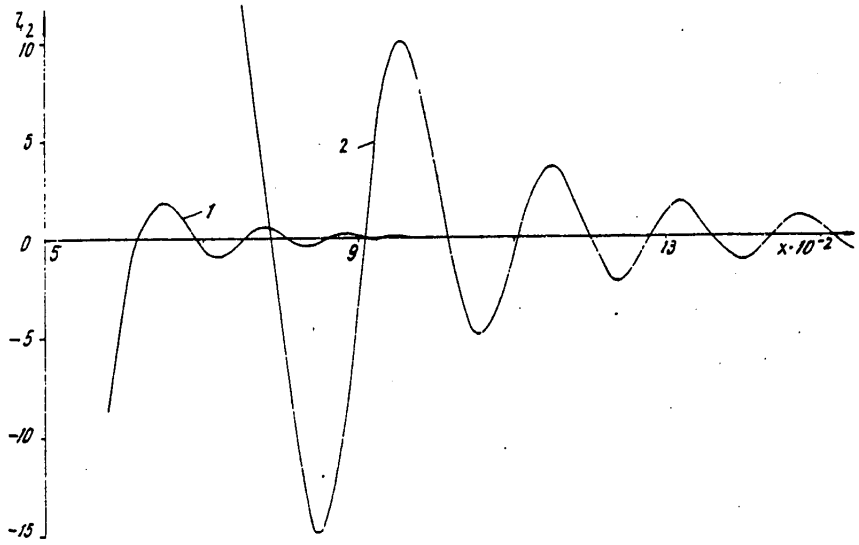

Fig. 3.

Changing with an adequately small interval r and taking into account that in the intervals $(0, r_0)$ and (r_0, ∞) the dependence between t and r is mutually unambiguous and that time increases with an increase in r in the interval $(0, r_0)$, but with an increase in r in (r_0, ∞) decreases, it is possible without finding the roots of the equation $M'_{1,2}(r) = 0$ to employ formulas (1.6) to form the pattern of behavior of ζ_1 and ζ_2 with time at a fixed point, computing t using the formula $t = x\tau^{-1}(r)$. Similarly, we obtain the dependence of ζ_1 and ζ_2 on x at a fixed moment in time. In this case x is determined from the expression $x = t\tau(r)$. The distributions of ζ_2 relative to x obtained in this way for t = 60 sec and relative to t for $x = 10^3$m in the case of a deltalike displacement of a sector of the

bottom with values of the parameters $E = 3 \cdot 10^9 N/m^2$, $\mu = 0.34$, $\rho = 870$ kg/m^3, $H = 10$ m are shown with an accuracy to the factor $a \cdot 10^{-4}$ in Figures 1-4. The curves 1-4 in Figures 1, 2 are given for $h = 1$ m. They correspond to dilatational forces 0, $1.68 \cdot 10^6$, $2.52 \cdot 10^6$, $3.03 \cdot 10^6$N/m. However, the dependence of the distribution of ζ_2 relative to x and t on ice thickness (Figures 3, 4) is illustrated in the case $Q = 0$. With other Q the pattern is qualitatively similar. The curves 1, 2 in Figures 3, 4 relate to thickness of the ice plate 1 and 2 m.

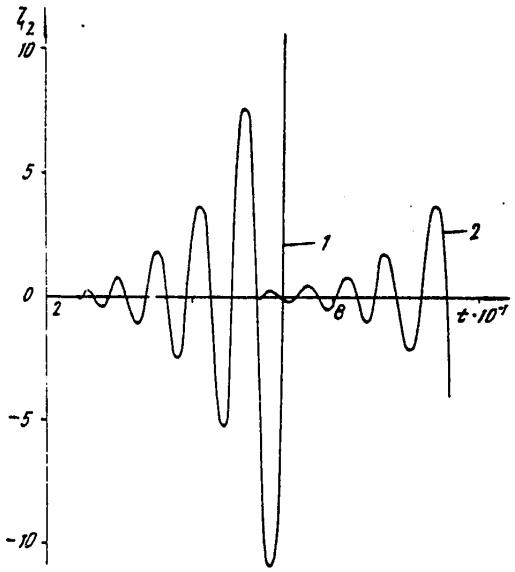

Fig. 4.

The extreme right values of each of the curves in Figures 2, 4 correspond to the moments in time close to the moment of passage of the trailing edge of the waves through a stipulated point. The extreme left points of the curves in Figures 1, 3 characterize the amplitude in the neighborhood of the trailing edge at a fixed moment in time. In this neighborhood the asymptotic formulas (1.6) do not apply, but the ζ_2 computed from them assumes an infinitely large value.

An analysis of the data in Figures 1-4 shows that with the course of time the vertical amplitude of the oscillations $\zeta_2(t)$ increases. The time for passage of the waves (1.6) through a stipulated point decreases with an increase in the dilatational force. It also decreases with an increase in the thickness of the ice plate. At a fixed moment in time the oscillations caused by elastic waves attenuate with distance from the epicenter of the disturbances both with an increase in h and with an increase in the dilatational force. The influence of longitudinal dilatation with a fixed force is manifested more clearly in the case of a lesser ice thickness.

2. Now we will analyze the process of development of waves arising under the influence of small vertical displacements of a sector of the bottom under ice compression conditions [2, 6, 7]. The generated wave movement is determined by the velocity potential φ satisfying the Laplace equation (1.2), initial and boundary conditions (1.3) at the bottom and

$$D_1\zeta_{xxxx} + Q_1\zeta_{xx} + \varkappa_1\zeta_{tt} + \zeta + \frac{1}{g}\varphi_z = 0, \quad \zeta_t = \varphi_z$$

at the undisturbed ice-water surface.

Solving the problem as in the case of longitudinal dilatation, for ζ we obtain the integral representation (1.4), where it must be assumed that $\theta_1 = 1 - Q_1 r^2 + D_1 r^4$. For a deltalike function $\psi(t)$ the integral (1.4) is reduced to (1.5), which we compute by the stationary phases method with $Q_1 < 2\sqrt{D_1}$, necessary for stability of the ice plate [2].

Assume that $Q_1 < Q_0$, where Q_0 is determined by the same expression as in [5]. Under such a condition the phase functions $M_{1,2}(r)$ behave qualitatively the same as under longitudinal dilatation conditions. This is attributable with the given condition to the qualitatively similar behavior of $\tau(r)$ for dilatational and compressive forces. In the first case $\tau(r)$ coincides with $\sigma(r)$ in Fig. 1 in [4], and in the second case with $\sigma(r)$ in Fig. 1 in [5], where the upper two curves are given for Q_1, satisfying the condition $Q_1 < Q_0$. A comparison of these figures, and also Fig. 2 from [4] with Fig. 4,b from [5], shows that in this case the condition of existence of stationary points for the phase functions $M_{1,2}(r)$ in the case of compressive forces $Q < \rho g Q_0$ is the same as in the case of dilatational forces. Accordingly, the type of ice-water surface under ice compression conditions with $Q < \rho g Q_0$ is determined, as in the case of dilatation, by formulas (1.6). A greater compressive force corresponds to a lesser velocity u_2 of the trailing edge of the ζ_1 and ζ_2 waves. The velocity u_1 of the leading edge of gravitational waves ζ_1 is not dependent on Q. The dependence of u_2 on the magnitude of the compressive force is clearly seen in Fig. 4,b in [5], where with $Q < Q_0$ it is characterized by minimum values on the upper two curves $u(r)$ and $\tau'(r)$, cited for the compressive forces 0 (upper curve) and $1.68 \cdot 10^6$ N/m respectively.

The influence of ice compression on the values of the local phase velocities $(\tau(r)/r)$ and lengths $(2\pi/r)$ of the developing waves is illustrated in [5] by the upper two curves in Fig. 4,a and Fig. 4,b respectively. The segments of the curves to the left of the minimum in the second of them are related to ζ_1, whereas to the right -- to ζ_2. It can be seen that with fixed $\nu = t/|x|$ the local length $\lambda_1 = 2\pi/r_1$ of the ζ_1 wave increases, whereas $\lambda_2 = 2\pi/r_2$ of the ζ_2 wave decreases with an increase in the compressive force Q. We have $\lambda_0 < \lambda_1 < \infty$, $0 < \lambda_2 < \lambda_0$, where λ_0, equal to $2\pi/r_0$, decreases with an increase in the compressive force. The gravitational ζ_1 and elastic ζ_2 waves with fixed local lengths have greater local phase velocities with a lesser compressive force. We note that the influence of the longitudinal compression on the examined wave characteristics is the opposite of the influence of longitudinal dilatational forces on them.

For an observer at the fixed point x the time of passage of elastic and gravitational waves increases with an increase in the compressive force. The greater the Q value, the trailing edge will be at a lesser distance from the epicenter of the

disturbances at a stipulated moment in time. The vertical amplitude of oscillations of the functions $\zeta_2(x)$ and $\zeta_2(t)$ decreases with an increase in Q.

Assume that $Q_0 < Q_1 < 2\sqrt{D_1}$. Then for $x > 0$ the phase function $M_1(r) = r + \nu\tau(r)$ has one $(-r_2)$, two $(-r_1, -r_2)$ or four $(-r_1, -r_2, r_3, r_4)$ stationary points, the roots of the equation $M_1'(r) = 0$ with satisfaction of the conditions $\nu^{-1} > u_1$, $u_2 < \nu^{-1} < u_1$, $\nu^{-1} < u_2$ respectively. Here $u_1 = \sqrt{gH}$; $u_2 = -\tau'(r_0)$, $\nu = t/|x|$; $0 < r_1 < r_3 < r_4 < r_2$; r_0 is the positive root of the equation $\tau''(r) = 0$; $\tau(r)$ is determined by formula (1.5), where it must be assumed that $\theta_1 = 1 - Q_1 r^2 + D_1 r^4$. For the phase function $M_2(r) = r - \nu\tau'(r)$ under similar conditions and $x > 0$ there will also be one (r_2), two (r_1, r_2) or four $(r_1, r_2, -r_3, -r_4)$ stationary points. For $x < 0$ the $M_{1,2}$ functions have the form $M_1(r) = -r + \nu\tau(r)$, $M_2(r) = -r - \nu\tau(r)$, and their stationary points differ from the stationary points in the case $x > 0$ only in sign. Taking this into account and considering f(x) to be even, from (1.5) we find

$$\zeta = \begin{cases} \zeta_2 + O\left(\frac{1}{|x|}\right), & |x| > u_1 t, \\ \sum_{k=1}^{2} \zeta_k + O\left(\frac{1}{|x|}\right), & u_2 t < |x| < u_1 t, \\ \sum_{k=1}^{4} \zeta_k + O\left(\frac{1}{|x|}\right), & |x| < u_2 t. \end{cases}$$

$$\zeta_k = \frac{1}{|x|} A(r_k) \cos\alpha_k, \quad A = \frac{\bar{f}(r)}{\theta_1(r)\, ch\, rH} \left[j\nu\tau''(r) \right]^{-1/2},$$

$$\alpha_k = \begin{cases} r_k |x| - t\tau(r_k) - (-1)^k \frac{\pi}{4}, & k = 1, 2, \\ r_k |x| + t\tau(r_k) + (-1)^k \frac{\pi}{4}, & k = 3, 4, \end{cases}$$

$$j = \begin{cases} 1, & k = 2, 4, \\ -1 & k = 1, 3. \end{cases}$$

It can be seen that wave movement is formed by one, two or four waves. The wave ζ_1 is gravitational, ζ_2 is elastic and ζ_3 and ζ_4 are caused by ice compression. The leading edges of the compressive waves move from the region of imparting of disturbances with the identical velocity u_2. A greater compressive force corresponds to a greater velocity u_2. This also follows from Fig. 4,b in [5], where u_2 is characterized by the modulus of the minimum value on the dotted segments of the curves

$u = \tau(r)$ with the numbers 3, 4, the upper of which corresponds to a compressive force $2.52 \cdot 10^6$ N/m, whereas the lower corresponds to a force $3.03 \cdot 10^6$N/m. Since the generated waves do not have trailing edges, the greater the Q_1 values, the greater will be the region covered with ζ_3, ζ_4 waves. The compressive waves move toward the epicenter of disturbances with local phase velocities equal to $v_{3,4} = \tau(r_{3,4})/r_{3,4}$. The character of the dependence of $v_{3,4}$ on the magnitude of the compressive force is shown in [5] in Fig. 4,a by the dotted segments of the curves 3, 4. With fixed ν the local lengths $\lambda_3 = 2\pi/r_3$ of the ζ_3 wave are greater than the lengths $\lambda_4 = 2\pi/r_4$ of the ζ_4 waves. In addition, $\lambda_1 > \lambda_3 > \lambda_0 > \lambda_4 > \lambda_2$. The leading edge of the gravitational waves ζ_1 is not dependent on Q_1. It is, as for $Q_1 < Q_0$, equal to $\sqrt{gH}$.

BIBLIOGRAPHY

1. Cherkesov, L. V., POVERKHNOSTNYYE I VNUTRENNIYE VOLNY (Surface and Internal Waves), Kiev, "Naukova Dumka," 1973, 247 pages.

2. Kheysin, D. Ye., DINAMIKA LEDYANOGO POKROVA (Dynamics of the Ice Cover), Leningrad, Gidrometeoizdat, 1967, 215 pages.

3. Bukatov, A. Ye., "Influence of Ice Cover on Unsteady Waves," MORSKIYE GIDROFIZICHESKIYE ISSLEDOVANIYA (Marine Hydrophysical Investigations), No 3, Sevastopol', pp 64-77, 1970.

4. Bukatov, A. Ye., "Influence of Longitudinal Dilatation on the Development of Flexural-Gravitational Waves in a Continuous Ice Cover," MORSKIYE GIDROFIZICHESKIYE ISSLEDOVANIYA, No 4, Sevastopol', pp 26-33, 1978.

5. Bukatov, A. Ye., "Influence of Longitudinal Compression on Unsteady Oscillations of an Elastic Plate Floating on the Surface of a Fluid," PRIKLADNAYA MEKHANIKA (Applied Mechanics), Vol 18, No 9, pp 33-39, 1980.

6. Timoshenko, S. P., KOLEBANIYA V INZHENERNOM DELE (Oscillations in Engineering), Moscow, "Nauka," 1967, 444 pages.

7. Kheysin, D. Ye., "Relationships Between Mean Stresses and Local Values of Internal Forces in a Drifting Ice Cover," OKEANOLOGIYA (Oceanology), Vol 18, No 3, pp 438-440, 1978.

INVESTIGATION OF TSUNAMI WAVES IN THE NEIGHBORHOOD OF ITURUP ISLAND

Sevastopol' TEORETICHESKIYE I EKSPERIMENTAL'NYYE ISSLEDOVANIYA POVERKHNOSTNYKH I VNUTRENNIKH VOLN in Russian 1980 (manuscript received 7 Jul 80) pp 74-78

[Article by R. A. Yaroshenya]

[Text]

Abstract: An attempt to find a correlation between the height of tsunamis at the shore and in the open ocean (at the tsunami focus) for Burevestnik village (Iturup Island) on the basis of computed and actual data on the height of tsunamis is described.

A complexity in predicting the height of a tsunami wave is that at the present time there is no real possibility, on the basis of the known magnitude of an earthquake, to obtain the necessary information on the field of wave disturbances at the focus of a tsunami. Measurements of the height of a tsunami wave at the focus are unavailable. However, in [2, 3, 7, 8] an attempt is made to establish a correlation between the magnitude of an earthquake and the height of a tsunami at the focus.

As a result of modeling it was possible to find the dependence between the basin depth, the maximum displacement of the bottom and the maximum rise at the source [7]. In studying the Niigata tsunami a correlation was established between the magnitude of the earthquake and the wave height at the source [8]. On the basis of an analysis of the results of theoretical investigations by Takahasi, Ichiye, Kadshiura, L. N. Sretenskiy, A. S. Stavrovskiy, it was demonstrated in [3] that in the region of the tsunami source the wave height can be assumed equal to the value of the vertical displacement of the bottom sector in the region of the earthquake focus. Source [2], in the form of a table, gives the dependence of tsunami height at the focus on earthquake magnitude and focal depth.

We will examine an analytical-numerical method making it possible to compute the height of the tsunami wave at the shore. The model of a basin filled with a fluid consists of a region of an ocean of a constant depth h_1, transitional to a zone of variable depth $h_2(x)$ and ending at the shore in a vertical wall. The x-axis is directed from the open sea to the shore, the z-axis is directed upward, the y-axis is directed along the shore. Within the framework of this model, using an analytical-numerical method, the tsunami wave heights are computed along the shore.

In this article, for Burevestnik village (Iturup Island), on the basis of computed and actual data on the height of a tsunami, an attempt has been made to find a correlation between the height of a tsunami at the shore and in the open ocean (at the tsunami focus).

In the approximation of the linear theory of long waves, with allowance for the action of Coriolis force, the system of equations has the form

$$\bar{u}_t - 2\omega\bar{v} = -g\bar{\zeta}_x, \quad \bar{v}_t + 2\omega\bar{u} = -g\bar{\zeta}_y, \quad \bar{\zeta}_t = -\left[(\bar{u}h)_x + (\bar{v}h)_y\right], \tag{1}$$

where $\bar{\zeta}$ is the rise in the level of the free surface; $\bar{u}$, $\bar{v}$ are the components of horizontal velocity; 2ω is the Coriolis parameter; h is basin depth (h_1 -- in the open ocean, h_2 -- in the shore zone).

The rise of the free surface for a tusunami wave running in at an angle from the open ocean has the form

$$\zeta = Ae^{i(mx+ny-\sigma t)}, \tag{2}$$

where A is the amplitude of this wave; m, n are the components of the wave vector on the x, y axes; b is the frequency of this wave. Using the periodicity conditions and seeking a solution of system (1) in the form

$$\left\{\bar{u}, \bar{v}, \bar{\zeta}\right\} = \left\{u, v, \zeta\right\} \cdot \exp\left\{i\left(ny - \sigma t\right)\right\}, \tag{3}$$

for determining the rise of the free surface in a region of variable depth ζ_2 and in the open ocean ζ_1 the ordinary differential equations are

$$gh_1\zeta_1'' + (\sigma^2 - 4\omega^2 - gh_1n^2)\zeta_1 = 0, \tag{4}$$

$$h_2\zeta_2'' + h_2'\zeta_2' - \zeta_2\left[\frac{2\omega h_2' n}{\sigma} + h_2 n^2 - \frac{1}{g}(\sigma^2 - 4\omega^2)\right] = 0. \tag{5}$$

Solving equation (4), we obtain

$$\zeta_1 = A_1 e^{imx} + B_1 e^{-imx}, \quad m = \sqrt{\frac{\sigma^2 - 4\omega^2}{gh_1} - n^2},$$

where A_1 and B_1 are arbitrary constants. The general solution of equation (5) is written in the form

$$\zeta_2 = A_2\varphi(x) + B_2\psi(x),$$

where A_2, B_2 are arbitrary constants; φ and ψ are two fundamental solutions of equation (5), determined numerically by the Runge-Kutta method.

For the rise in the free surface in the open ocean $\bar{\zeta}_1$ and in the coastal zone $\bar{\zeta}_2$ we obtain the expressions

$$\bar{\zeta}_1 = A_1 e^{i(mx+ny-\sigma t)} + B_1 e^{i(-mx+ny-\sigma t)},$$

$$\bar{\zeta}_2 = \left[A_2 \varphi(x) + B_2 \psi(x) \right] e^{i(ny - \sigma t)}$$

Here A_1 is the amplitude of the wave arriving from the abyssal region (we will consider it to be fixed); B_1 is the amplitude of the wave reflected in the abyssal region; the expression in brackets is the amplitude of a wave (dependent on x) moving along the shore in the coastal zone.

In order to find B_1, A_2, B_2 we will use the continuity conditions for the free surface profile and the horizontal velocities at the boundary of regions of constant and variable depth, and also the condition at the vertical wall. These conditions make it possible to obtain a system of three algebraic equations whose solution gives the sought-for values.

For Burevestnik village the proposed method was used in computing the rise of the level surface with approach of the tsunami wave to the shore. The basin model reflects its longitudinal section perpendicular to the shore. The depth of the open ocean is h_1 = 4 km. The zone of variable depth is broken down into regions whose depth and extent in each case with approach to the shore are h_2 = 2, 1, 0.5, 0.4, 0.005 km; L_1 = 60.5, 16.5, 242, 99, 143 km.

The computations were made for waves whose amplitude in the open ocean was 1 m, the periods being 107, 40, 33 minutes. The choice of periods is explained by the observational data. It is known [1, 4] that with passage of a tsunami precisely these periods predominate in the spectrum of ocean level fluctuations.

Source [4] gives the spectra of ocean level fluctuations with the passage of the close and distant tsunamis of 28 March-January 4, 1964, 14-16 May, 1966, 16-18 May 1968, 11-13 March, 1969, 22-25 September, 1969. Here it is also indicated that with the passage of distant tsunamis a long-period component appears in the spectrum which is absent in the spectrum of variations caused by near tsunamis.

The computations indicated that with the arrival of a tsunami wave from the open ocean at an angle to the shore, with an amplitude of 1 m and a period of 107 (distant tsunami), 40, 33 minutes (near tsunami) a wave is propagated along the shore whose amplitude is greater (by 60% for a distant tsunami and by 70% for a near tsunami) than the amplitude of the arriving wave. Since the wave is propagated along the shore, it can be regarded as an edge wave whose amplitude is 1/2-1/4 of the total amplitude.

In [6] a study was made of the record of level variations during the passage of waves during the Iturup tsunami (1958, 1963). It was demonstrated that the variations include a special component whose transformation in the transformation process is characteristic for edge waves on the shelf. The amplitude of these waves is 0.5-0.25 of the total amplitude and the maximum value is observed in those cases when the total group of waves approaches at an angle to the shelf. Thereby a wave component is excited which moves away from the shore along the normal with an amplitude up to 1/3 of the magnitude of the edge shelf waves.

Taking into account the conclusions in [6], we will assume that the maximum amplitude with approach of a tsunami to the shore, having an amplitude in the ocean of 1 m, will be 7 m (for a near tsunami) and 6 m (for a distant tsunami). A wave will

be reflected from the shore whose amplitude is 0.6 m (for a close tsunami) and 0.5 m (for a distant tsunami).

By comparing in situ observations of height of the wave (0.103 m) registered by the tide gage at Burevestnik village on 12 August 1969 with the passage of a tsunami (earthquake magnitude 8.2) [5] with the computed height (6 m), with the arrival of a wave with the amplitude 1 m from the abyssal region, for the actual tsunami we obtain an amplitude of the arriving wave or the wave height of the wave at the tsunami source of 0.2 m. Thus, the amplitude of the tsunami wave with approach to the shore increases by a factor of 6.

For other actual tsunamis [5] (28 March 1964, 15 May 1966, 16 May 1968, 23 November 1969) there was registry of amplitudes of variations several times less (0.42, 0.15, 0.2, 0.45 m respectively) than during the tsunami event of 12 August 1969; accordingly, the height of the tsunami at the source for them will be considerably less (0.02-0.1 m).

BIBLIOGRAPHY

1. Babiy, M. V. and Yaroshenya, R. A., "Results of Computations of Periods of Natural Level Fluctuations of Bays in the Example of Kasatka Bay," IZUCHENIYE TSUNAMI V OTKRYTOM OKEANE (Study of Tsunamis in the Open Ocean), Moscow, "Nauka," pp 43-47, 1977.

2. Ikonnikova, L. N. and Yaroshenya, R. A., TABLITSY VYSOT VOLN TSUNAMI (Tables of Heights of Tsunami Waves), Vladivostok, 1978, 150 pages.

3. Solov'yev, S. L. and Mileteyev, A. N., "Appearance of the Niigata Tsunami on the Shores of the USSR and Some Data on the Source of Waves," OKEANOLOGIYA (Oceanology), Vol 7, No 1, pp 104-116, 1967.

4. Yaroshenya, R. A., "Investigation of Natural Level Variations in Bays of the Kurile-Kamchatka Coast," TEORETICHESKIYE I EKSPERIMENTAL'NYYE ISSLEDOVANIYA PO PROBLEME TSUNAMI (Theoretical and Experimental Investigations on the Tsunami Problem), Moscow, "Nauka," pp 153-164, 1977.

5. Yaroshenya, R. A., "Clarification of the Principal Periods of Natural Level Variations in Bays of the Kurile-Kamchatka Coast," Archives of the Far Eastern Scientific Research Hydrometeorological Institute, Vladivostok, 1973, 403 pages.

6. Aida, I., "On the Edge Waves of the Iturup Tsunami," BULL. EARTHQUAKE RES. INST., Univ. Tokyo, 47, 467, No 1, pp 43-54, 1969.

7. Takahasi, R. and Hatori, Y., "A Model Experiment on the Tsunami Generation From Bottom Deformation Area of Elliptic Shape," BULL. EARTHQUAKE RES. INST., Tokyo, 40, No 4, pp 25-63, 1962.

8. Watanable, H., "Studies of the Tsunami on the Sanriku Coast of the Northeastern Honshu in Japan," GEOPHYS. MAG., No 1, pp 102-115, 1964.

GENERATION OF SEISMIC WAVES BY TSUNAMI WAVES PROPAGATING IN OCEAN WITH UNEVEN BOTTOM

Sevastopol' TEORETICHESKIYE I EKSPERIMENTAL'NYYE ISSLEDOVANIYA POVERKHNOSTNYKH I VNUTRENNIKH VOLN in Russian 1980 (manuscript received 3 Apr 80) pp 79-89

[Article by I. V. Lavrenov]

[Text] This article is devoted to the problem of short-range forecasting of tsunamis. The mechanism of generation of seismic waves in the earth's crust by tsunamis is examined. The resonance conditions for generation are revealed in an examination of the interaction of tsunami waves with irregularities on the ocean floor. The spectrum of Rayleigh waves is constructed in a case when tsunamis are propagated in an ocean whose bottom relief changes in one direction. The radiation of seismic waves has a directional character.

The problem of seismic waves generated by tsunamis has a direct relationship to the problem of short-range forecasting of tsunamis. This problem was raised for the first time in 1956 by L. N. Sretenskiy in [1]. Then it was examined by S. S. Voit in [8]. In these studies it was assumed that tsunamis during movement in an ocean with an elastic plane bottom excite seismic waves which are propagated considerably more rapidly than tsunamis. On the basis of observation of seismic waves it would be possible to judge the presence and character of tsunamis, thereby obtaining preliminary information for some time prior to the arrival of tsunami waves on the shore.

In source [2] a study was made of seismic waves generated by a tsunami, taking into account an analysis of elastic displacements of the earth's crust caused by tsunamis propagating at an angle to the shoreline.

In this article we examine the possible mechanism which would describe the generation of seismic waves by tsunami waves propagating in an ocean with an uneven bottom.

1. Assume that in a rectangular coordinate system (x, y, z) an elastic medium with $z \geqslant -h(x,y,z)$ is stipulated which is covered by a layer of homogeneous fluid $-[h_0 + \eta(x,y,t) \leqslant z \leqslant -h(x,y,t)$, where h_0 is the mean constant depth of the basin; h(x, y,t) is a function describing bottom relief; $\eta(x,y,t)$ is the deviation of the

free surface level of the fluid from the position of equilibrium (Fig. 1).

We will examine the wave movement of such a dynamic system. We will assume that bottom elasticity does not exert a significant influence on the propagation of fluid waves and that the height of the bottom irregularities is small in comparison with the mean depth of the basin $|h(x,y,t)| \ll 1$ and the slopes of the irregularities are small $|\text{grad } h(x,y,t)| \ll 1$.

On these assumptions the problem of wave movement of a fluid leads to the problem of wave propagation at the surface of a fluid in the presence of an uneven bottom. We will assume that the wave movement of the free surface of a fluid is described by the theory of long waves

$$\frac{\partial^2 \eta}{\partial t^2} - g \nabla_h \left(H \nabla_h \eta \right) = 0, \tag{1.1}$$

where $H = h_0[1 + \mathcal{E}(\vec{r})]$, $h = h_0 \mathcal{E}(\vec{r})$; ∇_h is the horizontal differential operator; g is the acceleration of free falling; r is the horizontal radius vector $r^2 = x^2 + y^2$.

The effect of the ocean on the bottom will be simulated by a system of normal pressures applied to the bottom from the direction of the ocean. Since an uneven bottom is examined, this boundary condition, related to the plane $z = 0$, gives not only a normal component to $z = 0$

$$\sigma_{zz} = -P = -\rho g \eta, \tag{1.2}$$

but also a tangential component

$$\vec{\sigma}_h = \left\{ \sigma_{xz}, \sigma_{yz} \right\} = P \nabla_h h, \tag{1.3}$$

where ρ is fluid density, wave pressure at the bottom P is taken in the approximation of hydrostatics.

Dynamic movements of the elastic medium relative to the position of equilibrium will be described by the vector of displacements $\vec{u}(\vec{r},z,t) = \{ U_x, U_y, U_z \}$, conforming to the equation

$$(\mu + \lambda) \operatorname{grad} \operatorname{div} \vec{U} + \Delta \vec{U} = \rho_r \frac{\partial^2 \vec{U}}{\partial t^2}, \tag{1.4}$$

where μ and λ are Lamé constants; ρ_r is the density of the elastic medium, which we will consider constant.

Thus, a system of linear equations with variable coefficients (1.1)-(1.4) is obtained. The wave equation (1.1) can be considered independently of (1.2)-(1.4). The solution of the remaining system of equations is obtained using equation (1.1).

The problem of the scattering of tsunami waves in an ocean with an uneven bottom has already been examined in the literature. For example, in [3] its solution was obtained in the approximation of the theory of long waves. Accordingly, we will not dwell on a detailed investigation of solution of equation (1.1). We note only

that the presence of bottom irregularities, whose height is considerably less than the mean depth of the ocean, leads to an attenuation of the mean wave field of long gravitational waves.

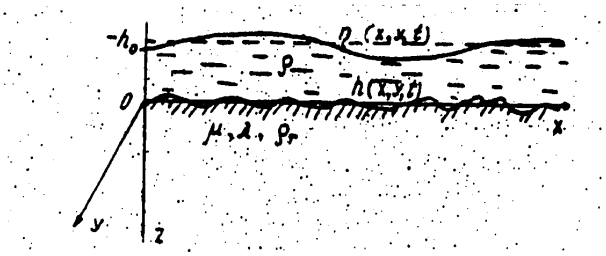

Fig. 1.

2. We will examine the problem of excitation of waves in an elastic homogeneous half-space by random boundary stresses.

Assume that at the boundary of a homogeneous elastic half-space at the time $t \geq 0$ the following stress is applied

$$\vec{\sigma}\left(\vec{r}, t\right) = \left\{\sigma_{xz}, \sigma_{yz}, \sigma_{zz}\right\}$$
$$\sigma_{xz} = \mu\left(\frac{\partial U_x}{\partial z} + \frac{\partial U_z}{\partial x}\right)\Big|_{z=0}, \quad \sigma_{yz} = \mu\left(\frac{\partial U_y}{\partial z} + \frac{\partial U_z}{\partial y}\right)\Big|_{z=0}, \tag{2.1}$$
$$\sigma_{zz} = 2\mu \frac{\partial U_z}{\partial z} + \lambda\left(\frac{\partial U_x}{\partial x} + \frac{\partial U_y}{\partial y} + \frac{\partial U_z}{\partial z}\right)\Big|_{z=0}.$$

Prior to the initial moment in time $t < 0$ the elastic medium was at rest

$$\vec{U} = \frac{\partial \vec{U}}{\partial t} = 0. \tag{2.2}$$

The boundary conditions (2.1) in combination with (1.4) and zero initial data constitute a closed system of equations.

The vector of elastic displacements $\vec{u}$ will be represented in the form of the sum

$$\vec{U} = \operatorname{grad} \varphi + \vec{V}, \tag{2.3}$$

where $\operatorname{div} \vec{V} = 0$; φ is scalar potential. We will rewrite (1.4) with (2.3) taken into account

$$\Delta \varphi = \alpha^2 \frac{\partial^2 \varphi}{\partial t^2}, \quad \Delta V_x = \beta^2 \frac{\partial^2 V_x}{\partial t^2}, \quad \Delta V_y = \beta^2 \frac{\partial^2 V_y}{\partial t^2}, \tag{2.4}$$
$$\Delta V_z = \beta^2 \frac{\partial^2 V_z}{\partial t^2}, \qquad \frac{\partial V_x}{\partial x} + \frac{\partial V_y}{\partial y} + \frac{\partial V_z}{\partial z} = 0.$$

Here $a = (\rho_T/\lambda + 2\mu)^{1/2}$ and $B(\rho_T/\mu)^{1/2}$ are parameters inverse to the velocities of the longitudinal and transverse waves. The boundary conditions assumed the form

$$\sigma_{xz} = \mu\left(2\frac{\partial^2\varphi}{\partial x\,\partial z} + \frac{\partial V_x}{\partial z} + \frac{\partial V_z}{\partial x}\right)\Big|_{z=0},\ \sigma_{yz} = \mu\left(2\frac{\partial^2\varphi}{\partial y\,\partial z} + \frac{\partial V_y}{\partial z} + \frac{\partial V_z}{\partial y}\right)\Big|_{z=0},\ \sigma_{zz} = \mu\left[\left(\beta^2 - 2a^2\right)\frac{\partial^2\varphi}{\partial t^2} + 2\frac{\partial^2\varphi}{\partial z^2} + 2\frac{\partial V_z}{\partial z}\right]\Big|_{z=0}. \tag{2.5}$$

Assume that $\vec{\sigma}(\vec{r},t)$ is a homogeneous random field with a zero mathematical expectation of the mean value $\langle\vec{\sigma}(\vec{r},t)\rangle = 0$. Then σ_i, φ, V_n and U_n (in order to shorten the writing we have introduced the indices i and n in place of x, y, z, i = 1, 2, 3; n = 1, 2, 3) will be represented in the form of Fourier-Stieltjes integrals

$$\sigma_i(\vec{r},t) = \int e^{i\vec{k}\vec{r}}\,d\tilde{\sigma}_i(\vec{k},t), \tag{2.6}$$

$$\varphi(\vec{r},z,t) = \int e^{i\vec{k}\vec{r}}\,d\tilde{\varphi}(\vec{k},z,t),\quad V_n(\vec{r},z,t) = \int e^{i\vec{k}\vec{r}}\,d\tilde{V}_n(\vec{k},z,t), \tag{2.7}$$

$$u_n(\vec{r},z,t) = \int e^{i\vec{k}\vec{r}}\,d\tilde{U}_n(\vec{k},z,t). \tag{2.8}$$

Here $\vec{k}$ is the horizontal wave vector $\vec{k} = \{k', k''\}$; $d\tilde{\sigma}_i$, $d\tilde{\varphi}$, $d\tilde{V}_n$, $d\tilde{U}_n$, are the components of Fourier-Stieltjes stresses, potentials and displacements. The initial functions $d\tilde{\varphi}$ and $d\tilde{V}_n$ are obtained in the form of Mellin integrals as a result of substitution of (2.6) and (2.7) into (2.4) and (2.5)

$$d\tilde{\varphi}(\vec{k},z,t) = \frac{1}{2\pi i}\int_{x-i\infty}^{x+i\infty}\Phi(\vec{k},\rho)\,e^{-zkd}\,e^{\rho t}\,d\rho,$$

$$d\tilde{V}_n(\vec{k},z,t) = \frac{1}{2\pi i}\int_{x-i\infty}^{x+i\infty}\Psi(\vec{k},\rho)\,e^{-zk\beta}\,e^{\rho t}\,d\rho, \tag{2.9}$$

where

$$\alpha = \left(1 + \frac{a^2\rho^2}{k^2}\right)^{1/2};\quad \beta = \left(1 + \frac{\beta^2\rho^2}{k^2}\right)^{1/2}.$$

We will take the residues at the poles of the integrands (2.9) with integration in the plane of the complex variable "p." As a result we obtain expressions determining the components of displacement of the elastic medium in a Rayleigh wave

$$d\tilde{U}_n(\vec{k},z,t) = \sum_{i=1}^{3} C_{in}(\vec{k},z)\int_0^t \sin\omega(t-\tau)\,d\tilde{\sigma}_i(\vec{k},\tau)\Big|_{\omega=v_R k}\,d\tau, \tag{2.10}$$

where v_R is the velocity of the Rayleigh wave, equal to $0.9194/\beta$ (on the assumption that $\mu = \lambda$); $C_{in}(\vec{k},z)$ is a tensor, setting in agreement the components of the vector $\vec{U}$ and the components of the vector $\vec{\sigma}$.

We obtain the correlation between the energy characteristics of the random field of the limiting stresses and the corresponding characteristics of the field of the Rayleigh wave. In the space of wave vectors $\vec{k}$ we introduce the spectrum of the field of stresses with the time shift t

$$D_{ij}\left(\vec{k}, t_0, t\right) = \frac{\langle d\tilde{\sigma}_i\left(\vec{k}_0, t_0\right) d\tilde{\sigma}_j^*\left(\vec{k}_0+\vec{k}, t_0+t\right)\rangle}{d\vec{k}}. \tag{2.11}$$

Here the brackets denote theoretical-probabilistic averaging, the asterisk denotes a complexly conjugate parameter. With i = j the components of the tensor D_{ij} represent spectral functions of each stress component. With $i \neq j$ the components of D_{ij} are the cross-spectral functions of the stress components, which, speaking in general, are complex. If the stress components are stationarily related, the components of the D_{ij} tensor are not dependent on the initial time t_0.

We introduce the spectrum of components of displacements in the Rayleigh wave

$$S_{nm}\left(\vec{k}, t, z\right) = \frac{\langle d\tilde{U}_n\left(\vec{k}_0, t, z\right) d\tilde{U}_m^*\left(\vec{k}_0+\vec{k}, t, z\right)\rangle}{d\vec{k}}, \tag{2.12}$$

in which we will examine only the autospectrum $S_n = \delta_{nm} S_{nm}$ (here δ_{nm} is the Kronecker symbol).

We obtain the correlation between $S_n(\vec{k}, t, z)$ and $D_{ij}(\vec{k}, t)$, using (2.10), (2.11) and (2.12).

$$S_n\left(\vec{k}, t, z\right) = \sum_{i=1}^{3}\sum_{j=1}^{3} C_{in}\left(\vec{k}, z\right) C_{jn}^*\left(\vec{k}, z\right) J_{ij}\left(\vec{k}, t\right), \tag{2.13}$$

where

$$J_{ij}\left(\vec{k}, t\right) = \int_0^t\int_0^t D_{ij}\left(\vec{k}, \tau'-\tau''\right)\left[\sin\omega\left(t-\tau'\right)\sin\omega\left(t-\tau''\right)\right]\Big|_{\omega=v_n\vec{k}} d\tau' d\tau'' =$$

$$= \int_0^t\int_0^t D_{ij}\left(\vec{k}, \tau'-\tau''\right)\frac{1}{2}\left[\cos\omega\left(\tau''-\tau'\right)-\cos\omega\left(2t-\tau'-\tau''\right)\right]\Big|_{\omega=v_n\vec{k}} d\tau' d\tau''.$$

We will replace the variables $\tau' - \tau'' = \tau$, $\tau' + \tau'' = \xi$ and carrying out one integration, we obtain an asymptotic expression for $J_{ij}(\vec{k}, t)$ with $\omega t \gg 1$

$$J_{ij}\left(\vec{k}, t\right) \simeq \frac{1}{2}\int_0^t \left(t-\tau\right) D_{ij}\left(\vec{k}, \tau\right)\cos\omega\tau\Big|_{\omega=v_n\vec{k}} d\tau.$$

For (2.13) with $t \to \infty$ we obtain

$$S_n\left(\vec{k}, t, z\right) \simeq t\left\{\pi\sum_{i=1}^{3}\sum_{j=1}^{3} C_{in}\left(\vec{k}, z\right) C_{jn}^*\left(\vec{k}, z\right) F_{ij}\left(\vec{k}, \omega\right)\Big|_{\omega=v_n\vec{k}}\right., \tag{2.14}$$

where

$$F_{ij}\left(\vec{k}, \omega\right) = \frac{1}{2\pi}\int_0^\infty D_{ij}\left(\vec{k}, \tau\right)\cos\omega\tau d\tau. \tag{2.15}$$

It follows from expression (2.14) that a resonance (linear in time) increase in the spectrum of Rayleigh waves occurs only in a case when in the spatial-temporal spectra of components of the stress field there is a set of frequencies and wave vectors corresponding to the dispersion relationship for these waves. A contribution to the spectral density of Rayleigh waves is made by both the autospectrum of the stress field, but also the cross-spectrum of stress components. Formula (2.14) is a singular generalization of [7] in which the generation of wind waves was studied.

In a linear formulation, without allowance for topography, the pressure field acting on the bottom does not afford the necessary conditions for the generation of seismic waves since in the latter case the frequency ω and the wave number $\vec{k}$ are related by the dispersion relationship $\omega^2 = g\vec{k}\ \mathrm{th}\ \vec{k}h_0$, which does not allow the phase velocity to exceed the $\sqrt{gh_0}$ value. Accordingly, the pressure spectrum does not contain the totality of frequencies and wave vectors corresponding to Rayleigh waves. We note that the resonance conditions for the generation of seismic waves are revealed not only in an examination of interactions of surface gravitational waves with bottom relief, but also in an analysis of nonlinear wave interactions between gravitational waves [5]. However, the mechanism of generation of seismic waves in the latter case is less effective for tsunami waves affecting with their wave movement the entire water layer of the ocean.

The mechanism of generation of Rayleigh waves, examined above, gives the same local increase in wave energy as that generated by the quasistationary and quasihomogeneous field of limiting stress. In the latter case the spectrum $F_{ij}(\vec{k}, \omega)$ from (2.14) is also a function of distance and time. The spectrum $S_n(\vec{k}, z, t)$ is determined not only by expression (2.14), but also by the energy related to inhomogeneity and nonstationary character of the distribution of the external field spectrum. Equation (2.14) is written in a more complete form, as was demonstrated in [4].

$$\frac{\partial S_n}{\partial t} + \dot{x}_i \frac{\partial S_n}{\partial x_i} + \dot{k}_i \frac{\partial S_n}{\partial k_i} = T_n\left(\vec{k}, t, \vec{r}, z\right), \tag{2.16}$$

where $T_n(\vec{k}, t, \vec{r}, z)$ is the expression in braces in (2.14); x_i and k_i are the components of the r and k vectors. In the absence of external forces (2.14) undergoes transformation into the equation derived in [6], the essence of which is that the energy spectrum remains constant along the direction of group velocity. In the absence of wave refraction the term

$$k_i \frac{\partial S_n}{\partial k_i}$$

disappears. Since the group velocity $\vec{V}_R = \dot{\vec{r}}$ remains constant, equation (2.16) can be easily integrated

$$S_n\left(\vec{k}, t, \vec{r}, z\right) = \int_{t_0}^{t} T_n\left(\vec{k}, t', \vec{r}_0 + \left(t' - t_0\right)\vec{V}_R, z\right) dt' + S_n\left(\vec{k}, t_0, \vec{r}_0, z\right) \tag{2.17}$$

where $\vec{r}_0 = \vec{r} - \vec{V}_R (t - t_0)$

As an example of the integration of (2.17) we will examine a simple case (Fig.2) where T_n is constant with respect to both t and $\vec{r}$ in some region with the given area Q and is equal to zero beyond its limits. The mean distance from the generation region to the observer is R, φ_0 is the angle between the ox-axis and the direction to the center of the region. If ABO is the path of propagation of the Rayleigh wave with the wave vector $\vec{k}$, then the spectrum S_n increases linearly from the

initial point A (where we will assume that $S_n = 0$) to the maximum value $l(\theta)T_n/V_R$ at the point B, where the propagation path of the considered wave emerges beyond the limits of the generation region (the distance RB is denoted $l(\theta)$). On the remaining segment of the path BO the spectrum of seismic waves S_n remains unchanged. Since here it is possible to convert from the variable $\vec{k}$ to ω and θ (where θ is the angle between the direction of wave propagation and the ox-axis), then

$$S_n(\vec{k}, t, z) = S_n(\omega, \theta, t, z). \tag{2.18}$$

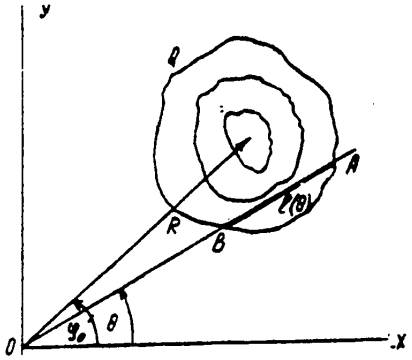

Fig. 2. Schematic representation of generation region and Rayleigh wave propagation path.

We introduce the new spectrum

$$f_n(\omega, z, y_0) = \frac{\omega}{V_R^2}\int_0^{2\pi} S(\omega, \theta, z)\,d\theta,$$

which we rewrite in the form

$$f_n(\omega, z, y_0) = \frac{\omega}{V_R^2}\int_0^{2\pi} l(\theta)\, T_n(\omega, \theta, z)\,d\theta. \tag{2.19}$$

The results are applicable only with $l(\theta) \gg 2\pi/k$.

The problem of finding the spectrum of Rayleigh waves is reduced to a determination of the stress field spectrum $F_{ij}(\vec{k}, \omega)$, capable of generating seismic waves.

3. We will examine the boundary conditions in the formulation of the problem (1.2) and (1.3). We will investigate only those components of stress which contain spectral components with high phase velocities satisfying the resonance conditions of generation of Rayleigh waves. Accordingly, we will limit ourselves only to the tangential stresses (1.3), since the normal component of stress (1.2) is not capable of generating seismic waves by reason of the factors indicated above.

We will write an expression for the spectral intensity of the field of shearing stresses (1.3). For this we will expand the wave fields $\eta(\vec{r}, t)$ and $\varepsilon(\vec{r})$ (as this was demonstrated in [3]) into Fourier integrals. Applying (2.11) and (2.15) and limiting ourselves only to the main term, containing the small parameter $\varepsilon(\vec{r})$ in the lowest power, we obtain

$$F_{\sigma_i \sigma_j}(\vec{k},\omega) = \delta(\rho g h_0)^2 \iint \left(a(\vec{k}_1)\, a^*(\vec{k}_1)\right) e^{(\gamma_1+\gamma_1^*)t}\, \Phi(\vec{k}_2)\, k_1^i k_1^j \cdot \delta(\vec{k}_1+\vec{k}_2-\vec{k})\, \delta(\omega-\omega_1)\, d\vec{k}_1\, d\vec{k}_2 , \tag{3.1}$$

where $(a(\vec{k}_1)a^*(\vec{k}_1))$ is the initial energy spectrum of the tsunami; $\gamma_1 + \gamma_1^* = 2\mathrm{Re}\gamma_1$ is the doubled decrement of attenuation of the tsunami wave field; $\Phi(\vec{k}_2)$ is the spectrum of the correlation function of bottom irregularities; $\delta(\vec{k})$ is the Dirac delta function; $\omega_1^2 = gh_0\, k_1^2$; $\vec{k}_1 = \{k_1', k_1''\} = \{k_1^i\}$.

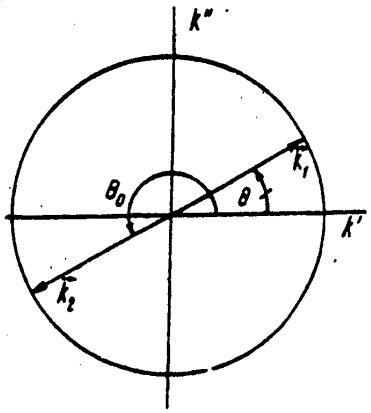

Fig. 3.

The great phase velocity $\omega/\vec{k}_1$, considerably exceeding the phase velocity of waves at the fluid surface $\omega_1/\vec{k}_1 = \sqrt{gh_0}$, can be discriminated from the spectrum in a case when $\vec{k}_1 \approx -\vec{k}_2$. As follows from (3.1), $\omega = \omega_1$. Thus, the condition of resonance excitation of the Rayleigh wave can be schematically represented in the following way (Fig. 3). The wave vector $\vec{k}_1$, describing the tsunami wave, and the wave vector of bottom irregularities $\vec{k}_2$, lie almost on the same circle and are opposite in direction. The radius of this circle determines the resonance frequency of the Rayleigh wave.

Expression (3.1) will be simplified in the range of large phase velocities

$$F_{\sigma_i \sigma_j}(\vec{k},\omega) \approx \delta(\rho g h_0)^2 \int \left(a(\vec{k}_1)\, a^*(\vec{k}_1)\right) e^{2\mathrm{Re}\gamma_1 t} \cdot \Phi(-\vec{k}_1)\, k_1^i k_1^j\, \delta(\omega-\omega_1)\, d\vec{k}_1 . \tag{3.2}$$

4. We will examine a case when bottom irregularities change only in one direction. Such a situation is possibly encountered in the coastal zone and in regions of submarine ocean mountains and the spectrum of irregularities has the form

$$\Phi(\vec{k}) = \frac{\Phi_0(|\vec{k}|)}{k}\, \delta(\theta-\theta_0) , \tag{4.1}$$

where θ_0 is the angle between the direction of roughness and the ox-axis.

In order to obtain some idea about seismic waves generated in such a special case it is also necessary to stipulate the spectrum of tsunami waves. However, here it is difficult to stipulate any specific spectrum. The evaluations cited by

different authors for the time being have an extremely ambiguous character for one and the same case. The principal difficulty in determining the basic parameters is related to the complexity in the precise registry of tsunami waves in the coastal zone, especially at the epicenter. We will assume that $(a(k_1)a^*(k_1))$ is dependent only on the modulus of the wave vector (as a rule, such vectors can describe tsunamis arising from the initial deviation of the free surface of the ocean when the form of this deviation is symmetric relative to the vertical axis passing through the epicenter).

If is assumed that the isolines of bottom irregularities are situated along the oy-axis, the examined case is easily illustrated. From the entire stress field acting on the bottom it is possible to discriminate only one main stress component which also for the most part determines the field of seismic waves at great distances. It is determined by the shearing stress along the ox-axis since only in this direction is there a change in bottom topography.

Thus, as a result of the substitution of the values (4.1) and (3.1) into (2.19) for distances considerably exceeding the characteristic dimensions of the generation region, it is possible to obtain the spectra of the components of displacements in the Rayleigh wave. For example, for the horizontal component we obtain

$$f_x(\omega, \varphi_0)\big|_{z=0} \cong f(\omega)\cos^4\varphi_0, \tag{4.2}$$

where

$$f(\omega) \simeq 0{,}745\ Q/R\ \beta^2\left(\frac{\rho}{\rho_T}\right)^2\ \sqrt{gh_0}\ \cdot\frac{\omega^3}{V_R^2}\ (a(\omega)a^*(\omega))\Phi(\omega)\,e^{2Re\gamma l}$$

Similarly

$$f_y(\omega, \varphi_0)\big|_{z=0} \cong 0{,}5\, f(\omega)\sin^2 2\varphi_0 \tag{4.3}$$

and

$$f_z(\omega, \varphi_0)\big|_{z=0} \cong 2{,}15\, f(\omega)\cos^2\varphi_0\,. \tag{4.4}$$

The radiation of Rayleigh waves has a directed character for a stipulated type of relief (Fig. 4). The radiation maximum falls primarily in the direction of the strongest change in bottom relief. In the full spectrum of the Rayleigh wave there is a predominance of a spectrum with a vertical displacement component.

The spectra of the Rayleigh wave components obtained in such a way give some idea concerning the directivity of the seismic precursors of tsunami waves. According to the proposed mechanism for the generation of seismic waves their excitation occurs when tsunamis encounter ocean bottom irregularities on their path. Participating in the generation are only quite extended bottom irregularities, as follows from resonance conditions. In a case when the correlation spectrum of bottom irregularities is nonisotropic, the radiation of seismic waves can have a directional character.

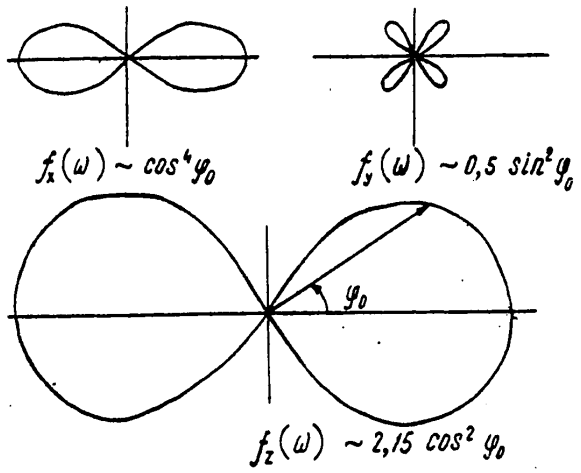

Fig. 4.

BIBLIOGRAPHY

1. Sretenskiy, L. N., "Excitation of Elastic Oscillations of a Semiplane by Wave Movement of a Fluid," BYULLETEN' SOVETA PO SEYSMOLOGII (Bulletin of the Council on Seismology), No 2, pp 12-26, 1956.

2. Stavrevskiy, A. S., "Elastic Displacements of the Earth's Crust Caused by a Tsunami Wave Propagating at an Angle to the Shoreline," TRUDY MGI (Transactions of the Marine Hydrophysical Institute), Vol 24, Moscow, pp 48-84, 1961.

3. Pelinovskiy, Ye. N., "Wave Propagation in a Statistically Inhomogeneous Ocean," NELINEYNYYE VOLNY (Nonlinear Waves), Moscow, "Nauka," 1979, 331 pages.

4. Hasselmann, E., "Statistical Analysis of Generation of Microseisms," REV. GEOPHYSICS, Vol 1, No 2, pp 177-210, 1963.

5. Hasselmann, K., "Feymann Diagrams and Interaction Rules of Wave-Wave Scattering Processes," REV. GEOPHYSICS, Vol 4, No 1, pp 1-32, 1966.

6. Longuet-Higgins, M. S., "On the Transformation of a Continuous Spectrum by Refraction," PROC. CAMBRIDGE PHIL. SOC., Vol 53, No 5, pp 226-229, 1957.

7. Phillips, O. M., "On the Generation of Waves by Turbulent Wind," J. FLUID. MECH., Vol 2, No 3, pp 417-445, 1957.

8. Voit, S. S., "On the Elastic Oscillations of the Ocean Bottom Caused by Tsunami Waves," SYMPOSIUM ON TSUNAMI AND STORM SURGES, Tokyo, pp 6-11, 1967.

EVOLUTION OF AXISYMMETRIC DISTURBANCES OF VISCOUS FLUID

Sevastopol' TEORETICHESKIYE I EKSPERIMENTAL'NYYE ISSLEDOVANIYA POVERKHNOSTNYKH I VNUTRENNIKH VOLN in Russian 1980 (manuscript received 18 Apr 80) pp 90-98

[Article by B. Yu. Sergeyevskiy]

[Text]

Abstract: Within the framework of the linear theory of long waves in a homogeneous fluid a study was made of the influence of friction on the process of development of wave movement caused by axisymmetric disturbances. The latter are characterized by both displacement of the free surface and by some velocity field. The analysis rests on computations of the integrals. Vertical friction is considered to be proportional to the mean integral horizontal velocity of movement; horizontal friction is taken into account in general form.

A large number of studies have been devoted to an investigation of waves from initial disturbances. A review of the results obtained by analytical and numerical methods in this region is contained in [1-7] and elsewhere. In this article we examine the problem of the evolution of an axisymmetric rise or velocity field in a homogeneous fluid, with viscosity being taken into account. We used vertically averaged equations of long waves in which horizontal friction is taken into account in general form and vertical friction is considered proportional to the mean integral horizontal velocity of motion. The analysis rests on numerical computation of the integrals. A similar investigation for an ideal fluid was made in [8]; plane waves in a viscous fluid were examined in [9].

1. We will examine a layer of a viscous incompressible homogeneous fluid of the constant depth H, unbounded in horizontal directions. At the time t = 0 the rise of the free surface of the fluid and the velocity field are known. Within the framework of the linear theory of long waves, with allowance for Coriolis force, we will investigate the developing unsteady motion of the fluid.

The mathematical formulation of the problem includes the system of three equations

$$u_t - \ell v = -g\zeta_x - ru + A\left(u_{xx} + u_{yy}\right), \qquad (1.1)$$
$$v_t + \ell u = -g\zeta_y - rv + A\left(v_{xx} + v_{yy}\right), \quad \zeta_t = -H\left(u_x + v_y\right)$$

with the initial conditions

$$u = u_0(x,y), \quad v = v_0(x,y), \quad \zeta = \zeta_0(x,y) \quad (t=0). \tag{1.2}$$

Here x, y are the horizontal coordinates; u(x,y,t), v(x,y,t) are the mean integral (vertically) projections of the velocity vector onto the x- and y-axes; ζ (x, y, t) are the rises of the free surface of the fluid, reckoned from the undisturbed position; $\ell = 2\omega \sin \varphi$; ω is the angular velocity of rotation; φ is local latitude; g is the acceleration of free falling; r and A are the friction and horizontal viscosity coefficients.

Applying the Fourier transform for the variables x, y and the Laplace time transform t, for the functions u, v and ζ we obtain the expressions

$$u = \frac{1}{4\pi^2} \int_{-\infty}^{\infty}\int (a_{11}\bar{u}_0 + a_{12}\bar{v}_0 + a_{13}\bar{\zeta}_0) \exp[i(mx+ny)]\, dm\, dn,$$

$$v = \frac{1}{4\pi^2} \int_{-\infty}^{\infty}\int (a_{21}\bar{u}_0 + a_{22}\bar{v}_0 + a_{23}\bar{\zeta}_0) \exp[i(mx+ny)]\, dm\, dn, \tag{1.3}$$

$$\zeta = \frac{1}{4\pi^2} \int_{-\infty}^{\infty}\int (a_{31}\bar{u}_0 + a_{32}\bar{v}_0 + a_{33}\bar{\zeta}_0) \exp[i(mx+ny)]\, dm\, dn,$$

where $\bar{u}_0(m, n)$, $\bar{v}_0(m,n)$, $\bar{\zeta}_0(m, n)$ are the Fourier transforms of the functions u_0, v_0, ζ_0;

$$a_{kj} = \frac{1}{2\pi i} \int_{s-i\infty}^{s+i\infty} \beta_{kj} [\alpha^3 + 2d\alpha^2 + (d^2+\rho^2)\alpha + dc^2k^2]^{-1} \exp(\alpha t)\, d\alpha,$$

$$\beta_{11} = \alpha(\alpha+d) + c^2n^2, \quad \beta_{12} = c^2mn - \alpha\ell, \quad \beta_{13} = -ig[n\ell + m(\alpha+d)], \tag{1.4}$$

$$\beta_{21} = -\alpha\ell - c^2mn, \quad \beta_{22} = \alpha(\alpha+d) + c^2m^2, \quad \beta_{23} = ig[m\ell - n(\alpha+d)],$$

$$\beta_{31} = iH[\ell n - m(\alpha+d)], \quad \beta_{32} = -iH[\ell m + n(\alpha+d)], \quad \beta_{33} = (\alpha+d)^2 + \ell^2,$$

$$\rho = \sqrt{\ell^2 + c^2k^2}, \quad d = r + Ak^2, \quad k = \sqrt{m^2+n^2}, \quad c = \sqrt{gH}, \quad s > 0.$$

The integrals (1.4) are computed using the theory of residues; the poles α are the roots of the cubic equation

$$\alpha^3 + 2d\alpha^2 + (d^2+\rho^2)\alpha + dc^2k^2 = 0, \tag{1.5}$$

which are easily found using the Cardano formula [10]. We will examine axisymmetric waves. Then the double integrals (1.3) can be transformed into single integrals. We will not use u_0, v_0, u, v, but u_0^*, v_0^*, u^*, v^*, where u_0^*, u^* are the radial and v_0^*, v^* are the tangential components of the velocity vector. Then transforming to polar coordinates both in the integrals (1.3) and in the transforms $\bar{u}_0$, $\bar{v}_0$, $\bar{\zeta}_0$,

and also carrying out a transition from u_0, v_0, ζ_0 and u, v, ζ to u_0^*, v_0^* and ζ_0 and u^*, v^*, ζ respectively, we obtain

$$u^* = \int_0^\infty \left(d_{11}\bar{u}_0^* + d_{12}\bar{v}_0^* + d_{13}\bar{\zeta}_0\right) J_0(kR)\,dk = \sum_{j=1}^{3} u_j(R,t), \tag{1.6}$$

$$v^* = \int_0^\infty \left(d_{21}\bar{u}_0^* + d_{22}\bar{v}_0^* + d_{23}\bar{\zeta}_0\right) J_1(kR)\,dk = \sum_{j=1}^{3} v_j(R,t), \tag{1.7}$$

$$\zeta = \int_0^\infty \left(d_{31}\bar{u}_0^* + d_{32}\bar{v}_0^* + d_{33}\bar{\zeta}_0\right) J_0(kR)\,dk = \sum_{j=1}^{3} \zeta_j(R,t). \tag{1.8}$$

Here J_0, J_1 are Bessel functions of the first kind;

$$Q = (\rho_1/3)^3 + (q/2)^2;\ \rho_1 = -d^2/3 + \rho^2;\ q = -2d^3/27 + d(c^2k^2 - 2\ell^2)/3;$$

$$\bar{u}_0^* = \int_0^\infty u_0^*(R)RJ_1(kR)\,dR;\ \bar{v}_0^* = \int_0^\infty v_0^*(R)RJ_1(kR)\,dR;\ \bar{\zeta}_0 = \int_0^\infty \zeta_0(R)RJ_0(kR)\,dR.$$

The coefficients d_{ij} (i, j = 1,3) entering into (1.6)-(1.8) have a different form in dependence on the sign on Q:

a) $Q < 0$,

(1.9)

$$d_{11} = k\sum_{i=1}^{3}\alpha_i(\alpha_i + d)s_i,\quad d_{12} = \ell k\sum_{i=1}^{3}\alpha_i s_i,\quad d_{13} = gk\sum_{i=1}^{3}(\alpha_i + d)s_i,$$

$$d_{21} = -d_{12},\quad d_{22} = k\sum_{i=1}^{3}\left[\alpha_i(\alpha_i + d) + c^2k^2\right]s_i,\quad d_{23} = -\ell g k^2\sum_{i=1}^{3}s_i,$$

$$d_{31} = -Hk^2\sum_{i=1}^{3}(\alpha_i + d)s_i,\quad d_{32} = -H\ell k^2\sum_{i=1}^{3}s_i,\quad d_{33} = k\sum_{i=1}^{3}\left[(\alpha_i + d)^2 + \ell^2\right]s_i,$$

$$s_i = \exp(\alpha_i t)/(3\alpha_i^2 + 4d\alpha_i + B),\quad B = d^2 + \rho^2,\quad \alpha_1 = 2\sqrt{-\rho_1/3}\cos(\varphi/3) - d/3,$$

$$\alpha_{2,3} = -2\sqrt{-\rho_1/3}\cos\left((\varphi \pm \pi)/3\right) - d/3,\quad a = 2d,\ \cos\varphi = -q/\left(2(-\rho_1/3)^{3/2}\right);$$

b) $Q > 0$.

$$d_{11} = k\left[a_1(a_1 + d)\lambda + z(\mu_2\mu_3 - a_3\nu_2\nu_3)\right],\quad d_{12} = \ell k\left[a_1\lambda + z(\mu_1\mu_3 + \mu a_3\nu_3)\right],$$

$$d_{13} = gk\left\{(a_1 + d)\lambda + z\left[(\mu_1 + d\nu)\mu_3 + a_3(2d\nu_1 + \mu)\nu_3\right]\right\},\quad d_{21} = -d_{12},$$

$$d_{22} = k\left\{\left[a_1(d + a_1) + k^2c^2\right]\lambda + z\left[(\mu_2 + \nu k^2c^2)\mu_3 - a_3(\nu_2 - 2d\nu_1 k^2c^2)\nu_3\right]\right\},$$

$$d_{23} = -g\ell k^2\left[\lambda + z(\nu\mu_3 + 2a_3\nu_1\nu_3)\right],$$

$$d_{31} = -Hk^2\left\{(a_1 + d)\lambda + z\left[(\mu_1 + d\nu)\mu_3 + a_3(2d\nu_1 + \mu)\nu_3\right]\right\},\quad d_{32} = d_{23}H/g,$$

$$d_{xy} = \lambda\left\{\left[(a_1+d)^2+\ell^2\right]\lambda+z\left[\left(\mu_2+6da_2f-d\mu_1+2d\left(\beta a_2+4df\right)+\right.\right.\right.$$
$$\left.\left.\left.+\left(\ell^2+d^2\right)\nu\right)\mu_3-2a_3\left(\beta\left(a_2+d\right)-df-\nu_1\left(\ell^2+d^2\right)\right)\nu_3\right]\right\},$$
$$a_1=A_1+A_2-\alpha/3,\quad a_2=-\left(A_1+A_2\right)/2-\alpha/3,\quad a_3=\sqrt{3}\left(A_1-A_2\right)/2, \qquad (1.10)$$

$$A_{1,2}=\left(-q/2\mp\sqrt{Q}\right)^{1/3},\ f=a_2^2+a_3^2,\ \mu=3f-\beta,\ \nu=3\left(a_2^2-a_3^2\right)+4da_2+\beta,$$
$$\mu_1=f\left(3a_2+4d\right)+\beta a_2,\ \nu_1=3a_2+2d,\ \lambda=\exp\left(a_1t\right)/\left(3a_1^2+4da_1+\beta\right),$$
$$\mu_2=3f^2+4da_2f+\beta\left(a_2^2-a_3^2\right)+d\mu_1,\ \nu_2=4df+2\beta a_2-\mu d,$$
$$\mu_3=\cos\left(ta_3\right),\quad \nu_3=\sin\left(ta_3\right),$$
$$z=2\exp\left(a_2t\right)/\left[f\left(9f+8d\nu_1\right)+\beta\left(6\left(a_2^2-a_3^2\right)+8da_2+\beta\right)\right].$$

If it is assumed that the friction and horizontal viscosity coefficients are equal to zero, then (1.6)-(1.8) will provide a solution of the similar problem for an ideal fluid [8].

A further investigation of u^*, v^*, ζ was made numerically using formulas (1.6)-(1.8) for the following model laws of change in u_0^*, v_0^* and ζ_0:

a) $$u_0^* = b_0\sqrt{2\varphi e}\ R\exp\left(-\varphi R^2\right); \qquad (1.11)$$

b) $$v_0^* = \rho_0\sqrt{2\varphi e}\ R\exp\left(-\varphi R^2\right);$$

c) $$\zeta_0 = a_0\exp\left(-\gamma R^2\right).$$

For the figures represented below a_0 = 1 m, $b_0 = \rho_0$ = 1 m/sec (max u_0^* = max v_0^* = 1 m/sec); H = $4\cdot10^3$ m; φ = 45°; $\gamma = 0.38\cdot10^{-9}$; $\gamma = 0.23\cdot10^{-9}$; the numerical values of the φ and γ parameters correspond to the characteristic half-width L_1 of the initial disturbance, equal to 10^5 m. By the half-width of the disturbance $f_0(R)$ is meant the maximum of the possible values R = L_1, for which $f_0(L_1) = 0.1 \max_R f_0(R)$.

In [8] an analysis was given of the velocity field and the form of the free surface of an ideal homogeneous rotating fluid caused by initial axisymmetric disturbances. It is shown that they cause the formation of time-attenuating annular waves and some stationary barotropic eddy at the center of the disturbance. Below we give an analysis of the influence of horizontal and vertical friction on the process of generation of these waves and time-attenuation of the indicated eddy formation.

Now we will examine the influence of vertical friction on the process of evolution of the initial rise of the free surface of the fluid and tangential velocities ($r \neq 0$, A = 0). Curve 1 in Fig. 1 gives the shape of the generated wave for the

initial rise ζ_0 in the form (1.11). Its profile is characterized by a rising wave and by a dropping wave which follows it. A comparison of curves 1, 2 in Fig. 1 reveals that vertical friction does not lead to qualitative changes in the shape of the wave but its amplitude value can be substantially reduced. This effect, as might be expected, is intensified with an increase in the vertical friction coefficient r. For example, if the value $\zeta^+ = \max |\zeta(R,t)|$ at the time t = 30 min with r = 0 is equal to 0.137 m, then with r = 10^{-4}, $2\cdot10^{-4}$, $3\cdot10^{-4}$, 10^{-3} sec^{-1} it can decrease to 0.123; 0.115; 0.107; 0.067 m respectively. With an increase in t the difference in the amplitudes of the ζ^+ waves with r = 0 and r $\neq$ 0 is intensified. This conclusion is illustrated in the table, where column 1 gives the ζ^+ values with r = 0 and column 2 gives the ζ^+ values with r = $2\cdot10^{-4}$ sec^{-1}.

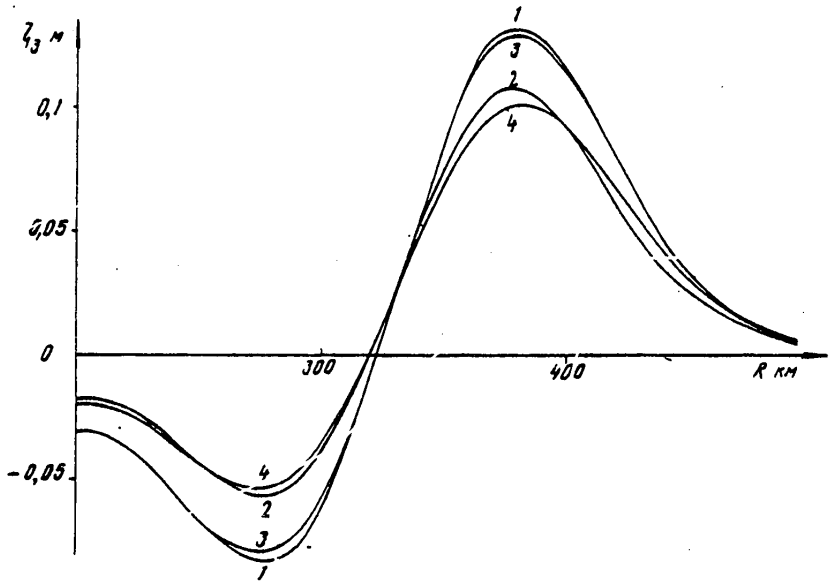

Fig. 1. Profiles of ζ_3 wave for t = 30 min: r = 0, A = 0 (curve 1); r = $3\cdot10^{-4}$ sec^{-1}, A = 0 (curve 2); r = 0, A = 10^5 $m^2\cdot sec^{-1}$ (curve 3); r = $3\cdot10^{-4}sec^{-1}$, A = 10^5 $m^2\cdot sec^{-1}$ (curve 4).

Figure 2,a illustrates the influence of vertical friction on the field of the tangential component of the velocity vector $v^* = v_3$. The curve marked with the symbol ∞ describes the v^* distribution in a stationary geostrophic eddy arising from the initial rise of the free surface of an ideal fluid. It can be seen that in a viscous fluid this eddy attenuates with time. With an increase in the friction coefficient r the attenuation of the eddy is intensified and accordingly the lifetime of the eddy is reduced. We note that allowance for vertical friction exerts no influence on the position of the maximum v_3 value.

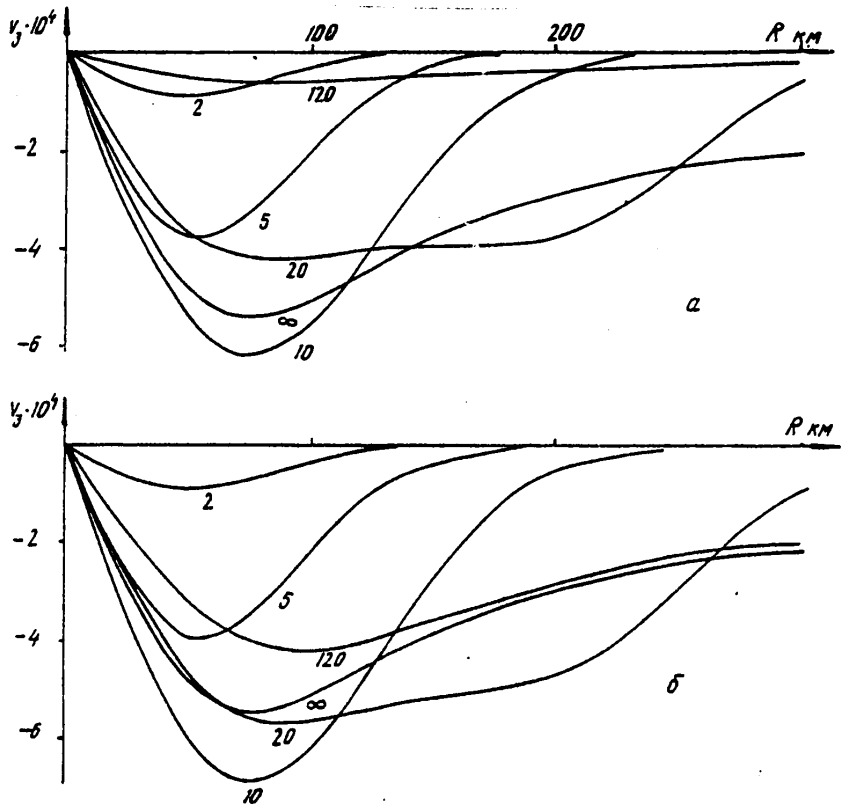

Fig. 2. Distribution $v_3 \cdot 10^4$ ($msec^{-1}$) for different moments in time (figures over the curves): a) $r = 10^{-3} sec^{-1}$, $A = 0$; b) $r = 0$, $A = 10^5 m^2 \cdot sec^{-1}$.

It was demonstrated in [8] that any initial distribution of tangential velocity (v_0^*) in an ideal fluid in the case of long waves virtually does not change in time.

Table

t minutes	t мин	1	2	3	4
	10	0,212	0,205	0,201	0,200
	20	0,166	0,155	0,162	0,146
	30	0,137	0,119	0,127	0,115
	40	0,116	0,095	0,109	0,090
	50	0,104	0,080	0,095	0,076
	60	0,095	0,071	0,085	0,067

The transpiring insignificant changes in hydrodynamic characteristics are attributable only to the effect of Coriolis force. Under the influence of vertical friction, with an increase in t the initial distribution of the tangential component of the velocity vector is considerably deformed, as can be seen from a comparison of curves 1, 2 (Fig. 3). With an increase in t the amplitude values $v^* = v_2$ decrease, but the position of the maximum value, as in the case of the initial displacement of the fluid surface, to all intents and purposes persists. Numerical computations made it possible to estimate the lifetime of such eddies. For example, with $r = 3 \cdot 10^{-4}$ sec^{-1} a decrease in the maximum velocity value by a factor of 10 occurs during a time interval of about 2 hours.

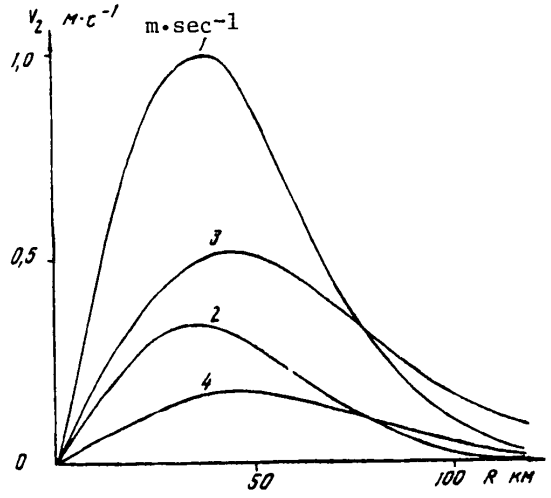

Fig. 3. Distribution v_2 ($m \cdot sec^{-1}$) for t = 0 (curve 1) and t = 1 hour: $r = 3 \cdot 10^{-4}$ sec^{-1}, A = 0 (curve 2); r = 0, $A = 10^5$ $m^2 \cdot sec^{-1}$ (curve 3); $r = 3 \cdot 10^{-4}$ sec^{-1}, $A = 10^5$ $m^2 \cdot sec^{-1}$ (curve 4).

3. We will examine the influence of horizontal friction on the process of evolution of the initial rises of the free surface and the field of tangential velocities (r = 0, $A \neq 0$). Horizontal friction, like vertical friction, favors a more rapid decrease in the amplitudes of the main wave and the descending wave in comparison with the case of an ideal fluid. A comparison of curves 1, 3 (Fig. 1) reveals that horizontal friction leads to some "spraying" of the wave in a radial direction. The dependence of the amplitude of the main wave ζ^+ (m) on time t (min) with r = 0, $A = 5 \cdot 10^4$ $m^2 \cdot sec^{-1}$ is given in column 3 in the table. With an increase in A the attenuation of ζ^+ with time will evidently occur more rapidly.

Figure 2,b shows the process of evolution of the field of tangential velocity caused by an initial rise of the free surface. It can be seen that with time due to horizontal friction, as well as due to vertical friction, there is a decrease

in the amplitude values v_3 and entry into a stationary geostrophic regime of movement does not occur. In contrast to the case $r \neq 0$, $A = 0$ under the influence of horizontal friction the position $\max_R |v_3(R)|$ with time is displaced into the region of high R values.

Horizontal friction also exerts a substantial influence on the initial distribution of the tangential component of the velocity vector, as follows from a comparison of curves 1, 3 (Fig. 3). It can be seen that the amplitude values $v^* = v_2$ decrease and the position $\max_R |v_2(R)|$ is displaced in the direction of high R values. Computations show that with an increase in the A coefficient the field of tangential velocity attenuates more rapidly and therefore the lifetime of the eddy decreases. It is several hours. For example, with $A = 10^5$ $m^2 \cdot sec^{-1}$ for $t = 2$ hours

$$\max_R |v_2(R)| = 0{,}3 \max_R |v_0^*|.$$

4. We will examine the joint effect of vertical and horizontal friction ($r \neq 0$, $A \neq 0$). An analysis indicated that the joint influence of vertical and horizontal friction leads to a decrease in the amplitudes of the head wave and decreasing wave and also to a "spraying" of the first in a horizontal direction. This is indicated by a comparison of curves 1 and 4 (Fig. 1). Wave attenuation, as might be expected, with $A \neq 0$ and $r \neq 0$ is more significant than when only vertical friction is considered or only horizontal friction. This is seen clearly also from the table given in section 2, in which column 4 gives the numerical values λ^+ (m) for $r = 2 \cdot 10^{-4}$ sec^{-1}, $A = 5 \cdot 10^4$ $m^2 \cdot sec^{-1}$. The computations also show that in general a change of the r coefficient exerts a considerably greater influence on the wave characteristics than a change in the A coefficient by the same number of times.

The joint influence of horizontal and vertical friction on the process of evolution of the initial distribution of the tangential component of the velocity vector v_0^* is illustrated by curves 1 and 4 (Fig. 3). It can be seen that with an increase in t under the influence of friction the amplitude values $v^* = v_2$ decrease and the position $\max_R |v_2(R)|$ is displaced in the direction of large R, as occurred due to horizontal friction. However, this decrease in v_2 with one and the same parameters of the problem exceeds the corresponding change occurring with allowance for horizontal friction alone.

BIBLIOGRAPHY

1. Sretenskiy, L. N., TEORIYA VOLNOVYKH DVIZHENIY ZHIDKOSTI (Theory of Wave Movements of Fluid), Moscow, "Nauka," 1977, 816 pages.

2. Kochin, N. Ye., K TEORII VOLN KOSHI-PAUSSONA (On the Theory of Cauchy-Poisson Waves), Vol 2, Moscow-Leningrad, Izd-vo AN SSSR, pp 137-154, 1949.

3. Voyt, S. S., "Long Waves and Tides," ITOGI NAUKI (Scientific Results), Vol 2, SER. OKEANOLOGII (Oceanological Series), Moscow, VINITI, pp 46-89, 1973.

4. Cherkesov, L. V., GIDRODINAMIKA POVERKHNOSTNYKH I VNUTRENNIKH VOLN (Hydrodynamics of Surface and Internal Waves), Kiev, "Nauka Dumka," 1976, 364 pages.

5. Potetyunko, E. N., Srubshchik, L. S. and Tsaryuk, L. B., "Use of the Stationary Phase Method in Some Studies of the Theory of Waves at the Surface of a Viscous Fluid," PMM (Applied Mathematics and Mechanics), Vol 34, No 1, pp 153-161, 1970.

6. Vol'tsinger, N. Ye. and Pyaskovskiy, R. V., OSNOVNYYE OKEANOGRAFICHESKIYE ZADACHI TEORII MELKOY VODY (Principal Oceanographic Problems in the Theory of Shallow Water), Leningrad, Gidrometeoizdat, 1968, 300 pages.

7. Kagan, B. A., GIDRODINAMICHESKIYE MODELI PRILIVNYKH DVIZHENIY V MORE (Hydrodynamic Models of Tidal Movements in the Sea), Leningrad, Gidrometeoizdat, 1968, 220 pages.

8. Dotsenko, S. F., Sergeyevskiy, B. Yu. and Cherkesov, L. V., "On Evolution of Axisymmetric Disturbances in a Fluid," MORSKIYE GIDROFIZICHESKIYE ISSLEDOVANIYA (Marine Hydrophysical Investigations), No 1, Sevastopol', pp 15-31, 1978.

9. Dotsenko, S. F., Sergeyevskiy, B. Yu. and Cherkesov, L. V., "Influence of Friction on Propagation of a Long Wave Caused by Initial Displacement of a Free Surface," POVERKHNOSTNYYE I VNUTRENNIYE VOLNY (Surface and Internal Waves), Sevastopol', Izd-vo AN Ukrainskoy SSR, pp 87-94.

10. Korn, G. and Korn, T., SPRAVOCHNIK PO MATEMATIKE DLYA NAUCHNYKH RABOTNIKOV I INZHENEROV (Handbook on Mathematics for Scientific Workers and Engineers), Moscow, "Nauka," 1974, 832 pages.

EFFECT OF VISCOSITY AND BETA-EFFECT ON GENERATION OF LONG WAVES IN OCEAN BY ATMOSPHERIC WAVES

Sevastopol' TEORETICHESKIYE I EKSPERIMENTAL'NYYE ISSLEDOVANIYA POVERKHNOSTNYKH I VNUTRENNIKH VOLN in Russian 1980 (manuscript received 19 Jun 80) pp 99-107

[Article by V. F. Ivanov]

[Text]

Abstract: The author gives the derivation of an equation for the complex amplitude of a wave taking into account the influence of viscosity, the β- effect, bottom relief and wave shearing stresses. Simple formulas are derived for wave velocities, taking into account the surface and bottom friction layers, as well as formulas for wave shearing stresses expressed through periodic fluctuations of atmospheric pressure. It has been established that the influence of viscosity and the β-effect is manifested for the most part in the resonance region and leads to a change in the resonance amplitudes and frequencies.

It is known that atmospheric disturbances at the ocean surface [1-3] are one of the important sources of generation of internal waves in the ocean. At the same time, in the upper surface layer of the ocean, due to allowance for turbulent friction, there can be intensive turbulent wave movements caused by fluctuations of atmospheric pressure. In most studies [1, 3, 4] devoted to an investigation of the boundary layers and generation of internal waves only the bottom boundary layer is taken into account and also the boundary layers forming at the discontinuities of a multilayer fluid. At the ocean surface it is customary to stipulate the normal stresses and shearing stresses are usually not taken into account at all [1-4] or are taken into account but are not related to fluctuations of atmospheric pressure [5, 8, 12].

In this article we give the derivation of an equation for the complex amplitude of a wave and formulas for wave velocities, taking into account the surface and bottom friction layers, and investigate the joint influence of viscosity and the β-effect on the generation of long waves in the ocean by atmospheric waves.

Within the framework of the linear theory of long waves, with allowance for vertical turbulent viscosity and the effect of Coriolis force, assuming the movements to be periodic, we will write the initial equations in the form

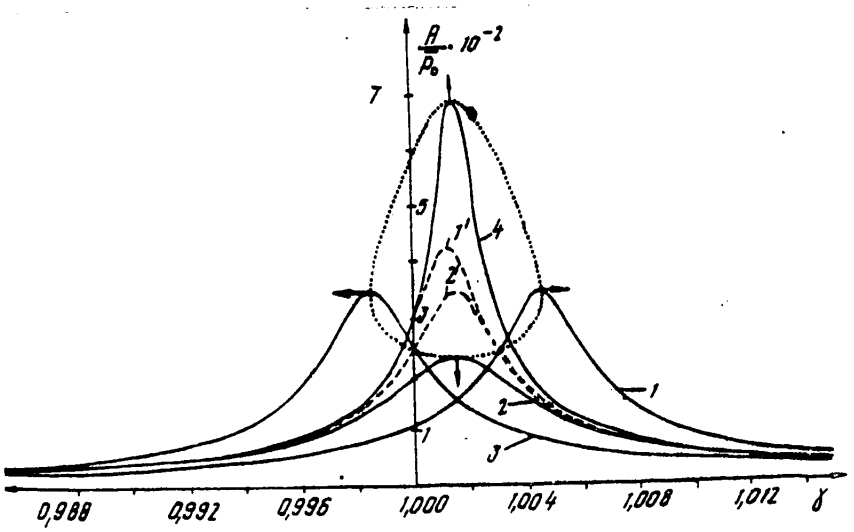

Fig. 1.

Table 1

ψ \ θ	0	90	180	270
10	425,3 (1,0028)	398,5 (1,0012)	427,6 (0,9997)	458,8 (1,0012)
20	424,4 (1,0028)	375,9 (1,0012)	426,8 (0,9998)	490,6 (1,0012)
30	423,1 (1,0025)	359,9 (1,0012)	425,4 (0,9999)	516,7 (1,0012)
40	421,7 (1,0024)	351,0 (1,0012)	423,4 (1,0000)	530,8 (1,0012)
50	420,0 (1,0022)	349,4 (1,0012)	421,6 (1,0002)	529,0 (1,0012)
60	418,6 (1,0020)	355,1 (1,0012)	419,6 (1,0004)	511,3 (1,0012)
70	417,5 (1,0018)	368,4 (1,0012)	418,4 (1,0007)	482,5 (1,0012)
80	416,8 (1,0015)	389,1 (1,0012)	417,1 (1,0010)	449,0 (1,0012)

$$i\sigma u + \ell v = \frac{1}{\rho_0}\frac{\partial p}{\partial x} - \nu\frac{\partial^2 u}{\partial z^2}, \tag{1}$$

$$i\sigma v - \ell u = \frac{1}{\rho_0}\frac{\partial p}{\partial y} - \nu\frac{\partial^2 v}{\partial z^2}, \tag{2}$$

$$-i\sigma\zeta + \int_{\gamma}^{H}\left(\frac{\partial u}{\partial x} + \frac{\partial v}{\partial y}\right)dz = 0 \tag{3}$$

with vertical boundary conditions. At the ocean surface with $z = -\zeta(x,y)$

$$p = p_a, \tag{4}$$

$$\rho_0\nu\frac{\partial u}{\partial z} = -\tau_x, \quad \rho_0\nu\frac{\partial u}{\partial z} = -\tau_y, \tag{5}$$

at the ocean floor with $z = H(x,y)$ (the bottom is considered fixed) for velocity of a wave current we apply the attachment conditions

$$u = v = w = 0. \tag{6}$$

Here $\ell = 2\omega\sin\varphi$, φ is latitude; the x-axis is directed to the east, the y-axis is directed to the north and the z-axis is directed downward. Since henceforth we will be interested in wave movements in the ocean generated by atmospheric waves, p_a and p represent wave pressures in the atmosphere and ocean, τ_x and τ_y are wave shearing stresses, ν is the coefficient of turbulent friction of water, $\nu = 10^2\cdot\text{cm}^2/\text{sec}$ [7].

For a homogeneous ocean, with (4) taken into account, we have

$$p = p_a + \rho_0 g\zeta \tag{7}$$

And the system (1) and (2) is reduced to one equation relative to u

$$\nu^2\frac{\partial^4 u}{\partial z^4} + 2i\sigma\nu\frac{\partial^2 u}{\partial z^2} - (\sigma^2 - \ell^2)u = \sum_{n=1}^{2} L_n(p), \tag{8}$$

where

$$L_n = \frac{1}{2\rho_0[\sigma + (-1)^n\ell]}\left[i\frac{\partial}{\partial x} + (-1)^n\frac{\partial}{\partial y}\right].$$

The solution of (8) is sought in the form

$$u = \sum_{n=1}^{2} C_n, \quad v = i\sum_{n=1}^{2}(-1)^n C_n. \tag{9}$$

where

$$C_n = A_n e^{(1-i)\alpha_n z} + B_n e^{-(1-i)\alpha_n z} - L_n(p),$$

$$\alpha_n = \sqrt{\frac{\sigma + (-1)^n\ell}{2\nu}}, \quad \sigma > \ell.$$

Taking (5) and (6) into account, for C_n we obtain

$$C_n = \frac{1}{4\rho_0 \nu \alpha_n}\left[(1+i)\tau_x + (-1)^n (1-i)\tau_y\right] e^{-(1-i)\alpha_n' z} - L_n(\rho) + L_n(\rho)_{z=H} \cdot e^{-(1-i)\alpha_n (H-z)} \tag{10}$$

In (10) the first terms correspond to the drift velocity of the wave current; the second terms correspond to the gradient current and the third terms correspond to the bottom current.

In the derivation of formulas (9) we will neglect the terms

$$e^{-2(1-i)\alpha_r' H}$$

in comparison with 1, since everywhere we assume that the depth of the ocean is greater than the thickness of the boundary layer. They are correct for $\delta > \ell$ at some distance from the critical latitudes.

We will express the drift part of the wave current through fluctuations of atmospheric pressure. For this purpose we will examine a system of equations for periodic movements in the near-water layer of the atmosphere, which on the assumption of the linear theory of long waves for periodic movements has the same form as (1) and (2). In this case we replace ν by ν' (ν' is the coefficient of turbulent friction of air, $\nu' = 10^4 \cdot cm^2 \cdot sec$ [7, 9]); by p is meant atmospheric wave pressure.

As the boundary conditions we take

$u = u_0$, $v = v_0$ with $z = 0$; u, v are limited with $z = -\infty$. (11)

Then the solution of (1) and (2), by analogy with [8], for the atmosphere is written in the form

$$u = \sum_{n=1}^{2} D_n, \qquad v = i \sum_{n=1}^{2} (-1)^n D_n, \tag{12}$$

where

$$D_n = A_n e^{(1-i)\alpha_n' z} + B_n e^{-(1-i)\alpha_n' z} + \int_0^z F_n \operatorname{sh}\left[(1-i)\alpha_n'(z-\xi)\right] d\xi. \tag{13}$$

Here

$$\alpha_n' = \sqrt{\frac{\delta + (-1)^n \ell}{2\nu'}}, \qquad F_n = \frac{(1-i)}{4\rho_0 \alpha_n' \nu}\left[i\frac{\partial p}{\partial x} + (-1)^n \frac{\partial p}{\partial y}\right].$$

Satisfying the boundary conditions (11) and differentiating u and v for z for

$$\tau_x = -\rho_0 \nu' \left(\frac{\partial u}{\partial z}\right)_{z=0}, \qquad \tau_y = -\rho_0 \nu' \left(\frac{\partial v}{\partial z}\right)_{z=0}, \tag{14}$$

we obtain the expressions

$$\tau_x = \sum_{n=1}^{2} \tau_n, \qquad \tau_y = i \sum_{n=1}^{2} (-1)^n \tau_n, \tag{15}$$

where

$$\tau_n = -\frac{(1-i)}{4\alpha_n'}\left[i\frac{\partial p_a}{\partial x} + (-1)^n \frac{\partial p_a}{\partial y}\right].$$

In (15) we will neglect terms with u_0 and v_0 since they are small in comparison with the others, but we will assume that $p = p_a$ with $z = 0$. These expressions are an analogue of the formulas for the components of wind shearing stress [7].

In (10) we will replace τ_x by τ_y using formulas (15). Then we have

$$C_n = -\sqrt{\frac{\nu'}{\nu}}\, L_n(p_a)\, e^{-(1-i)\alpha_n z} - L_n(p) + L_n(p)_{z=H}\, e^{-(1-i)\alpha_n (H-z)}. \tag{16}$$

Substituting u and v from (9) into (3), with (7) and (16) taken into account, for the complex amplitude of a wave on the β-plane we obtain

$$\underbrace{H\Delta\zeta_1}_{\text{I}} + \underbrace{I(H,\zeta_1) + \frac{i\ell}{\sigma} J(H,\zeta_1)}_{\text{II}} + \underbrace{\frac{(\sigma^2-\ell^2)}{g}\zeta_1}_{\text{III}} + \underbrace{q_x H\frac{\partial\zeta_1}{\partial y} - iq_y H\frac{\partial\zeta_1}{\partial x}}_{\text{IV}} - \underbrace{(1+i)\, q_T \Delta\zeta_1}_{\text{V}} = \underbrace{-(1+i)\frac{1}{\rho_0}\sqrt{\frac{\nu'}{\nu}}\, q_T\, \Delta p_a}_{\text{VI}}, \tag{17}$$

where

$$\zeta_1 = \zeta + \frac{1}{\rho_0 g} p_a; \qquad I(H,\zeta_1) = \frac{\partial H}{\partial x}\frac{\partial\zeta_1}{\partial x} + \frac{\partial H}{\partial y}\frac{\partial\zeta_1}{\partial y};$$

$$J(H,\zeta_1) = \frac{\partial H}{\partial x}\frac{\partial\zeta_1}{\partial y} - \frac{\partial H}{\partial y}\frac{\partial\zeta_1}{\partial x}; \quad q_x = \frac{2\beta\ell}{\sigma^2-\ell^2}; \quad q_y = \frac{\beta(\sigma^2+\ell^2)}{\sigma(\sigma^2-\ell^2)};$$

$$q_T = \frac{\sqrt{2\nu}}{4\sigma(\sigma^2-\ell^2)^{1/2}}\left[(\sigma+\ell)^{1/2} + (\sigma-\ell)^{1/2}\right]; \quad \beta = 2\omega a^{-1}\cos\varphi, \quad a = 6{,}4\cdot 10^8\ \text{см}.$$

In the derivation of equation (17) we will neglect the secondary effects of the variability of ℓ and H, related to viscosity, since we are considering a deep ocean ($H \geqslant 5\cdot\alpha_1^{-1}$). Their contribution does not exceed several percent in comparison with the fundamental terms II and IV, which were retained. For a deep ocean and small periods (about several hours) it is also possible to neglect viscosity (term V), leaving term I.

Now we will integrate the continuity equation

$$\frac{\partial u}{\partial x} + \frac{\partial v}{\partial y} + \frac{\partial w}{\partial z} = 0 \tag{18}$$

for z from 0 to z, and using the boundary condition $w = i\sigma\zeta$ at the surface, we obtain

$$w = i\sigma\zeta + \sum_{n=1}^{2} W_n, \tag{19}$$

where

$$W_n = \frac{i}{2\rho_0[\sigma+(-1)^n\ell]}\left\{\frac{(1+i)}{2\alpha_n}\sqrt{\frac{\nu'}{\nu}}\,\Delta p_a\,(1-e^{-(1-i)\alpha_n z}) + \right.$$

$$+ I\Delta p - \frac{\beta z}{[\sigma+(-1)^n\ell]}\left[i\frac{\partial p}{\partial x} + (-1)^n\frac{\partial p}{\partial y}\right] +$$

$$\left. + \left[I(H,p) - i(-1)^n J(H,p) - \frac{(1+i)}{2\alpha_n}\Delta p\right] e^{-(1-i)\alpha_n (H-z)}\right\}.$$

Specific computations were made for an ocean of a constant depth. Assume that a plane wave of atmospheric pressure moves over the ocean

$$\bar{p}_a = p_0 e^{i(kr - \sigma t)}, \tag{20}$$

where r = x cos θ + y sin θ; θ is the angle between the direction of wave propagation and the x-axis; p_0 is the amplitude of a wave of atmospheric pressure. In an ocean of constant depth it generates a wave in the form

$$\bar{\zeta} = \zeta_0 e^{i(kr - \sigma t)} \tag{21}$$

and with the amplitude ζ_0. From (17), with $p_a = p_0 e^{ikr}$ and $\zeta = \zeta_0 e^{ikr}$ taken into account with $H = H_0 = \text{const}$, we find an expression relating the complex amplitude of a wave in the ocean to the amplitude of a wave in the atmosphere

$$\zeta_0 = p_0 \left[\frac{1 + (1+i)\gamma^2 \sqrt{\nu'/\nu}\, q_T H_0^{-1}}{1 - \gamma^2 + (1+i)\gamma^2 q_T H_0^{-1} + \gamma (q_y \cos\theta + i q_x \sin\theta) k_0^{-1}} - 1 \right], \tag{22}$$

where

$$\gamma = \frac{k}{k_0}; \qquad k_0 = \sqrt{\frac{\sigma^2 - f^2}{gH_0}}.$$

Here k_0 is the wave number (space frequency) corresponding to free oscillations in the absence of viscosity and the β-effect. Using (22) we determine the wave amplitude (absolute ζ_0 value) and its phase

$$A = \sqrt{R^2 + I^2}, \qquad \varphi = \operatorname{arctg} \frac{I}{R}, \tag{23}$$

where R and I are the real and imaginary parts of formula (22). If it is assumed that $\nu' = 0$, in the absence of the β-effect resonance occurs when

$$\gamma_p = \frac{1}{\sqrt{1 - q_T}}, \quad A_p = \frac{p_0 \sqrt{(1 - q_T)^2 + q_T^2}}{q_T}, \quad \varphi = \operatorname{arctg} \frac{1 - q_T}{q_T}. \tag{24}$$

We will assume that H = 1000 m, φ = 30°, p_0 = 100 Pa. It follows from (24) that resonance sets in with $\gamma > 1$, that is, with a space frequency higher than k_0 and a phase close to 90°. Since $q_T << 1$, the shift is small. With γ = 1 the amplitude already decreases by a factor of $\sqrt{2}$ and the phase is equal to 45°. Here and in the text which follows A and A_p are indicated in centimeters.

The figure shows the dependence of the dimensionless amplitudes ($\bar{p}_0 = (\rho_0 g)' \rho_0$) on the dimensionless space frequency γ. The dashed curves 1',2', corresponding to periods of 2 and 3 hours, were computed in the presence of viscosity; the solid curves 1-4, relating to 3 hours, for θ equal to 0, 90, 180 and 270°, were obtained taking into account both viscosity and the β-effect. It can be seen that allowance for vertical turbulent viscosity leads to a shift in the resonance curves to the right (to the left if the dependence of dimensionless wave amplitude on the dimensionless time frequency $\gamma = \sigma/\sigma_0$ [2] is examined). This shift increases with an increase in the period, but the wave amplitude decreases. As a result of the joint effect of viscosity and the β-effect, even for identical periods, in dependence on the θ angle, there is a change in wave amplitude and a shift of the resonance curves.

For example, if the wave propagated to the east ($\theta = 0$) the resonance curve 1 is shifted to the right relative to the dashed curve 2', computed in the absence of the β-effect. For a wave propagating to the west ($\theta = 180°$) the shift of curve 3 occurs to the left. Their resonance amplitudes are virtually identical. If the wave is propagated to the south or north there is no shift of the resonance curves but the resonance amplitude with $\theta = 90°$ (curve 2) is less, whereas with $\theta = 270°$ (curve 4) it is greater than when only viscosity is taken into account. With an increase in the wave period these differences become greater. This also corresponds to an increase in the circles, one of which, with T = 3 hours, represented by the dashed line, is shown in this figure. Each point taken on it corresponds to the resonance amplitude value computed with a smooth change in the θ angle from 0 to 360°. An analysis of the results of computations shows that the influence of viscosity, and also the joint influence of viscosity and the β-effect on wave amplitude, is manifested for the most part in the region close to resonance ($0.98 \leqslant \gamma \leqslant 1.02$). Beyond it these effects are not significant (all the curves for different periods and θ angles virtually merge). With respect to wave phase, with $\gamma < \gamma_p$ it is negative, whereas with $\gamma > \gamma_p$ it is positive, that is, a wave generated in the ocean with an increase in γ first lags in phase behind the atmospheric wave and then for $\gamma > \gamma_p$ begins to "outpace" it, changing very rapidly at 180° with $\gamma \to \gamma_p$. We note that all the curves in the figure were computed in the presence of wave shearing stresses in (22). However, allowance for them does not lead to a substantial increase in wave amplitude for the considered periods, but is more important in computing the velocity of the wave current.

Now we will clarify how a change in the Coriolis parameter exerts an influence on wave amplitude. It was demonstrated in [1] that for free oscillations, corresponding to small periods of about 1-8 hours, a change in the Coriolis parameter exerts little influence on the wave amplitude. For forced oscillations such will be the case only far from resonance, whereas near it the role of the Coriolis parameter increases.

The table gives the values of the resonance amplitudes A_p (T = 2 hours, $\beta \neq 0$) as a function of latitude φ for four values of the θ angle, equal to 0, 90, 180 and 270°. The figures in parentheses correspond to γ_p values corresponding to these resonance amplitudes. It can be seen that if the wave is propagated to the west or east, its amplitude varies little with latitude. However, the greater the latitude, the greater will be the γ value at which resonance is attained for $\theta = 180°$ and the lesser will be the γ value for $\theta = 0°$. If the wave is propagated to the south or north, resonance is attained with virtually identical γ values, but with an increase in latitude the wave amplitude for $\theta = 90°$ first decreases and in the region of the middle latitudes attains a minimum value, and then increases. On the other hand, for an angle $\theta = 270°$ the resonance amplitude of the wave attains a maximum value near the middle latitudes.

Summary

An equation was derived for the complex amplitude of a wave taking into account the influence of viscosity, the β-effect and variable ocean depth. Simple formulas were also derived for the velocity components of a wave current, taking the surface and bottom friction layers into account, and for wave shearing stresses caused by periodic fluctuations of atmospheric pressure.

It is shown that the influence of viscosity, the β-effect and change in the Coriolis parameter on wave amplitude for small periods (of the order of several hours) is manifested for the most part in the resonance region and leads to both a change in the resonance amplitude of the wave and to a shift in the resonance frequency.

BIBLIOGRAPHY

1. Cherkesov, L. V., GIDRODINAMIKA POVERKHNOSTNYKH I VNUTRENNIKH VOLN (Hydrodynamics of Surface and Internal Waves), Kiev, "Naukova Dumka," 1976, 384 pages.

2. Zadorozhnyy, A. I. and Khartiyev, S. M., "Long Internal Waves in a Continuously Stratified Viscous Fluid Caused by Atmospheric Pressure Fluctuations," POVERKHNOSTNYYE I VNUTRENNIYE VOLNY (Surface and Internal Waves), Sevastopol', Izd. MGI AN Ukrainskoy SSR, pp 153-162, 1979.

3. Levkov, N. P. and Cherkesov, L. V., "Boundary Layers of Surface and Internal Long Waves," IZV. AN SSSR: FAO (News of the USSR Academy of Sciences: Physics of the Atmosphere and Ocean), 3, 9, pp 304-310, 1973.

4. Levkov, N. P., "Dissipation of Surface Waves Generated by Periodic Atmospheric Disturbances," MORSKIYE GIDROFIZICHESKIYE ISSLEDOVANIYA (Marine Hydrophysical Investigations), No 4, Sevastopol', pp 76-83, 1973.

5. Vapnyar, D. U., PLANETARNYYE VOLNY I TECHENIYA V EKVATORIAL'NOY ZONE OKEANA (Planetary Waves and Currents in the Equatorial Zone of the Ocean), Kiev, "Naukova Dumka," 1976, 222 pages.

6. Sustavov, Yu. V. and Chernysheva, Ye. S., "Numerical Modeling of Internal Tides in the Faeroe-Shetland Region," POVERKHNOSTNYYE I VNUTRENNIYE VOLNY, Sevastopol', Izd-vo AN Ukrainskoy SSR, pp 168-177, 1978.

7. Sarkisyan, A. S., CHISLENNYY ANALIZ I PROGNOZ MORSKIKH TECHENIY (Numerical Analysis and Prediction of Sea Currents), Leningrad, Gidrometeoizdat, 1977, 182 pages.

8. Kochergin, V. P., TEORIYA I METODY RASCHETA OKEANICHESKIKH TECHENIY (Theory and Methods for Computing Ocean Currents), Moscow, "Nauka," 1978, 127 pages.

9. Gossard, E. E., Khuk, U. Kh., VOLNY V ATMOSFERE (Atmospheric Waves), Moscow, "Mir," 1978, 532 pages.

10. Magulin, V. V., Medvedev, V. I., Mustel', Ye. R. and Parygin, V. N., OSNOVY TEORII KOLEBANIY (Principles of the Theory of Oscillations), Moscow, "Nauka," 1978, 392 pages.

11. Golubev, Yu. N. and Ivanov, V. F., "Influence of Bottom Relief and the β-Effect on Long Barotropic Waves," POVERKHNOSTNYYE I VNUTRENNIYE VOLNY, Sevastopol', Izd. MGI AN Ukrainskoy SSR, pp 102-109, 1978.

12. Krauss, W., "On Currents, Internal and Inertial Waves in a Stratified Ocean Due to Variable Winds." Part 1, DEUT. HYDROGR. Z., 29, 3, pp 87-96, 1976.

GENERATION OF LONG WAVES IN OCEAN OVER LOCAL BOTTOM RISE BY ATMOSPHERIC WAVES

Sevastopol' TEORETICHESKIYE I EKSPERIMENTAL'NYYE ISSLEDOVANIYA POVERKHNOSTNYKH I VNUTRENNIKH VOLN in Russian 1980 (manuscript received 19 Jun 80) pp 108-117

[Article by V. F. Ivanov]

[Text]

Abstract: With allowance for surface and bottom friction layers a study was made of the generation of long waves in the ocean propagating over a bottom rise through the action of atmospheric waves. It was established that in the surface layer the drift wave velocity component makes a substantial contribution to total wave velocity, especially for shorter wave lengths. It is noted that the influence of viscosity, the β-effect and bottom relief on the elements of the generated waves is reflected more significantly in the region close to resonance and in the neighborhood of the peak of the underwater rise.

Recently interest has increased in study of the variability of oceanological fields caused by periodic oscillations in the atmosphere having characteristic periods from several days to months [1]. Nevertheless, it is of interest to investigate wave movements in the ocean in the range from several hours to a day, emphasizing the upper surface layer in which intensive wave movements can exist. In many studies [2, 3] in which a study has been made of the influence of viscosity on the generation of surface and internal waves by atmospheric disturbances in most cases the investigation was confined to the bottom boundary layer and the depth of the ocean was assumed to be constant. An investigation of wave movements at the bottom with allowance for viscosity in a basin of variable depth was made in [5].

In this article, by numerical methods, with allowance for the surface and bottom friction layers, a study is made of the generation of long waves by periodic atmospheric pressures in a homogeneous ocean of variable depth.

Assume that a plane wave of atmospheric pressure

$$\hat{p}_a = p_0 e^{i(kr - \sigma t)}, \quad (1)$$

moves over the ocean. Here r = x cos θ + y sin θ; θ is the angle between the direction of wave propagation and the x-axis. In a region of the ocean of a constant depth it generates a wave in the form

$$\hat{\zeta} = \zeta_0 e^{i(kr-\sigma t)}, \tag{2}$$

which propagates over a local bottom rise having a domelike configuration [5]. The bottom relief of the underwater rise changes in conformity to the formula

$$H = H_0 - H_1 \cos^2 \frac{\pi x}{2l_1} \cos^2 \frac{\pi y}{2l_2} \quad \text{when} \quad |x| \leq l_1, \ |y| \leq l_2, \tag{3}$$

$$H = H_0 \quad \text{when} \quad |x| > l_1, \ |y| > l_2.$$

where l_1 and l_2 are the horizontal dimensions of the region at the base of the underwater rise; H_0 is maximum ocean depth; H_1 is the elevation of the bottom rise. We will investigate deformation of waves in the ocean generated by atmospheric waves over the underwater rise and we will study the structure of wave velocities.

The equation for the complex amplitude of a wave with allowance for viscosity, the β-effect, bottom relief, wave shearing and normal stresses at the surface, expressed through atmospheric pressure gradients, is written in the form

$$\sigma\zeta + \sum_{n=1}^{2} \frac{g}{2[\sigma+(-1)^n l]} \left\{ H \cdot \Delta\zeta_1 - \frac{(1+i)}{2\alpha_n} \Delta\zeta_1 - \frac{\rho H}{[\sigma+(-1)^n l]} L_n(\zeta_1) + \right.$$
$$\left. + L_n(\zeta_1) \cdot L_n^*(H) \right\} = - \sum_{n=1}^{2} \frac{(1+i)}{4\rho_0 \alpha_n [\sigma+(-1)^n l]} \sqrt{\frac{\nu'}{\nu}} \Delta p_a, \tag{4}$$

where $l = 2\omega \sin\varphi$; φ is latitude; $\zeta_1 = \zeta + p_a/g\rho_c$;

$$\alpha_n = \sqrt{\frac{\sigma+(-1)^n l}{2\nu}}; \quad L_n = i\frac{\partial}{\partial x} + (-1)^n \frac{\partial}{\partial y};$$

and L_n^* is a complexly conjugate operator; ν' and ν are the coefficients of turbulent viscosity of air and sea water. In accordance with [4] we will assume that they are equal to $\nu' = 10^4$ cm^2/sec, $\nu = 10^2$ cm^2/sec. In [6], within the framework of the linear theory of long waves, for $\sigma > l$ the equation (4) was derived in which we will neglect the secondary effects of the variability of l and H, associated with viscosity, since their role is small for the deep ocean when the depth H > h, where h is the thickness of the boundary layer ($h = 5 \cdot \alpha_1^{-1}$).

Knowing ζ and p_a it is possible to compute the velocity components of the wave current using the formulas

$$u = \sum_{n=1}^{2} c_n, \quad v = i \sum_{n=1}^{2} (-1)^n c_n, \tag{5}$$

where

$$c_n = -\sqrt{\frac{\nu'}{\nu}}\bar{L}_n(p_a)\,e^{-(1-i)\alpha_n z} - \bar{L}_n(p) + \bar{L}_n(p)_{z=H}\,e^{-(1-i)\alpha_n (H-z)},$$
$$\bar{L}_n = \frac{1}{2\rho_0[\sigma + (-1)^n \ell]}\,L_n. \tag{6}$$

In formulas (5), (6) the first terms correspond to the drift velocity of the wave current (we will denote the components of drift velocity by u_{dr} and v_{dr}), the second terms correspond to the gradient velocity and the third to bottom velocity.

The solution of system (4) is taken in the form

$$\zeta = \bar{\zeta} + \tilde{\zeta}, \tag{7}$$

where $\tilde{\zeta}$ is a disturbance introduced by bottom relief;

$$\zeta = \zeta_0\, e^{ikr}. \tag{8}$$

the solution with $H = H_0 = \text{const}$. The complex amplitude of the wave ζ_0 with allowance for

$$p_a = p_0\, e^{ikr} \tag{9}$$

is found from (4), assuming the ocean depth to be constant,

$$\zeta_0 = p_0\,\frac{(A-B)}{\rho_0(\sigma + gB)}, \tag{10}$$

where

$$A = \sum_{n=1}^{2} \frac{(1+i)k^2}{4\alpha_n[\sigma + (-1)^n \ell]}\sqrt{\frac{\nu'}{\nu}};$$
$$B = \sum_{n=1}^{2} \frac{k}{2[\sigma + (-1)^n \ell]}\left\{k\left[\frac{(1+i)}{2\alpha_n} - H_0\right] + \frac{\rho H_0}{[\sigma + (-1)^n \ell]}\left[\cos\theta - i(-1)^n \sin\theta\right]\right\}.$$

Since beyond the local bottom rise the ocean depth is considered constant, the disturbances introduced by bottom relief attenuate far from the underwater rise. Accordingly, the horizontal dimensions L_1 and L_2 ($L_1 > \ell_1$, $L_2 > \ell_2$) of the investigated region must be such that at its outer boundaries it can be assumed [5] that

$$\tilde{\zeta} = 0. \tag{11}$$

At the internal points of the considered region we determine amplitude from equation (4). Substituting (7) into it, with (8) and (9) taken into account, we obtain an inhomogeneous equation relative to $\tilde{\zeta}$

$$\sigma\tilde{\zeta} + \sum_{n=1}^{2} \frac{g}{2[\sigma + (-1)^n \ell]}\left\{H\Delta\tilde{\zeta} - \frac{(1+i)}{2\alpha_n}\Delta\tilde{\zeta} - \frac{\rho H}{[\sigma + (-1)^n \ell]}\,L_n(\tilde{\zeta}) + \right.$$
$$\left. + L_n(\tilde{\zeta})\,L_n^*(H)\right\} = -\left\{\left[g(B+C) + \sigma\right]\zeta_0 + \frac{1}{\rho_0}(B + C - A)p_0\right\}e^{ikr}, \tag{12}$$

where $$C=\sum_{n=1}^{2}\frac{k}{2[\sigma+(-1)^n\ell]}\left[\cos\theta-i(-1)^n\sin\theta\right]\left[i\frac{\partial H}{\partial x}-(-1)^n\frac{\partial H}{\partial y}\right].$$

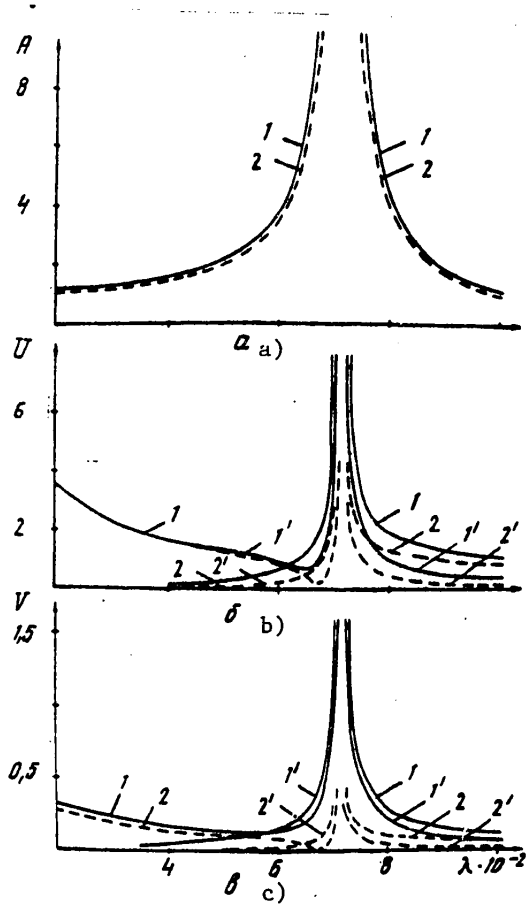

Fig. 1.

The derivatives in (12) are replaced by central finite-difference ratios and the derived system of algebraic equations is solved by the Seidel iteration method.

Specific computations of wave elements were made for parameters of the problem which then were not changed (the linear dimensions were given in kilometers): $\ell_1 = \ell_2 = 48$; $L_1 = L_2 = 30$; $H_0 = 1$; $H_1 = 0.94$; $\varphi = 30°$, the amplitude of the atmospheric pressure was assumed equal to $p_0 = 100$ Pa, the interval of the computation grid was $h_0 = 4$ km.

Emphasis was on an investigation of the influence of bottom relief on wave amplitude and wave velocities and study of their spatial structure.

Figure 1a,b,c shows the dependence of the maximum amplitudes of the wave A and surface wave velocities U and V on λ for T = 2 and $\beta = 0$, computed for variable (curves 1 and 1') and constant (curves 2 and 2') bottom relief (here and in the text which follows U and V are indicated in centimeters per second, A in centimeters, λ in kilometers, ν and ν' in square centimeters per second, T is in hours. Curves 1 and 2 were obtained taking into account all the terms in (4) and (5) and 1' and 2' for $\nu' = 0$. In Fig. 1,a the curves 1' and 2' have been omitted because they are close to 1 and 2. This small difference is attributable to the fact that allowance for tangential friction at the surface ($\nu' \neq 0$) has little effect on wave amplitude (by only several percent), but exerts a more significant influence on wave movements in the surface layer (Fig. 1,b,c). In this case the greatest differences in the amplitudes of U_n, V_n from U_{gr}, V_{gr}, computed for the cases $\nu' = 10^4$ and $\nu' = 0$ respectively, are observed on the slopes and at the base of the resonance curves. It should be noted that for $\lambda > \lambda$ (λ is the resonance wave length) the amplitudes of velocities $U_n > U_{gr}$, $V_n > V_{gr}$, whereas for $625 < \lambda < \lambda_p$, on the other hand, $U_n < U_{gr}$, $V_n < V_{gr}$. The influence of bottom relief on wave amplitude is more significant near resonance and on the amplitudes U and V in the entire resonance region ($3 \leqslant \lambda \leqslant 12$).

Now we will examine a case when $\lambda = \lambda_p$. An analysis of the results of computations shows that during resonance the influence of tangential friction with z = 0 exerts little effect both on the wave amplitude and on the amplitude of velocities. For example, for the period T = 1 with $\nu' = 10^4$ the amplitudes A_p, U_p and V_p are approximately 1.7% greater than the corresponding amplitudes with $\nu' = 0$, whereas for T = 2 -- by 2.5%. At the same time, the influence of bottom relief on wave elements is manifested more strongly and increases with approach to resonance. For the amplitudes of velocities this increase is considerably greater than for the wave amplitude. For example, for T = 1 with $\nu' = 10^4$ A_p is 15.2% greater for variable bottom relief than for constant bottom relief, U_p is greater by a factor of 2.3 and V_p by a factor of 14.2. For T = 2 this increase is: A_p by 4.1%, U_p and V_p by factors of 1.7 and 5.5 respectively, that is, with an increase in the period the role of bottom relief decreases.

Returning to Fig. 1,b,c we see that with a decrease in wave length its amplitude far from resonance decreases, whereas the velocities U_n and V_n increase. This increase is attributable to an increase in the role of the components of drift wave velocities U_{dr} and V_{dr}.

Table 1 gives the values U_{dr} and V_{dr} (upper and lower lines respectively), computed with the use of formulas (5), (6) for six periods and different wave lengths. It follows from this table that with an increase in the period of oscillations and a decrease in wavelength U_{gr} and V_{gr} increase by several times and allowance for them is important in the surface layer, especially for shorter wave lengths.

Figure 2 shows the fields of amplitudes of surface velocities U and V, computed using formulas (5) for T = 2 and two wave lengths $\lambda = 825$ and $\lambda = 800$. The solid curves correspond to the total velocities U_n and V_n, whereas the dashed curves correspond to the gradient velocities U_{gr} and V_{gr}, computed without allowance for the terms U_{dr} and V_{dr}. An analysis of the U_n and U_{gr} fields shows that at the center of the underwater rise there is one large disturbance on both sides of which there are two additional lobes. Qualitatively the U_n and U_{gr} fields for $\lambda = 800$ agree well

with one another although there is a small quantitative difference. The maximum amplitudes $U_n = 0.91$, $U_{gr} = 1.00$. For $\lambda = 625$ the U_n and U_{gr} fields have only an external similarity. A more detailed analysis indicates that the U_n field at the center has a minimum ($U_n = 0.3$) and U_{gr} has a maximum ($U_{gr} = 0.82$). Within the additional lobes U_n is greater and U_{gr} is less than outside them.

Table 1

T \ λ	200	400	600	800	1000
2	3,56 0,30	1,78 0,15	1,19 0,10	0,89 0,07	0,71 0,06
4	7,27 1,21	3,63 0,61	2,42 0,40	1,82 0,30	1,45 0,24
8	14,30 2,83	5,65 1,41	3,77 0,94	2,83 0,71	2,26 0,57
8	15,89 5,30	7,95 2,65	5,30 1,77	3,97 1,32	3,18 1,06
10	21,37 8,90	10,68 4,45	7,12 2,97	5,34 2,23	4,27 1,78
12	28,25 14,13	14,13 7,06	9,42 4,71	7,06 3,53	5,65 2,83

Table 2

	θ \ λ	6[illegible]	750	705	725	714,76
P	0	9,83 9,83	10,33 10,03	38,3 42,1	36,0 32,9	432 293
	180	9,04 9,45	10,33 10,65	38,4 35,2	36,0 33,7	432 295
U		1,92 [illegible]	2,33 2,27	7,96 8,78	7,87 7,21	91,7 65,7
	180	[illegible],92 1,68	2,32 2,38	8,16 7,46	7,68 8,45	91,7 65,9
V		0,407 0,416	[illegible],476 0,462	[illegible],86 1,83	1,62 1,49	19,0 13,7
	180	0,408 0,400	0,474 0,482	1,71 1,56	1,59 1,75	18,1 13,8

The V_n and V_{gr} fields behave otherwise. Both qualitatively and quantitatively they differ greatly from one another. For example, the V_n field for $\lambda = 625$ to the left of the direction of movement of the wave ($y > 0$) is more intense and has two maxima.

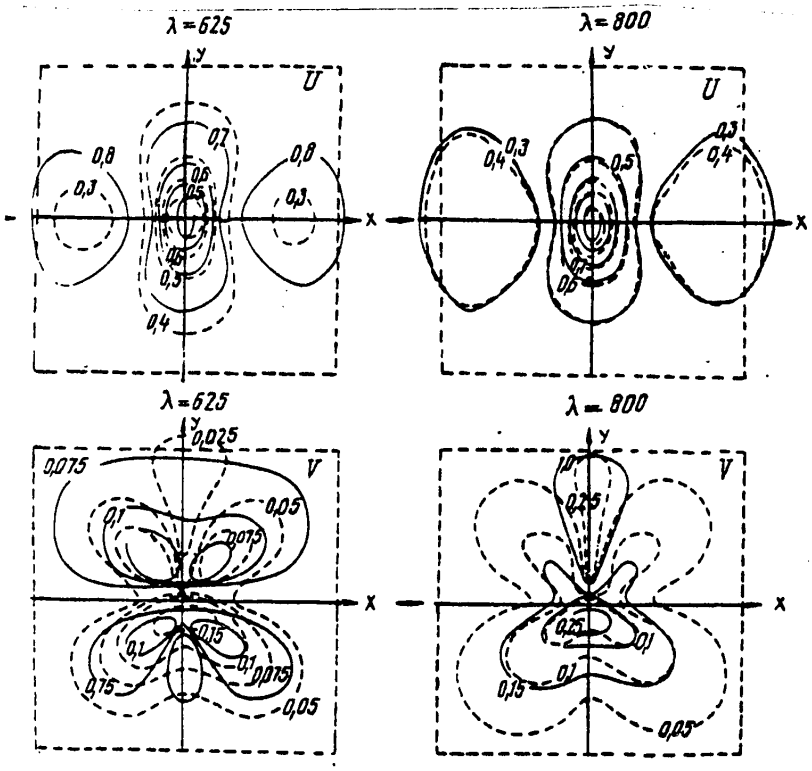

Fig. 2.

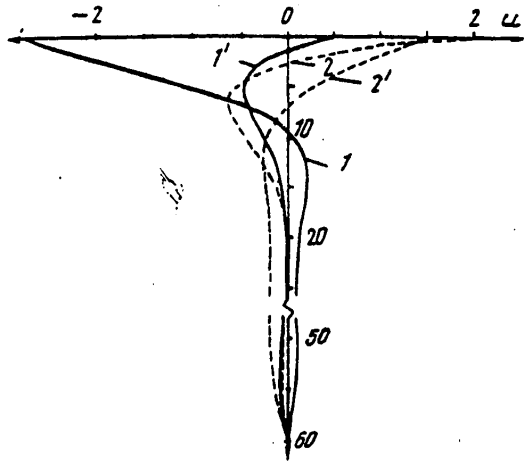

Fig. 3a.

To the right of the x-axis ($y<0$) it is weaker and consists of two lobes, each of which has its own maximum. The isolines of the V_{gr} field, on the other hand, are clustered to a greater degree to the right of the x-axis, but at the left there are two lobes with a maximum and a separate lobe along the y-axis ($y>0$) with a minimum. For $\lambda = 800$ the V_n and V_{gr} fields agree better qualitatively than for $\lambda = 625$. They have a great quantitative difference. For example, the V_n field is more intense than V_{gr} (Fig. 2).

The presence of a β-effect is reflected for the most part in the resonance region $675 < \lambda < 750$ ($1.059 > \gamma > 0.953$, where $\gamma = \lambda_p \mu$, $\lambda_p = 714.76$). It can be seen (Table 2) that for $\lambda = 675$ and $\lambda \geq 750$ the influence of the β-effect and bottom relief on the amplitudes of waves and velocities is small and does not exceed 2-3% (the upper lines correspond to the values of the maximum amplitudes A, U, V, computed without taking the β-effect into account and the lower lines -- with the β-effect taken into account). With approach to resonance their role increases. For example, for $\lambda = 705$ and $\lambda = 725$ the maximum amplitudes A, U and V change by 8-10% in comparison with a case when the β-effect is absent.

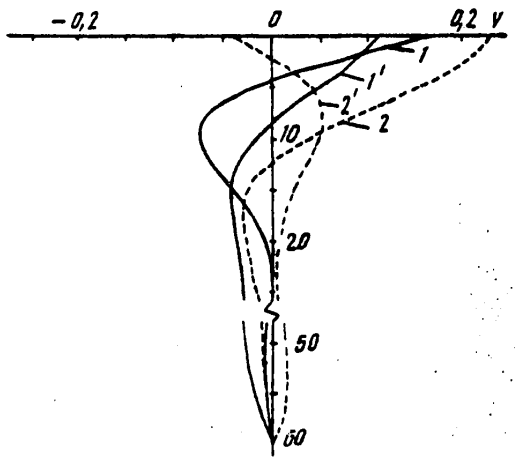

Fig. 3b.

If $\beta = 0$, the amplitudes of the waves virtually do not change for waves propagating in forward ($\theta = 0°$) and backward ($\theta = 180°$) directions, but the amplitudes of velocities change by only 2-3% for $\lambda = 705$ and $\lambda = 725$. For these same wave lengths, but with allowance for the β-effect, this difference is more significant and for both the wave amplitude and for velocities is approximately 15-17%. In addition, if $\beta = 0$ and $\lambda < \lambda_p$, the amplitudes A, U and V_0 are less for $\theta = 0°$ and greater for $\theta = 180°$ than in the presence of a β-effect. In the case $\lambda > \lambda_p$ the opposite picture is observed.

With resonance ($\lambda = \lambda_p$) the role of the β-effect is manifested in a decrease in the maximum amplitudes of the wave elements. For example, the amplitude of the wave is 32% less and the amplitudes of velocities are approximately 28% less than

in the absence of the β-effect. It must be noted that in a resonance case even with $\beta \neq 0$ the maximum amplitudes of velocities and waves virtually do not change for $\theta = 0$ and $\theta = 180°$. The joint influence of the β-effect and bottom relief increases not only with approach to resonance, but also with approach to the peak of the underwater rise. Nevertheless, qualitatively the fields of amplitudes A_β, U_β and V_β do not experience significant changes. In this case the V field is more intense to the right of the direction of movement of the wave both during its propagation in a straight line and in the opposite direction. In a study of the role of the β-effect we assumed $\gamma' = 0$ in order to evaluate better its influence on the amplitudes of gradient wave velocities.

Figure 3 shows profiles of the velocities u and v, computed for the period T = 2 hours at the time t = 0 (solid curves) and after a quarter-period t = 0.25T (dashed curves) for a point situated at the center of the bottom rise (x = 0, y = 0). Curves 1 and 2 correspond to $\lambda = 200$, curves 1' and 2' correspond to $\lambda = 400$. The analysis indicates that as time passes the profiles of the velocities u and v experience considerable changes both in value and direction. For example, the velocity u for $\lambda = 200$ has a clearly expressed maximum at a depth of 6.5 m at the time t = 0.25T, and for $\lambda = 400$ -- with t = 0. The v profiles behave similarly, but in contrast to u the v velocities have a rather distinct maximum for $\lambda = 200$ and t = 0 (curve 1), and also for $\lambda = 400$ and t = 0.25T (curve 2').

Summary

Allowance for surface shearing stresses has little effect on wave amplitude for short periods (of about several hours) in comparison with the normal stresses, but is more important in computing the velocity of the wave current, especially in the surface layer for shorter wave lengths.

The influence of bottom relief, and also the joint influence of the β-effect and bottom relief is manifested to the greatest degree near resonance and near the peak of the underwater rise.

BIBLIOGRAPHY

1. Lappo, S. S., SREDNEMASSHTABNYYE DINAMICHESKIYE PROTSESSY OKEANA, VOZBUZHDAYEMYYE ATMOSFEROY (Intermediate Dynamic Processes in the Ocean Excited by the Atmosphere), Moscow, "Nauka," 1979, 181 pages.

2. Cherkesov, L. V., GIDRODINAMIKA POVERKHNOSTNYKH I VNUTRENNIKH VOLN (Hydrodynamics of Surface and Internal Waves), Kiev, "Nauka Dumka," 1976, 364 pages.

3. Levkov, N. P., "Dissipation of Surface Waves Generated by Periodic Atmospheric Disturbances," MORSKIYE GIDROFIZICHESKIYE ISSLEDOVANIYA (Marine Hydrophysical Investigations), No 4, Sevastopol', pp 76-83, 1973.

4. Sarkisyan, A. S., CHISLENNYY ANALIZ I PROGNOZ MORSKIKH TECHENIY (Numerical Analysis and Prediction of Sea Currents), Leningrad, Gidrometeoizdat, 1977, 182 pages.

8. Golubev, Yu. N. and Ivanov, V. F., "Deformation of a Long Wave Over an Underwater Mountain," MORSKIYE GIDROFIZICHESKIYE ISSLEDOVANIYA, No 1, Sevastopol', pp 32-43, 1978.

6. Ivanov, V. F., "Influence of Viscosity and the β-Effect on the Generation of Long Waves in the Ocean by Atmospheric Waves," in this collection of articles, pp 99-107.

INFLUENCE OF FLUID VISCOSITY ON WAVE RESISTANCE TO SYSTEM OF NORMAL STRESSES DISTRIBUTED IN SEGMENT

Sevastopol' TEORETICHESKIYE I EKSPERIMENTAL'NYYE ISSLEDOVANIYA POVERKHNOSTNYKH I VNUTRENNIKH VOLN in Russian 1980 (manuscript received 19 Jun 80) pp 118-123

[Article by L. G. Yeremenko]

[Text]

Abstract: In this article the wave resistance of a viscous fluid is represented by the L. N. Sretenskiy integral. An asymptotic solution is obtained in the case of an arbitrary viscosity. Known solutions are obtained in the case of vanishing viscosity. Numerical computations indicate the presence of such regions of parameters in which even a small viscosity gives results differing substantially from the results for an ideal fluid in these same regions of the values of the parameters.

In a linear formulation we solve the problem of computing the wave resistance R of a viscous fluid covered by a viscous film with the steady movement of normal pressures p_*, uniformly distributed in a segment [1, 2], over the surface of the fluid

$$u\frac{\partial \bar{v}}{\partial x}=-\frac{1}{\rho}\nabla p+\nu\Delta\bar{v},\quad \operatorname{div}\bar{v}=0, \tag{1}$$

$$p=-\int_{-\infty}^{\infty}p_*(x)\frac{\partial\zeta}{\partial x}\,dx; \tag{2}$$

with z = 0

$$-p+2\mu\frac{\partial v_z}{\partial z}+\rho g\zeta-\alpha\frac{\partial^2\zeta}{\partial x^2}=-p_*(x), \tag{3}$$

$$p=p+\rho g z,\quad \mu\left[\frac{\partial v_x}{\partial z}+\frac{\partial v_z}{\partial x}\right]=0, \tag{4}$$

$$u\frac{\partial\zeta}{\partial x}=v_z; \tag{5}$$

$$v_x,\ v_z,\ \rho \to 0 \text{ when } z \to -\infty; \tag{6}$$

$$\frac{\partial \rho}{\partial x},\ v_x,\ v_z,\ \rho,\ \frac{\partial v_x}{\partial x},\ \frac{\partial v_z}{\partial x} \to 0 \text{ when } |x| \to \infty, \tag{7}$$

$$\rho_*(x) = \begin{cases} Q, & |x| \le \ell, \\ 0, & |x| > \ell. \end{cases} \tag{8}$$

Here ρ is fluid density; ν is the kinematic viscosity coefficient; u is the velocity of movement of normal pressures; ρ_f is the density of the surface film; v_x and v_z are the velocity components of the fluid; α is reduced surface tension [5]; ζ is the rise of the free surface; ρ is fluid pressure; P is the dynamic component of fluid pressure.

The origin of coordinates is set on the undisturbed fluid surface. The oz-axis is directed vertically upward.

The system (1)-(8) is solved by use of an integral Fourier transform of x. Inverting, we obtain the following integral expression for rise of the free surface:

$$\zeta = -\frac{1}{\sqrt{2\pi}\rho} \int_{-\infty}^{\infty} \frac{e^{-i\xi x} |\xi| \bar{\rho}_*(\xi)\, d\xi}{(2\nu\xi^2 - i\xi u)^2 + (g|\xi| + \beta|\xi|^3) - 4\nu^{3/2}|\xi|^3 \sqrt{\nu\xi^2 - i\xi u}}, \tag{9}$$

$$\bar{\rho}_*(\xi) = \frac{1}{\sqrt{2\pi}} \int_{-\infty}^{\infty} \rho_*(x) e^{i\xi x}\, dx.$$

After some transformations the integral expression of wave resistance is represented in the form

$$R = -\frac{2Q^2}{\pi\rho} \int_{-\infty}^{\infty} \frac{i \sin^2 \xi\ell\, |\xi|\, d\xi}{\xi\left([2\nu\xi^2 - i\xi u]^2 + (g|\xi| + \beta|\xi|^3) - 4\nu^{3/2}|\xi|^3 \sqrt{\xi^2\nu - i\xi u}\right)}, \tag{10}$$

$$\beta = \alpha/\rho.$$

Investigating the expression for $|q|$ at the extremum,

$$|q| = \left| \frac{4\nu^{3/2}|\xi|^3 \sqrt{\nu\xi^2 - i\xi u}}{(2\nu\xi^2 - i\xi u)^2 + g|\xi| + \beta|\xi|^3} \right|,$$

it can be demonstrated that for all ξ $(-\infty < \xi < +\infty)$ the following evaluation is correct

$$|q| < c = \frac{1}{\sqrt{1+\gamma}} < 1, \quad \gamma = \frac{g + \xi^2\beta}{\nu^2 |\xi|^3}.$$

By virtue of this evaluation the wave resistance (10) can be written in the form of a converging series [3, 4]

$$R = \sum_{n=0}^{N} R_n + R_N = \sum_{n=0}^{N} \int_{-\infty}^{\infty} \frac{i \sin^2 \xi\ell\, |\xi| \cdot q^n\, d\xi}{\xi\left[(2\nu\xi^2 - i\xi u)^2 + (g|\xi| + \beta|\xi|^3)\right]} + R_N. \tag{11}$$

We will make a replacement of variables $\mathcal{E} = gv/u^2$ and then write the main term of the expansion

$$R = -\frac{2Q^2}{\pi\rho g}\int_0^\infty \frac{i\sin^2 v/Fr^2\, dv}{v[4\Phi^2 v^3 - (4i\Phi - \Gamma)v^2 - v + 1]} +$$

$$+\frac{2Q^2}{\pi\rho g}\int_0^\infty \frac{i\sin^2 v/Fr^2\, dv}{v[4\Phi^2 v^3 + (4i\Phi + \Gamma)v^2 - v + 1]}, \qquad (12)$$

where

$$\Phi = \frac{vQ}{u^3}; \quad Fr = \frac{u}{\sqrt{gl}}; \quad \Gamma = \frac{1}{We} = \frac{\beta Q}{u^4};$$

WE is the Weber number, Fr is the Froude number.

We will break down the integrands (12) into simple factors

$$R = -\frac{Qi}{\pi\rho g}\left\{\sum_{j=1}^{3}\frac{1}{12\Phi v_j^2 - 8\Phi v_j i - 1}\left[-\frac{1}{v_j}\int_0^\infty \frac{dv}{v} + \frac{1}{v_j}\int_0^\infty \frac{\cos 2v/Fr^2}{v}dv + \right.\right.$$

$$+\frac{1}{v_j}\int_0^\infty \frac{dv}{v - v_j} - \frac{1}{v_j}\int_0^\infty \frac{\cos 2v/Fr^2}{v - v_j}dv\Big] - \sum_{j=1}^{3}\frac{1}{12\Phi^2\tilde{v}_j^2 + 8\Phi\tilde{v}_j i - 1}\left[-\frac{1}{\tilde{v}_j}\int_0^\infty \frac{dv}{v} + \right.$$

$$\left.\left. + \frac{1}{\tilde{v}_j}\int_0^\infty \frac{\cos 2v/Fr^2}{v}dv + \frac{1}{\tilde{v}_j}\int_0^\infty \frac{dv}{v - \tilde{v}_j}dv - \frac{1}{\tilde{v}_j}\int_0^\infty \frac{\cos 2v/Fr^2}{v - \tilde{v}_j}dv\right]\right\}. \qquad (13)$$

Here v_j and $\tilde{v}_j$ are the roots of the equations respectively:

$$4\Phi^2 v^3 - (4i\Phi - \Gamma)v^2 - v + 1 = 0, \quad 4\Phi^2 \tilde{v}^3 + (4i\Phi + \Gamma)\tilde{v}^2 - \tilde{v} + 1 = 0.$$

Using expressions 3.722.7, 8.232.2 from [6], we finally obtain

$$R = \frac{Q^2 i}{\pi\rho g}\left\{\sum_{j=1}^{3}\frac{1}{v_j(12\Phi^2 v_j^2 - 8\Phi v_j i - 1)}\left\{-C - \ln\frac{2}{Fr^2} - \right.\right.$$

$$-\frac{1}{\ln v_j} + \cos\left(\frac{2}{Fr^2}v_j\right)ci\left(\frac{2}{Fr^2}v_j\right) + \sin\left(\frac{2}{Fr^2}v_j\right)\left[si\left(\frac{2}{Fr^2}v_j\right) + \right. \qquad (14)$$

$$\left.\left. + \pi\right]\right\} - \sum_{j=1}^{3}\frac{1}{(12\Phi^2\tilde{v}_j^2 + 8\Phi\tilde{v}_j - 1)\tilde{v}_j}\left\{-C - \ln\frac{2}{Fr^2} - \frac{1}{\ln\tilde{v}_j} + \right.$$

$$+\cos\left(\frac{2}{Fr^2}\bar{v}_j\right)\left[\operatorname{ci}\left(\frac{2}{Fr^2}\bar{v}_j\right)+\sin\left(\frac{2}{Fr^2}\bar{v}_j\right)\left[\operatorname{si}\left(\frac{2}{Fr^2}\bar{v}_j\right)+\pi\right]\right]\Bigg\}. \qquad (14)$$

The residual of the series can be represented in the following way:

$$R_N=-\frac{2Q^2}{\pi\rho g}\int_{-\infty}^{\infty}\frac{i\sin^2 v\ell}{\left(4\varphi^2|v|^3-4i\varphi v^2+Fv^2-|v|+1\right)v}\,\frac{q^N}{1-q}\,dv.$$

We will evaluate R_N with respect to absolute value, assuming N = 2k. Then $|R_N|$ + $2|J|$, where

$$|J_1|\leq\int_0^{\infty}\frac{|q^2|^k\sqrt[4]{\varphi^2v^3+1+Fv^2}\,dv}{v\sqrt{\left(4\varphi^2v^3+Fv^2-v+1\right)^2+16\varphi^2v^4}\left(\sqrt[4]{\varphi^2v^3+1+Fv^2}-\sqrt[4]{\varphi^2v^3}\right)}.$$

It can be shown [5] that

$$\left|\frac{\sqrt[4]{\varphi^2v^3+Fv^2+1}}{\sqrt{\left(4\varphi^2v^3+Fv^2-v+1\right)^2+16\varphi^2v^4}\left(\sqrt[4]{\varphi^2v^3+1+Fv^2}-\sqrt[4]{\varphi^2v^3}\right)}\right|<\frac{(1+Fv^2)^{-1}}{\varepsilon^4\,2\sqrt{2}}.$$

Then for $|J_1|$ we obtain

$$|J_1|<\frac{1}{2\sqrt{2}}\int_0^{\infty}\frac{q^{2k}}{\varepsilon^4v\left(1+Fv^2\right)}\,dv.$$

We will break down the integration interval into two parts [0, A] and [A, ∞)

$$|J_1|<\frac{1}{2\sqrt{2}}\int_0^{A}\frac{q^{2k}\,dv}{v\varepsilon^4\left(1+Fv^2\right)}+\frac{1}{2\sqrt{2}}\int_A^{\infty}\frac{q^{2k}\,dv}{v\varepsilon^4\left(1+Fv^2\right)}$$

and in the segment [A, ∞) we evaluate $|q|<\varepsilon$ as unity. Then

$$|J_1|<\frac{1}{2\sqrt{2}}\int_0^{A}\varphi^{k-2}v^{3(k-5)/2}dv+\frac{1}{2\sqrt{2}}\int_A^{\infty}\frac{dv}{Fv^3}<\frac{1}{2\sqrt{2}}\varphi^{k-2}\frac{A^{3k/2-4}}{3k/2-4}+\frac{1}{2\sqrt{2}}\,\frac{1}{2FA^2}.$$

We will select A from the consideration that both terms on the right-hand side of the latter inequality are of the same order of magnitude

$$\varphi^{k-2}A^{3(k-4)/2}=\frac{1}{FA^2},\quad A^{3(k-2)/2}=\frac{1}{F\varphi^{k-2}},\quad A=\frac{1}{F^{2/(3k-4)}\varphi^{(2k-4)/(3k-4)}}.$$

Thus, we obtain the following evaluation of the residue of the series:

$$|R_n|<\frac{1}{\sqrt{2}}\,\varphi^{\frac{4k-8}{3k-4}}\cdot F^{\frac{8-3k}{3k-4}}\cdot\frac{6-3k}{3k-8}.$$

Numerical analysis of problem. In the case of steady movement of the normal stresses distributed in a segment we made computations of the total resistance using formula (14) for the cases $\beta = 0$ and $\beta \neq 0$, and also using the L. N. Sretenskiy formulas [7] for the wave resistance of an ideal fluid and for the wave resistance of an ideal fluid with a correction for viscosity

$$R_u=\frac{4Q^2}{\rho g}\sin^2\frac{1}{Fr^2},\qquad R=R_u-\frac{4Q^2}{\rho g}\,\frac{2\varphi}{\pi}\ln\frac{1}{Fr^2\varphi}.$$

The computations were made for different Fr and WE numbers. It follows from the computations that the influence of viscosity in essence is expressed only for velocities of movement greater than 20 m/sec. The presence of a region of a sharp rise and fall of the wave resistance of a viscous fluid is of interest, whereas for an ideal fluid a tendency of wave resistance to a limiting constant value is characteristic. The influence of a surface film is important only in the rise region.

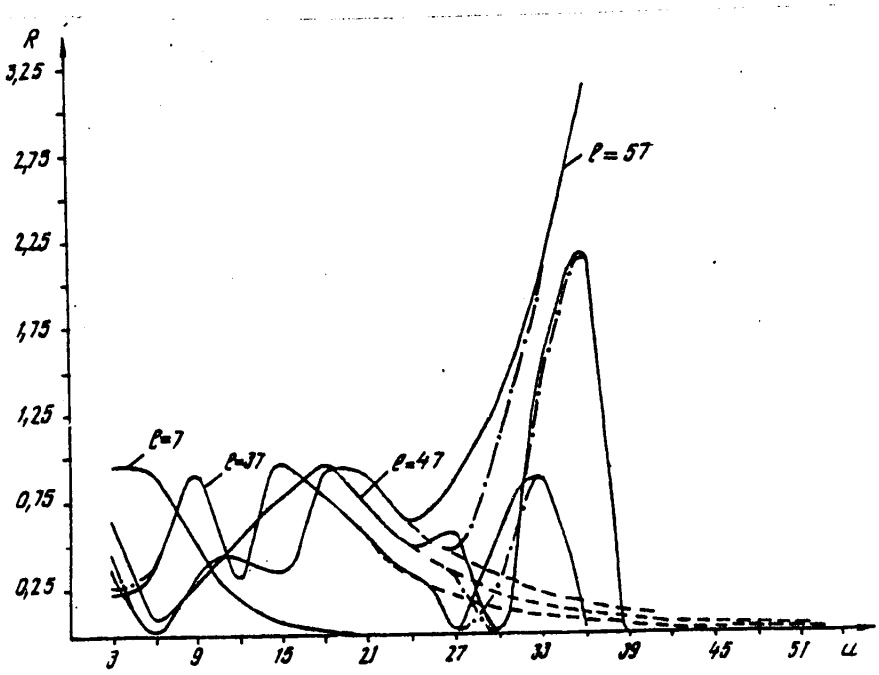

Fig. 1. Wave resistance: of moving pressure

$$p_* = \begin{cases} Q, & |x| \leqslant \ell \\ 0, & |x| > \ell \end{cases};$$

_____ for a viscous fluid; _._ for a viscous fluid with allowance for surface tension; _ _ _ _ for an ideal fluid.

For velocity values less than 20 m/sec the computed values of wave resistance for all four expressions coincide with a great accuracy.

L. N. Sretenskiy [1] derived his formulas by the method of expanding the integrand of wave resistance into a series in powers of viscosity near vanishing viscosity. The correction for viscosity obtained by this method was insignificant. In this study we have investigated this same L. N. Sretenskiy integral, but have obtained

a different asymptotic expansion of this integral for arbitrary viscosity, from which the L. N. Sretenskiy solution is obtained as a special case.

The curves presented in this study show that it is possible to indicate the zones of values of the parameters for which the influence of viscosity is important.

A clarification of the influence of different factors on wave resistance is necessary in developing means for lessening it.

BIBLIOGRAPHY

1. Sretenskiy, L. N., TEORIYA VOLNOVYKH DVIZHENIY ZHIDKOSTI (Theory of Wave Movements of a Fluid), Moscow-Leningrad, ONTI NKTP SSSR, 1936, 108 pages.

2. Kochin, N. Ye., Kibel', I. A. and Roze, N. V., TEORETICHESKAYA GIDROMEKHANIKA (Theoretical Hydromechanics), Vol 1, Moscow, Fizmatgiz, 1963, 445 pages.

3. Potetyunko, E. N., "Asymptotic Analysis of Surface Waves of a Viscous Fluid With Small and Large Times," DAN SSSR (Reports of the USSR Academy of Sciences), Vol 210, No 5, pp 1040-1042, 1973.

4. Potetyunko, E. N., "Asymptotic Analysis of Surface Waves on a Viscous Fluid of Infinite Depth," IZV. SKNTs VSh. SER. YESTESTV. NAUK (News of the Northern Caucasus Scientific Center of Higher Schools. Natural Sciences Series) [Expansion Unconfirmed], pp 71-74, 1973.

5. Yeremenko, L. G. and Potetyunko, E. N., "Analysis of Waves and Wave Resistance of a Viscous Fluid With Allowance for a Surface Film," GIDROMEKHANIKA VYSOKIKH SKOROSTEY (Hydromechanics of High Velocities), Leningrad, "Sudostroyeniye," 313, pp 145-153, 1980.

6. Gradshteyn, N. S. and Ryzhik, I. M., TABLITSY INTEGRALOV, SUMM, RYADOV I PROIZVEDENIY (Tables of Integrals, Sums, Series and Products), Moscow, Fizmatgiz, 1963, 1100 pages.

7. Sretenskiy, L. N., "Waves on the Surface of a Viscous Fluid," TRUDY TsAGI (Transactions of the Central Aerohydrodynamics Institute), No 541, Moscow, pp 1-34, 1951.

8. PROBLEMY PRIKLADNOY GIDROMEKHANIKI SUDNA (Problems in the Applied Hydromechanics of a Ship), Leningrad, "Sudostroyeniye," 1975, 251 pages.

LONG SURFACE AND INTERNAL WAVES GENERATED BY NONAXISYMMETRIC INITIAL DISTURBANCES

Sevastopol' TEORETICHESKIYE I EKSPERIMENTAL'NYYE ISSLEDOVANIYA POVERKHNOSTNYKH I VNUTRENNIKH VOLN in Russian 1980 (manuscript received 18 Mar 80) pp 124-135

[Article by S. F. Dotsenko and B. Yu. Sergeyevskiy]

[Text]

Abstract: In a linear formulation the authors examine the process of development of spatial long waves in a two-layer fluid caused by initial displacements of the free surface and interfaces of the layers. A study was made of the influence of asymmetry of the initial disturbance on the developing unsteady surface and internal waves. The rises are modeled by a set of a finite number of identical (but displaced relative to one another) axisymmetric displacements of a special type, for which the solution of the problem is expressed through elementary functions. It is shown that for extended initial disturbances waves radiated perpendicularly to the greatest axis of the rise are dominant. A comparison with both plane and axisymmetric waves is presented. Regions for which the spatial waves are close to plane waves are determined.

The process of evolution of nonaxisymmetric initial displacements of the free surface and the interfaces of layers of a two-layer fluid is examined. The influence of the asymmetry of the initial disturbance on the developing surface waves was investigated earlier in [1, 5, 6].

1. A basin of the constant depth H, filled with an ideal incompressible two-layer fluid, unbounded in horizontal directions, is examined. The thickness and density of the upper layer are h_1 and ρ_1 respectively; for the lower layer, h_2 and ρ_2, the corresponding parameters are $\rho_1<\rho_2$, $H = h_1 + h_2$. At the time $t = 0$ the free surface and interface are displaced from the horizontal positions and the velocity field is absent. Within the framework of the linear theory of long waves we will investigate the influence of asymmetry of the mentioned initial disturbances on the process of formation and propagation of surface and internal waves.

We will examine the auxiliary axisymmetric problem. The mathematical formulation of the latter in a cylindrical coordinate system includes the two equations [2]

$$\zeta_{1tt} = c_1^2 \Delta \zeta_1 + c_2^2 \Delta(\gamma \zeta_1 + \varepsilon \zeta_2), \quad \zeta_{2tt} = c_2^2 \Delta(\gamma \zeta_1 + \varepsilon \zeta_2) \tag{1.1}$$

with the initial conditions

$$\zeta_1 = \zeta_{01}(R), \quad \zeta_{1t} = 0, \quad \zeta_2 = \zeta_{02}(R), \quad \zeta_{2t} = 0 \quad (t=0), \tag{1.2}$$

where $R = \sqrt{x^2 + y^2}$; x, y are horizontal coordinates; ζ_{0i} are arbitrary functions allowing the use of the Fourier transform; ζ_1 and ζ_2 are the deviations of the free surface and interface of the layers from undisturbed positions:

$$\Delta = \frac{1}{R}\frac{\partial}{\partial R}\left(R\frac{\partial}{\partial R}\right); \quad c_i = \sqrt{g h_i}; \quad \gamma = \rho_1 \rho_2^{-1}; \quad \varepsilon = 1 - \gamma; \quad i = 1, 2.$$

The solution of problem (1.1), (1.2) in integral form is found using a standard scheme using the Laplace transform of t and the Hankel transform for R. The final expressions for $\zeta_i(R,t)$ have the form

$$\zeta_i(R,t) = \zeta_i' = \sum_{k=1}^{2} \zeta_{ik}(R,t), \quad \zeta_{ik} = \int_0^\infty D_{ik}(r,t) F_k(r) J_0(rR)\, dr, \tag{1.3}$$

where J_0 is a Bessel function of the first kind;

$$F_k = \int_0^\infty R \zeta_{0k}(R) J_0(rR)\, dR; \quad D_{11} = \frac{1}{2} r (a_1 \mu_1 + a_2 \mu_2);$$

$$D_{12} = \frac{1}{2} c_2^2 \varepsilon r (\beta_1 u_1^{-2} \mu_1 + \beta_2 u_2^{-2} \mu_2); \quad D_{21} = \gamma \varepsilon^{-1} D_{12};$$

$$D_{22} = \frac{1}{2} r \left[(d_1 - c_1^2 \gamma \beta_1 u_1^{-2}) \mu_1 + (d_2 - c_2^2 \gamma \beta_2 u_2^{-2}) \mu_2 \right];$$

$$u_{1,2} = \sqrt{\frac{1}{2}(c^2 \pm \Lambda)}; \quad c = \sqrt{gH}; \quad \Lambda = \sqrt{c^4 - 4 c_1^2 c_2^2 \varepsilon}; \quad a_{1,2} = 1 \pm (c^2 - 2\varepsilon c_2^2)\Lambda^{-1};$$

$$\beta_{1,2} = 1 \pm c^2 \Lambda^{-1}; \quad d_{1,2} = 1 \pm (c_2^2 - c_1^2)\Lambda^{-1}; \quad \mu_i = \cos(r u_i t).$$

With $\varepsilon << 1$ the D_{ij} coefficients are written in a simpler form, more convenient for analysis, retaining only the most important terms

$$\begin{aligned} D_{11} &= (1 - \varepsilon h_2^2 H^{-2}) r \cos rct + \varepsilon h_2^2 H^{-2} r \cos r u_2 t, \\ D_{12} &= \varepsilon h_2 H^{-1} r (\cos rct - \cos r u_2 t), \quad D_{21} = \varepsilon^{-1} D_{12}, \\ D_{22} &= (h_2 - h_1) H^{-1} r \cos rct + 2 h_1 H^{-1} r \cos r u_2 t, \quad u_2 = \sqrt{h_1 h_2 H^{-2} \varepsilon}. \end{aligned} \tag{1.4}$$

We will examine model initial displacements of the free surface and interface of layers in the form

$$\zeta_{oi}(R) = A_i \ell_i^3 \left(R^2 + \ell_i^2\right)^{-3/2}, \quad \left(A_i, \ell_i = const, \ \ell_i > 0\right). \tag{1.5}$$

Then the integrals ζ_{ik} in (1.3) are computed using formulas 6.554(4), 6.623(2) from [3]. Finally we find

$$\zeta_{11} = A_1 \ell_1 \sum_{j=1}^{2} \alpha_j s_{ij}, \quad \zeta_{21} = A_1 \gamma c_2^2 \ell_1 \sum_{j=1}^{2} \beta_j s_{1j} \omega_j^{-2},$$
$$\zeta_{12} = A_2 \varepsilon c_2^2 \ell_2 \sum_{j=1}^{2} \beta_j s_{2j} \omega_j^{-2}, \quad \zeta_{22} = A_2 \ell_2 \sum_{j=1}^{2} \left(\alpha_j - \gamma c_2^2 \beta_j \omega_j^{-2}\right) s_{2j}, \tag{1.6}$$

where

$$s_{ij} = \frac{1}{4}\left[2\ell_i^2 \cos\left(\frac{3}{2}\varphi_{ij}\right) + N_{ij} \sin\left(\frac{3}{2}\varphi_{ij}\right)\right] T_{ij}^{-3/4};$$

$$T_{ij} = M_{ij}^2 + N_{ij}^2; \quad M_{ij} = R^2 + \ell_i^2 - \omega_j^2 t^2; \quad N_{ij} = 2\ell_i \omega_j t;$$

the angles $\psi_{ij} \in [0, \pi]$ also satisfy the system of equations

$$\sin\varphi_{ij} = N_{ij} T_{ij}^{-1/2}, \quad \cos\varphi_{ij} = M_{ij} T_{ij}^{-1/2}.$$

An analysis of the process of formation and propagation of long waves for this case is contained in [4].

The solution of the axisymmetric problem makes it possible to study some features of development of spatial waves in more complex cases when the initial displacements of the free surface and interface of fluid layers do not have cylindrical symmetry. We will use, as in [1], where the case of a homogeneous fluid was examined, the very simple method for modeling of such wave processes. It rests on the algebraic addition of a finite number of identical initial axisymmetric displacements of the form (1.5), whose centers are situated at different points (x_{ij}, y_{ij}) in the horizontal plane (i = 1 is the undisturbed free surface of the fluid $z = 0$; i = 2 is the interface of the layers $z = -h_1$).

Assume that

$$\zeta_i^0 = A_i A_{oi} \sum_{j=n_i}^{n_i} \zeta_{oi}\left(R_{ij}\right),$$
$$R_{ij} = \sqrt{\left(x - x_{ij}\right)^2 + \left(y - y_{ij}\right)^2}, \quad A_{oi}^{-1} = \max_{x,y}\left\{\sum_{j=n_i}^{n_i} \zeta_{oi}\left(R_{ij}\right)\right\}, \tag{1.7}$$

where n_i are natural numbers; i = 1, 2. Then, due to the linearity of the problem from formulas (1.3), (1.5)-(1.7), we obtain

$$\zeta_i(x, y, t) = A_i A_{oi} \sum_{j=n_i}^{n_i} \sum_{k=1}^{2} \zeta_{ik}\left(R_{ij}, t\right). \tag{1.8}$$

With t = 0 the maximum values of displacements of the surface and interface of the fluid layers are equal to R_1 and R_2 respectively.

The simplest case is that examined below when the points (x_{ij}, y_{ij}) lie on a straight line at an identical distance ΔL_i from one another. Without limitations on universality it can be assumed that this line coincides with the Ox-axis; the point (x_{i0}, y_{i0}) is at the origin of coordinates. Then in formulas (1.7), (1.8) $x_{ij} = j\Delta L_i$, $y_{ij} = 0$ $(i = 1,2;\ j = 0, \pm n_i)$ the displacements $\zeta_i(x,y,t)$ are even functions of x and y. This makes it possible to limit ourselves to an analysis of waves only in the region $x \geqslant 0$, $y \geqslant 0$.

The asymmetry of the initial rise of the indicated type is conveniently evaluated by the parameter ν_i, equal to the ratio of the characteristic length $2L_{1i}$ of the rise to its characteristic width $2L_{2i}$ ($\nu_i = L_{1i}L_{2i}^{-1}$). If as the conditional boundary of the initial rise we take the isoline on which $\zeta_i^\circ(x,y) = 0.1A_i$, then as L_{1i} it is desirable to take the maximum distance from it to the origin of coordinates, and as L_{2i} it is desirable to take the minimum distance from it to the origin of coordinates.

A further analysis of waves was made using the formulas (1.3), (1.6). The values h_1, h_2, ε were taken equal to 0.8, 4.2 km, 10^{-3} respectively, as is characteristic for the ocean floor. It was also assumed that $\ell_1 = \ell_2 = 52.4$ km, $\Delta L_1 = \Delta L_2 = 30$ km. In all the figures presented below the distance is measured in kilometers.

2. Assume that $A_1 = 1$, $A_2 = 0$. In this case at the time t = 0 the free surface of the fluid deviates from the position of equilibrium; the interface of the layers is horizontal.

In an axisymmetric case from (1.3), (1.4) we obtain approximate expressions for ζ_1 and ζ_2

$$\zeta_1 = \left(1 - \varepsilon h_2^2 H^{-2}\right)\eta_1 + \varepsilon h_2^2 H^{-2}\eta_2,\quad \zeta_2 = h_2 H^{-1}\eta_1 - h_2 H^{-1}\eta_2, \tag{2.1}$$

where

$$\eta_1 = \int_0^\infty r\cos rct\, F_1(r) J_0(rR)\, dr;\quad \eta_2 = \int_0^\infty r\cos r\omega_2 t F_1(r) J_0(rR)\, dr, \tag{2.2}$$

and η_1 coincides with the precise expression for the rise of the free surface of a homogeneous fluid.

It follows from formulas (2.1), (2.2) and the results of [4] that the initial axisymmetric displacement of the fluid surface leads to the formation of surface and internal waves attenuating with time. The first terms in formulas (2.1) correspond to a surface wave; the second terms correspond to an internal wave. A surface wave is slightly distorted due to inhomogeneity of the fluid and in the process of its propagation causes a displacement of the interface of layers of the same sign which is less by a factor of Hh_2^{-1}. The velocity of propagation η_1 is evidently close to c. The amplitude of the developing purely internal wave is maximum at the interface of the layers; at the free surface it is $H(\varepsilon h_2)^{-1}$ times less

and the velocity of its propagation is $u_2 \ll c$. Due to the linearity of the initial mathematical problem the mentioned general properties of unsteady waves in a two-layer fluid are correct for nonaxisymmetric initial displacements of the type (1.7).

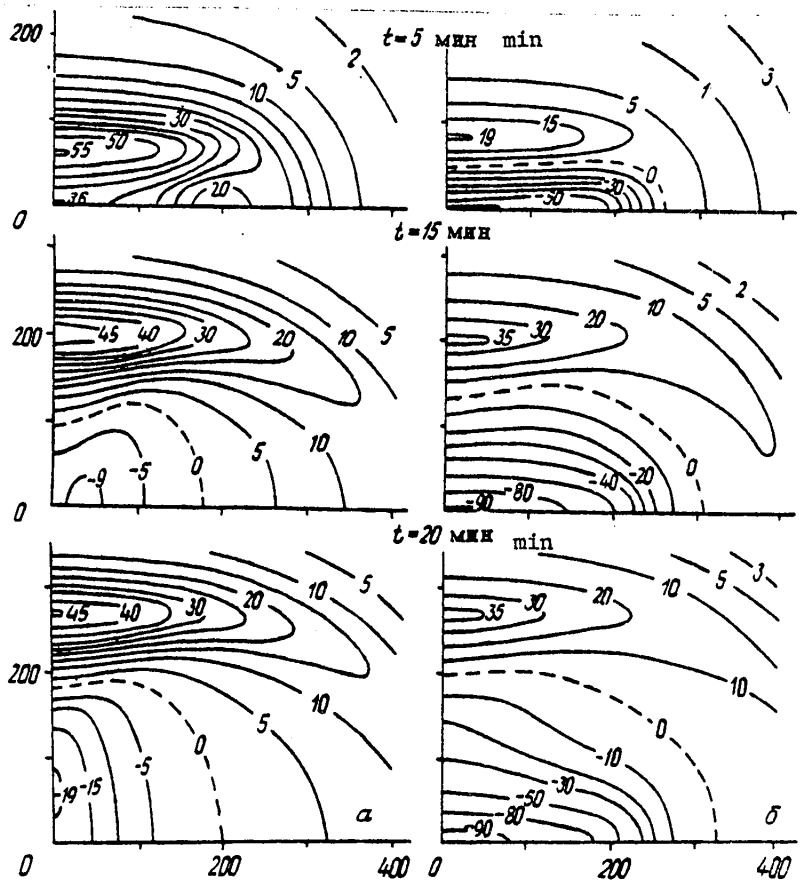

Fig. 1. Form of free surface and interface of layers in initial stage of wave development ($A_1 = 1$, $A_2 = 0$): a) isolines $10^2 z_1$; b) isolines $10^2 z_2$.

The process of development of unsteady surface and internal waves in the case of an initial displacement of the free surface of the fluid with $n_1 = 7$ ($L_{11} = 295$ km, $L_{21} = 145$ km, $\nu_1 = 2.04$ is illustrated in Figures 1 and 2.

Thus, the initial displacement of the free surface of the fluid in the process of its evolution leads to the formation of a spatial surface wave ζ_1 attenuating with time (Fig. 1,a) and disturbances of the interface of the layers ζ_2 (Fig. 1,b), representing (see (2.1)) a superpositioning of the developing internal wave and

the "response" of the surface wave at the density jump. In the initial stage of wave development there is a subsidence of the central part of the rise ζ_1°. The maximum ζ_1 values with $t>0$ are situated on the Oy-axis and move along it in opposite directions with velocities close to c.

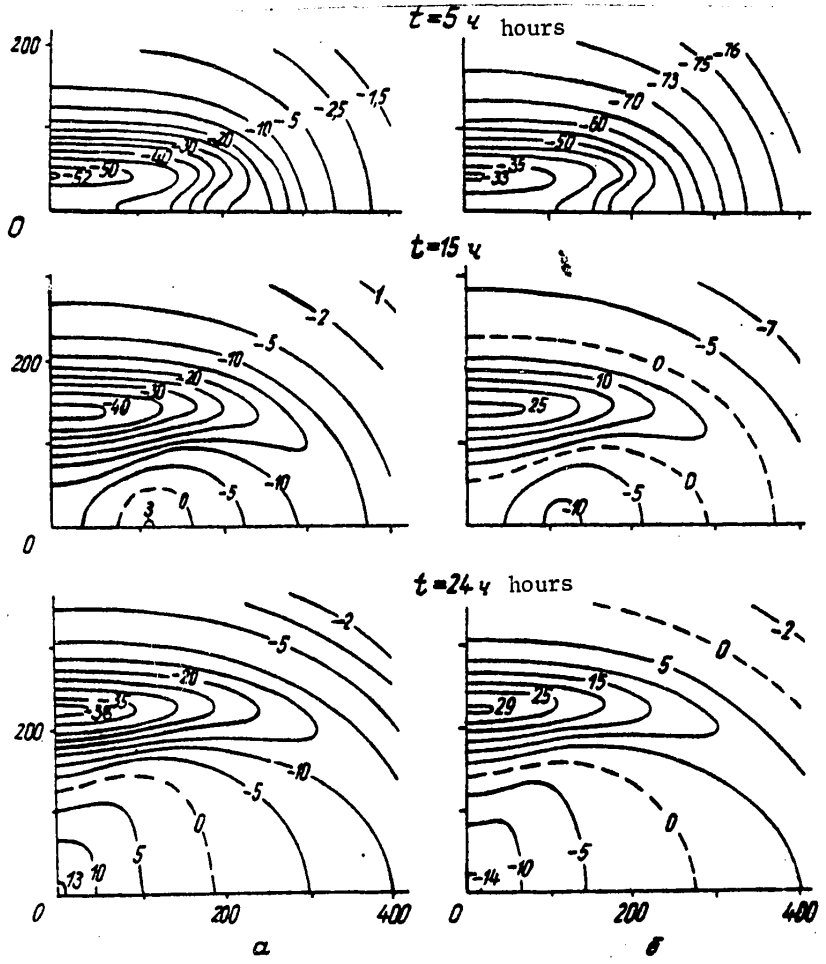

Fig. 2. Form of free surface and interface of layers with large t (A_1 = 1, A_2 = 0): a) isolines 10^2 ζ_2; b) isolines 10^5 ζ_1.

At a definite moment in time $t = t_0$ ($5<t_0<15$ min) at two points $\pm x_0$ on the Ox-axis ($x_0>0$) the displacement ζ_1 becomes equal to zero and thereafter two nonintersecting regions with $\zeta_1 < 0$ are formed, these being situated symmetrically relative to the Oy-axis. With an increase in t there is a broadening of these regions and their joining into one (t = 15 min), taking in the origin of coordinates. Points with a maximum depression of the free surface with $t<20$ min are

displaced along the Ox-axis in the direction of the origin of coordinates and then move along the Oy-axis in opposite directions, following the corresponding isoline of maximum amplitude. At an adequate distance from the origin of coordinates the ζ_1 isolines constitute closed curves, as is characteristic for axisymmetric waves.

In the process of submergence of the central part of the initial rise of the free surface ζ_1 the generation of an internal wave occurs. Initially it is a region of negative ζ_2 values;

$$\max_{x,y} |\zeta_2|$$

is situated at the origin of coordinates (Fig. 1,b). In addition to a local depression of the density jump, an internal rise wave is formed which corresponds to the main surface wave and moves with the velocity of long waves in a homogeneous fluid. It is the "response" of a surface wave, as was mentioned at the beginning of this section. Its amplitude, as mentioned earlier, is Hh_2^{-1} times less than the amplitude of the surface wave.

In accordance with Fig. 1,b, in the neighborhood of the origin of coordinates in the initial stage of movement of the fluid a region of negative ζ_2 values is formed, elongated along the Ox-axis. In the process of its evolution, when the main disturbances of the free surface become small, purely internal waves are formed (Fig. 2,a); the velocity of their propagation is $u_2 \ll c$. It follows from a comparison of Figures 1,a and 2,a that the spatial structure of the surface and internal waves qualitatively has much in common if $-\zeta_2$ is considered, rather than ζ_2.

In the process of propagation of this internal wave it exerts a reverse effect on the free surface of the fluid. The developing surface waves (Fig. 2,b) constitute a "response" of the internal wave at the free surface of the fluid. Their amplitude is less by a factor greater than 10^3 than the maximum vertical displacements within the fluid. The spatial structure of ζ_1 and ζ_2 with $t > 15$ hours is different; especially the positive ζ_1 values are localized in an annular region, which was not observed for internal waves.

At one and the same moment in time t the amplitude of a purely internal wave is slightly dependent on the relative density drop ε, but the velocity of its propagation and the amplitude of the surface waves caused by it decrease substantially with a decrease in ε.

Thus, the initial displacement of the free surface of a two-layer fluid in the course of its development can generate internal waves whose amplitude is of the same order of magnitude as the amplitude of the initial disturbance. Such waves attenuate considerably more slowly than surface waves and are dominant after departure of the main surface waves from the region of the initial displacement of the free surface of the fluid. In all cases for initial displacements of the fluid surface elongated along the Ox-axis the waves of greatest amplitude are radiated in the direction of the Oy-axis. Such a directivity of radiation of unsteady waves is observed even with ν_1 values extremely close to 1.

Assume that $A_1 = 0$, $A_2 = 1$. In this case at the time t = 0 the free surface is horizontal, the interface of the layers is displaced from the position of equilibrium.

In an axisymmetric case from (1.3), (1.4) we obtain approximate expressions for ζ_1 and ζ_2

$$\zeta_1 = \varepsilon h_2 H^{-1} (\xi_1 - \xi_2), \quad \zeta_2 = \varepsilon h_2^2 H^{-2} \xi_1 + (1 - \varepsilon h_2^2 H^{-2}) \xi_2, \tag{3.1}$$

where

$$\xi_1 = \int_0^\infty r \cos rct\, F_2(r) J_0(rR)\, dr; \quad \xi_2 = \int_0^\infty r \cos r u_2 t\, F_2(r) J_0(rR)\, dr. \tag{3.2}$$

It follows from formulas (3.1), (3.2), (1.7) and the results in [4] that the initial axisymmetric density jump leads to the formation of surface and internal waves. The first terms in formulas (3.1) correspond to a surface wave; the second terms correspond to an internal wave. The amplitude of the surface wave is of the order of $O(\varepsilon)$ and therefore is substantially less than the amplitude of the internal wave. It is evident that $\zeta_2 \approx \xi_2$.

The process of development of unsteady surface and internal waves in the case of initial displacement of the interface of layers in the form (1.5), (1.7) with $n_2 = 7$ ($L_{12} = 295$ km, $L_{22} = 145$ km, $\nu_2 = 2.04$) is illustrated in Figures 3, 4.

The initial displacement of the interface of layers of the fluid (Fig. 3,a) in the process of its development generates surface waves of two types: first, purely surface waves propagating with the velocity c (Fig. 3), second, disturbances of the free surface, caused by inhomogeneity of the fluid (Fig. 4,b), propagating with the velocity of internal waves u_2. The formation of surface waves of the first type caused a slow subsidence of the central part of the initial displacement of the density jump. These waves constitute two regions of positive ζ_1 values propagating in opposite directions and having maximum amplitude values on the Oy-axis (Fig. 3). Thereafter the deformations of the initial rise ζ_2° and the free surface increase at the origin of coordinates, which lead to the formation of slowly evolving internal waves (Fig. 4,a), which correspond to qualitatively similar surface deformations of the fluid of opposite sign, representing the above-mentioned second class of surface waves of small amplitude (Fig. 4,b). All the considered waves are essentially three-dimensional. For initial displacements of the interface of layers elongated along the Ox-axis the waves of greatest amplitude are radiated in the direction of the Oy-axis.

It is clear from a comparison of Figures 1,a, 2,a, 3,a and 4,a that the spatial structure of the fields of purely internal and purely surface waves has much in common, although these classes of waves have essentially different propagation velocities. This conclusion can also be drawn from formulas (2.1), (2.2), (3.1), (3.2). In accordance with (1.7), the spatial structure of the mentioned surface waves is described by the sum of the integrals ζ_1 or ξ_1, for internal waves -- ζ_2 or ξ_2. It is evident that with $\zeta_1^\circ = \zeta_2^\circ$, as a result of the replacement $\tau = u_2 c^{-1} t$ the integrals ζ_2 and ξ_2 assume a form similar to ζ_1 and ξ_1.

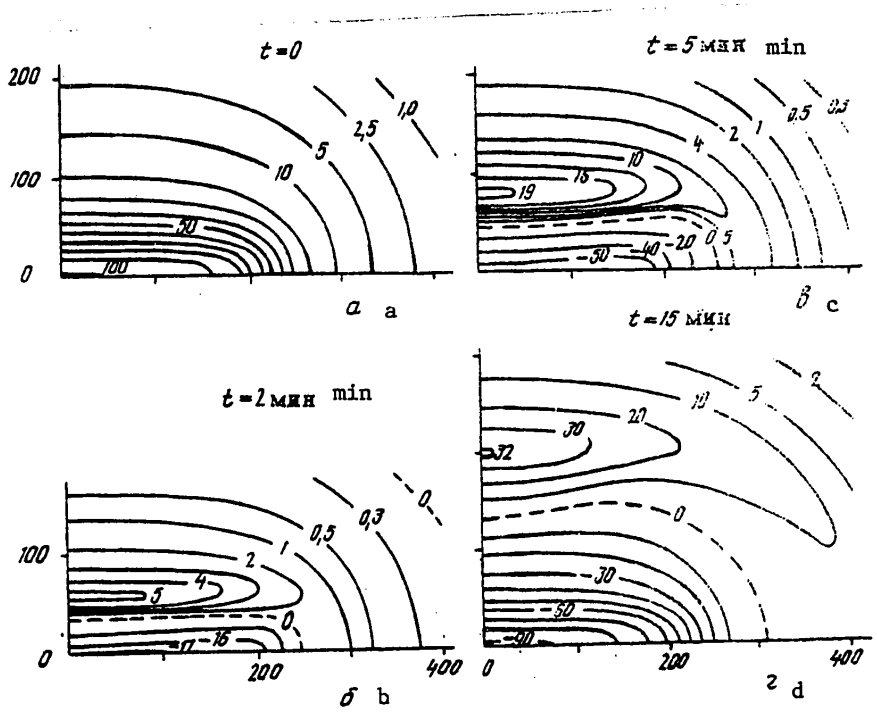

Fig. 3. Form of free surface in initial stage of wave development ($A_1 = 0$, $A_2 = 1$): a) isolines $10^2\,\zeta_2^\circ$; b, c, d) isolines $10^5\,\zeta_1^\circ$.

The amplitude of the internal wave to a considerable degree is dependent on the initial parameters of the problem and this dependence is particularly important in the case of large t values. A change in h_1, h_2 and δ, leading to an increase in u_2, not only accelerates the development process, but also decreases the amplitude of the internal wave at a particular moment in time, all other conditions being equal.

4. We will examine the influence of asymmetry of the initial disturbance on the amplitude of surface and internal waves. We will assume that $A_1^+ = \max_{x,y} \zeta_1(x,y,t)$ with $A_1 = 1$, $A_2 = 0$ and $A_2^+ = \max_{x,y} \zeta_2(x,y,t)$ with $A_1 = 0$, $A_2 = 1$. The $\nu_i = 1$ value corresponds to axisymmetric waves and $\nu_i = \infty$ corresponds to plane waves.

The computed expressions $A_i^+ = A_i^+(\nu_i, t)$ are represented in Fig. 5. The ν_i values are indicated on the corresponding curves. It therefore follows that $A_i^+(1,t) < A_i^+(\nu_2,t) < A_i^+(\infty, t)$ with $\nu_i > 1$. Accordingly, for initial rises of the free surface and the interface of the layers elongated along the Ox-axis, with their identical width, the amplitudes of the developing waves are greater than in an axisymmetric case and increase with an increase in ν_i. It is evident that $A_i^+(\infty, t) \approx 0.5$ with large t, but $A_i^+(\nu_i, t) \to 0$ with $t \to \infty$.

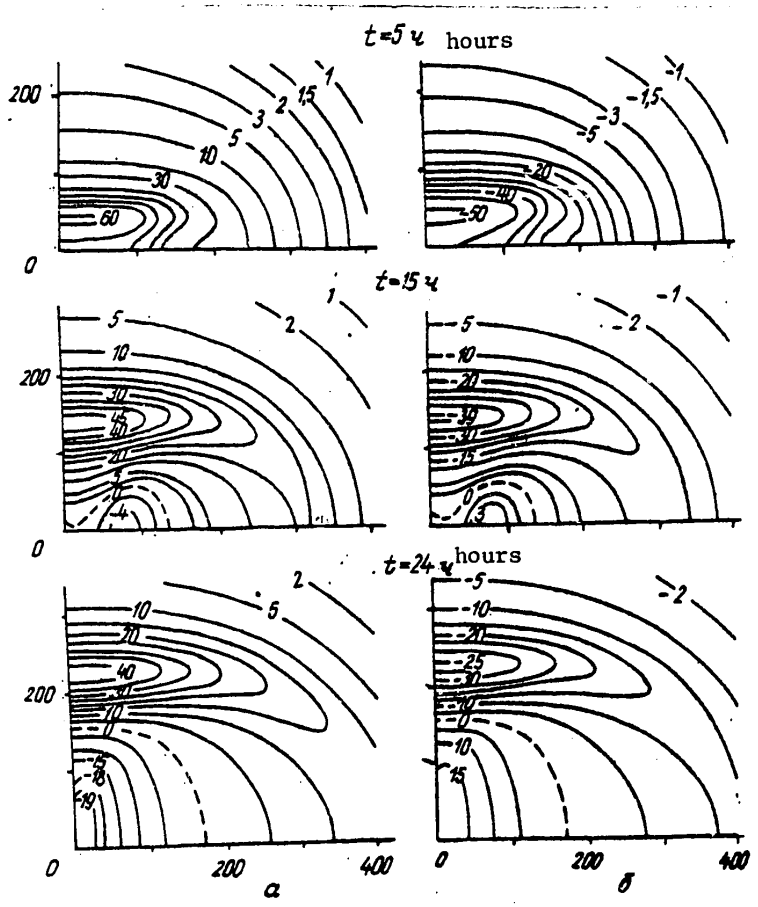

Fig. 4. Form of free surface and interface of layers with large t ($A_1 = 0$, $A_2 = 1$): a) isolines $10^2\zeta_2$; b) isolines $10^5\zeta_1$.

In conclusion we will examine the problem of regions in the plane xOy for which the form of the spatial wave differs little from the form of a plane wave. We will assume that for such regions

$$|\zeta_i(x, y, t) - \zeta_i^{\infty}(y, t)| \leq 0{,}1 A_i, \quad (4.1)$$

where ζ_i^{∞} is the displacement corresponding to a plane wave ($\nu_i = \infty$). The results of computations of the boundaries of these regions for an internal wave ($i = 2$) in the case $A_1 = 0$, $A_2 = 1$ are shown in Fig. 6 ($n_2 = 7$). The inequality (4.1) is satisfied in one (in the initial stage) or two time-dependent regions of ellipsoidal shape situated symmetrically relative to the Ox-axis (Fig. 6). With an increase in t they withdraw from the origin of coordinates with the velocity u_2, decrease in size monotonically along the Ox-axis, but change little in the direction of the Oy-axis. At some moment in time this region ceases to exist. With an increase

in ν_2 the size of the regions along the Ox-axis in the time interval during which they exist increases.

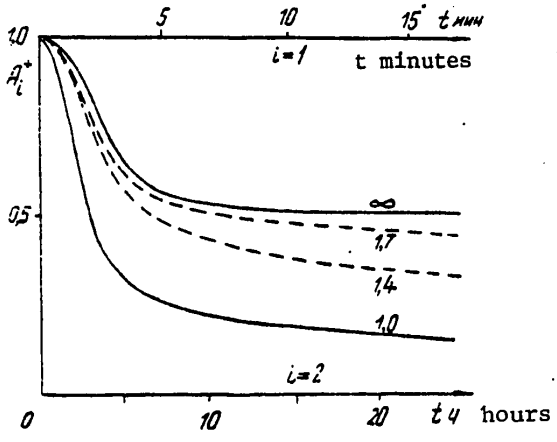

Fig. 5. Dependence of A_i^+ on t for different ν_i values.

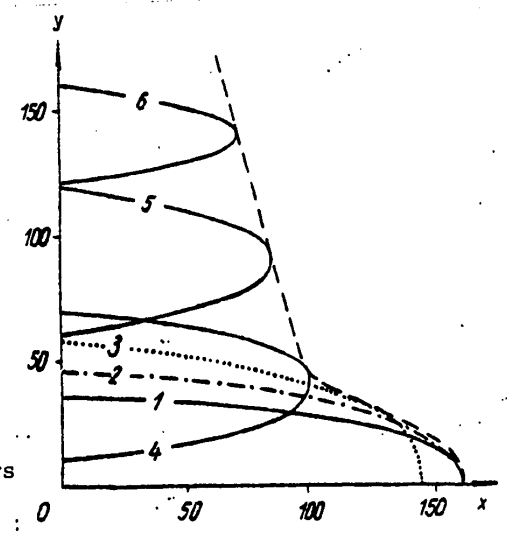

Fig. 6. Boundaries of regions for internal waves within which the inequality (4.1) is satisfied. The curves 1-6 correspond to the values t = 0; 1; 2; 5; 10; 15 hours.

Similar results are correct for surface waves ζ_1 caused by initial displacement of the free surface of the fluid [1].

BIBLIOGRAPHY

1. Dotsenko, S. F., Sergeyevskiy, B. Yu. and Cherkesov, L. V., "Long Waves From Nonaxisymmetric Initial Displacements of the Free Surface of a Fluid," EVOLYUTSIYA TSUNAMI OT OCHAGA DO VYKHODA NA BEREG (Evolution of Tsunamis From the Focus to Emergence on Shore), in press.

2. Sekerzh-Zen'kovich, T. Ya., "Propagation of Initial Disturbances Along a Free Surface and Along the Interface of a Fluid Consisting of Two Layers of Different Density," TRUDY MGI (Transactions of the Marine Hydrophysical Institute), Vol 17, Moscow, Izd-vo AN SSSR, pp 48-58, 1959.

3. Gradshteyn, I. Z. and Ryzhik, I. M., TABLITSY INTEGRALOV, SUMM RYADOV I PROIZVEDENIY (Tables of Integrals, Sums of Series and Products), Moscow, Fizmatgiz, 1963, 1100 pages.

4. Dotsenko, S. F. and Sergeyevskiy, B. Yu., "Axisymmetric Long Waves in a Two-Layer Fluid From Initial Disturbances," POVERKHNOSTNYYE I VNUTRENNIYE VOLNY (Surface and Internal Waves), Sevastopol', Izd. MGI AN Ukrainskoy SSSR, pp 119-128, 1979.

5. Sen, A. R., "Surface Waves on Fluid of Finite Depth Due to Arbitrary Surface Impulse and Elevation," J. TECHNOL., Vol 4, No 2, pp 105-118, 1959.

6. Chaudhuri Kripasindhu, "Waves in Shallow Water Due to Arbitrary Surface Disturbances," APPL. SCIENT. RES., Vol 19, No 3-4, pp 274-284, 1968.

INTERNAL WAVES FROM INITIAL DISTURBANCES IN A TWO-LAYER FLUID

Sevastopol' TEORETICHESKIYE I EKSPERIMENTAL'NYYE ISSLEDOVANIYA POVERKHNOSTNYKH I VNUTRENNIKH VOLN in Russian 1980 (manuscript received 3 Apr 80) pp 136-142

[Article by A. A. Novik]

[Text]

Abstract: A solution of the plane problem of gravitational waves arising at the horizontal discontinuity of two flows of fluid of different density is obtained and investigated.

We will examine two flows of an ideal fluid situated one beneath the other and extending without limit in a vertical direction. Assume that the lower flow has the velocity c_1 and the density ρ_1; the upper flow has the velocity and density c_2 and ρ_2 and $\rho_1 > \rho_2$. At the initial moment in time $t = 0$ the fluid particles are imparted any additional velocity and the initially horizontal discontinuity changes somewhat. It is necessary to find the form of the discontinuity at any moment in time $t > 0$.

We will cite the equations and boundary conditions of the problem of internal waves. We will use the horizontal line of separation of flows in an undisturbed state as the x-axis, whereas the y-axis is directed vertically upward. We will assume that the xy coordinate system moves in the plane of motion in a horizontal direction with the constant velocity

$$c = \frac{\rho_1 c_1 + \rho_2 c_2}{\rho_1 + \rho_2}. \tag{1}$$

Then the linearized boundary conditions at the discontinuity assume the form [2]

$$\rho_1\left[\frac{\partial \varphi_1}{\partial t} + \frac{\rho_2(c_1-c_2)}{\rho_1+\rho_2}\frac{\partial \varphi_1}{\partial x} + g\eta\right] = \rho_2\left[\frac{\partial \varphi_2}{\partial t} - \frac{\rho_1(c_1-c_2)}{\rho_1+\rho_2}\frac{\partial \varphi_2}{\partial x} + g\eta\right], \tag{2}$$

$$\frac{\partial \eta}{\partial t} + \frac{\rho_2(c_1-c_2)}{\rho_1+\rho_2}\frac{\partial \eta}{\partial x} = \frac{\partial \varphi_1}{\partial y}, \tag{3}$$

$$\frac{\partial \eta}{\partial t} - \frac{\rho_1(c_1-c_2)}{\rho_1+\rho_2}\frac{\partial \eta}{\partial x} = \frac{\partial \varphi_2}{\partial y}. \tag{4}$$

Here g is the acceleration of gravity; $\eta(x;t)$ is the deviation of the discontinuity from the position of equilibrium; $\varphi_1(x,y;t)$ and $\varphi_2(x,y;t)$ are the potentials of the velocity of wave movement of the lower and upper fluids; the derivatives of the functions φ_1 and φ_2 are taken with y = 0.

The problem of internal waves is usually formulated in the following way. It is necessary to find such a solution φ_1 of the Laplace equation in the lower half-plane, becoming equal to zero together with the first-order partial derivatives with $y = -\infty$, and such a solution φ_2 of this same equation in the upper half-plane, having a similar behavior with $y = \infty$, which on the axis y = 0 would satisfy the two boundary conditions obtained from (2)-(4) by exclusion of the function η, and also some initial conditions. With known velocity potentials the discontinuity equation is found using formula (2) by simple differentiation.

2. An analysis of the equations and the boundary conditions makes it possible to simplify the problem somewhat.

First, the right-hand sides of the kinematic conditions (3) and (4) are the normal derivatives of the velocity potentials on the x-axis. Accordingly, regarding φ_1 and φ_2 as solutions of the Neumann problem for the lower and upper half-planes, it is possible to represent them in the form of the corresponding potentials of a simple layer and to check to see that the dependence

$$\frac{\partial}{\partial t}(\varphi_1+\varphi_2)=\frac{c_1-c_2}{\rho_1+\rho_2}\frac{\partial}{\partial x}(\rho_1\varphi_1-\rho_2\varphi_2)\cdot$$

exists between them on the x-axis. Using this additional expression, following from the continuity of motion, the boundary conditions for the velocity potentials are transformed to a form similar to the Cauchy-Poisson condition at the free surface,

$$\frac{\partial^2\varphi_1}{\partial t^2}+j\ell\frac{\partial^2\varphi_1}{\partial x^2}+j\frac{\partial\varphi_1}{\partial y}=0,\quad \frac{\partial^2\varphi_2}{\partial t^2}+j\ell\frac{\partial^2\varphi_2}{\partial x^2}-j\frac{\partial\varphi_2}{\partial y}=0,$$

where

$$j=\frac{\rho_1-\rho_2}{\rho_1+\rho_2}g,\quad \ell=\frac{\rho_1\rho_2(c_1-c_2)^2}{g(\rho_1^2-\rho_2^2)}\cdot$$

For determining the ordinate of the discontinuity we also derive the simpler formula

$$\eta=-\frac{1}{j}\left[\frac{\partial\varphi_1}{\partial t}+\frac{\rho_2(c_1-c_2)}{\rho_1+\rho_2}\frac{\partial\varphi_2}{\partial x}\right]_{y=0}\cdot \qquad (5)$$

Second, in this problem the initial values of the functions φ_1, φ_2 and η have a physical sense. However, the difference in the kinematic conditions (3)-(4) shows that at the initial moment a zero velocity should correspond to a zero displacement of the discontinuity, and on the contrary, a zero displacement corresponds to equal velocities of the particles. This means that it is possible to stipulate only two functions arbitrarily, for example,

$$\eta(x;0)=f(x),\quad \rho_1\varphi_1(x,0;0)-\rho_2\varphi_2(x,0;0)=-F(x), \qquad (6)$$

where F(x) characterizes the difference in the impulse pressures imparted to the boundary particles of fluid flows. Using conditions (6), it is possible to find the initial values of the functions φ_1, φ_2, η and their first time derivatives [2]. In particular, the second initial condition for the function η has the form

$$\frac{\partial \eta(x;0)}{\partial t} = \frac{1}{\rho_1+\rho_2}\,\tilde{F}'(x),$$

where $\tilde{F}'(x)$ is the Gilbert transform of the derivative of the F(x) function.

The separation of the boundary and initial conditions affords possibilities for use or application of the methods of the theory of functions of a complex variable. On the basis of formula (5) using complex potentials it is possible to introduce the function s(z;t), analytical with respect to z = x + iy in the lower half-plane, whose real part with y = 0 coincides with η and obtain for it the equation

$$\frac{\partial^2 s}{\partial t^2} + j\ell\frac{\partial^2 s}{\partial z^2} + ij\frac{\partial s}{\partial z} = 0 \qquad (7)$$

and the initial conditions

$$s(x;0) = f(x) + i\tilde{f}(x),\quad \frac{\partial s(x;0)}{\partial t} = \frac{1}{\rho_1+\rho_2}\left[\tilde{F}'(x) - iF'(x)\right].$$

3. We will examine the following solution of equation (7):

$$E(z;t) = -\frac{i}{2\sqrt{j\ell}}\,e^{-i\frac{z}{2\ell}}\,H_0^{(1)}\left(\frac{1}{2\ell}\sqrt{z^2+j\ell t^2}\right).$$

Taking into account the ambiguity of the Hankel function of the first kind entering into it the real E_1 and imaginary E_2 parts of the limiting value of this solution on the real axis from the direction of the lower half-plane are represented by the formulas

$$E_1(x;t) = \frac{1}{2\sqrt{j\ell}}\left[N_0(\rho)\cos\xi - J_0(\rho)\sin|\xi|\right],$$

$$E_2(x;t) = -\frac{1}{2\sqrt{j\ell}}\left[N_0(\rho)\sin|\xi| + J_0(\rho)\cos\xi\right]\operatorname{sign} x.$$

Here $J_0(P)$ is the Bessel function; $N_0(P)$ is the Neumann function;

$$\rho = \sqrt{\xi^2+\tau^2};\quad \xi = \frac{x}{2\ell};\quad \tau = t\sqrt{\frac{1}{4\ell}}.$$

The general solution of the problem of internal waves is written in the form of the convolution

$$\eta = \frac{\partial E_1(x;t)}{\partial t} * f(x) - \frac{\partial E_2(x;t)}{\partial t} * \tilde{f}(x) +$$
$$+ E_1(x;t) * \frac{1}{\rho_1+\rho_2}\,\tilde{F}'(x) + E_2(x;t) * \frac{1}{\rho_1+\rho_2}\,F'(x). \qquad (8)$$

4. We will investigate the type of internal waves caused by the concentrated initial displacement of the discontinuity of the flows at the point x = 0 with the total area Q, that is, with $f(x) = Q\delta(x)$, $F(x) = 0$. In this case from formula (8) we obtain

$$\eta = Q\frac{\partial}{\partial t}\left[E_1(x;t) - \tilde{E}_2(x;t)\right].$$

The Gilbert transform $\tilde{E}_2$ in the x-coordinate consists of two parts: the function $E_1(x;t)^2$, taken with a minus sign, and a nonwave addition, whose t derivative is of the order of τ/P^2. Accordingly, with large P values we obtain

$$\eta \simeq \frac{Q\tau}{\sqrt{2\pi}\,\ell\rho^{3/2}}\cos\left(\rho - |\xi| - \frac{\pi}{4}\right). \qquad (9)$$

We will study the wave movement described by formula (9). As a result of the symmetry of the rise η relative to the y-axis it is possible to limit ourselves to the case when $x > 0$.

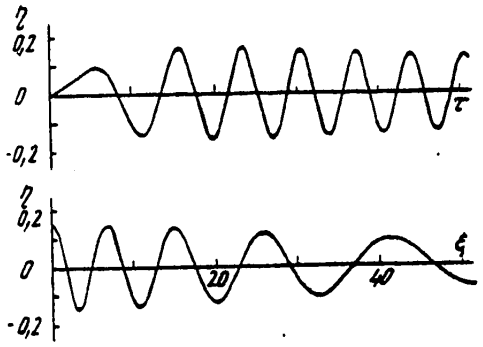

Fig. 1.

The general nature of the waves is schematically represented in Fig. 1, which is a graph of movement of the discontinuity of the flows at the fixed point x and the instantaneous pattern of waves at some moment in time t. As unity for the vertical scale we adopt the value $Q/\sqrt{2\pi\ell}$, and the parameters ξ and τ are equal to

$$\xi = \frac{13\pi}{4(\sqrt{3}-1)} = 13{,}95, \quad \tau = \frac{57\pi}{4} = 44{,}77.$$

We will examine the phase change $\theta - P - \xi$, caused by transition along the x-axis from a particular wave to the next, that is, $\Delta Q = 2\pi$. Carrying out differentiation for x and introducing the notation $-\Delta x = \lambda$, we obtain a general expression for the wave length λ as a function of ξ

$$\lambda = 4\pi\ell\frac{\rho}{\rho - \xi}. \qquad (10)$$

Formula (10) shows that with adequately large τ the origin of coordinates generates waves of the length

$$\lambda = 4\pi\ell = \frac{4\pi}{g}\frac{\rho_1\rho_2}{\rho_1^2-\rho_2^2}(c_1-c_2)^2, \tag{11}$$

which, with advance along the x-axis are distended and at the points corresponding to sufficiently large $\mathcal{E}$ their length becomes almost the same ($8\pi x^2/9t^2$) as for waves at the free surface of a deep fluid [3].

Similarly, a general expression is found for the wave period T as a function of τ

$$T = 2\pi\sqrt{\frac{4\ell}{j}}\frac{\rho}{\tau}. \tag{12}$$

With $\tau \ll \mathcal{E}$ the internal waves have periods of about $4\pi x/jt$, which are $\rho_1+\rho_2/\rho_1-\rho_2$ times greater than the period of the waves at the surface of the deep fluid. With the course of time the period T decreases and when $\tau \gg \mathcal{E}$ becomes close to its limiting value

$$T = 2\pi\sqrt{\frac{4\ell}{j}} = \frac{4\pi}{g}\frac{\sqrt{\rho_1\rho_2}}{\rho_1-\rho_2}|c_1-c_2|. \tag{13}$$

This means that upon the elapsing of an adequately long time interval the fluid level in this place will experience almost periodic oscillations.

The formula for the phase velocity

$$c_\varphi = \sqrt{j\ell}\,\frac{\tau}{\rho-\xi}$$

shows that the waves move with a constant acceleration equal to $j/2\theta$, which is $\rho_1-\rho_2/\rho_1+\rho_2$ times less than the acceleration of waves at the free surface. In addition, the phase velocity of the shortest waves (11) is equal to

$$c_\varphi = \sqrt{j\ell} = \frac{\sqrt{\rho_1\rho_2}}{\rho_1+\rho_2}|c_1-c_2|. \tag{14}$$

The group velocity of the internal waves, like the waves at the surface of a deep fluid, is equal to x/t.

Thus, in a coordinate system moving in the plane of movement in a horizontal direction with the mean mass velocity of the floes (1) and related to the x, y axes, series of waves of the length $4\pi\ell$ are propagated from the origin of coordinates in both directions; these waves move to infinity, being distended in length and accelerating. As time passes the distension and the acceleration of the waves attenuates greatly, as a result of which a considerable part of the discontinuity is covered with waves whose length, period and phase velocity are given approximately by formulas (11), (13) and (14); their numerical values are cited in the table.

In a fixed coordinate system these extremal characteristics of the waves are as follows:

$$\lambda = 4\pi\ell\sqrt{1+\frac{c^2}{j\ell}}\left(\sqrt{1+\frac{c^2}{j\ell}}+\frac{c}{\sqrt{j\ell}}\right),$$
$$T = 2\pi\sqrt{\frac{4\ell}{l}}\left(\sqrt{1+\frac{c^2}{j\ell}}+\frac{c}{\sqrt{j\ell}}\right), \quad c_{ph}=\sqrt{j\ell+c^2}. \tag{15}$$

Table 1

ρ_2/ρ_1	$c_1 - c_2$ m/sec		
	0.1	1	10
	Maximum length of internal waves, m		
0.001	0.0001	0.001	0.13
0.01	0.0001	0.01	1.28
0.1	0.001	0.13	12.94
0.9	0.06	6.07	606.78
0.99	0.64	63.73	6372.69
0.999	6.4	640.17	64016.74
	Minimum period of internal waves, sec		
0.001	0.004	0.04	0.4
0.01	0.013	0.13	1.29
0.1	0.045	0.45	4.8
0.9	1.22	12.15	121.52
0.99	12.74	127.46	1274.55
0.999	128.03	1280.33	12803.35
	Minimum phase velocity of propagation of internal waves, m/sec		
0.001	0.003	0.032	0.32
0.01	0.01	0.099	0.99
0.1	0.029	0.287	2.87
0.9	0.05	0.499	4.99
0.99	0.05	0.5	5
0.999	0.05	0.5	5

We note in conclusion that formulas (13) and (15) for the wave period were derived by L. N. Sretenskiy [1] from a special solution of the problem obtained in the form of a Fourier integral and evaluated using the stationary phase method.

BIBLIOGRAPHY

1. Sretenskiy, L. N., "Cauchy-Poisson Problem for the Discontinuity of Two Flowing Currents," IZV. AN SSSR: SER. GEOFIZ. (News of the USSR Academy of Sciences: Geophysical Series), No 6, pp 505-513, 1955.

2. Novik, A. A., "Formulation of the Problem of Waves at the Discontinuity of Two Infinite Currents of an Incompressible Fluid," Manuscript deposited at the All-Union Institute of Scientific and Technical Information, 3 October 1979, No 3457-79.

3. Stoker, Dzh., VOLNY NA VODE (Waves on Water), Moscow, IL, 1959, 618 pages.

INVESTIGATION OF EFFECT OF VERTICAL DENSITY STRUCTURE ON INTERNAL WAVES

Sevastopol' TEORETICHESKIYE I EKSPERIMENTAL'NYYE ISSLEDOVANIYA POVERKHNOSTNYKH I VNUTRENNIKH VOLN in Russian 1980 (manuscript received 25 Apr 80) pp 143-150

[Article by S. M. Khartiyev and L. V. Cherkesov]

[Text]

Abstract: The effect of vertical density structure on the kinematic characteristics of free internal gravitational waves is investigated. The investigations are made both for averaged density distributions and for models with a vertical fine structure.

At the present time a considerable percentage of the investigations devoted to the fine vertical structure of the ocean are directed to a study of the role played by internal waves during its formation [1, 2, 8]. Closely akin to these investigations are the problems related to the influence of fine structure itself on the field of internal waves [3, 4, 9]. Due to the experimental studies carried out in these directions it was possible to obtain a considerable number of different estimates of the size of microscale inhomogeneities having the nature of stratification. Such estimates, in turn, made it possible to choose the models most completely taking into account the real density distribution in the ocean [3] and making it possible to analyze the distorting effect of fine structure on internal waves [4, 9].

In this article, in contrast to [3, 4, 9], we study the dependence of the elements of internal waves on fine structure parameters. In comparison with [3, 4], we give a more detailed analysis of the influence of characteristic vertical scales of the "fine stratification" ("sheets" with a thickness from 10 cm to 3 m were taken into account) and high local values of the Väisälä-Brunt frequency on the kinematic characteristics of internal waves.

We will examine a plane layer of an ideal inhomogeneous incompressible fluid of a constant depth H. Assume that the density in an undisturbed state changes in conformity to the law

$$\bar{\rho}_0(\bar{z}) = \begin{cases} \rho_1 & \text{with} \quad -H_1 \leqslant \bar{z} \leqslant 0, \\ \bar{\rho}_0(z) & \text{with} \quad -H_2 < \bar{z} < -H_1, \\ \rho_2 & \text{with} \quad -H \leqslant \bar{z} \leqslant -H_2, \end{cases}$$

where

$$\bar{R}_0(\bar{z}) = -\bar{z}\frac{\Delta\rho}{\Delta H} + \frac{\rho_1 H_2 - H_1\rho_2}{\Delta H},$$

ΔH is the thickness of the thermocline ($\Delta H = H_2 - H_1$); $\Delta\rho$ is the total density drop ($\Delta\rho = \rho_2 - \rho_1$).

We will arbitrarily break down the thermocline ($-H_2 \leqslant \bar{z} \leqslant -H_1$) into m parts, retaining ΔH and $\Delta\rho$ invariable

$$\Delta H = \sum_{i=1}^{n} \Delta h_i + \sum_{j=1}^{m-n} \Delta H_j, \quad \Delta\rho = \sum_{i=1}^{n} \Delta\rho_i. \qquad (1)$$

Here we use ΔH_j to denote the thickness of the homogeneous layers (laminae) and Δh_j is used to denote the thickness of interlayers having the density drop $\Delta\rho_i$ ("sheets").

Thus, we obtain

$$\bar{\rho}_m(\bar{z}) = \begin{cases} \rho_1 & \text{with} \quad -H_1 \leqslant \bar{z} \leqslant 0, \\ \bar{R}_m(\bar{z}) & \text{with} \quad -H_2 \leqslant \bar{z} \leqslant -H_1, \\ \rho_2 & \text{with} \quad -H \leqslant \bar{z} \leqslant -H_2, \end{cases}$$

where $\bar{R}_m(\bar{z})$ is the new density distribution containing fine structure elements.

We will investigate the kinematic characteristics of free internal gravitational waves for an averaged stratification model $\bar{\rho}_0(\bar{z})$ and for a model with a fine structure $\bar{\rho}_m(\bar{z})$. Comparing the results of these investigations, we study the influence of the parameters of fine structure (m, ΔH_j, Δh_i, $\Delta\rho_i$) on the modal composition of internal waves.

As the initial equations of motion we will take a linearized system of Euler equations. We will select the origin of coordinates on the undisturbed free surface of the ocean. We will relate the dimensionless variables with the dimensional variables by the expressions

$$z = Hz, \quad \bar{x} = Hx, \quad \bar{\zeta} = H\zeta, \quad \bar{t} = \sqrt{g^{-1}H}\,t, \quad \bar{v}_x = \sqrt{gH}\,v_x,$$
$$\bar{v}_z = \sqrt{gH}\,v_z, \quad \rho = \bar{\rho}_\ell(0)gH\rho, \quad \bar{\rho}_\ell = \bar{\rho}_\ell(0)\rho_\ell, \quad \bar{\rho} = \bar{\rho}_\ell(0)\rho.$$

Here the function $\bar{\zeta}(\bar{x}, \bar{t})$ determines the form of the free surface; $\bar{v}_x$, $\bar{v}_z$ are the horizontal and vertical components of the velocity vector of the wave disturbance; $\bar{\rho}_\ell(\bar{z})$ is stationary density ($\ell = 0, m$), $\bar{p}$, $\bar{\rho}$ are the dynamic increments of pressure and density. Seeking periodic solutions in time t and in the horizontal coordinate x in the form

$$(\rho, p, v_x, v_z, \zeta) = [P(z), R(z), U(z), W(z), S]\exp[i(kx - \sigma t)],$$

we arrive at an equation relative to the amplitude of the vertical velocity component W(z)

$$\frac{d}{dz}\left(\rho_\ell \frac{dW}{dz}\right) - W\left(\frac{d\rho_\ell}{dz}\frac{1}{\sigma^2} + \rho_\ell\right)k^2 = 0 \qquad (2)$$

with the boundary conditions

$$\frac{dW}{dz} - \frac{k^2}{\sigma^2}W = 0 \quad \text{with } z = 0,\ W = 0 \text{ with } z = -1. \qquad (3)$$

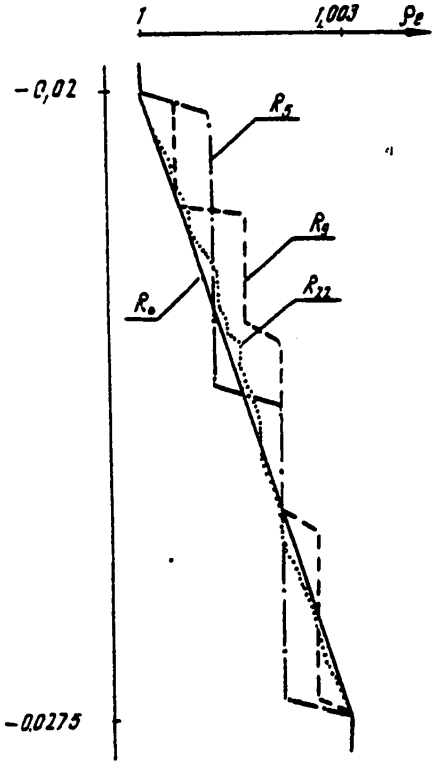

Fig. 1.

A solution of the boundary-value problem (2)-(3) was obtained numerically by its reduction to the Cauchy problem with subsequent use of the Runge-Kutta method [6, 7]. With stipulation, for computations of the continuous distributions ρ_0, ρ_m it was assumed that the density in the interlayers Δh_i changes linearly.

Figure 1 shows models $\rho_\ell(z)$ (ℓ = 0, 5, 9, 22). Their numerical characteristics for dimensionless variables are represented in Table 1. The points $\tilde{z}_i$ in the table correspond to the depths ($\tilde{z}_i = -10^2 \cdot z_i$, $-1 \leqslant z_i \leqslant 0$) at which the density values $\rho_m(\tilde{z}_i)$ (change in density between these points is assumed to be linear) are stipulated. The maximum values of the Väisälä-Brunt frequency for the ρ_m distributions are given in the third line in Table 1. Assume that $H = 4 \cdot 10^3$ m. Then H_1 = 80 m, H_2 = 120 m; the thickness of the "sheets" Δh_i is equal to 1 m with m = 1, 0.5-1 m with m = 9 and 0.1-3 m with m = 22.

The kinematic characteristics of the internal waves corresponding to the $\rho_\ell(z)$ distributions are given in Figures 2, 3. The solid lines correspond to the model ρ_0; the dot-dash lines correspond to ρ_5; and the dashed and dotted lines correspond to ρ_9 and ρ_{22} respectively.

Figure 2,a,b shows dispersion curves of the second, third, fourth and fifth modes of internal waves (the figures designate the number of the mode). Between the curves of the models ρ_0, ρ_5, ρ_9 there is a discrepancy which already becomes significant in the region of quite long waves $1 < k < 5$. For example, with k = 3 the period of oscillations of the third internal mode of the ρ_5 model will then be 1 1/2 times less than the period of this same mode in the case of an averaged stratification. With $1 < k < 5$ the dispersion dependences are close to linear.

Table 1

0		5		9		22		m
1		3		5		12		n
0,6325		1,9986		2,8333		0,6957		$\bar{N}$
$\tilde{z}_i$	$\rho_0(\tilde{z}_i)$	$\tilde{z}_i$	$\rho_5(\tilde{z}_i)$	$\tilde{z}_i$	$\rho_9(\tilde{z}_i)$	$\tilde{z}_i$	$\rho_{22}(\tilde{z}_i)$	i
0	1	0	1	0	1	0	1	1
2	1	2	1	2	1	2	1	2
2,75	1,003	2,025	1,001	2,6125	1,0005	2,00625	1,000025	3
100	1,003	2,35	1,001	2,1375	1,0005	2,08125	1,000525	4
		2,375	1,002	2,15	1,0015	2,1	1,000525	5
		2,725	1,002	2,275	1,0015	2,10625	1,00055	6
		2,75	1,003	2,3	1,002	2,125	1,00055	7
		100	1,003	2,5	1,002	2,2	1,00105	8
				2,525	1,0025	2,21875	1,00105	9
				2,725	1,0025	2,22125	1,001062	10
				2,75	1,003	2,23375	1,001062	11
				100	1,003	2,23875	1,001075	12
						2,25125	1,001075	13
						2,2575	1,001	14
						2,275	1,001	15
						2,35	1,0014	16
						2,375	1,0014	17
						2,45	1,0017	18
						2,475	1,0017	19
						2,55	1,002	20
						2,575	1,002	21
						2,65	1,0025	22
						2,675	1,0025	23
						2,75	1,003	24
						100	1,003	25

In the region $k>5$ the behavior of the dispersion curves becomes more complex. Here in models with a fine structure ρ_5, ρ_9 resonance zones are formed [5] and anomalies appear in the neighborhood of the so-called critical frequencies at which some characteristic value of one waveguide coincides with some value of the other [3]. For model ρ_9, which contains the greatest number of "sheets" and in these interlayers having the maximum (in comparison with ρ_5) local values of the Väisälä-Brunt frequency, the anomalous effect is expressed more strongly than for ρ_5. This is evidently attributable to the fact that with an increase in the local values of the Väisälä-Brunt frequency N_i the region of characteristic frequencies of individual waveguides (Δh_i) expands accordingly ($\sigma<N_i$) and the probability of coincidence of the characteristic values of the different "sheets" increases. The greater the number of poorly interrelated waveguides (that is, the number of "sheets"), evidently, the more probable will be the cases of coincidence of their characteristic frequencies. We will mention the ranges of critical frequencies for the fifth, fourth and third modes of internal waves of the model ρ_9. With $0.4\leqslant k\leqslant 10$ we obtain

$$0{,}25 < \sigma_3 \cdot 10^2 < 0{,}31,$$
$$0{,}31 < \sigma_4 \cdot 10^2 < 0{,}38,$$
$$0{,}38 < \sigma_5 \cdot 10^2 < 0{,}45.$$

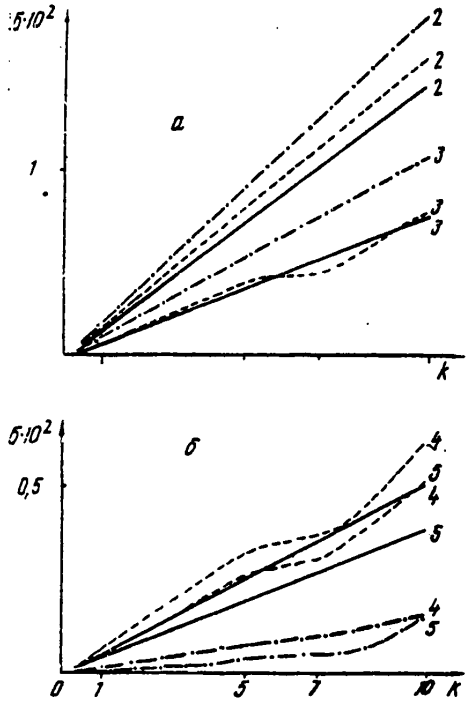

Fig. 2.

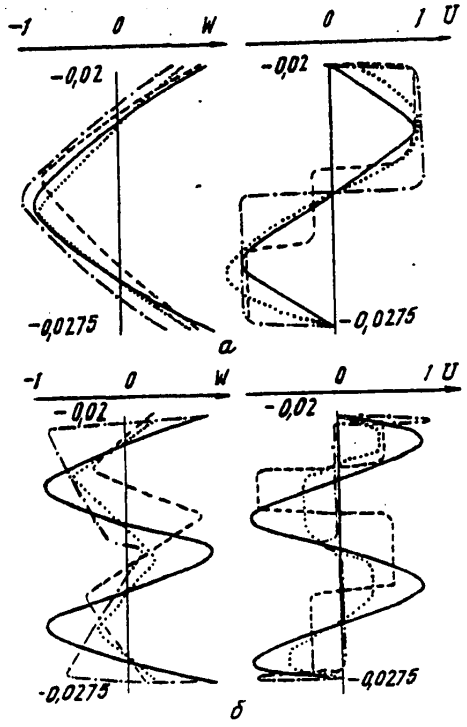

Fig. 3.

Table 2 gives the ratios of the maximum values of group velocities for the first five modes of internal waves of the models ρ_9 and ρ_0 (V_9/V_0). The strongest influence of the fine structure on group velocities is observed (beginning with the third mode) in the region $5 \leqslant k \leqslant 7$ in which all the ranges of critical frequencies $0.25 < \sigma \cdot 10^2 < 0.45$ (Fig. 2) fall. In this region the group velocities for the averaged model greatly exceed the "fine stratification" values. With $7 < k \leqslant 10$ the group velocity V_g increases sharply and becomes greater in value than V_0, but this difference is already less significant than in the region $5 \leqslant k \leqslant 7$.

Thus, an increase in the number n of "sheets" with high local values of the Väisälä-Brunt frequency in the structure of the thermocline (with retention of the relationships (1) and a weak correlation between the waveguides) leads for the most part to the clearest manifestation of anomalies in the dispersion curves, which exerts a substantial effect on the group velocity of the internal waves. However in quantitative estimates the decisive role is played by the parameter m -- the total number of layers. For example, the anomalous effect for the ρ_5 distribution is expressed more weakly than for ρ_9. Nevertheless, the discrepancy in the dispersion curves

for models ρ_5 and ρ_0 is far more significant than in the case ρ_9 and ρ_0 (Fig. 2). That is, despite the fact that with an increase in m there can be rather strong anomalous effects in the dispersion relationships, the discrepancy between the dispersion curves of models ρ_0 and ρ_m, as might be expected, decreases with an increase in m.

Table 2

k	$5 \leqslant k \leqslant 7$					$7 < k \leqslant 10$				
№	1	2	3	4	5	1	2	3	4	5
v_9/v_0	1	1,070	0,43	0,5	0,57	1	1,09	1,33	1,6	1,5

Although the relative changes introduced by the fine structure in the region of short waves increase (for example, the frequency of oscillations for one and the same wavelength can decrease by several times), this is not reflected very appreciably, evidently, in the amplitudes of the internal waves. It was demonstrated in [9] that for the region $1/2 \leqslant \sigma^2/N_0^2 \leqslant 3/4$ the relative changes in amplitudes constitute less than 10%. From this point of view, the sector $\sigma^2/N_0^2 < 1/2$ (Fig. 2) is of definite interest because for it there are already rather considerable discrepancies in the periods of oscillations of internal waves having a quite great length.

Figure 3 shows the depth distributions of the amplitudes of the third and fifth modes of the vertical and horizontal components of the velocity vector of wave disturbance, computed for the models ρ_ℓ (ℓ = 0, 5, 9, 22) with k = 10 and related to their maximum values. It can be seen that the presence of elements of fine structure leads to a displacement of the nodal and extremal points in the thermocline, which in depth fall for the most part in the interlayers Δh_i. Such a distribution of extrema for the high modes causes a concentration of movement in rather narrow "sheets" (Fig. 3,b). However, this effect occurs only for the ρ_5 model. In comparing the fine vertical structure in the models ρ_5, ρ_9, ρ_{22}, we note that the "sheets" (Δh_i) alternate successively with laminae (ΔH_j). In the ρ_5 model the ratios $\Delta H_j/\Delta h_i$ will be maximum. Thus, one of the necessary conditions for the concentration of the higher modes in layers with high local values of the Väisälä-Brunt frequency is the existence of a weak correlation between the "sheets" in the vertical density structure. A numerical analysis indicated that the velocity profiles, computed from models with a fine structure, are more sensitive (especially the horizontal component, Fig. 3) to changes in the wave number than the profile with an averaged stratification. For example, the amplitude of the fifth mode of the vertical velocity component for the ρ_9 model at emergence from the thermocline with k = 10 attains its maximum value; with k = 3 this value will already be 22% of the maximum. The amplitude values W(z) for the third mode of the ρ_5 model (with k = 3) and the fifth model of the ρ_{22} model (with k = 10) at the entry into the thermocline and upon emergence from it constitute 50% of the maximum, whereas for the averaged stratification (ρ_0 model) these values, all other conditions being equal, will be maximum. Such a redistribution of extrema and frequencies, introduced by the fine structure (Figures 2, 3), can exert a substantial influence on the kinematic characteristics of internal waves beyond the limits of the thermocline. For example, for the third mode of the ρ_5 model the

value of the vertical velocity component with x = 0, k = 3 at the depth H/2 at the times t = 500π, 1000π will constitute 0.23, 0.18 of the maximum (unity) respectively; in the case of an averaged density, all other conditions being equal, -0.1, -0.46. Thus, the distorting effect of fine structure will lead to a change in the intensity and direction of velocity beyond the limits of the thermocline.

Now we will clarify how the dimensions of the "sheets" Δh_i exert an influence on the elements of internal waves. We will take an averaged stratification $\rho_0(z)$ with the parameters H = $4 \cdot 10^3$ m, H_1 = 80 m, H_2 = 120 m, $\Delta\rho$ = 0.0006 g/cm^3, N_0 = 0.014 Hz. We will model the fine structure by the ρ_5 distribution containing three identical waveguides (Δh_i = 2 m, $\Delta\rho_1$ = 0.0002 g/cm^3), two of which are situated on the boundaries of the thermocline and one in the middle. The density distribution $\tilde{\rho}_5(z)$ is obtained from the ρ_5 model by decreasing Δh_i (i = 1, 2, 3) by a factor of 4 and retaining the former ΔH, $\Delta\rho$ values. Computations indicated that the vertical structure of the modes of internal waves of the model $\tilde{\rho}_5$ almost do not differ from the vertical structure of the corresponding modes of the ρ_5 model with one and the same k values. However, there can be a strong discrepancy in the periods of oscillations of these modes of identical structure. For example, with k = 10 the periods of oscillations of the fourth mode of the ρ_5, $\tilde{\rho}_5$ models are related as 1:2 respectively, although with respect to vertical structure the modes of the ρ_5 and $\tilde{\rho}_5$ models virtually coincide.

BIBLIOGRAPHY

1. Fedorov, K. N., TONKAYA TERMOKHALINNAYA STRUKTURA VOD OKEANA (Fine Thermohaline Structure of Ocean Waters), Leningrad, Gidrometeoizdat, 1976, 183 pages.

2. Dykman, V. Z. and Panteleyev, N. A., "Correlation Between the Fine Structure in the Ocean and Internal Waves and Turbulence," MORSKIYE GIDROFIZICHESKIYE ISSLEDOVANIYA (Marine Hydrophysical Investigations), No 4, Sevastopol', pp 132-147, 1977.

3. Goncharov, V. V., "Some Features of Internal Waves in the Ocean," TSUNAMI I VNUTRENNIYE VOLNY (Tsunamis and Internal Waves), Sevastopol', Izd. MGI AN Ukrainskoy SSR, pp 87-96, 1976.

4. Navrotskiy, V. V., "Internal Waves and Fine Structure in the Ocean," DAN SSSR (Reports of the USSR Academy of Sciences), Vol 231, No 5, pp 1080-1083, 1976.

5. Ekkart, K., "Internal Waves in the Ocean," VNUTRENNIYE VOLNY (Internal Waves), Moscow, "Mir," pp 95-115, 1964.

6. Bukatov, A. Ye., et al., "Internal Waves of a Tidal Period in the Equatorial Zone of the Indian Ocean," OKEANOLOGIYA (Oceanology), Vol 13, No 5, pp 788-795, 1978.

7. Ageyev, M. I., et al., BIBLIOTEKA ALGORITMOV (Archives of Algorithms), No 1, Moscow, "Sov. Radio," 1975, 175 pages.

8. Woods, J. D. and Wiley, R. L., "Billow Turbulence and Ocean Microstructure," DEEP SEA RES., Vol 19, No 1, pp 87-121, 1972.

9. Bell, T. H., Jr., "A Numerical Study of Internal Wave Propagation Through Ocean Fine Structure," DTSCH. HYDROGR. Z., 27, No 5/6, pp 193-202, 1974.

EFFECT OF FINE STRATIFICATION ON INTERNAL WAVES GENERATED BY PERIODIC ATMOSPHERIC DISTURBANCES

Sevastopol' TEORETICHESKIYE I EKSPERIMENTAL'NYYE ISSLEDOVANIYA POVERKHNOSTNYKH I VNUTRENNIKH VOLN in Russian 1980 (manuscript received 12 Dec 80) pp 151-158

[Article by S. M. Khartiyev and L. V. Cherkesov]

[Text]

Abstract: A study was made of the influence of vertical density structure on the kinematic characteristics of internal waves generated by surface disturbances, periodic in time, occurring in a limited region. The investigation is carried out both for an averaged stratification and for a distribution with a vertical fine structure.

An investigation of the influence of vertical density structure on the elements of free internal gravitational waves was carried out in [1-5].

In this article we examine the distorting effect of fine stratification on the kinematic characteristics of internal waves generated by surface disturbances, periodic in time, occurring in a limited region.

1. Assume that pressures in the form

$$\bar{p}_0(\bar{x},\bar{t}) = \bar{a} f(\bar{x}) \cdot e^{i\bar{\sigma}\bar{t}},$$

are applied to the free surface of an inhomogeneous ideal incompressible fluid of finite depth, where f is an even continuous function equal to zero with $|x| > \bar{B}$. We have investigated the kinematic characteristics of internal waves arising under the influence of the applied pressure system, with averaged stratification $\bar{\rho}_0(z)$ and in the case of a distribution with a fine structure $\bar{\rho}_m(\bar{z})$. Comparing the results of these investigations we will evaluate the distorting influence of fine structure on internal waves.

We will select the origin of coordinates at the undisturbed free surface. The z-axis is directed vertically upward. We will relate the dimensionless variables and the dimensional relationships

$$\bar{x} = Hx, \quad \bar{z} = Hz, \quad \bar{t} = \sqrt{Hg^{-1}}\,t, \quad \bar{v}_{x\ell} = \sqrt{gH}\,v_{x\ell}, \quad \bar{v}_{z\ell} = \sqrt{gH}\,v_{z\ell},$$

$$\bar{\zeta}_\ell = H\zeta_\ell, \quad \bar{\eta}_\ell = H\eta_\ell, \quad \bar{\rho}_\ell = \bar{\rho}_\ell(0)R_\ell, \quad \bar{p}_\ell = \bar{p}_\ell(0)p_\ell, \quad \bar{p}_\ell = \bar{p}_\ell(0)gHp_\ell,$$

$$\bar{p}_0 = \bar{p}_\ell(0)gHp_0, \quad \bar{a} = \bar{\rho}_\ell(0)gHa, \quad \bar{b} = Hb.$$

where ρ_ℓ is the density distribution in an undisturbed state ($\ell = 0, m$); $\bar{v}_{x\ell}$, $\bar{v}_{z\ell}$ are the horizontal and vertical velocity components; $\bar{\zeta}_\ell$ are the free surface rises; $\bar{\eta}_\ell$ is the deviation of the streamline at a particular depth from the undisturbed position; $\bar{p}_\ell$, $\bar{R}_\ell$ are the dynamic increments to pressure and density. The linearized level of movement and boundary conditions in dimensional variables have the form (the subscript ℓ in formulas (1)-(8) are omitted as a simplification)

$$\rho\frac{\partial v_x}{\partial t} = -\frac{\partial p}{\partial x}, \quad \rho\frac{\partial v_z}{\partial t} = -\frac{\partial p}{\partial z} - R; \tag{1}$$

$$\frac{\partial v_x}{\partial x} + \frac{\partial v_z}{\partial z} = 0, \quad \frac{\partial R}{\partial t} + \frac{d\rho}{dz}v_z = 0; \tag{2}$$

$$p = \zeta = p_0, \quad \partial\zeta/\partial t = v_z \qquad \text{with } z = 0,\ v_z = 0 \text{ with } z = -1. \tag{3}$$

2. Solving the boundary-value problem (1)-(3) much as was done in [6, 7], for the vertical velocity component we obtain the expression

$$v_z = \frac{ai\sigma}{\sqrt{2\pi}}\int_{-\infty}^{\infty}\frac{k^2\bar{f}(k)}{\Delta(k)}W(k,z)e^{ikx}\,dk\,e^{i\sigma t}, \tag{4}$$

where $\bar{f}$ is the Fourier transform of the function f;

$$\Delta(k) = \sigma^2 W'(k,0) - k^2 W(k,0), \tag{5}$$

and the function W satisfies the equation (the prime and the superscript k denote the derivatives of z and k respectively)

$$(\rho W')' - k^2[\rho' + \sigma^2\rho]\sigma^{-2}W = 0 \tag{6}$$

with the initial conditions

$$W(k,-1) = 0, \quad W'(k,-1) = 1. \tag{7}$$

The integrand in (4) has singularities with k values satisfying the equation

$$\Delta(k) = 0. \tag{8}$$

We will demonstrate that this equation has only purely imaginary and real roots. We mill multiply (6) by a function complexly conjugate with W and we will integrate along the segment $-1 \leqslant z \leqslant 0$. Taking into account the conditions (7) and expression (8) we obtain

$$k^2 = \frac{\int_{-1}^{0} \rho |W'|^2 dz}{|W(k,0)|^2 - \int_{-1}^{0} (\rho' + \sigma^2 \rho) |W|^2 dz} \sigma^2.$$

It therefore follows that all the k values can be only purely imaginary or real numbers situated symmetrically on a complex plane relative to the point k = 0.

For computing the integral (4) the integration path (4) will be deformed into a contour running along the real axis and passing around the poles situated on it in small semicircles in such a way that the natural radiation condition is satisfied. Computing the integral by the residues method, we obtain

$$Re\, v_{z\ell} = \sum_{i=0}^{\infty} W_{\ell i}. \qquad (9)$$

where

$$W_{\ell i} = -a\sqrt{2\pi}\, \sigma \frac{k_i^2 \bar{f}(k_i)}{\Delta_k'(k_i)} W_\ell(k_i, z) \cos(k_i x + \sigma t).$$

The sum in (9) is taken for all real roots of equation (8) because the contribution from the complex roots attenuates exponentially with an increase $|x|$ of the disturbance (the solution is considered far from the pressure region).

The solution of the Cauchy problem (6)-(7) and equation (8) was obtained numerically with use of the Runge-Kutta method [8]. By determining $V_{z\ell}$ it is easy to find η_ℓ, $V_{x\ell}$ respectively from the kinematic condition and continuity equation.

3. We will carry out the further investigation for the density distribution ρ_0, ρ_1 (Fig. 1, $H_1 = 0.02$, $H_2 = 0.0425$) and the f function in the form

$$f(x) = \begin{cases} 1, & |x| = 5. \\ 0, & |x| > 6. \end{cases}$$

Figure 2 is a graph of the dependence of the amplitude $\tilde{W}_\ell$ ($\max|V_{z\ell}|$ during the period T at a particular depth) on the vertical velocity component as a function of z. The solid curve corresponds to $\ell = 0$, the dashed line corresponds to $\ell = 7$. The computations were made with a = 1, b = 39.15, $x_0 = -100$ for the periods $T_1 = 1571$, $T_2 = 1142$, $T_3 = 898$ (the characteristics in dimensional variables for different depths are given in Table 1). We note that it was not possible to satisfy computations for $T < T_3$ as a result of the dispersion of the numerical method.

It can be seen (Fig. 2) that fine structure exerts a substantial influence on the depth distribution of the maximum values of amplitudes of the vertical velocity component of the wave disturbance. With a decrease in the period of oscillations

the difference in the amplitudes of $\widetilde{W}_0$, $\widetilde{W}_T$ is intensified. The fine stratification can both increase ($T = T_1$, T_2 and decrease ($T = T_3$) the amplitude of $\widetilde{W}_\ell$. The strongest discrepancy in the W_0, W_T values is observed for the period T_3 at the emergence from the thermocline ($\widetilde{z} = -42.5$, $\widetilde{z} = z \cdot 10^3$), where the absolute maximum $\widetilde{W}_\ell$ is attained. Here $\widetilde{W}_7 = 3.13 \cdot \widetilde{W}_0$.

Table 1

$H \cdot 10^{-3}$ м	$\bar{H}_1$ м	$\bar{H}_2$ м	Δh_i м				$\bar{\sigma} \cdot 10^{-3}$ м	$\lvert\bar{x}_0\rvert \cdot 10^{-3}$ м	T_i ч hours		
			1	2	3	4			1	2	3
2	40	85	1	1,5	0,5	2	78,3	200	6,23	4,53	3,56
	80	170	2	3	1	4	156,6	400	8,81	6,41	5,03
	120	255	3	4,5	1,5	6	234,9	600	10,79	7,85	6,17

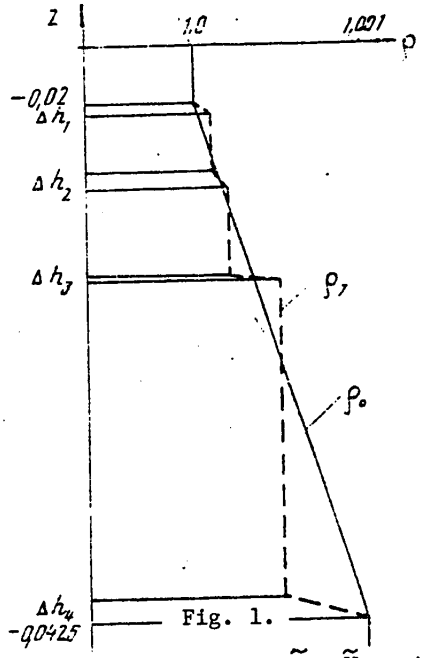

Fig. 1.

We note that the difference in the amplitudes $\widetilde{W}_0$, $\widetilde{W}_7$ exists not only in the thermocline region ($-42.5 \leqslant z \leqslant -20$), but also beyond its limits. For example, during the period T_2 in the upper homogeneous layer with $-20 \leqslant \widetilde{z} \leqslant -5$ $\widetilde{W}_0$ exceeds $\widetilde{W}_7$ by more than a factor of 2. The same picture is observed during the period T_1 in the region $-20 \leqslant z \leqslant -15$.

For the period T_3 the greatest difference in the values $\widetilde{W}_0$, $\widetilde{W}_7$ is observed in the entire lower homogeneous layer where the amplitude $\widetilde{W}_7$ exceeds by a factor greater than 2 the corresponding $\widetilde{W}_0$ value. The computations indicated that such a strong discrepancy in the amplitudes $\widetilde{W}_0$, $\widetilde{W}_7$ during the period T_3 is attributable primarily to substantial differences in the modal composition of the internal waves for the models ρ_0, ρ_7.

Figure 3 shows the functions $W\ell_i$, $V\ell_i$ ($V\ell_i$ are the harmonics of horizontal velocity, $i = 0, 1, 2, \ldots$), computed at the time $t = 310$, when $V_z\ell$ during the period T_3 attains (in absolute value) its maximum level. It can be seen that in the case of averaged stratification there is obviously a dominance of the harmonics $W\ell_0$,

$V_{\ell 0}$ in the entire depth, that is, surface waves. In the case of a fine stratification with the formation of the velocity profile $V_{z\ell}$ the most important role is played by internal waves (in particular, the first internal mode). A similar manifestation of the fine structure is also observed during formation of the horizontal velocity profile. The structure of the internal modes V_{7i}, in contrast to V_{0i}, has a clearly expressed power-law character (Fig. 3,b).

Table 2 gives the maximum (in absolute value) values of the parameters and $V_{x\ell}$ during the period T with $z = -H_1, -H_2$ ($\eta_\ell = \max_T |\eta_\ell| \cdot 10$, $V_{x\ell} = \max_T |V_{x\ell}| \cdot \ell = 0.7$). Since the profile of horizontal velocity in homogeneous layers forms straight lines parallel to the z-axis, the $\tilde{V}_{x\ell}$ values will also be correct for the regions $-1 \leqslant z \leqslant -H$, $-H_1 \leqslant z \leqslant 0$. The differences in the amplitudes $\tilde{V}_{x0}$, $\tilde{V}_{x7}$ in the upper and lower homogeneous layers in comparison with $\tilde{V}_{z0}$, $\tilde{V}_{z7}$ (Fig. 2) are not so significant. The discrepancy is greatest when $T = T_2$ in the upper homogeneous layer, where $\tilde{V}_{x7} = 1.96\ V_{x0}$.

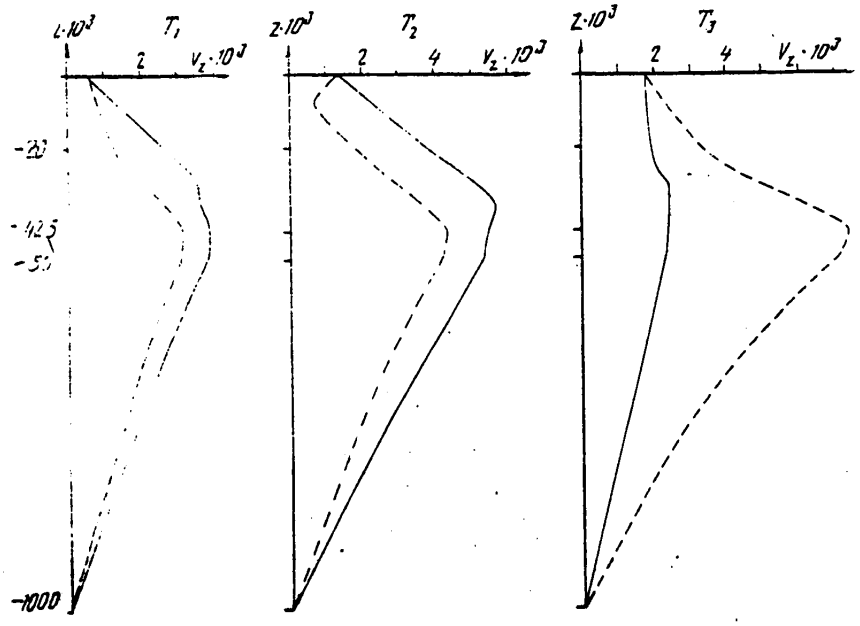

Fig. 2.

The greatest difference in the $\tilde{\eta}_0$ and $\tilde{\eta}_7$ values at the entrance into the thermocline are observed during the periods T_1 and T_2, for which $\tilde{\eta}_7 = 0.28\ \tilde{\eta}_0$, $\tilde{\eta}_7 = 0.43\ \tilde{\eta}_0$ respectively. With $T = T_3$ the picture changes. A considerable discrepancy in the $\tilde{\eta}_i$ values is observed with emergence from the thermocline, where the fine stratification increases the amplitude of the oscillations by a factor greater than 3.

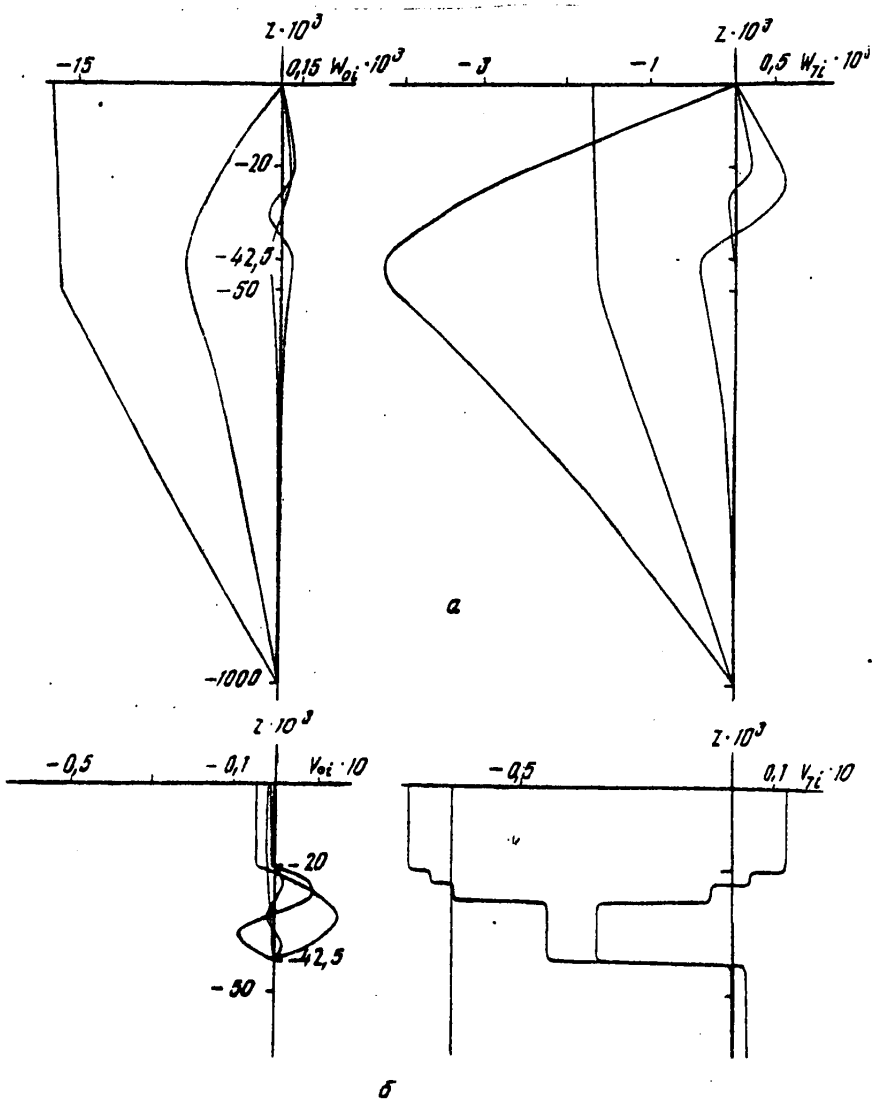

Fig. 3.

Proceeding on the basis of the data in Table 2, we will give the limits of change of the $\bar{V}_{xl}$ and $\bar{\eta}_l$ parameters for the periods $\bar{T}_j$ (j = 1, 2, 3).

In the case of an averaged stratification $\bar{\rho}_0(\bar{z})$ with an ocean depth H = 4 km and atmospheric pressure a = $2 \cdot 10^2$ Pa we obtain

$$0.14 \leqslant V_{x0} \leqslant 0.24 \text{ (m/sec)}, \quad 5.6 \leqslant \bar{\eta}_0 \leqslant 19.2 \text{ (m)}.$$

For the model ρ_7, all other conditions being equal, we have

$$0.15 \leqslant V_{x7} \leqslant 0.32 \text{ (m/sec)}, \quad 4.1 \leqslant \bar{\eta}_7 \leqslant 21.2 \text{ (m)}.$$

Table 2

T	T_1		T_2		T_3	
z	$-H_1$	$-H_2$	$-H_1$	$-H_2$	$-H_1$	$-H_2$
$\tilde{v}_{x0}$	1,76	1,38	1,65	2,33	2,21	2,38
$\tilde{v}_{x7}$	1,54	1,45	3,24	2,27	1,99	2,51
$\tilde{\rho}_0$	7,43	9,62	6,96	9,60	2,80	3,20
$\tilde{\rho}_7$	2,06	7,43	3,02	7,93	4,79	10,60

4. We will estimate the amplitudes of the kinematic characteristics of internal waves at the ocean surface. The fine stratification of the thermocline exerts virtually no influence on the amplitude of the vertical velocity component of the wave disturbance at the free surface (Fig. 2). The distorting effect of fine structure on the horizontal component is more significant. For the periods T_1 and T_3 the discrepancies in the amplitudes $\tilde{V}_{x0}$, $\tilde{V}_{x7}$ at the free surface are 10 and 14% respectively (V_{x0} - 100%). With $T = T_2$ this value will already be equal to 96%. Computations have shown that such a strong discrepancy in the amplitudes of $\tilde{V}_{x0}$, $\tilde{V}_{x7}$ for the period T_2 is attributable to the distorting effect which the fine structure exerts on the modal composition of the internal waves (the fine stratification exerts virtually no influence on the surface mode, that is, $V_{00}(0,t) = V_{70}(0,t)$).

Conclusions

Fine stratification exerts a significant influence on the depth distribution of the kinematic characteristics of the wave disturbance; depending on the period of oscillations it can both increase and decrease them.

As a result of the distorting influence of fine structure on the modal composition of internal waves the profiles of horizontal and vertical velocities in the thermocline region can experience structural changes of considerable amplitude (the values of the vertical velocity component can more than triple).

The distorting effect of fine structure exists not only in the thermocline region, but also beyond its limits; in the upper homogeneous layer it exerts the strongest influence on the horizontal velocity component, whereas in the lower homogeneous layer it exerts the strongest influence on the vertical velocity component.

The presence of a fine stratification of the thermocline can lead to an appreciable increase (by a factor of 2) in the amplitudes of the horizontal velocity of the wave disturbance at the ocean surface, but this leaves the vertical velocity value unchanged.

BIBLIOGRAPHY

1. Marchuk, G. I. and Kagan, B. A., "Internal Gravitational Waves in a Really Stratified Ocean," IZV. AN SSSR: FIZIKA ATMOSFERY I OKEANA (News of the USSR Academy of Sciences: Physics of the Atmosphere and Ocean), Vol 6, No 4, pp 412-422, 1970.

2. Fedorov, K. N., "Internal Waves and Vertical Thermohaline Microstructure of Ocean," VNUTRENNIYE VOLNY V OKEANE (Internal Waves in Ocean), Novosibirsk, Izd-vo VTs SO AN SSSR, pp 90-118, 1972.

3. Goncharov, V. V., "Some Characteristics of Internal Waves in the Ocean," TSUNAMI I VNUTRENNIYE VOLNY (Tsunamis and Internal Waves), Sevastopol', Izd-vo MGI AN UkrSSR, pp 87-96, 1976.

4. Navrotskiy, V. V., "Internal Waves and Vertical Structure of Water Temperature in Ocean," OSOBENNOSTI STRUKTURY I DINAMIKI VOD TIKHOGO OKEANA (Characteristics of Structure and Dynamics of Waters in Pacific Ocean), Vladivostok, Izd-vo DNTs AN SSSR, pp 101-117, 1978.

5. Khartiyev, S. M. and Cherkesov, L. V., "Investigation of the Influence of the Vertical Structure of Density on Internal Waves," in this collection of articles, pp 143-150.

6. Bukatov, A. Ye. and Cherkesov, L. V., "Internal Waves From Periodic Surface Disturbances," IZV. AN SSSR: FIZIKA ATMOSFERY I OKEANA, Vol 7, No 6, pp 648-657, 1971.

7. Cherkesov, L. V., POVERKHNOSTNYYE I VNUTRENNIYE VOLNY (Surface and Internal Waves), Kiev, "Naukova Dumka," 1973, 247 pages.

8. Ageyev, M. I., et al., BIBLIOTEKA ALGORITMOV (Library of Algorithms), Moscow, "Sov. Radio," No 1, 1975, 175 pages.

EVALUATION OF POSSIBLE VALUES OF PARAMETERS OF INTERNAL WAVES IN SOUTH POLAR FRONT ZONE

Sevastopol' TEORETICHESKIYE I EKSPERIMENTAL'NYYE ISSLEDOVANIYA POVERKHNOSTNYKH I VNUTRENNIKH VOLN in Russian (manuscript received 7 Jul 80) pp 159-167

[Article by N. P. Bulgakov and R. A. Yaroshenya]

[Text]

Abstract: On the basis of hydrological data with the use of a frontal zone model the authors give an evaluation of the possible values of elements of the field of internal waves for the south polar front.

Data from in situ observations [19, 20] indicate that frontal zones are regions of increased intensity of internal waves in the ocean. This explains the interest in a model study of these zones as one of the important factors in the generation of internal waves.

In sources [2, 17, 18, 26, 27] the frontal zone is modeled by a jet of constant width. Beyond the limits of the jet the fluid is assumed to be motionless. The effect of Coriolis force and the slope of the free surface and the discontinuity is taken into account.

Within the framework of a three-layer model of the ocean [4] a study was made of a thermal frontal zone constituting a rising or subsidence of cold waters, which is attributable to the curvature of a density discontinuity.

A frontal zone in the form of a region with a constant horizontal density gradient in a two-layer ocean was examined in [2, 3, 5]. The velocities of flow, related to a horizontal density gradient, are assumed to be of the same order of magnitude with the velocities of wave disturbances. We note that in the enumerated studies the indicated models of a front were used for studying the general laws of generation of internal waves outside and inside frontal zones of different types, but were not used in precomputing the parameters of internal waves in any specific frontal zone in the ocean.

In this article an attempt is made to obtain an evaluation of the possible values of the parameters of long-period internal waves for the south polar front (SPF). The analysis is made on the basis of hydrological data with use of an earlier developed model of a frontal zone described in detail in [2, 3].

The principal objective was, assuming the amplitude and frequency of an oncoming barotropic wave to be known, to detect the dependence of elements of the generated internal waves on the parameters of the SPFZ (south polar front zone) (width of zone, depth and latitude, thickness of layers, horizontal and vertical density drops). The choice of this zone is attributable to the relatively good study of this feature.

In solving the formulated problem it is important to know the spatial-temporal variability of the position of the frontal zone and its genetic characteristics. However, among the investigators of the SPFZ there is no unanimous opinion concerning these matters. The authors of [4] analyzed different points of view concerning the spatial-temporal variability of the SPFZ; an attempt was made to evaluate its position and clarify its genetic characteristics.

In 1937 Deacon [21] was the first to determine the position of the SPFZ as relatively stable (the distance between extremal positions did not exceed 60 miles); he defined the frontal zone as the boundary region between subantarctic and antarctic surface waters. On the basis of the temperature distribution in the water layer he advanced the hypothesis that the position of the SPFZ is governed by bottom topography, by the movement of deep and bottom waters. In 1946 Mackintosh [24] fixed the changes in the position of the zone to be 24-29 miles.

V. N. Botnikov [6], on the basis of data from the Soviet Antarctic Expedition of 1955-1958, and also the materials of the "Discovery" expedition, examined the vertical distribution of temperature and established that the 2° isotherm at the horizon 100-300 m characterizes the northern boundary of the SPFZ and that the deviation of the position of the SPFZ from the mean does not exceed 60 miles. Yu. A. Ivanov [11] assigns a decisive role in the formation of the fronts to the nonuniformity of the wind field; he defines dynamic frontal zones (zones with extremal vertical velocities -- divergence and convergence) and accompanying physical frontal zones in which there are clearly expressed physicochemical characteristics. Theoretical computations made it possible to detect a great seasonal variability of the geographic position of the south polar front zone -- up to a total of about 8° in latitude.

However, the author of [14] notes the erroneousness of some premises adopted in [11]. These led to a discrepancy between the theoretical computed values of displacement of the frontal zone and the values cited by other authors based on experimental estimates. At the same time it was demonstrated that Deacon's ideas concerning the decisive effect of deep and bottom waters, and also bottom topography, on the position of the front agree with the results of hydrological observations. This same study [14] gives a hydrological section along 55°W through the region of the south polar frontal zone (Fig. 1). Figure 1 shows that over a distance of 20 miles (between stations 4 and 5) the temperature decrease is 2°. Data in the literature make it possible to conclude that there is a relatively low variability in position of the south polar frontal zone.

However, it is demonstrated in sources [1, 7, 9, 10, 15] that the positions of the SPFZ substantially differ from one another (Fig. 2).

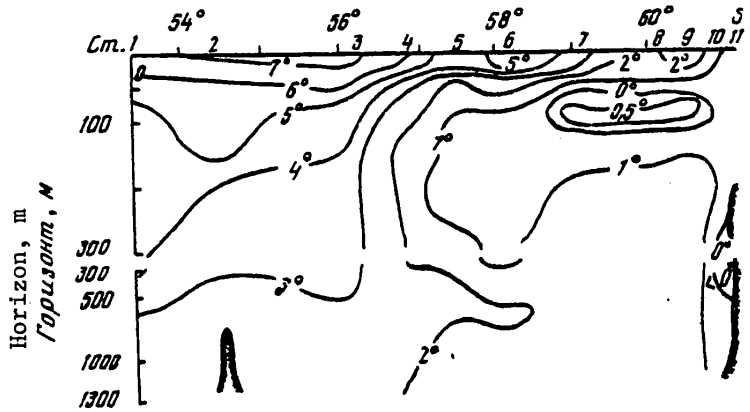

Fig. 1. Distribution of water temperature.

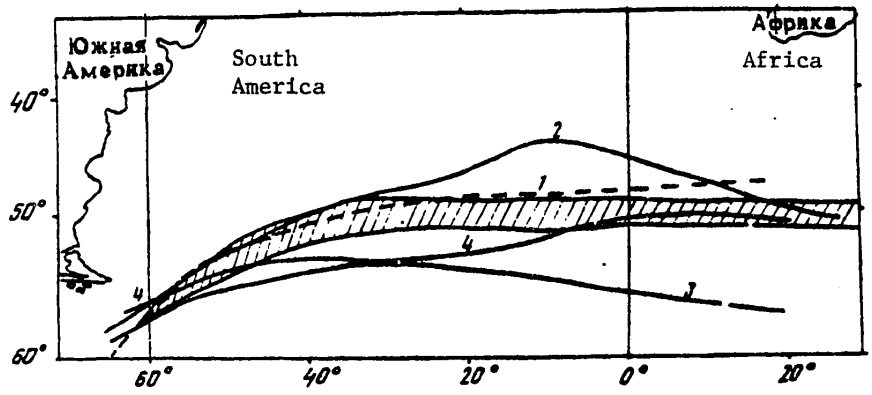

Fig. 2. Positions of south polar front according to data published by Bulatov (1), Burkov, et al. (2), Gruzinov (3) and Stepanov (4); shaded region -- south polar front zone from ATLAS OF THE OCEANS.

R. P. Bulatov [7] defined ocean fronts as the boundaries between macroscale systems of ocean circulations having an opposite direction of movements of waters situated in different climatic zones and discriminated on the basis of the general background of geostrophic circulation. Such a scheme was compiled using dynamic heights computed from averaged observations at different spatial-temporal scales (for one, five and forty degree squares with mean monthly, mean annual and semiannual values). The zone of the south polar front virtually does not react to a change in averaging scales.

The authors of [9], on the basis of data on geostrophic circulation, prepared from mean long-term hydrological data for 5° squares, defined oceanic fronts as regions of crowding of the dynamic contour lines between adjacent circulations.

V. M. Gruzinov [10] developed a scheme of geographic zones in the world ocean, the basis for which is the natural boundaries which are the main oceanic fronts. The south polar frontal zone is one of those zones in the ocean between two main circulations and the boundary between different vertical water structures.

In the ATLAS OF THE OCEANS [1] the south polar frontal zone is represented as a boundary region of displacement of different types of water structure.

V. N. Stepanov [16] demonstrated that the position of five types of fronts, among which one is the south polar front, is closely associated with geographic zonality. The south polar front is less active and is discriminated from the maximum horizontal gradients of thermohaline characteristics, the maximum vertical and horizontal current velocities, and the discontinuities of macrocirculation systems and water masses. On the basis of computations of circulation in the entire layer of ocean waters in accordance with the A. S. Sarkisyan model [13] Stepanov determined the position of quasistationary fronts, also examined the vertical position of the front and discriminated a stable position of the dynamic zones in the entire ocean layer at 0, 200, 500, 1000, 2000 and 3000 m.

A special point of view on the genetic characteristics of the south polar zone is expressed in [8, 12, 22].

The thought that the boundary between the warm and cold waters of the ocean emerges at the surface in the region of the polar fronts was expressed for the first time by Defant [22] in 1928.

N. P. Bulgakov [8], on the basis of his investigations, demonstrated a correlation between the main thermocline and the polar fronts.

V. V. Klepikov [12] pointed out that at approximately 40°S the isotherms characterizing the main thermocline rise toward the ocean surface. The mean annual temperature of the water surface here is 3.5°; it is characteristic for the lower boundary of the main thermocline. The sharply expressed maximum water temperature gradients at the horizons 100 and 200 m serve as proof that the SPFZ is associated with processes manifested not only at the ocean surface, but also in the deep layers. The mean horizontal temperature gradient is approximately 0.1°/km. The fronts associated with the main thermocline are called the main fronts. They are usually situated at 40-60°S. The frontal layer extends to a depth of 500-1000 m and the frontal surface slopes to the horizon in the range from several minutes of angle to 1-2°.

In [25] the south polar frontal zone is characterized as a region of high meridional temperature gradients observed in the surface waters around Antarctica at 50°S. On the basis of a review of the studies it was possible to discriminate some of its characteristics. The lower boundary of the zone is situated at a depth of 200-300 m and the isotherm 2°C is characteristic for it. The temperature minimum is related to the seasonal thermocline and the position of the front varies from 44 to 60°S.

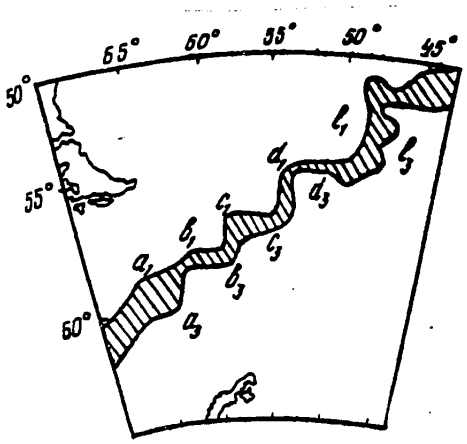

Fig. 3. Position of south polar frontal zone.

In [23] the author cites a diagram of the south polar frontal zone. From this it can be judged that the width of the zone varies in the range 20-200 km (Fig. 3).

Such a diversity of judgments concerning the spatial-temporal variability and genetic characteristics of the south polar frontal zone makes it necessary to select the parameters of zones in definite ranges for computing the generated internal waves.

The section cited in [14] confirms the correctness of choice of a two-layer model of the south polar frontal zone (Fig. 1). The upper layer of the frontal zone model is characterized by a horizontal density gradient. The SPFZ around Antarctica varies from 45 to 60°S; the maximum depth here on the average is 4 km.

The thickness of the upper layer (frontal layer), since the ocean in the model is assumed to be two-layered, varies, according to data from different authors, from 100 to 1000 m. The density in the neighborhood of the investigated frontal zone is taken from [15].

As the initial system of equations describing wave movement within the frontal zone we write a system of equations of long waves

$$u_{1t} - 2\omega v_1 = g\rho_{12}^{-1}\left(\rho_{12}\zeta_1\right)_x, \quad v_{1t} + u_1\left(2\omega + V_{1x}\right) = 0,$$
$$u_{2t} - 2\omega v_2 = -g\rho_2^{-1}\left[\rho_{12}\left(\zeta_2 - \zeta_1\right) + \rho_2\zeta_2\right]_x, \quad v_{2t} + u_2(2\omega + V_{2x}) = 0,$$
$$\zeta_{1t} - \zeta_{2t} = -\rho_{12}^{-1} h_1 \left(u_1\rho_{12}\right)_x, \quad \zeta_{2t} = -h_2 u_{2x}.$$

All the notations, description of the model and solution method were set forth in [3, 5].

As demonstrated by the computations, the amplitudes of the internal waves at the periphery of the frontal zone (regions I, III, Fig. 1 [3, 5]) are essentially dependent on the width ℓ with a fixed value of the density drop $\Delta\rho(\Delta\rho = \rho_{13} - \rho_{11})$

within the frontal zone. The width of the SPFZ is not constant in different regions (Fig. 3) and varies from 20 to 200 km. The greatest values of the amplitudes of internal waves are observed in those regions where ℓ is minimum (regions b_1, b_3; d_1, d_3) and can attain 50% of the amplitude of the oncoming barotropic wave. Relatively small values of the amplitudes of internal waves must be expected in those places where the width ℓ is maximum (regions a_1, a_3; c_1, c_3; ℓ_1, ℓ_3). True, the minimum values of the amplitudes of internal waves in this case may not be attained with the largest ℓ (ℓ = 200 km for the SPFZ), but with lesser values ($100 \leqslant \ell \leqslant 200$ km). The maximum values of the amplitudes of internal waves in the regions a_1, a_3; c_1, c_3; ℓ_1, ℓ_3 do not exceed 10% of the amplitude of the oncoming barotropic wave.

Since the thickness h_1 of the layer of the frontal zone in different regions (according to data from different authors) varies from 100 to 1000 m, then, assuming the mean depth of the layer to be equal to 500 m, we find that due to the deviation of h_1 from the mean value the above-mentioned values of the amplitudes of internal waves can vary. In the region $500 < h_1 < 1000$ m they can increase by 5-20%, and in the region $100 < h_1 < 500$ -- decrease by a factor of 1.1-2.5.

The considered SPFZ falls in the limits 45-60°S. As indicated by computations, the deviation of φ from its mean value (φ_{mean} = 52°) exerts little influence on the amplitudes of the internal waves and does not exceed 10% of their values, corresponding to $\varphi = \varphi_{mean}$.

The dependence of the amplitudes of the internal waves on frequency σ of the oncoming wave is more important. The values of the amplitudes cited above correspond to $\sigma = 7 \cdot 10^{-5} sec^{-1}$; for $\sigma = 1.4 \cdot 10^{-4}$ the amplitudes of the internal waves are less than for $\sigma = 7 \cdot 10^{-5} sec^{-1}$. Under the condition $20 < \ell < 50$ km they are less by 10-30% and with $50 < \ell < 200$ they are less by a factor of 1.5-4.5.

It is characteristic that the frontal zone, with its intersection by a barotropic wave, plays the role of a source of internal waves moving in both directions from its boundaries. The amplitudes of the waves propagating in the direction of the barotropic wave are greater than the amplitudes of the internal waves moving in the opposite direction (reflected waves). In the regions $\ell \sim 200$ km their values are close, whereas in the regions $\ell \sim 20$ km they differ by a factor of 5-10.

BIBLIOGRAPHY

1. ATLAS OKEANOV. ATLANTICHESKIY I INDIYSKIY (Atlas of the Oceans), Leningrad, GUNIO MO SSSR, 1977, 306 pages.

2. Babiy, M. V. and Cherkesov, L. V., "Influence of a Frontal Zone on the Generation of Internal Waves," TSUNAMI I VNUTRENNIYE VOLNY (Tsunamis and Internal Waves), Sevastopol', Izd-vo MGI AN UkSSR, pp 67-75, 1976.

3. Babiy, M. V. and Yaroshenya, R. A., "Generation of Internal Waves in the Neighborhood of a Frontal Zone," POVERKHNOSTNYYE I VNUTRENNIYE VOLNY (Surface and Internal Waves), Sevastopol'. Izd-vo MGI AN UkSSR, pp 146-153, 1978.

4. Babiy, M. V. and Yaroshenya, R. A., "Generation of Internal Waves of a Frontal Zone of the Thermal Crest Type," POVERKHNOSTNYYE I VNUTRENNIYE VOLNY, Sevastopol', Izd-vo MGI AN UkSSR, pp 186-194, 1979.

5. Babiy, M. V. and Yaroshenya, R. A., "Generation of Internal Waves Within a Frontal Zone Simulated by a Horizontal Density Gradient," POVERKHNOSTNYYE I VNUTRENNIYE VOLNY, Sevastopol', Izd-vo MGI AN UkSSR, pp 113-118, 1979.

6. Botnikov, V. N., "Geographical Position of the Zone of Antarctic Convergence in the Antarctic Ocean," INFORMATSIONNYY BYULLETEN' SAE (Information Bulletin of the Soviet Antarctic Expedition), No 41, Moscow, "Morskoy Transport," pp 19-24, 1963.

7. Bulatov, R. P., "Investigation of Water Circulation in the Atlantic Ocean at Different Spatial-Temporal Scales," OKEANOLOGICHESKIYE ISSLEDOVANIYA (Oceanographic Research), No 22, pp 7-93, 1972.

8. Bulgakov, N. P., "Principal Features of Structure and Position of the Subarctic Front in the Northwestern Part of the Pacific Ocean," OKEANOLOGIYA (Oceanology), Vol 7, No 5, pp 879-888, 1967.

9. Burkov, V. A., Bulatov, R. P. and Neyman, V. G., "Macroscale Features of Water Circulation in the World Ocean," OKEANOLOGIYA, Vol 13, No 3, pp 395-403, 1973.

10. Gruzinov, V. M., FRONTAL'NYYE ZONY MIROVOGO OKEANA (Frontal Zones of the World Ocean), Moscow, Gidrometeoizdat, 198 pages.

11. Ivanov, Yu. A., "Frontal Zones in Antarctic Waters. Results of Investigations Under the IGY Program," OKEANOLOGICHESKIYE ISSLEDOVANIYA (Oceanological Research), No 3, pp 30-51, 1961.

12. Klepikov, V. V., "Polar Fronts and the Main Thermocline in the Oceans," VESTNIK LGU (Herald of Leningrad State University), No 28, Issue 3, pp 151-157, 1969.

13. Sarkisyan, A. S., OSNOVY TEORII I RASCHET OKEANICHESKIKH TECHENIY (Principles of Theory and Computation of Ocean Currents), Leningrad, Gidrometeoizdat, 1966, 123 pages.

14. Solyankin, Ye. V., "Dynamics of Some Frontal Zones in the South Atlantic," TRUDY VNIRO (Transactions of the All-Union Scientific Research Institute of Fishing and Oceanography), Vol 75, Moscow, pp 96-106, 1972.

15. Stepanov, V. N., "Density Field of Water in the World Ocean," OKEANOLOGIYA, Vol 17, No 5, pp 778-784, 1975.

16. Stepanov, V. N., "Dynamic Zones in the Oceans and Atmosphere," IZV. AN SSSR: SER. GEOGR. (News of the USSR Academy of Sciences: Geographical Series), No 3, pp 5-14, 1978.

17. Chernysheva, Ye. S., "Investigation of the Parameters of Internal Waves on the Basis of a Numerical Solution of the Equations of Hydrodynamics for a Two-Layer Fluid," KOMPLEKSNYYE ISSLEDOVANIYA V MIROVOM OKEANE (Multisided Investigations in the World Ocean), Moscow, pp 28-31, 1975.

18. Shari, V. P., "Internal Waves in a Two-Layer Ocean," TRUDY 17-y NAUCHNOY KONFERENTSII MFTI (Transactions of the 17th Scientific Conference of the Moscow Physicotechnical Institute), 1971, SER. AEROFIZIKA I PRIKLADNAYA MATEMATIKA (Series on Aerophysics and Applied Mathematics), Dolgoprudnyy, pp 48-54, 1972.

19. Beckerle, I. C., "Detection of Internal Waves From Doppler Shift Observations," TRANS. AMER. GEOPHYS. UNION, Vol 47(1), p 110, 1966.

20. Beckerle, I. C., "Doppler Shifted Waves Relative to a Towed Sensor in a Thermal Front Region," DEEP SEA RES., Vol 22, No 3, pp 197-200, 1975.

21. Deacon, G. E. R., "The Hydrology of the Southern Ocean," DISCOVERY REP., 15, pp 1-124, 1937.

22. Defant, A., PHYSICAL OCEANOGRAPHY, Volumes 1-2, London, Pergamon Press, Vol I, p 730, 1961; Vol II, p 598, 1960.

23. Georgi, D. T., "Fine Structure in the Antarctic Polar Front Zone: Its Characteristics and Possible Relationship to Internal Waves," J. GEOPHYS. RES., Vol 83, No C9, pp 4579-4588, 1978.

24. Mackintosh, N. A., "The Antarctic Convergence and the Distribution of Surface Temperatures in Antarctic Waters," DISCOVERY REP., 23, pp 177-212, 1946.

25. Taylor, H. W., Gordon, A. Z. and Molinelli, E., "Climatic Characteristics of the Antarctic Polar Front Zone," J. GEOPHYS. RES., Vol 83, No C9, pp 4572-4578, 1978.

26. Yasui, M., "Internal Waves in the Open Ocean. An Example of Internal Waves Progressing Along the Oceanic Frontal Zone," THE OCEANOGR. MAG., Vol 12, No 12, pp 157-185, 1961.

27. Yasui, M., "Internal Waves in the Open Ocean. Internal Waves of Long Periods at Ocean Weather Station 'Tango'," THE OCEANOGR. MAG., Vol 12, No 2, pp 185-205, 1961.

VARIABILITY OF ENERGY DENSITY OF INTERNAL WAVES WITH DEPTH IN AN INHOMOGENEOUSLY STRATIFIED OCEAN

Sevastopol' TEORETICHESKIYE I EKSPERIMENTAL'NYYE ISSLEDOVANIYA POVERKHNOSTNYKH I VNUTRENNIKH VOLN in Russian 1980 (manuscript received 17 Mar 80) pp 168-174

[Article by V. Z. Dykman and A. A. Slepyshev]

[Text]

Abstract: It is shown that with an increase in the Väisälä-Brent frequency the energy density of internal waves decreases as a result of a limitation of the amplitudes of waves due to local shear hydrodynamic instability. The theoretically derived dependence of the fluxes of the kinetic energy of internal waves to turbulence on the Väisälä-Brent frequency agrees with experimental data.

The experimental data obtained in the course of implementation of work under the "Polimode" program on the 14th, 16th, 17th and 18th voyages of the scientific research vessel "Akademik Vernadskiy" indicate that the density of potential energy of the internal waves is not constant; it is dependent on local hydrological conditions [1]. For example, in the region of the seasonal thermocline in the "Polimode" polygon with an increase in the Väisälä-Brent frequency N from 3 to 15 cycles per hour the potential energy of the wave field E decreases by more than an order of magnitude. On the other hand, the rate of influx of kinetic energy to small-scale turbulence ε, determined by the method described in [3], considerably increases [2].

Thus, it is entirely natural to postulate the existence of an interrelationship between these two processes. Figure 1 shows the relative distribution of ε and σ_ξ^2 -- the normalized dispersion of vertical displacements, proportional to the density of potential energy of internal waves. The physical nature of this interrelationship is evidently as follows: with an increase in vertical density gradients as a result of limitation of the amplitude of waves due to the appearance of local hydrodynamic instability of the wave movement the wave energy decreases. The energy supply of small-scale turbulence occurs due to the dissipation of wave energy. It is shown in the article that under definite conditions with an increase in the Väisälä-Brent frequency the rate of dissipation of wave energy increases

simultaneously with an increase in the rate of influx of kinetic energy to turbulence.

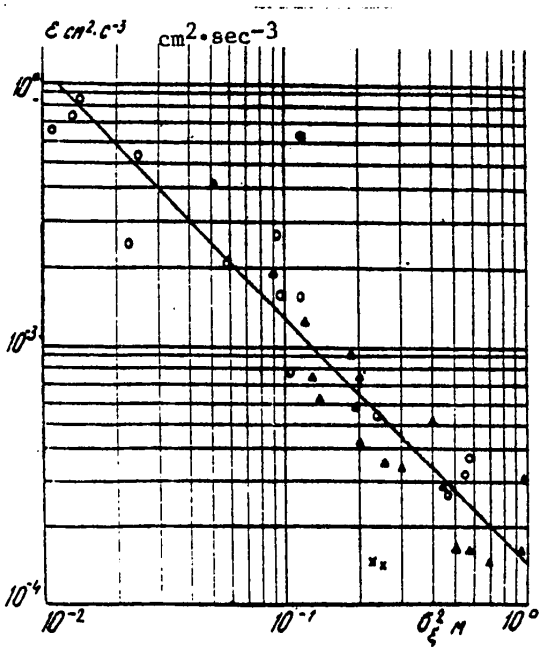

Fig. 1.

The presently existing empirical model of the spectrum of internal waves, constructed by Garrett and Munk [6] on the basis of a generalization of experimental data, does not take into account the dependence of the energy density of waves on local hydrological conditions, and accordingly, does not give an explanation of its observed inconstancy. The density of potential energy of internal waves is proportional to the normalized dispersion of vertical displacements, which is determined using the formula [7]

$$\sigma_\xi^2 = \bar{N}^2 \int_{\gamma_{min}}^{\gamma_{max}} P_\xi(\gamma)\, d\gamma, \quad \gamma = \frac{m}{\bar{N}}, \tag{1}$$

where γ_{max} and γ_{min} are the dimensions of the "floating" spectral window, equal to 1 and 0.1 cycle/m respectively; $\bar{N} = N/N_0$; N is the Väisälä-Brunt frequency; N_0 = 1 cycle/hour. The evaluations σ_ξ^2 when using the Garrett-Munk model in the indicated spectral interval are 0.1 m^2, whereas according to experimental data σ_ξ^2 varies by more than an order of magnitude with a change in the Väisälä-Brunt frequency on the average from 8 to 15 cycles/hour.

What is the reason for the decrease in σ_ξ^2 with an increase in the Väisälä-Brunt frequency? It should be noted that Garrett and Munk examined an isotropic wave field in the absence of shear velocity and did not discuss the problem of the

role of hydrodynamic instability in the formation of the spectrum of internal waves. Phillips, for a three-layer model of the ocean with a Väisälä-Brunt frequency, experiencing a jump in the thermocline, demonstrated that the wave amplitude decreases in the jump layer due to local hydrodynamic instability. The energy density N^2a^2 is limited, in accordance with [5]

$$N^2a^2 < \frac{4N^2}{k_h^2}\left(\frac{N}{\nu} - \frac{\nu}{N}\right)^2, \tag{2}$$

or equivalently

$$N^2a^2 < \frac{4N^4\nu^4}{\left(N^2-\nu^2\right)k_h^2}. \tag{3}$$

The upper boundary for the energy density of internal waves decreases with an increase in N. It will be demonstrated below that under conditions when the Väisälä-Brent frequency slowly changes in distances comparable with the scales of internal waves the level at which there is a limitation of their amplitude as a result of the appearance of local hydrodynamic instability decreases continuously with an increase in N. This means that the density of the potential energy of waves decreases with an increase in the vertical density gradients.

The criterion of local shear hydrodynamic stability has the form

$$R_i = \frac{N^2}{\left[\left(\partial\bar{u}/\partial z\right)^2 + \left(\partial\bar{v}/\partial z\right)^2\right]} > \frac{1}{4}. \tag{4}$$

Using the WKB approximation, it is possible to find the relationship between the vertical velocity gradients and the amplitude of rises of internal waves. The disturbance of the velocity field and the rise are in this case examined in the form

$$\bar{u} = \bar{u}_0 e^{i\theta(\vec{x},t)}, \quad \zeta = A\left(\vec{x},t\right)e^{i\theta(\vec{x},t)}, \tag{5}$$

where $\bar{u}_0(\vec{x},t)$ and $A(\vec{x},t)$ are slowly changing functions of the space and time coordinates; $\theta(\vec{x},t)$ is a phase function for which there is satisfaction of the relationships correct for the wave packets [4],

$$\frac{\partial\theta}{\partial x_i} = k_i, \quad \frac{\partial\theta}{\partial t} = -\nu. \tag{6}$$

Here $k_i = \{k, \ell, m\}$ are the components of the wave vector; ν is frequency; k_h is the horizontal wave vector.

The linearized system of equations of hydrodynamics has the form

$$\frac{\partial}{\partial t}u - fv = -\frac{\partial p}{\partial x}, \tag{7}$$

$$\frac{\partial}{\partial t}v + fu = -\frac{\partial p}{\partial y}, \tag{8}$$

$$\frac{\partial}{\partial t}w - g\rho = -\frac{\partial p}{\partial z}, \tag{9}$$

$$\frac{\partial}{\partial x}u + \frac{\partial}{\partial y}v + \frac{\partial}{\partial z}w = 0, \tag{10}$$

$$\frac{\partial \rho}{\partial t} + \frac{N^2}{g}w = 0, \tag{11}$$

where u, v, w are the velocity components of wave movement along the x, y and z axes (the x-and y-axes lie in the horizontal plane and the z-axis is directed vertically upward respectively); P is the deviation of pressure from hydrostatic; ρ is the deviation of density from the mean; f is the Coriolis parameter.

It follows from equations (4)-(8) in the WKB approximation that there is a correlation between the amplitude of the rise and the amplitudes of the horizontal velocity components

$$uu^* = \frac{m^2}{(k^2+l^2)^2}\left(\nu^2k^2+f^2l^2\right)\zeta\zeta^*, \tag{12}$$

$$vv^* = \frac{m^2}{(k^2+l^2)^2}\left(\nu^2l^2+f^2k^2\right)\zeta\zeta^*. \tag{13}$$

The value of the amplitude of horizontal velocity hence is expressed through the amplitude of the rise in the following way:

$$uu^* + vv^* = \frac{m^2}{k^2+l^2}\left(\nu^2+f^2\right)\zeta\zeta^*. \tag{14}$$

The value of the vertical gradient of horizontal velocity is expressed through the amplitude of the rises

$$\left(\frac{\partial u}{\partial z}\right)^2 + \left(\frac{\partial v}{\partial z}\right)^2 = \frac{1}{2}\frac{m^4}{k^2+l^2}\left(\nu^2+f^2\right)\zeta\zeta^2. \tag{15}$$

Substituting the derived expression for the gradient of horizontal velocity through the amplitude of the rise under the condition of hydrodynamic stability (4), we obtain the limitation on the level of the density of potential energy of the wave packets (WP)

$$N^2\zeta\zeta^* < \frac{4N^2}{m^4}\left(k_h^2+m^2\right). \tag{16}$$

Averaging (16) for the totality of WP in the same spectral range in which the dispersions of the normalized rises were experimentally determined, we obtain an expression for the energy density of internal waves

$$E = \frac{A}{N^2}. \tag{17}$$

The A constant is determined experimentally. The wave packets with approach to the thermocline, that is, with an increase in the Väisälä-Brunt frequency, lose energy; the energy losses of the wave packet in a unit time evidently can be used as the

influx of kinetic energy to turbulence after averaging for the totality of WP.

In order to determine the energy losses of the wave packet in a unit time we will compute the time derivative along the WP trajectory, that is, the right-hand side of expression (16).

The differentiation operator has the form

$$\frac{d_0}{dt} = \frac{d}{dt} + C_{g_i} \frac{\partial}{\partial x_i}, \tag{18}$$

where C_{g_i} are the components of the group velocity of the WP. With the use of the operator (18) we have in mind that in a horizontally homogeneous case we have the relationship [9]

$$\frac{\partial_0 k_h}{\partial t} = 0, \quad \frac{\partial_0 \nu}{\partial t} = 0, \quad \frac{\partial_0 z}{\partial t} = \frac{\partial \nu}{\partial m}. \tag{19}$$

After differentiation we obtain

$$j = -\frac{d_0}{dt}\left(N^2 \xi \xi^*\right) = \frac{16N^2 \frac{\partial N}{\partial z} k_h^3}{m^3 \sqrt{k_h^2 + m^2}}. \tag{20}$$

For wave packets with an upward-directed vertical component of group velocity there are energy losses and the energy fluxes are positive; however, if the vertical component of group velocity is directed downward, the energy density does not decrease and the energy losses of the WP are nil.

For determining the fluxes of kinetic energy of internal waves to turbulence we average (19) for the totality of wave packets

$$J = \int_{m_{min}}^{m_{max}} \int_{0}^{k_{h\,max}} \frac{16N^2 \frac{\partial N}{\partial z} k_h^3 2\pi}{m^3 \sqrt{k_h^2 + m^2}} dk_h\, dm = BN^2 \frac{\partial N}{\partial z}. \tag{21}$$

The B constant is experimentally determined.

Figure 2 shows the dependence (17) of energy density on the Väisälä-Brunt frequency. The A constant was assumed equal to $2 \cdot 1$ m^2 (cycles/hour)^2.

If in the region of the seasonal thermocline there is a current with a vertical velocity shear, after allowance for current velocity shears under conditions of hydrodynamic stability (4) the expression for the density of potential energy is transformed to the form

$$E = A \cdot N^{-4}\left(N^2 - U_z^2/4\right). \tag{22}$$

Accordingly, in a current with a vertical velocity shear the energy density of internal waves also decreases.

Figure 3 shows the dependence of the fluxes of kinetic energy to turbulence on the Väisälä-Brunt frequency (theoretical curve). The Väisälä-Brunt frequency gradient $\partial N/\partial z$ was assumed to be constant with depth, equal to 0.4 cycle/hour·m; the

constant B = $3.9 \cdot 10^{-4} m^4 \cdot hour^3$.

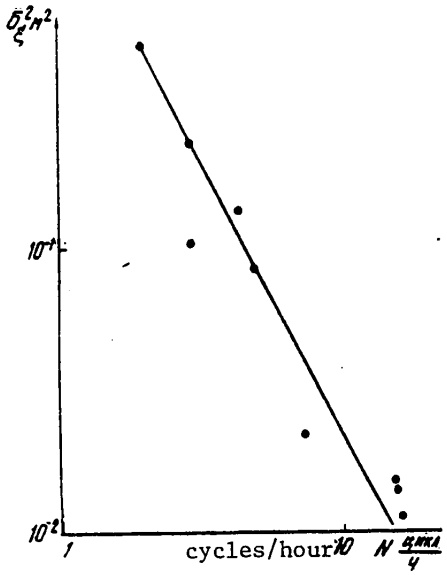

Fig. 2.

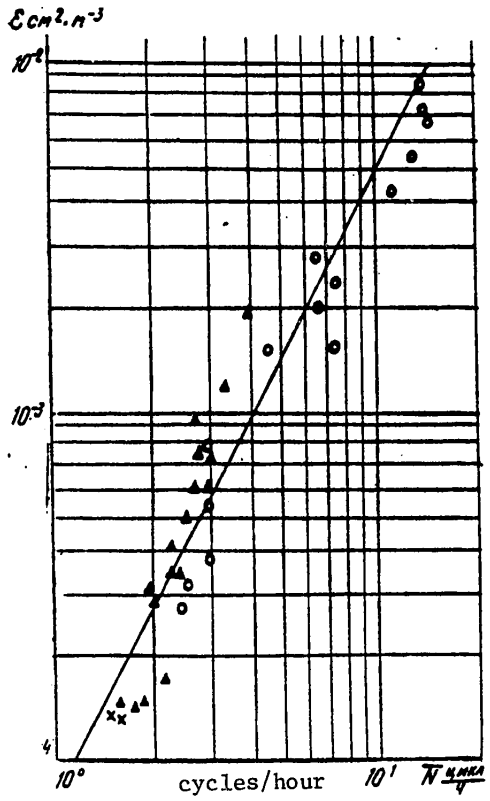

Fig. 3.

However, if $\partial N / \partial z$ increases with an increase in the Väisälä-Brunt frequency, the theoretical curve in the case of large Väisälä-Brunt frequencies exceeds the experimental data. The presence of currents with a vertical velocity shear will change the energy influx to turbulence, in particular, with $\partial^2 U / \partial z^2 < 0$ the rate of influx of kinetic energy will be less than was determined in accordance with (21).

Thus, the derived dependences of the rate of influx of kinetic energy on the conditions of density stratification are confirmed by the cited experimental data.

BIBLIOGRAPHY

1. Dykman, V. Z., Yefremov, O. I. and Kiseleva, O. A., "Investigations of the Fine Vertical Structure of the Temperature Field in Eddy Formations of a Synoptic Scale," in press.

2. Dykman, V. Z. and Kiseleva, O. A., "Interrelationship of the Fine Structure of Internal Waves and Small-Scale Turbulence," in press.

3. Ozmidov, R. V., GORIZONTAL'NAYA TURBULENTNOST' I TURBULENTNYY OBMEN B OKEANE (Horizontal Turbulence and Turbulent Exchange in the Ocean), Moscow, "Nauka," 1968, 105 pages.

4. Korotayev, G. K., "Spectral Energy Density of Wave Packets," MORSKIYE GIDROFIZICHESKIYE ISSLEDOVANIYA (Marine Hydrophysical Investigations), No 2, Sevastopol', pp 41-47, 1977.

5. Phillips, G., DINAMIKA VERKHNEGO SLOYA OKEANA (Dynamics of the Upper Layer of the Ocean), Moscow, "Mir," 1969, 139 pages.

6. Garrett, C. J. R. and Munk, W. H., "Space Time Scales of Internal Waves," JGR, Vol 80, No 3, pp 291-297, 1975.

7. Hayes, S. P., Joyce, T. M. and Millard, R. C., "Measurement of Vertical Fine Structure in the Sargasso Sea," JGR, Vol 80, No 3, pp 314-319, 1975.

8. Brethertone, F. P. and Garrett, C. J. R., "Wavetrains in Homogeneous Moving Media," PROC. ROY. SOC., Ser A, 302, No 1471, pp 529-554, 1968.

EFFECT OF SURFACE FILM ON NATURAL OSCILLATIONS OF FREE BOUNDARY OF FLUID

Sevastopol' TEORETICHESKIYE I EKSPERIMENTAL'NYYE ISSLEDOVANIYA POVERKHNOSTNYKH I VNUTRENNIKH VOLN in Russian 1980 (manuscript received 19 Jun 80) pp 175-181

[Article by T. M. Pogorelova]

[Text]

Abstract: The effect of a film on the attenuation of surface waves is investigated. The dispersion law was formulated: a precise solution of the frequency equation is found. For any values of the parameters of the problem simple asymptotic representations are obtained for the dimensionless complex frequency s as a function of the wave number ξ (and wave lengths L). The dependence of the period of oscillations and the logarithmic decrement of attenuation on wave length is found.

In many practical problems in geophysics it is desirable to investigate the influence of a surface film on the wave movement of a fluid. The studies of V. G. Levich were devoted to this problem [2]. He examined the problem of the natural oscillations of a fluid with a surface-active film taken into account. He found approximate solutions of the frequency equation under definite conditions superposed on the parameters of the problem.

In addition, studies [1, 3, 4] were devoted to the problem of the natural oscillations of the free boundary of a fluid without a film. In [1] the analytical dependence between the frequency of the free oscillations and the wave length was investigated numerically by the Graffe method for a number of values of parameters of the problem. An analytical dependence of the complex frequency on wave number was found by E. N. Potetyunko in [4].

In this article we give an analysis of influence of the film on the logarithmic decrement of attenuation and the wave period for the problem of the natural oscillations of a semi-infinite fluid covered with a film. The influence of the film is "conveyed" into the boundary condition of the problem.

1. Formulation of problem. We will examine free oscillations, periodic along the Ox-axis, for an infinitely deep two-layer viscous fluid occupying the lower half-space,

$$\begin{cases} \dfrac{\partial \bar{V}_1}{\partial t} = -\dfrac{1}{\rho_1}\nabla p_1 + \nu_1 \Delta \bar{V}_1 + g\bar{k}, \quad \operatorname{div} \bar{V}_1 = 0, \quad p_1 = p_1 + \rho_1 g(h-z), \\ \dfrac{\partial \bar{V}_2}{\partial t} = -\dfrac{1}{\rho_2}\nabla p_2 + \nu_2 \Delta \bar{V}_2 + g\bar{k}, \quad \operatorname{div} \bar{V}_1 = 0, \quad p_2 = p_2 - \rho_2 gz + \rho_1 gh; \end{cases} \tag{1.1}$$

with z = 0

$$\begin{cases} -p_2 + \rho_2 g\zeta_2 + 2\mu_2 \dfrac{\partial V_{2z}}{\partial z} - \alpha_2 \dfrac{\partial^2 \zeta_2}{\partial x^2} = -p_1 + \rho_1 g\zeta_2 + 2\mu_1 \dfrac{\partial V_{1z}}{\partial z}, \\ \mu_2\left(\dfrac{\partial V_{2z}}{\partial x} + \dfrac{\partial V_{2x}}{\partial z}\right) = \mu_1\left(\dfrac{\partial V_{1z}}{\partial x} + \dfrac{\partial V_{1x}}{\partial z}\right), \\ V_{1z} = V_{2z}, \quad V_{1x} = V_{2x}, \quad \partial\zeta_2/\partial t = V_{2z}, \end{cases} \tag{1.2}$$

$$\frac{\partial V_{1x}}{\partial z} + \frac{\partial V_{1z}}{\partial x} = 0, \quad \frac{\partial \zeta_1}{\partial t} = V_{1z}, \quad z = h; \quad z \to -\infty, \ \bar{V}_2 = 0, \ p_2 = 0;$$

$$-p_1 + \rho_1 g\zeta_1 - \rho_1 hg + 2\mu_1 \frac{\partial V_{1z}}{\partial z} - \alpha_1 \frac{\partial^2 \zeta_1}{\partial x^2} = 0, \qquad z = h. \tag{1.3}$$

Here α_1, α_2 are the coefficients of surface tension at the upper and lower discontinuities respectively; ρ_1, ρ_2 are the densities of the upper and lower fluid; ν_1, ν_2 are the coefficients of the kinematic viscosities of the upper and lower fluids; ζ_1, ζ_2 are the disturbances of the free surface and discontinuity. The origin of coordinates is taken on the undisturbed discontinuity of the fluids, the Oz-axis is directed vertically upward; h is the thickness of the upper layer ($h \to 0$).

2. In place of precise satisfaction of the equations of motion of the upper layer from (1.1) we require their satisfaction in an integral sense: we will integrate the equations of motion of the upper layer in the thickness h with the boundary conditions (1.2) and (1.3).

As a result, the initial problem is reduced to the following boundary-value problem:

$$\begin{cases} \dfrac{\partial V_{2x}}{\partial t} = -\dfrac{1}{\rho_2}\dfrac{\partial p_2}{\partial x} + \nu_2\left(\dfrac{\partial^2 V_{2x}}{\partial x^2} + \dfrac{\partial^2 V_{2x}}{\partial z^2}\right), \\ \dfrac{\partial V_{2z}}{\partial t} = -\dfrac{1}{\rho_2}\dfrac{\partial p_2}{\partial z} + \nu_2\left(\dfrac{\partial^2 V_{2z}}{\partial x^2} + \dfrac{\partial^2 V_{2z}}{\partial z^2}\right), \quad \dfrac{\partial V_{2x}}{\partial x} + \dfrac{\partial V_{2z}}{\partial z} = 0; \end{cases} \tag{2.1}$$

the boundary conditions with z = 0 are

$$-p_2 + \rho_2 g\zeta_2 + 2\mu_2 \frac{\partial V_{2z}}{\partial z} - \alpha_2 \frac{\partial^2 \zeta_2}{\partial x^2} = 0, \qquad \frac{\partial V_{2z}}{\partial x} + \frac{\partial V_{2x}}{\partial z} = 0,$$

$$\partial\zeta_2/\partial t = V_{2z}; \quad z \to -\infty, \quad p_2, \bar{V}_2 \to 0. \tag{2.2}$$

Here $\alpha_0 = \alpha_1 = \alpha_2$.

3. We will seek solution of system (2.1) in the form

$$V_{2x} = F_1(z)e^{i\xi x}e^{\sigma t}, \quad V_{2z} = F_2(z)e^{i\xi x}e^{\sigma t}, \quad \rho_2 = F_3(z)e^{i\xi x}e^{\sigma t}, \tag{3.1}$$

where σ is the frequency of the natural oscillations; ξ is the wave number ($\xi = 2\pi/L$; L is the wave length).

Substituting the solution (3.1) into system (2.1), we find

$$\begin{aligned} V_{2x} &= i\left(\frac{\delta c_2}{\xi}e^{\delta z} - \frac{c_1\xi}{\rho_2\sigma}e^{\xi z}\right)e^{i\xi x}\cdot e^{\sigma t}, \\ V_{2z} &= \left(c_2 e^{\delta z} - \frac{\xi c_1}{\rho_2\sigma}e^{\xi z}\right)e^{i\xi x}\cdot e^{\sigma t}, \qquad \rho_2 = c_1 e^{\xi z}\cdot e^{i\xi x}\cdot e^{\sigma t}. \end{aligned} \tag{3.2}$$

Here $\delta = \sqrt{\xi^2 + \sigma/\nu_2}$; $\mathrm{Re}\,\delta > 0$. Satisfying the boundary conditions (2.2), we obtain the following system relating the unknown constants c_1 and c_2:

$$\begin{cases} -c_1\frac{1}{\sigma}\left[\sigma^2 + g\xi + 2\nu_2\sigma\xi^2 + \beta_0\xi^3\right] + c_2\rho_2\left[g + 2\nu_2\sigma\delta + \beta_0\xi^2\right] = 0, \\ -2c_1\xi^3 + \rho_2\sigma c_2\left[2\xi^2 + \sigma/\nu_2\right] = 0. \end{cases} \tag{3.3}$$

Excluding (3.3) in system c_1 and c_2, we obtain the frequency equation

$$-\sigma^2 - \beta_0\xi^3 - \xi g + 4\nu_2^2\xi^3\sqrt{\xi^2 + \sigma/\nu_2} - 4\xi^4\nu_2^2 - 4\xi^2\nu_2\sigma = 0. \tag{3.4}$$

Solving this equation we find the dependence of σ on the wave number ξ.

We will carry out a replacement of the variables in (3.4)

$$\sigma = s\xi^2\nu_2, \tag{3.5}$$

where s is dimensionless frequency. Then equation (3.4) assumes the form

$$(\delta^2+1)^2 - 4\delta + 1/\lambda = 0. \tag{3.6}$$

Here

$$\frac{1}{\lambda} = \frac{\beta_0\xi^2 + g}{\xi^3\nu_2^2}, \qquad \delta = \sqrt{1+s}, \qquad \beta_0 = \frac{\alpha_1 + \alpha_2}{\rho_2}. \tag{3.7}$$

4. The roots of the dispersion equation (3.6) are algebraic functions of the parameter λ and are represented in the broadened plane "δ" as a four-valued function of λ [4, 5]

$$\delta(\lambda) = \sum_{k=\mu}^{\infty} A_k(\lambda - \lambda_0)^{k/r}, \quad \lambda_0 \neq \infty, \quad \delta(\lambda) = \sum_{k=\mu}^{\infty} A_k/\lambda^k, \quad \lambda_0 = \infty. \tag{4.1}$$

Substituting (4.1) into (3.6), we obtain the following representation for the complex frequency s:

$$0 \leq \lambda < \lambda_*, \quad s = \sum_{n=0}^{\infty} c_n \lambda^{\frac{1}{4}(n-2)} - 1, \tag{4.2}$$

$$c_n = \frac{1}{c_0}\left[2a_{n-3} - c_{n-2} - \frac{1}{2}\sum_{k=2}^{n-2} c_k c_{n-k}\right], \quad n \geq 5,$$

$$c_0 = a_0^2, \quad c_1 = 0, \quad c_2 = -1, \quad c_3 = 2/a_0, \quad c_4 = 0,$$

$$a_n = \frac{1}{2a_0}\left[c_n - \sum_{k=2}^{n-2} a_k a_{n-k}\right], \quad n \geq 5,$$

$$a_0 = \sqrt{2}(1 \pm i)/2, \quad a_1 = 0, \quad a_2 = -1/2a_0, \quad a_3 = 1/a_0^2, \quad a_4 = -1/8a_0^3; \tag{4.3}$$

$$\lambda_* - \delta' < \lambda < \lambda_* + \delta', \quad s = \sum_{n=0}^{\infty} c_n \varepsilon^n - 1,$$

$$\varepsilon_{1,2} = \pm\sqrt{\frac{1}{\lambda_*} - \frac{1}{\lambda}}, \quad c_n = \frac{B_1 a_n}{2} + \sum_{k=1}^{n-1} a_k a_{n-k}, \quad n \geq 2,$$

$$c_0 = b_*^2, \quad c_1 = B_1/2B, \quad B = 6b_*^2 + 2, \quad B_1 = 4b_*,$$

$$a_n = -\frac{1}{2Ba_1}\left[B\sum_{k=2}^{n-1} a_k a_{n-k+1} + B_1\sum_{k=1}^{n-1} d_k a_{n-k} + \sum_{k=1}^{n-2} d_k d_{n-k-1}\right], \quad n \geq 3,$$

$$a_1 = \frac{1}{\sqrt{B}}, \quad a_2 = -\frac{B_1}{2B^2}, \quad d_k = \sum_{m=1}^{k} a_m a_{k-m+1}, \quad k \geq 1;$$

(4.4)

$$\lambda > \lambda_*, \quad s = \sum_{n=0}^{\infty} \frac{c_n}{\lambda^n} - 1,$$

$$c_n = \sum_{k=0}^{n} a_k a_{n-k}, \quad n \geq 1, \quad c_0 = a_0^2, \quad a_0 = 1,$$

and the second value a_0 satisfies the equation

$$a_0^3 + a_0^2 + 3a_0 - 1 = 0,$$

$$a_n = -\frac{1}{4A}\left[2A_1\sum_{k=1}^{n-1} a_k a_{n-k} + \sum_{k=1}^{n-1} c_k c_{n-k}\right], \quad n \geq 2,$$

$$a_1 = -1/4A, \quad A_1 = a_0^2 + 1, \quad A = a_0^3 + a_0 + 1;$$

$$\lambda_* = \frac{1}{4b_* - (b_*^2+1)^2},$$

B_* is a positive root of the equation

$$b_*^3 + b_* - 1 = 0.$$

5. Limiting ourselves to the first terms in formulas (4.2)-(4.4), we have the following simple representations for the complex frequency s:

$$0 \leq \lambda < \lambda_*, \quad \mathrm{Re}\, s_{1,2} \simeq \sqrt{2}\lambda^{1/4} - 2, \quad \mathrm{Im}\, s_{1,2} \simeq \pm\left(\lambda^{-1/2} - \sqrt{2}\lambda^{1/4}\right); \tag{5.1}$$

$$\lambda = \lambda_*, \quad s_1 = s_2 \simeq b_*^2 - 1 \quad \text{(double root)}; \tag{5.2}$$

$$\lambda > \lambda_*, \quad s_{1,2} \simeq a_0^2 - 1 - \frac{a_0}{2(a_0^3 + a_0 + 1)} \cdot \frac{1}{\lambda}. \tag{5.3}$$

Here

$$a_{01} = 1; \quad a_{02} = 0{,}286598; \quad b_* = 0{,}682328; \quad \lambda_* = 1{,}719841. \tag{5.4}$$

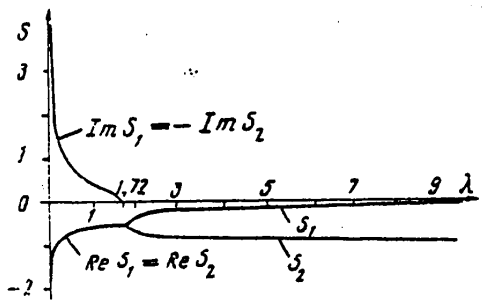

Fig. 1.

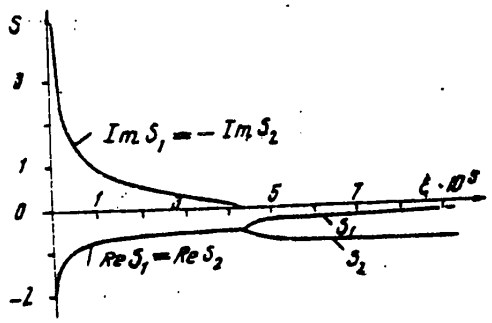

Fig. 2.

Figure 1 shows the dependence Re $S_{1,2}$ and Im $S_{1,2}$ on the parameter λ. For $\lambda < \lambda_*$ s is a complex parameter which corresponds to the presence of periodic attenuating oscillations. If $\lambda = \lambda_*$, then $s_1 = s_2$ (double root point) corresponds to an aperiodic solution; when $\lambda > \lambda_*$ there are two real branches of the roots s_1 and s_2, which corresponds to the presence of aperiodic movements.

If we return to the wave number ξ, we see that the critical value of the dimensionless parameter λ_* corresponds to ξ_*, being a positive root of the equation

$$\frac{1}{\lambda_*} = \frac{\xi^2 p_2 + 1}{\xi^3 p_1}, \quad p_1 = \frac{\nu_2^2}{g}, \quad p_2 = \frac{\alpha_1 + \alpha_2}{\rho_2 g}, \tag{5.5}$$

$$(\xi_* = 4{,}299853 \cdot 10^6), \quad p_1 = 4 \cdot 10^{-7}, \quad p_2 = 0{,}1.$$

Figure 2 shows the dependence of Re $S_{1,2}$ and Im $S_{1,2}$ on the wave number ξ. With $0 < \xi < \xi_*$ s is a complex value: $\xi = \xi_*$, $S_1 = S_2$ is a double real root; with $\xi > \xi_*$ there are two real branches of the roots S_1 and S_2.

6. Next we construct the dependence of Re and Im of the frequency s on the wave length $L = 2\pi/\xi$.

$$0 < L < L_*. \quad s_{1,2} \simeq a_0^2 - 1 - \frac{a_0}{2(a_0^3+a_0+1)} \cdot \frac{L(L^2+4\pi^2 p_2)}{8\pi^3 p_1}; \tag{6.1}$$

$$L = L_*, \quad s_1 = s_2 \simeq b_*^2 - 1; \tag{6.2}$$

$$L > L_*. \quad Re\, s_{1,2} \simeq \sqrt{2}\left[\frac{8\pi^3 p_1}{L(L^2+4\pi^2 p_2)}\right]^{1/4} - 2,$$

$$Im\, s_{1,2} \simeq \pm\left\{\left[\frac{8\pi^3 p_1}{L(L^2+4\pi^2 p_2)}\right]^{-1/2} - \sqrt{2}\left[\frac{8\pi^3 p_1}{L(L^2+4\pi^2 p_2)}\right]^{1/4}\right\} \tag{6.3}$$

Here L_* is a positive root of the equation $-\lambda_* L^3 - 4\pi^2 p_2 \lambda_* L + 8\pi^3 p_1 = 0$.

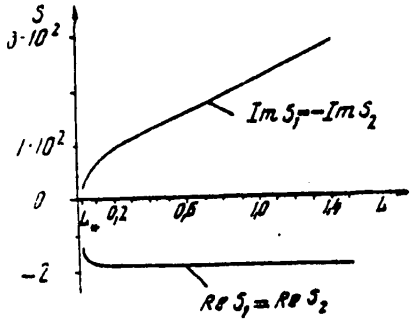

Fig. 3

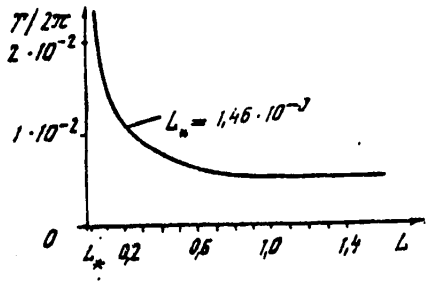

Fig. 4

Figure 3 shows the dependence of the complex frequency s (Re $S_{1,2}$, Im $S_{1,2}$) on the wave length; Figure 4 shows the dependence of the period of oscillations on wave length. When $L > L_*$

$$T \simeq 2\pi \frac{[64\pi^6 p_1^2 L(L^2+4\pi^2 p_2)]^{1/4}}{L^{3/4}(L^2+4\pi^2 p_2)^{3/4} - [4(8\pi^3 p_1)^3]^{1/4}}.$$

Comparing the results with the results for free oscillations of a fluid without a film we find that the film increases the logarithmic decrement of attenuation of a wave and increases the period of oscillations. The critical length of a wave, less than which the movement has an aperiodic character, increases.

BIBLIOGRAPHY

1. Sretenskiy, L. N., "Waves at the Surface of A Viscous Fluid," TRUDY TsAGI (Transactions of the Aerohydrodynamic Institute), No 541, Moscow, pp 1-34, 1941.

2. Levich, V. G., FIZIKO-KHIMICHESKAYA GIDRODINAMIKA (Physicochemical Hydrodynamics), Moscow, Fizmatgiz, 1959, 699 pages.

3. Oborotov, I. P., "Gravitational Waves at the Surface of a Viscous Fluid of Finite Depth," OKEANOLOGIYA (Oceanology), Vol 3, No 4, pp 610-625, 1963.

4. Potetyunko, E. N., "Natural Oscillations of a Viscous Fluid of Infinite Depth," MATEMATICHESKIY ANALIZ I YEGO PRILOZHENIYA (Mathematical Analysis and Its Applications), Vol 6, Rostov, RGU, 1974, 85 pages.

5. Markushevich, A. I., TEORIYA ANALITICHESKIKH FUNKTSIY (Theory of Analytical Functions), Volumes 1, 2, Second Edition, Moscow, "Nauka," 1967, 1968, 486 pages, 624 pages.

EFFECT OF VISCOSITY ON DISSIPATION OF INTERNAL WAVES

Sevastopol' TEORETICHESKIYE I EKSPERIMENTAL'NYYE ISSLEDOVANIYA POVERKHNOSTNYKH I VNUTRENNIKH VOLN in Russian 1980 (manuscript received 23 Mar 80) pp 182-188

[Article by N. P. Levkov]

[Text]

Abstract: In the first approximation a study was made of the influence of horizontal and vertical exchange of momentum on the dissipation of internal waves in a stratified ocean with a real density distribution. It has been established that in the region of the short-wave spectrum of frequencies the first approximation is inadequate; in the case of long waves there is a similarity with the law of dissipation of surface waves and it can be assumed that the first approximation to all intents and purposes is a precise solution of the problem.

In [4] The author presented a theoretical investigation of the influence of horizontal and verical exchange of momentum on the dissipation of surface and internal waves in a stratified ocean. It was assumed that the solution of the "ideal" problem is known. But in [4] it was impossible to find even one fundamental solution W_{10} of equation (6) in a general case. Two methods are now known for overcoming this difficulty.

First, having an analytical expression for the density value, it is possible to find approximate solutions of this equation outside the turning points and in their neighborhood; then asymptotic splicing of these solutions is carried out [7]. Proceeding along these lines, it is necessary to approximate the density measurement data by the function $\rho(z)$ and then find an approximate solution of the problem.

On the other hand [3,6], the ocean can be regarded as N layers of fluid $[0, H] = [0, H_1) + (H_1, H_2] + \ldots + [H_{N-1}, H_N]$. The density measurement data for the entire depth of the real ocean can be approximated by some continuous function for which in each of N sectors it is easy to obtain one precise sought-for solution W_j (for example, for $\rho_j = \rho_{j0} \exp k_j z$). Satisfying the boundary conditions for attachment at the bottom, the equality of the velocity and stress components at the discontinuities and the absence of stresses at the free surface, we obtain a solution of the formulated problem.

The movement of a fluid in each of N layers is described [4] by the system of equations

$$A_z\varphi'' + A_z\frac{\rho'}{\rho}\varphi' + \left(i\sigma - r^2 A_L\right)\varphi - \frac{i}{\sigma r^2}W' = 0,$$

$$A_z W^{IV} + 2A_z\frac{\rho'}{\rho}W''' + \left(i\sigma - r^2A_L - r^2A_z + A_z\frac{\rho''}{\rho}\right)W'' + \left(i\sigma - 2r^2A_L\right)\frac{\rho'}{\rho}W' + \tag{1}$$

$$+r^2\left(-i\sigma + r^2A_L + A_L\frac{\rho''}{\rho} - i\frac{g}{\sigma}\frac{\rho'}{\rho}\right)W - 4\omega^2 i\sigma r^2\left(\varphi' + \frac{\rho'}{\rho}\varphi\right) = 0,$$

the boundary conditions have the form

$$W = W' = \varphi = 0 \quad \text{when } z = 0;$$

$$W_j = W_{j+1}, \quad W_j' = W_{j+1}', \quad \varphi_j = \varphi_{j+1},$$

$$A_z i m W_j'' - 2\omega A_z\sigma n r^2\varphi_j' + A_L i m r^2 W_j =$$

$$= A_z i m W_{j+1}'' - 2\omega A_z\sigma n r^2\varphi_{j+1}' + A_L i m r^2 W_{j+1},$$

$$A_z i n W_j'' + 2\omega\sigma A_z m r^2\varphi_j' + A_L i n r^2 W_j = \tag{2}$$

$$= A_z i n W_{j+1}'' + 2\omega\sigma A_z m r^2\varphi_{j+1}' + A_L i n r^2 W_{j+1},$$

$$A_z\left(W_j''' + \frac{\rho'}{\rho}W_j''\right) - \left(-i\sigma + 2A_z r^2 + r^2A_L\right)W_j' + r^2A_L\frac{\rho'}{\rho}W_j - 4\omega^2\sigma i r^2\varphi_j =$$

$$= A_z\left(W_{j+1}''' + \frac{\rho'}{\rho}W_{j+1}''\right) - \left(-i\sigma + 2A_z r^2 + r^2A_L\right)W_{j+1}' + r^2A_L\frac{\rho'}{\rho}W_{j+1} -$$

$$-4\omega^2 i\sigma r^2\varphi_{j+1} \quad \text{when} \quad z = H_j \quad (j = 1\div N-1);$$

$$A_z i m W'' - 2\omega A_z\sigma n r^2\varphi' + A_L i m r^2 W = A_z i n W'' + 2\omega A_z\sigma m r^2\varphi' + A_L i n r^2 W = 0,$$

$$-i\sigma A_z\left(W''' + \frac{\rho'}{\rho}W''\right) + \left(\sigma^2 + 2i\sigma A_z r^2 + i\sigma r^2A_L\right)W' - \left(gr^2 + i\sigma r^2A_L\frac{\rho'}{\rho}\right)W -$$

$$-4\omega^2\sigma^2 r^2\varphi = 0 \quad \text{when} \quad z = H_N = H.$$

The general solution of the equations of motion in each case represents the totality of (7) and (11) [4]. We will limit ourselves to the first approximation. Satisfying the boundary conditions, we obtain the determinant Δ_1 of the order of 6N. Making some identical transforms with its rows and expanding into a series in powers of ε_1 and ε_2, we reduce the finding of r_0, r_1 and r_2 to computation of the Jacobian determinant Δ of the order 2N.

$$\Delta - \frac{(\sigma^2-4\omega^2)^N r_0^2 A_1}{2\rho_1\rho_2\cdots\rho_N}\left(\frac{1}{\alpha_1^2 ch\beta_1 H}+\frac{1}{\alpha_2^2 ch\beta_2 H}\right)=0. \qquad (3)$$

Here the notations in [4] have been retained.

$$J_j = J_{j0} + J_{j1}, \quad J_{10} = a_{11}^0, \quad J_{11} = a_{11}^1, \quad J_{20} = J_{10}\cdot a_{22}^0,$$

$$J_{21} = J_{11} a_{22}^0 + J_{10} a_{22}^1 - a_{21}^0 a_{12}^1, \quad J_{j0} = J_{j-1,0} a_{jj}^0 - J_{j-2,0} a_{j-1,j}^0 a_{j,j-1}^0,$$

$$J_{j1} = J_{j-1,0} a_{jj}^1 + J_{j-1,1} a_{jj}^0 - J_{j-2,0} a_{j-1,j}^1 a_{j,j-1}^0 - J_{j-2,0} a_{j-1,j}^0 a_{j,j-1}^1 -$$

$$- J_{j-2,1} a_{j-1,j}^0 a_{j,j-1}^0, \qquad a_{kj} = a_{kj}^0 + a_{kj}^1;$$

$$a_{11}^1 = \frac{i\sqrt{A_2}}{2\sigma} W_{10}'\left(\frac{\alpha_2^2}{\alpha_1} th\beta_1 H + \frac{\alpha_1^2}{\alpha_2} th\beta_2 H\right),$$

$$a_{11}^0 = W_{10}, \qquad a_{12}^1 = \frac{a_{11}^1}{\rho W_{10} W_{10}'} \cdot \text{ when } z = 0;$$

$$a_{2j,2j-1}^0 = W_{j0}, \quad a_{2j,2j-1}^1 = -\frac{i\sigma r^2 A_1}{\sigma^2-4\omega^2} W_{j0} + W_{j1} c_1 + W_{j2} c_2,$$

$$a_{2j,2j}^0 = W_{j0}\int \frac{dz}{\rho W_{j0}^2}, \quad a_{2j,2j}^1 = -\frac{i\sigma r^2 A_1}{\sigma^2-4\omega^2} a_{2j,2j}^0 + \bar{W}_{j1} c_1 + \bar{W}_{j2} c_2,$$

$$a_{2j,2j+1}^1 = \frac{i\sigma r^2 A_1}{\sigma^2-4\omega^2} W_{j+1,0}, \quad a_{2j+1,2j}^0 = \frac{\sigma^2-4\omega^2}{\rho W_{j,0}},$$

$$a_{2j+1,2j}^1 = \frac{i r^2 A_1}{\sigma\rho W_{j0}}\left(\sigma^2+4\omega^2\right) + \left(\sigma^2-4\omega^2\right)\left[\left(\bar{W}_{j1}' - \frac{W_{j0}'}{W_{j0}}\bar{W}_{j1} - W_{j1}'\int\frac{dz}{\rho W_{j0}^2} + \right.\right.$$

$$\left.\left. + \frac{W_{j0}'}{W_{j0}} W_{j1}\int\frac{dz}{\rho W_{j0}^2}\right) c_1 + \left(\bar{W}_{j2}' - \frac{W_{j0}'}{W_{j0}}\bar{W}_{j2} - W_{j2}'\int\frac{dz}{\rho W_{j0}^2} + \frac{W_{j0}'}{W_{j0}} W_{j2}\int\frac{dz}{\rho W_{j0}^2}\right) c_2\right],$$

$$a_{2j+1,2j+1}^0 = \left(\sigma^2-4\omega^2\right)\left(\frac{W_{j0}'}{W_{j0}} W_{j+1,0} - W_{j+1,0}'\right),$$

$$a_{2j+1,2j+1}^1 = ir^2 A_1 \frac{\sigma^2+4\omega^2}{\sigma(\sigma^2-4\omega^2)} a_{2j+1,2j+1}^0 - \left(\sigma^2-4\omega^2\right)\frac{W_{j+1,0}}{W_{j0}}\left[\left(\frac{W_{j0}'}{W_{j0}} W_{j1} - \right.\right.$$

$$\left.\left. - W_{j1}'\right) c_1 + \left(\frac{W_{j0}'}{W_{j0}} W_{j2} - W_{j2}'\right) c_2\right], \quad a_{2j+1,2j+2}^0 = -\frac{\sigma^2-4\omega^2}{\rho W_{j+1,0}},$$

$$a^1_{2j+1,2j+2} = -\frac{ir^2 A_L\left(\sigma^2+4\omega^2\right)}{\sigma\rho\, W_{j+1,0}} \qquad \text{when} \quad z = H_j \quad \left(j=1\div N-1\right);$$

$$a^0_{2N,2N-1} = \left(\sigma^2-4\omega^2\right) W'_{N0} - gr^2 W_{N0}, \; a^1_{2N,2N-1} = \frac{ir^2 A_L}{\sigma}\left(\sigma^2+4\omega^2\right) W'_{N0} +$$

$$+\left(\sigma^2-4\omega^2\right)\left(W'_{N1}\varepsilon_1 + W'_{N2}\varepsilon_2\right) - i\sigma r^2 A_L \frac{\rho'}{\rho} W_{N0} - g W_{N0} \times$$

$$\times\left(2rr_1\varepsilon_1 + 2rr_2\varepsilon_2 - \frac{i\sigma r^4 A_L}{\sigma^2-4\omega^2}\right) - gr^2\left(W_{N1}\varepsilon_1 + W_{N2}\varepsilon_2\right),$$

$$a^0_{2N,2N} = \left(\sigma^2-4\omega^2\right)\left(W'_{N0}\int\frac{dz}{\rho W^2_{N0}} + \frac{1}{\rho W_{N0}}\right) - gr^2 W_{N0}\int\frac{dz}{\rho W^2_{N0}},$$

$$a^1_{2N,2N} = \frac{ir^2 A_L}{\sigma}\left(\sigma^2+4\omega^2\right)\left(W'_{N0}\int\frac{dz}{\rho W^2_{N0}} + \frac{1}{\rho W_{N0}}\right) +$$

$$+\left(\sigma^2-4\omega^2\right)\left(\bar{W}'_{N1}\varepsilon_1 + \bar{W}'_{N2}\varepsilon_2\right) - i\sigma r^2 A_L \frac{\rho'}{\rho} W_{N0}\int\frac{dz}{\rho W^2_{N0}} - g W_{N0}\left(2rr_1\varepsilon_1 +\right.$$

$$\left.+2rr_2\varepsilon_2 - \frac{i\sigma r^4 A_L}{\sigma^2-4\omega^2}\right)\int\frac{dz}{\rho W^2_{N0}} - gr^2\left(\bar{W}_{N1}\varepsilon_1 + \bar{W}_{N2}\varepsilon_2\right) \quad \text{when } z = H.$$

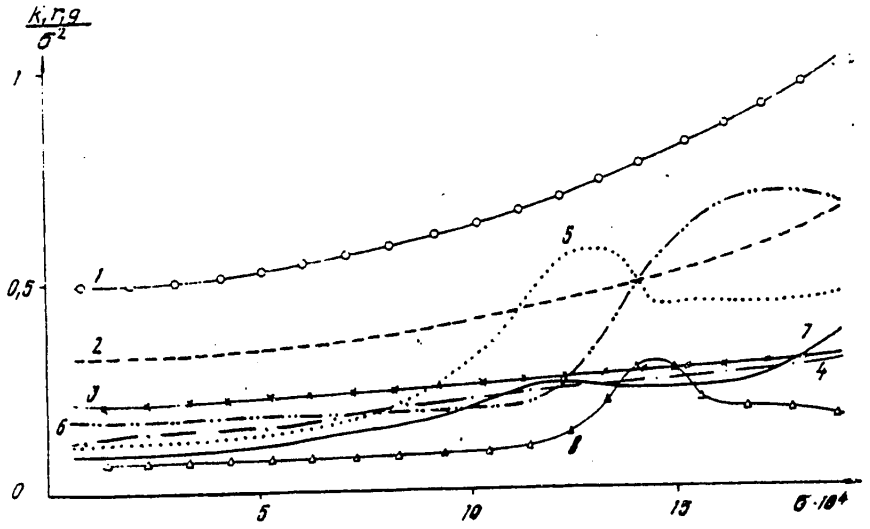

Fig. 1. Change in decrement of attenuation due to horizontal exchange.

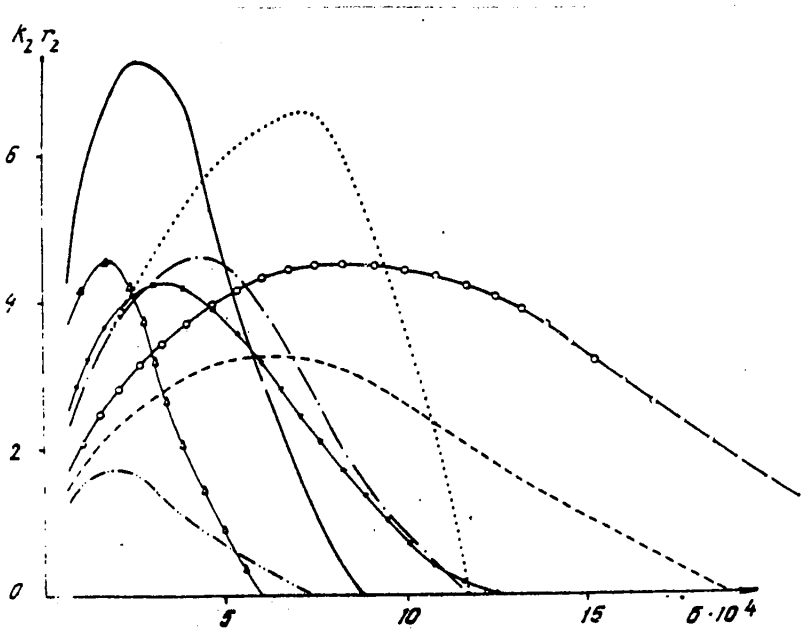

Fig. 2. Change in decrement of attenuation due to vertical exchange.

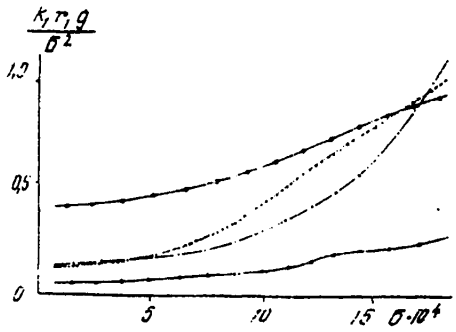

Fig. 3.

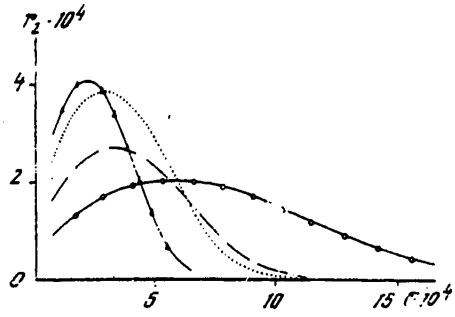

Fig. 4.

Here W_{j0} is one of the solutions of equation (6) [4]; W_{jk} are the viscous additives to this solution; W_{jk} are the viscous additives to another solution of equation (6) in the j-th layer; a_{kj} are elements of the determinant Δ not equal to zero; the prime denotes the derivative of z. The integration constants are selected in such a way that with $z = H_{j-1}$ the integrals are equal to zero. Then $\Delta = J_{2N}$. Substituting this value into equation (3), we obtain an equation for determining the wave number (or numbers) r_0 and the components r_1 and r_2 of the decrement of attenuation γ.

It is known [5] that under the conditions $\sigma > 2\omega$, $\sigma^2 + g\,\rho'/\rho > 0$ for the entire depth in the entire fluid one surface wave arises which does not attenuate with distance, and with

$$\min\left(\sigma^2 + g\frac{\rho'}{\rho}\right) < 0,$$

in addition to the surface wave, another set of nonattenuating internal waves develops. In the presence of vertical and horizontal exchange of momentum, all the waves attenuate with distance.

For the purpose of finding the value of the decrement of attenuation γ we made computations using density measurement data [1] (Fig. 1,2) and [2] (Figures 3, 4). The figures denote the numbers of the internal modes to which the curves correspond; the fictitious parts of r_1 and r_2 are represented in m^{-1}. In this case

$$k_1 = 10^{-6} \cdot \frac{(j-3)^2 + 2}{4j}$$

(j is the number of the mode) $k_2 = 5 \cdot 10^3$ for curve 4 and $k_2 = 10^4$ in all the remaining cases.

An analysis of the computations shows that for clarifying the influence of vertical exchange A_z on the dissipation of internal waves a first approximation of the expansion in ε_2 is inadequate since in the short-wave region it tends to 0. The j-th mode attains its maximum with a wavelength $\lambda_j \sim BH/\sqrt{j}$. For longer waves the r_2 value changes proportionally to $(1 + i)\sqrt{\sigma}$. Depending on the stratification, different modes attenuate with distance differently. Cases are possible when the lower modes (the waves are longer) attenuate more rapidly than the higher modes. It can only be assumed, by analogy with surface waves [4], that with $\lambda_j/H > 10$ r_2 will be virtually the precise value of the decrement of attenuation γ, caused by the presence of exchange A_2.

What is the influence of horizontal exchange A_L on the dissipation of internal waves and is a first approximation adequate for clarifying the qualitative and quantitative aspects of this influence? With an increase in frequency, regardless of the mode number, in the case of long waves the r_1 value increases as σ^2 and is equal approximately to

$$r_1 = i \frac{r_0^3 H \sqrt{gH} (\sigma^2 + 4\omega^2)}{2\sigma(\sigma^2 - 4\omega^2)},$$

in the case of short waves the order of the increase increases and r_1 has an oscillatory character. In all probability, as in the case of surface waves [4], for a clarification of the influence of the horizontal exchange of momentum A_L on the dissipation of internal waves it is adequate to use a first approximation. An exhaustive answer can be given only after comparison of the results of this work with a second approximation or with a precise solution of the formulated problem.

BIBLIOGRAPHY

1. Bukhatov, A. Ye., Pukhtyar, L. D. and Cherkesov, L. V., "Internal Waves," KOMPLEKSNYYE OKEANOGRAFICHESKIYE ISSLEDOVANIYA CHERNOGO MORYA (Multisided Investigations of the Black Sea) (in press).

2. Bukhatov, A. Ye., et al., "Internal Waves of a Tidal Period in the Equatorial Zone of the Indian Ocean," OKEANOLOGIYA (Oceanology), Vol 18, No 5, pp 788-795, 1978.

3. Goncharov, V. V., "Some Characteristics of Internal Waves in the Ocean," TSUNAMI I VNUTRENNIYE VOLNY (Tsunamis and Internal Waves), Sevastopol', Izd. MGI UkrSSR, pp 87-96, 1976.

4. Levkov, N. P., "Free Oscillations of a Stratified Viscous Fluid," in this collection of articles, pp 189-197.

5. Odulo, A. V., "Vertical Structure of Planetary Waves in a Stratified Ocean," MORSKIYE GIDROFIZICHESKIYE ISSLEDOVANIYA (Marine Hydrophysical Investigations), No 6, Sevastopol', pp 82-94, 1971.

6. Fliegel, M. and Hunkins, K., "Internal Wave Dispersion Calculated Using the Thomson-Haskell Method," J. PHYS. OCEAN., Vol 5, No 3, pp 541-548, 1975.

7. Hyun, J. M., "Internal Wave Dispersion in Deep Oceans Calculated by Means of Two-Variable Expansion Techniques," J. OCEAN. SOCIETY JAPAN, Vol 32, No 1, pp 11-20, 1976.

FREE OSCILLATIONS OF A STRATIFIED VISCOUS FLUID

Sevastopol' TEORETICHESKIYE I EKSPERIMENTAL'NYYE ISSLEDOVANIYA POVERKHNOSTNYKH I VNUTRENNIKH VOLN in Russian 1980 (manuscript received 23 Jan 80) pp 189-197

[Article by N. P. Levkov]

[Text]

Abstract: A study was made of the influence of vertical and horizontal exchange of momentum on the dissipation of waves in a stratified fluid of constant depth. The solution is found by expansion of the sought-for functions into a series in two small parameters with an accuracy to values of the second order of magnitude inclusive. A comparison of the derived expressions with the precise solution of the problem is presented in the example of a homogeneous ocean.

The characteristics of internal waves in an ideal stratified fluid of constant depth have been studied quite well [2, 9, 10]. A study was also made of the influence of viscosity on the dissipation of surface and internal waves in the case of a piecewise-constant [5, 7, 11] or exponental [4, 8] density distribution.

In this article a study is made of the influence of vertical A_z and horizontal A_L exchange of momentum on the dissipation of waves in an unbounded basin of constant depth H with an arbitrary stratification. It is assumed that the coefficients A_z and A_L are constant.

Within the framework of a linear theory, with Coriolis force taken into account, the motion of the fluid is described by the equations

$$\begin{aligned} u_t - 2\omega v &= \frac{1}{\rho}\left[-p_x + \bar{\mu}(u_{xx}+u_{yy}) + (\mu u_z)_z + \bar{\mu}_z w_x\right], \\ v_t + 2\omega u &= \frac{1}{\rho}\left[-p_y + \bar{\mu}(v_{xx}+v_{yy}) + (\mu v_z)_z + \bar{\mu}_z w_y\right], \\ w_t + g\frac{\rho^*}{\rho} &= \frac{1}{\rho}\left[-p_z + \bar{\mu}(w_{xx}+w_{yy}) + (\mu w_z)_z + \mu_z w_z\right], \end{aligned} \tag{1}$$

$$u_x + v_y + w_z = 0, \qquad \rho_t^* + \rho_z w = 0$$

with the boundary conditions

$$u = v = w = 0 \text{ with } z = 0, \tag{2}$$

$$A_z u_z + A_L w_x = A_z v_z + A_L w_y = 0, \quad p - 2\mu w_z = \rho g \zeta, \quad \zeta_t = w \text{ with } z = H.$$

Here $\mu = A_z \rho$; $\bar{\mu} = A_L \rho$, ρ is the density of the fluid in an undisturbed state; ρ^* is the dynamic additive of density;

$$p = P - g \int_z^H \rho \, dz;$$

P is dynamic pressure.

We will seek a solution of equations (1) in the form of harmonic functions exp[i (mx + ny - σt)]. We introduce φ in such a way that

$$u = i\frac{m}{r^2} w' - 2\omega\sigma n\varphi, \quad v = i\frac{n}{r^2} w' + 2\omega\sigma m\varphi, \quad \rho^* = -\frac{i}{\sigma}\rho' w, \quad \frac{p}{\rho} = \frac{A_z}{r^2} w''' + \frac{A_z}{r^2}\frac{\rho'}{\rho} w'' + \left(\frac{i\sigma}{r^2} - A_L\right) w' + A_L \frac{\rho'}{\rho} w - 4\omega^2 i\sigma\varphi, \quad r^2 = m^2 + n^2. \tag{3}$$

The prime denotes differentiation for z. Then the system (1) assumes the form

$$A_z \varphi'' + A_z \frac{\rho'}{\rho}\varphi' + \left(i\sigma - r^2 A_L\right)\varphi - \frac{i}{\sigma r^2} w' = 0.$$

$$A_z w^{IV} + 2A_z \frac{\rho'}{\rho} w''' + \left(i\sigma - r^2 A_L - r^2 A_z + A_z \frac{\rho''}{\rho}\right) w'' + \left(i\sigma - 2r^2 A_z\right)\frac{\rho'}{\rho} w' + \tag{4}$$

$$+ r^2\left(-i\sigma + r^2 A_L + A_L \frac{\rho''}{\rho} - i\frac{g}{\sigma}\frac{\rho'}{\rho}\right) w - 4\omega^2 i\sigma r^2\left(\varphi' + \frac{\rho'}{\rho}\varphi\right) = 0.$$

The system of two equations (4) is easily reduced to one sixth-degree differential equation with variable coefficients

$$A_z^2\left(w^{VI} + A_5 w^{V}\right) + A_z\left(A_4 w^{IV} + A_3 w'''\right) + A_2 w'' + A_1 w' + A_0 w = 0. \tag{4a}$$

The boundary conditions (2) are transformed to

$$\varphi = w = w' = 0 \text{ with } z = 0,$$

$$\varphi' = A_z w'' + A_L r^2 w = A_z w''' + \left(i\sigma - r^2 A_L - 2r^2 A_z\right) w' -$$

$$- \frac{igr^2}{\sigma} w - 4\omega^2 i\sigma r^2 \varphi = 0 \text{ with } z = H. \tag{5}$$

With $A_L = A_z = 0$

$$w'' + \frac{\rho'}{\rho} w' - r^2 \frac{\sigma^2 + g\rho'/\rho}{\sigma^2 - 4\omega^2} w = 0. \tag{6}$$

We will assume that one solution of equation (6) w_{10} is known, which is not equal to zero with z = 0. Then the second fundamental solution is

$$w_{20} = w_{10} \int \frac{dz}{w_{10}^2 \rho}.$$

We will select the integration constant in such a way that w_{20} becomes equal to zero with z = 0. Expanding the sought-for function w and the wave number r into a series [1] in two small parameters $\varepsilon_1 = A_L H \sqrt{gH}$ and $\varepsilon_2 = \sqrt{A_z / H \sqrt{gH}}$, we find two fundamental solutions of equation (4a). It is possible to find these solutions with any degree of accuracy. We will limit ourselves to the second approximation. Assume

$$\begin{aligned} w &= w_0 + w_1\varepsilon_1 + w_2\varepsilon_2 + w_3\varepsilon_2^2 + w_4\varepsilon_1\varepsilon_2 + w_5\varepsilon_1^2 + O(\varepsilon^3), \\ r &= r_0 + r_1\varepsilon_1 + r_2\varepsilon_2 + r_3\varepsilon_2^2 + r_4\varepsilon_1\varepsilon_2 + r_5\varepsilon_1^2 + O(\varepsilon^3), \end{aligned} \tag{7}$$

where $\varepsilon = \max(\varepsilon_1, \varepsilon_2)$. Substituting expressions (7) into equation (4a) and equating the coefficients with equal degrees of ε_1 and ε_2, we obtain five differential equations for finding the viscous additives to the fundamental solutions of equation (6)

$$w_k'' + \frac{\rho'}{\rho} w_k' - r_0^2 \frac{\sigma^2 + g\rho'/\rho}{\sigma^2 - 4\omega^2} w_k = h_k \qquad (k = 1 \div 5), \tag{8}$$

where

$$h_1 = h_2 \frac{r_1}{r_2} + \frac{i r_0^2 H \sqrt{gH}}{\sigma^2 - 4\omega^2} \left[\left(2\sigma r_0^2 + \sigma \frac{\rho''}{\rho} + r_0^2 \frac{g\rho'}{\sigma\rho} \right) w_0 - \sigma \left(2w_0'' + \frac{\rho'}{\rho} w_0' \right) \right],$$

$$h_2 = 2 r_0 r_2 \frac{\sigma^2 + g\rho'/\rho}{\sigma^2 - 4\omega^2} w_0,$$

$$h_3 = \frac{\sigma^2 + g\rho'/\rho}{\sigma^2 - 4\omega^2} \left(2 r_0 r_2 w_2 + r_2^2 w_0 + 2 r_0 r_3 w_0 \right) + \frac{i\sigma H \sqrt{gH}}{\sigma^2 - 4\omega^2} \left[w_0^{IV} + 2\frac{\rho'}{\rho} w_0''' - r_0^2 w_0'' + \right.$$

$$\left. + \frac{\rho''}{\rho} w_0'' - 2 r_0^2 \frac{\rho'}{\rho} w_0' + \frac{4\omega^2}{\sigma^2} \left(w_0^{IV} + 2\frac{\rho'}{\rho} w_0''' + \frac{\rho''}{\rho} w_0'' \right) \right],$$

$$h_4 = 2 \frac{\sigma^2 + g\rho'/\rho}{\sigma^2 - 4\omega^2} \left[r_0 r_1 w_2 + r_0 r_2 w_1 + \left(r_1 r_2 + r_0 r_4 \right) w_0 \right] + \frac{i\sigma H \sqrt{gH}}{\sigma^2 - 4\omega^2} \left[2 r_0 r_2 \left(2 r_0^2 + \right. \right.$$

$$\left. \left. + \frac{\rho''}{\rho} \right) w_0 + r_0^2 \left(r_0^2 + \frac{\rho''}{\rho} \right) w_2 - \left(1 + \frac{4\omega^2}{\sigma^2} \right) \left(r_0^2 w_2'' + 2 r_0 r_2 w_0'' \right) -$$

$$-\frac{4\omega^2}{\sigma^2}\frac{\rho'}{\rho}\left(r_0^2 w_2' + 2r_0 r_2 w_0'\right)\Big],$$

$$h_5 = \frac{\sigma^2+g\rho'/\rho}{\sigma^2-4\omega^2}\left[2r_0 r_1 w_1 + \left(r_1^2+2r_0 r_3\right)w_0\right] - \frac{4\omega^2 r_0^4 H^3 g}{\sigma^2\left(\sigma^2-4\omega^2\right)}\left(w_0'' + \frac{\rho'}{\rho}w_0'\right) +$$

$$+\frac{i\sigma H\sqrt{gH}}{\sigma^2-4\omega^2}\left[2r_0 r_1\left(2r_0^2+\frac{\rho''}{\rho}\right)w_0 + r_0^2\left(r_0^2+\frac{\rho''}{\rho}\right)w_1 -\right.$$

$$\left.-\left(1+\frac{4\omega^2}{\sigma^2}\right)\left(r_0^2 w_1'' + 2r_0 r_1 w_0''\right) - \frac{4\omega^2}{\sigma^2}\frac{\rho'}{\rho}\left(r_0^2 w_1' + 2r_0 r_1 w_0'\right)\right].$$

The zero approximations of the two solutions are denoted by w_{10} and w_{20}. Then from (8) we find [3]

$$w_{jk} = w_{20}\int_0^z w_{10} h_{jk}\rho\, dz - w_{10}\int_0^z w_{20} h_{jk}\rho\, dz. \tag{9}$$

Here the subscript j is additionally introduced; j = 1 corresponds to w_{10}, j = 2 - w_{20}.

Thus, in the second approximation there are two fundamental solutions W_1 and W_2 of equation (4a). We seek the lacking four fundamental solutions of this equation with a small parameter and a higher derivative [6] in the form

$$W_{j+2} = Z_1(z,\varepsilon_1,\varepsilon_2)\exp\frac{Z_2(z,\varepsilon_1,\varepsilon_2)}{\varepsilon_2} \quad (j=1\div 4), \tag{10}$$

where the functions $Z_{1,2}(z, \varepsilon_1, \varepsilon_2)$ are stipulated in the form of series in powers of ε_1 and ε_2. Substituting the series (10) into equation (4a) and comparing the coefficients with identical powers of ε_1 and ε_2, in the second approximation

$$W_{j+2} = \frac{1}{\sqrt{\rho}}\exp\left(\beta_j z + \bar{\alpha}_j\right), \tag{11}$$

where

$$\beta_j = \frac{\alpha_j}{\sqrt{A_z}}; \quad \alpha_{1,2} = \sqrt{-i\left(\sigma\pm 2\omega\right)+r_0^2 A_L}; \quad \alpha_{3,4} = -\alpha_{1,2};$$

$$\bar{\alpha}_j = \frac{1}{4\alpha_j\sqrt{A_z}}\int_0^z\left[\frac{3\rho'' A_z}{\rho} - \frac{5(\rho')^2 A_z}{2\rho^2} + 4r_0 A_L\left(r_1\varepsilon_1 + r_2\varepsilon_2\right) + \right.$$

$$\left.+\frac{r_0^2 A_z}{\alpha_j^2}\left(i\frac{g}{\sigma} - \frac{\alpha_j A_L}{\sqrt{A_z}}\right)\frac{\rho'}{\rho} + (-1)^j\frac{2\omega i r_0^2 A_z}{\alpha_j^2}\right]dz.$$

Substituting expressions (11) into the differential equations (4) and equating the coefficients with the lower powers of ε, it is easy to confirm that (11) are solutions of (4). The expressions for φ, corresponding to the fundamental solutions W_{j+2}, assume the form

$$\Phi_{j-2} = \frac{(-1)^j \beta_i W_{j-2}}{2\omega\sigma r^2}\left(1 - \frac{\rho'}{2\beta_i\rho} + \bar{\Phi}_j\right),$$

where

$$\bar{\Phi}_j = \frac{1}{2\alpha_j^2}\left\{\frac{3A_z\rho''}{2\rho} - \frac{5A_z(\rho')^2}{4\rho^2} - r^2A_z - r^2A_z\frac{\omega+(-1)^j\sigma}{2\omega\alpha_j^2}\left(i\frac{g}{\sigma} - \beta_j A_z\right)\frac{\rho'}{\rho} + \right.$$

$$\left. + \frac{\sqrt{A_z}}{2z}\int_0^z\left[\frac{5\sqrt{A_z}(\rho')^2}{2\rho^2} - 3\sqrt{A_z}\frac{\rho''}{\rho} - \frac{r^2\sqrt{A_z}}{\alpha_j^2}\left(\frac{ig}{\sigma} - \beta_j A_z\right)\frac{\rho'}{\rho}\right]dz\right\};$$

$$\bar{\Phi}_j(0) = \lim_{z\to 0}\bar{\Phi}_j(z).$$

With an accuracy to higher-order values, the general solution of the formulated problem is as follows:

$$w = \sum_{j=1}^{6} C_j W_j.$$

Satisfying the boundary conditions and equating the coefficients of expansion of the determinant into a series in powers of ε to zero, we obtain equations for determining the wave number r_0, and also r_1, r_2, r_3, r_4 and r_5, the fictitious parts of which give the decrement of attenuation of a wave with the length $\lambda = 2\pi/r_0$

$$L_1 w_{20} = 0, \quad L_1 = (\sigma^2 - 4\omega^2)\frac{d}{dz} - gr_0^2, \quad L_1 w_{21} - 2gr_0 r_1 w_{20} = -r_0^2 L_3 w_{20},$$

$$L_{2,3} = i\sigma H\sqrt{gH}\left(\frac{gr_0^2}{\sigma^2 - 4\omega^2} \pm \frac{\rho'}{\rho} + \frac{\sigma^2+4\omega^2}{\sigma^2}\frac{d}{dz}\right), \tag{12}$$

$$L_1 w_{22} - 2gr_0 r_2 w_{20} = \frac{i(\sigma^2-4\omega^2)\sqrt{H\sqrt{gH}}(\alpha_1^3 + \alpha_2^3)}{2\sigma\rho(0)[w_{10}(0)]^2 w_{20}\rho\alpha_1\alpha_2},$$

$$L_1 w_{23} - g(r_2^2 + 2r_0 r_3)w_{20} - 2gr_0 r_2 w_{22} + \left(2\sigma - \frac{g\rho'}{\sigma\rho}\frac{\sigma^2+4\omega^2}{\sigma^2-4\omega^2}\right)ir_0^2 H\sqrt{gH}w_{20}' +$$

$$+ \frac{iH\sqrt{gH}(\sigma^2+4\omega^2)\rho'(0)w_{20}'(0)}{2\sigma(\sigma^2-4\omega^2)\rho(0)w_{10}(0)}L_1 w_{10} + \frac{\sqrt{H\sqrt{gH}}}{2\sigma w_{10}(0)}\left(\frac{\sigma-2\omega}{\alpha_1} + \frac{\sigma+2\omega}{\alpha_2}\right)\times$$

$$\times\left[w_{20}'(0)(L_1 w_{12} - 2gr_0 r_2 w_{10}) - w_{10}'(0)(L_1 w_{22} - 2gr_0 r_2 w_{20})\right] = 0,$$

$$L_1 w_{24} - 2g(r_1 r_2 + r_0 r_4)w_{20} - 2gr_0(r_1 w_{22} + r_2 w_{21}) +$$

$$+L_2(r_0^2 w_{22}+2r_0 r_2 w_{20})+\frac{\sqrt{H\sqrt{gH}}\,w'_{20}(0)}{2\sigma w_{10}(0)}\left(\frac{\sigma-2\omega}{\alpha_1}+\frac{\sigma+2\omega}{\alpha_2}\right)\times$$

$$\times(L_1 w_{11}-2gr_0 r_1 w_{10}+r_0^2 L_3 w_{10})+r_0^2 H^2\sqrt{g\sqrt{gH}}\left[\frac{i\omega w'_{20}(0)}{\sigma^2 w_{10}(0)}\times\right.$$

$$\left.\times\left(\frac{1}{\alpha_1}-\frac{1}{\alpha_2}\right)L_1 w_{10}-\frac{\sigma r_0^2 w_{20}}{\sigma^2-4\omega^2}\left(\alpha_1^2\frac{\sigma-\omega}{\alpha_2}+\alpha_2^2\frac{\sigma+\omega}{\alpha_1}\right)\right]=0,$$

$$L_1 w_{25}-g(r_1^2 w_{20}+2r_0 r_5 w_{20}+2r_0 r_1 w_{21})+L_2(r_0^2 w_{21}+2r_0 r_1 w_{20})+$$

$$+\frac{2gH^3 r_0^4(\sigma^4+4\omega^2\sigma^2-8\omega^4)}{\sigma^2(\sigma^2-4\omega^2)}w'_{20}=0 \quad \text{with } z=H.$$

The values w_{jk} are found from equation (8). The values of the velocity components u, v and w with an accuracy to the arbitrary constant C in the first approximation are determined by the expressions

$$u=\frac{C}{r_0^2}\left[\left(im-\frac{2\omega}{\sigma}n\right)w'_{20}-(im+n)F_1(z)-(im-n)F_2(z)+\right.$$

$$\left.+(im+n)F_3(z)+(im-n)F_4(z)\right],$$

$$v=\frac{C}{r_0^2}\left[\left(in+\frac{2\omega}{\sigma}m\right)w'_{20}-(in-m)F_1(z)-(in+m)F_2(z)+\right.$$

$$\left.+(in-m)F_3(z)+(in+m)F_4(z)\right], \qquad (13)$$

$$w=C\left\{w_2+\frac{(\alpha_1^3+\alpha_2^3)i\sqrt{A_z}\,w_{10}}{2\sigma\alpha_1\alpha_2\rho(0)w_{10}^2(0)}-\sqrt{A_z}\left[\frac{F_1(z)}{\alpha_1}+\frac{F_2(z)}{\alpha_2}+\frac{F_3(z)}{\alpha_1}+\frac{F_4(z)}{\alpha_2}\right]\right\},$$

$$F_{1,2}(z)=\frac{(\sigma\mp2\omega)\,ch\,\beta_{1,2}(H-z)}{2\sigma\rho(0)w_{10}(0)\,ch\,\beta_{1,2}H}, \qquad F_{3,4}(z)=\frac{r_0^2 A_z w_{20}(H)\,ch\,\beta_{1,2}z}{2\sqrt{A_z}\,\alpha_{1,2}\,ch\,\beta_{1,2}H}.$$

It can be seen (13) that the influence of viscosity on the velocity field is reflected most substantially at the bottom and at the free surface. The second and third terms of the expressions for the horizontal velocity components u and v represent, in fact, a mathematical description of the change in the velocity in the bottom boundary layer. The last terms of the first two expressions (13) determine the boundary layer at the free surface. With a high horizontal exchange value it can attain values comparable to the bottom boundary layer.

We will examine the simplest case. Assume that ρ= const. Then the solutions of equations (6) and the viscous additive to it (8) will be

$$w_{10}=\exp\beta z, \qquad w_{20}=\frac{1}{\beta\rho}\,sh\,\beta z,$$

$$w_{1k}=\frac{B_k}{2\beta^2}(\beta z\exp\beta z-\operatorname{sh}\beta z),\quad w_{2k}=\frac{B_k}{2\rho\beta^3}(\beta z\operatorname{ch}\beta z-\operatorname{sh}\beta z),$$

where

$$\beta=\frac{\sigma r_0}{\sqrt{\sigma^2-4\omega^2}};\quad B_1=\frac{2i\sigma r_0}{\sigma^2-4\omega^2}\left[r_0H\sqrt{gH}(r_0^2-\beta^2)-ir_1\sigma\right];\quad B_2=\frac{2\sigma^2r_0r_2}{\sigma^2-4\omega^2}.$$

The equations for determining the wave number r_0 and the first approximation r_1 and r_2 (12) assume the form

$$g\beta\operatorname{th}\beta H=\sigma^2,$$

$$\frac{4ir_0\beta^2}{\sigma}(\sigma^2+2\omega^2)H\sqrt{gH}-4\sigma^2r_1+r_0B_1\left(\frac{\sigma^2}{\beta^2}+\frac{\sigma^4H}{\beta^2g}-gH\right)=0, \tag{14}$$

$$4\sigma^2r_2-r_0B_2\left(\frac{\sigma^2}{\beta^2}+\frac{\sigma^4H}{\beta^2g}-gH\right)=\frac{2\rho^2\sqrt{H\sqrt{gH}}}{\operatorname{sh}2\beta H}(\alpha_1^3+\alpha_2^3).$$

For long waves

$$r_0=\sqrt{\frac{\sigma^2-4\omega^2}{gH}},\quad r_1=ir_0\frac{\sigma^2+2\omega^2}{\sigma}\sqrt{\frac{H}{g}},\quad r_2=(1+i)\frac{(\sigma+2\omega)^{3/2}+(\sigma-2\omega)^{3/2}}{4\sigma\sqrt{2H\sqrt{gH}}} \tag{15a}$$

for short waves

$$r_0=\frac{\sigma\sqrt{\sigma^2-4\omega^2}}{g},\quad r_1=r_0\frac{2iH\sigma^3}{g}\sqrt{\frac{H}{g}},\quad r_2=\frac{2(1+i)\sigma^2\sqrt{H\sqrt{gH}}\left[(\sigma+2\omega)^{3/2}+(\sigma+2\omega)^{3/2}\right]}{g^2\sqrt{2}\exp(2\sigma^2H/g)} \tag{15b}$$

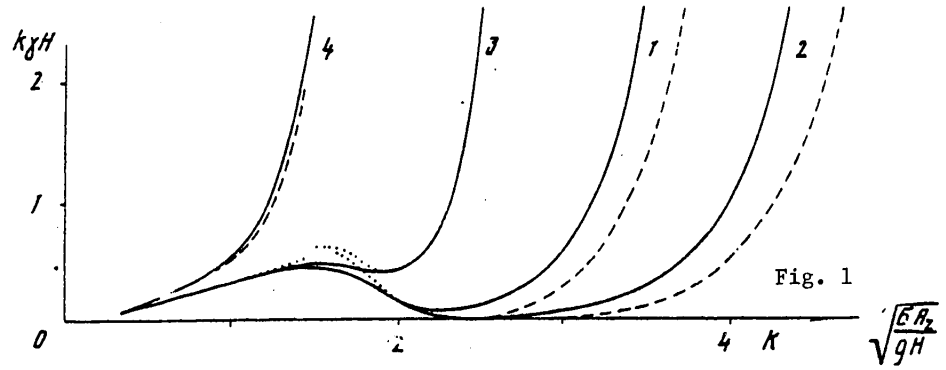

Fig. 1

For the purpose of explaining the influence of higher-order terms on the decrement of attenuation γ we made computations of the values r_1 and r_2 using formulas (14) with $\omega=0$, H = 4000 m (Fig. 1) and H = 100 m (Fig. 2); the dashed curves 1 and 5 correspond to $A_L = A_z = 200$ cm$^2\cdot$sec^{-1}, k = 10^4; curve 2 $A_L = A_z = 2$ cm$^2\cdot$sec^{-1}, k = 10^5; curves 3 and 6 -- $A_L = 50\,A_z = 10^4$ cm$^2\cdot$sec^{-1}, k = 10^4; curve 4 -- $A_L = 5\cdot10^3\,A_z = 10^6cm^2\cdot$sec^{-1}, k = 10^4. The solid curves represent the change in the decrement of attenuation corresponding to the same parameters, but computed using precise formulas derived in [5]; the dotted curves are plotted using the approximate formulas (15a) with $r_0 H<1$ or (15b) with $r_0 H>1$.

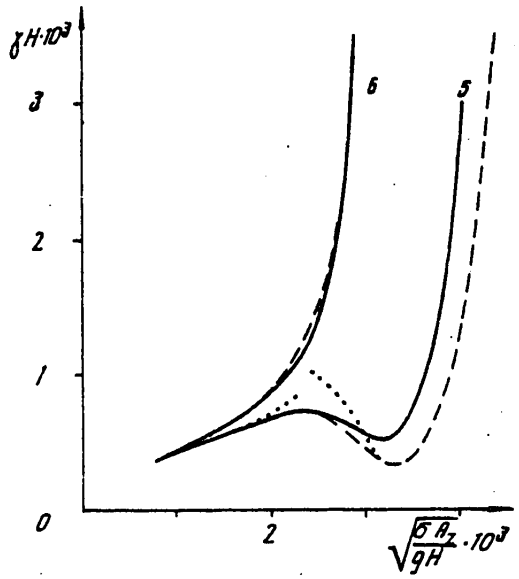

Fig. 2.

Comparing the solid, dashed and dotted curves we see that in the region of long waves they all coincide. However, in the region of short waves with $A_L >> A_z$ they also coincide (curves 3, 4, 6); with $A_L = A_z$ the values of the dashed and dotted curves are half as great as the true γ value. This is attributable to the fact that for short waves the contributions of the A_L and A_z values to the γ value are equivalent. However, numerical computations were made taking into account only the first approximation of the expansion in the small parameter ε_2, which with $r_0 H >> 1$ becomes equal to zero. In the range of waves with a length of the order of several depths, regardless of the relationship between A_L and A_z, the approximation (14) seems quite good; the short-wave and long-wave approximations (15) give somewhat exaggerated results.

In connection with the above, it is desirable to examine the second approximation of the expansion in the small parameter ε. For short waves

$$r_3 = r_1 \frac{\sigma^2 - 2\omega^2}{\sigma^2 - 4\omega^2}.$$

The r_4 and r_5 values, regardless of the length of the surface waves, exert no appreciable influence on the value of the decrement of attenuation.

Thus, the first approximation for ε_1 and the second for ε_2 give a virtually precise solution of the formulated problem.

BIBLIOGRAPHY

1. Vazov, V., ASIMPTOTICHESKIYE RAZLOZHENIYA RESHENIY OBYKNOVENNYKH DIFFERENTSIAL'NYKH URAVNENIY (Asymptotic Expansions of Solutions of Ordinary Differential Equations), Moscow, "Mir," 1968, p 172.

2. Goncharov, V. V., "Some Characteristics of Internal Waves in the Ocean," TSUNAMI I VNUTRENNIYE VOLNY (Tsunamis and Internal Waves), Sevastopol', Izd. MGI AN UkSSR, pp 87-96, 1976.

3. Yerugin, N. P., KNIGA DLYA CHTENIYA PO OBSHCHEMU KURSU DIFFERENTSIAL'NYKH URAVNENIY (Book for Reading in the General Course on Differential Equations), Minsk, "Nauka i Tekhnika," 1972, 660 pages.

4. Zadorzhnyy, A. I., "Attenuation of Long Waves in an Exponentially Stratified Sea," MORSKIYE GIDROFIZICHESKIYE ISSLEDOVANIYA (Marine Hydrophysical Investigations), No 3, Sevastopol', pp 96-110, 1975.

5. Levkov, N. P., "Dissipation of Surface Waves Generated by Periodic Atmospheric Disturbances," MORSKIYE GIDROFIZICHESKIYE ISSLEDOVANIYA, No 4, Sevastopol', pp 76-83, 1973.

6. Moiseyev, N. N., ASIMPTOTICHESKIYE METODY NELINEYNOY MEKHANIKA (Asymptotic Methods of Nonlinear Mechanics), Moscow, "Nauka," 1969, 800 pages.

7. Nerkesov, L. V., GIDRODINAMIKA POVERKHNOSTNYKH VNUTRENNIKH VOLN (Hydrodynamics of Surface and Internal Waves), Kiev, "Naukova Dumka," 1976, 364 pages.

8. Dore, B. D., "The Decay of Oscillations of a Nonhomogeneous Fluid Within a Container," PROC. OF THE CAMBRIDGE PHIL. SOCIETY, Vol 65, No 1, pp 301-307, 1969.

9. Fliegel, M. and Hunkins, K., "Internal Wave Dispersion Calculated Using the Thomson-Haskell Method," J. PHYS. OCEAN., Vol 5, No 3, pp 541-548, 1975.

10. Hyun, J. M., "Internal Wave Dispersion in Deep Ocean Calculated by Means of Two-Variable Expansion Techniques," J. OCEAN. SOCIETY JAPAN, Vol 32, No 1, pp 11-20, 1976.

11. Johns, B. and Cross, M., "The Decay of Internal Wave Modes in a Multilayered System," DEEP SEA RES., Vol 16, No 2, pp 185-195, 1969.

5303 - END -
CSO: 8144/1944